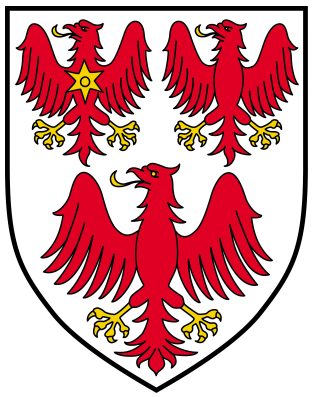
Investigation of the Contribution of Cutaneous HPV E6 Proteins towards the Development of Non Melanoma Skin Cancer

AMY FRANCES HOLLOWAY

The Queen's College





A thesis submitted to the Medical Sciences Division of the University of Oxford in partial fulfilment of the requirements for the Degree of Doctor of Philosophy

Michaelmas Term 2012

Department of Oncology
The Weatherall Institute of Molecular Medicine
University of Oxford

Abstract

Investigation of the Contribution of Cutaneous HPV E6 Proteins towards the Development of Non Melanoma Skin Cancer

Amy Frances Holloway D.Phil Medical Oncology

The Queen's College Michaelmas Term 2012

Sunlight is the main aetiological agent in the development of non melanoma skin cancer (NMSC), the most commonly diagnosed cancer in the fair skinned population. Mounting epidemiological and molecular data suggest that infection with cutaneous Human papillomavirus (HPV) may act as a co-factor in the early stages of NMSC development. The viral E6 protein can inhibit the apoptotic response to UV-induced damage, partly through proteasomal degradation of the pro-apoptotic protein BAK. Upon UV damage, BAK undergoes a series of activating modifications that are linked to changes in phosphorylation status. BAK activation commits a cell to apoptosis through mitochondrial permeabilisation.

The aim here was to elucidate the underlying mechanism of HPV5 E6-mediated BAK degradation. Mutation of lysine 113 in BAK and siRNA knockdown of a novel HPV5 E6 associated ubiquitin ligase, HERC1, prevented HPV5 E6 mediated-BAK degradation. A proximity ligation *in situ* assay showed an interaction between HERC1 and BAK in cells, which was dependent on the presence of the E6 protein and UV irradiation. Probing the BAK conformation and phosphorylation status suggests E6 targets a dephosphorylated BAK monomer before mitochondrial permeabilisation occurs, leading to the proposal of a mechanism for the interaction of BAK with HERC1 which depends on the activation status of BAK and a putative BH3 domain identified in HERC1.

Additional work identifies β_1-integrin as an interacting protein of a conserved YHDW amino acid motif at the C-terminus of certain β1 HPV E6 proteins. Only expression of E6 proteins with the YHDW motif (HPV5 and 8) in keratinocytes disrupted β_1-integrin membrane localisation, altered expression of β_1-integrin downstream effectors, such as focal adhesion kinase, and increased cell migration. Mutation of W157A in the HPV5 E6 YHDW motif reduced these effects.

Together, this work furthers the understanding of mechanisms by which infection with HPV may promote the early stages of NMSC development.

Acknowledgements

I would like to thank my supervisor, Alan Storey, for the opportunity to do a D.Phil and for providing opportunities to travel and present this work. I am also grateful for his guidance and encouragement throughout this project. My thanks also go to other members of the lab: Ghadeer Almuhaini, Abul Azad, Joanna Fox and Christine Tomlins for their continued help, useful discussion, entertaining company and occasional declarations of 'that's odd'.

My gratitude goes to other members of the Weatherall Institute of Molecular Medicine for helpful advice, friendly nods and smiles in the corridor and provision of urgently required reagents and desperately needed cake. Special thanks to Peter Thomas for his assistance with microscopy.

I would also like to thank Cancer Research UK for funding this studentship and The Queen's College for additional financial support to attend a conference in Italy.

I am grateful to the friends I have made in Oxford for providing excellent company and alcohol in both the good and more challenging times.

My thanks also go to my family for their support and occasional help moving!

Presentations

The work in this thesis has been presented at the following events:

2009 Targeted Degradation of BAK by HPV5 E6 Following UVB Irradiation

DNA Tumour Virus Meeting, 14-19 July, Oxford (poster)

2011 Identification of a HECT domain E3 Ligase used by HPV5 E6 to Target an Active Conformation of BAK in Response to UVB Irradiation

The University of Oxford Medical Sciences Division D.Phil Student's Day, 12 July, Oxford (oral presentation)

2011 Identification of a HECT domain E3 Ligase used by HPV5 E6 to Target an Active Conformation of Bak in Response to UVB Irradiation

DNA Tumour Virus Meeting, 19-24July, Trieste, Italy (oral presentation)

with thanks to The Queen's College, Oxford, for the award of a travel grant

2012 How to Kill a Killer: HPV's Life and Death Decisions at the Mitochondria

The Weatherall Institute of Molecular Medicine Student Presentation Day, 19 January, Oxford (oral presentation)

Table of Contents

Abstract i

Acknowledgements ii

Presentations iii

Table of Contents iv

List of Figures x

List of Tables xiv

Abbreviations xv

Chapter 1 Introduction 1

1.1 Skin 1

1.1.1 Skin Structure and Function 1

1.1.2 Epidermal Structure and Keratinocyte Differentiation 2

1.1.3 Junctions 6

1.1.3.1 Integrin Based Junctions 8

1.2 Apoptosis 11

1.2.1 Extrinsic Pathway 11

1.2.2 Intrinsic Pathway 13

1.2.2.1 The BCL-2 Family Proteins 14

1.2.3 p53-Induced Apoptosis 19

1.3 Non Melanoma Skin Cancer 21

1.3.1 UV-induced DNA Damage and Repair 23

1.3.2 Apoptosis and UV in Keratinocytes 26

1.4 Human Papillomavirus 27

1.4.1 Cancer and α-HPV Epidemiology 29

1.4.2 NMSC and β-HPV 32

1.4.2.1 Epidermodysplasia Verruciformis 32

1.4.2.2 HPV Infection in the Immune Suppressed Population 32

1.4.2.3 Immunocompetent Population 33

1.4.3 HPV Life Cycle 36

1.4.4 HPV Genome Structure 39

1.4.5 Virus-Encoded Proteins 40
1.4.5.1 L1 and L2 40
1.4.5.2 E1 and E2 41
1.4.5.3 E4 and E5 43
1.4.5.4 E6 45
1.4.5.5 E7 54
1.4.6 The Proteasome 58
1.4.6.1 HPV and the Proteasome 60
1.4.7 Models of HPV Infection and Cancer 63
1.5 Summary and Aims 66
Chapter 2 Materials and Methods 68
2.1 Mammalian Cell Culture 68
2.1.1 Media 68
2.2 Cell Lines and Maintenance 68
2.2.1 Cell Lines 68
2.2.2 Mycoplasma Testing 69
2.2.3 UVB Irradiation of Cells 69
2.2.4 Cyclohexamide Treatment 70
2.2.5 Storage and Recovery of Cell Lines 70
2.3 Transfection of Mammalian Cells 70
2.3.1 DNA Transfections 70
2.3.2 siRNA Transfections 71
2.3.3 Retrovirus Production and Transduction 72
2.4 Protein Techniques 73
2.4.1 Whole Cell Extracts 73
2.4.1.1 Protein Extraction Buffers 74
2.4.2 Sodium Dodecyl Sulphate Polyacrylamide Gel Electrophoresis 74
2.4.3 Western Blotting 76
2.4.4 Immunoprecipitation (IP) 77
2.4.4.1 Immunoprecipitation Buffers 78
2.4.5 Peptide Pull-Down Assay 78

2.4.6 BH3 Peptide Pull-Down 80
2.4.7 Mitochondrial Fractionation 80
2.4.8 BAK Dimerisation Assay 80
2.4.9 Expression of Fusion Proteins in *E. coli* 81
2.4.9.1 Purification of GST-HPV5 E6 from Bacteria 81
2.4.9.2 Purification of His-BAKΔC from Bacteria 82
2.4.9.3 Purification of HERC1 Mini-gene MBP Fusion Proteins 83
2.4.10 *In Vitro* Ubiquitination Assay 84
2.5 Molecular Biology Techniques 84
2.5.1 Polymerase Chain Reaction 84
2.5.1.1 RNA Isolation from Cells 84
2.5.1.2 Reverse Transcription of RNA 85
2.5.1.3 Real Time Quantitative Polymerase Chain Reaction 86
2.5.1.4 High Fidelity Polymerase Chain Reaction 90
2.5.1.5 Taq Polymerase Chain Reaction 90
2.5.1.6 Agarose Gel Electrophoresis 92
2.5.2 Vector Construction 92
2.5.2.1 Restriction Digest and Ligation 92
2.5.3 Mutagenesis 94
2.5.4 Plasmid DNA Preparation 95
2.5.4.1 Bacterial Transformation 95
2.5.4.2 Plasmid Purification 95
2.5.4.3 DNA Sequencing 96
2.6 Flow Cytometry 96
2.6.1 BAK N-terminal Conformation Change Assay 96
2.6.2 Active Caspase-3 97
2.6.3 Cytochrome *c* Release 98
2.7 Immunocytochemistry 99
2.7.1 Proximity Ligation *In Situ* Assay 100
2.8 Cell Migration Assays 100
2.9 Statistics 101

Chapter 3 Investigation Into the Mechanism of HPV E6 Targeting of BAK Following DNA Damage....102

3.1 Introduction....102

3.2 Aim....103

3.3 Results....104

3.3.1 Construction of pEFIRES vector expressing the HPV5 E6 sequence 104

3.3.2 Generation of HCT116 DKO stable cell lines expressing pEFIRES and pEFIRES-5E6 105

3.3.3 Effects on BAK levels in HCT116 WT BAK cells expressing HPV5 E6 following UVB irradiation 108

3.3.4 Levels of p53 and E6AP in response to UVB in HCT116 WT BAK cells expressing HPV5 E6 109

3.3.5 BAK is targeted to the proteasome by HPV5 E6 in HCT116 WT BAK cells 109

3.3.6 Caspase-3 activation in HPV5 E6 expressing HCT116 WT BAK cells in response to UVB....113

3.3.7 Generation of a BAK lysine mutant 117

3.3.8 Characterisation of the BAK K113R mutant 119

3.3.9 Requirement of K113 for HPV5 E6-mediated degradation of BAK .124

3.3.10 Caspase-3 activation in response to UVB in HCT116 K113R cells expressing HPV5 E6 125

3.3.11 Phosphorylation status of Y108 in response to UVB in HCT116 WT BAK cells expressing HPV5 E6....129

3.3.12 Phosphorylation status of S117 in HCT116 WT BAK cells expressing HPV5 E6 in response to UVB....130

3.3.13 Binding of p53 to BAK in HCT116 WT BAK cells expressing HPV5 E6 in response to UVB....132

3.3.14 Investigation of the BAK N-terminal conformational change in response to UVB irradiation in HCT116 WT BAK and HT1080 cells expressing the HPV5 E6 protein 133

3.3.15 Temporal regulation of BAK degradation in HPV5 E6 expressing HCT116 WT BAK and HT1080 cells 135

3.3.16 Targeting of a BAK mutant unable to expose the hydrophobic pocket for degradation by the HPV5 E6 protein 138

3.3.17 Investigation of outer mitochondrial membrane integrity in response to UVB in HCT116 WT BAK pEFIRES-expressing cells 141

3.4 Discussion 143

Chapter 4 Investigation of a novel E6 associated E3 ubiquitin ligase 149

4.1 Introduction 149

4.2 Aim 151

4.3 Results 153

4.3.1 *herc1* knockdown in HCT116 DKO cells 153

4.3.2 Investigation of HERC1 involvement in HPV5 E6-mediated degradation of BAK in HCT116 cells 157

4.3.3 Requirement of HERC1 for HPV5 E6-mediated BAK degradation in HEKa cells 161

4.3.4 Interaction of HERC1 with BAK *in vivo* 164

4.3.5 Investigation of a putative HERC1 BH3 sequence 173

4.3.6 Construction of a HERC1 mini-gene 177

4.3.7 *In vitro* HPV5 E6-mediated ubiquitination assay of BAK using the HERC1 mini-gene 188

4.4 Discussion 197

Chapter 5 Identification of binding partners of the HPV5 E6 C-terminal motif 205

5.1 Introduction 205

5.2 Aim 208

5.3 Results 208

5.3.1 Identification of the YHDW motif interacting proteins 208

5.3.2 Point mutation of the HPV5 E6 YHDW motif 213

5.3.3 Western blot for junctional and cytoskeletal proteins in N-TERT cells expressing HPV E6 constructs 216

5.3.4 Immunofluorescent staining of β_1-integrin and FAK in keratinocyte cell lines 220

5.3.5 Integrin-β_1 immunofluorescence in PM1 cells 222

5.3.6 Integrin-β_1 immunofluorescence using saponin permeabilisation ...224

5.3.7 Paxillin localisation by immunofluorescence 224

5.3.8 Investigation of filamentous actin cytoskeletal arrangement in N-TERT cells expressing HPV E6 constructs during migration 226

5.3.9 Investigation of migration rates in N-TERT cells expressing HPV E6 constructs 228

5.4 Discussion..... 235

General Discussion 241

Appendices 245

References 249

List of Figures

Figure 1.1 Structure of the epidermis 3

Figure 1.2 Schematic of epidermal cell junctions 7

Figure 1.3 Apoptosis pathways 12

Figure 1.4 The BCL-2 proteins 15

Figure 1.5 Schematic of the 'direct' and 'indirect' models of BCL-2 effector protein activation 18

Figure 1.6 Formation of pyrimidine dimers upon UVB irradiation 24

Figure 1.7 Papillomavirus phylogenetic tree 28

Figure 1.8 Comparison of the structure of uninfected and HPV-infected epithelium during the viral life cycle 37

Figure 1.9 Genome organisation of β-HPV 39

Figure 1.10 Structure of the HPV E6 proteins 46

Figure 1.11 Model of high-risk α-HPV E6-mediated p53 degradation 51

Figure 1.12 Summary of the function of HPV E6 and E7 proteins 55

Figure 1.13 Disruption of the cell cycle by the E7 protein 56

Figure 1.14 Schematic of HECT domain and RING finger E3 ligase-mediated ubiquitination 61

Figure 2.1 Example raw RT-QPCR data 88

Figure 3.1 Schematic of BAK activation 104

Figure 3.2 Construction of pEFIRES vector encoding the HPV5 E6 gene 106

Figure 3.3 pEFIRES-5E6 expression in HCT116 WT BAK cells 107

Figure 3.4 Levels of BAK, p53 and E6AP in response to UVB in HCT116 WT BAK cells expressing pEFIRES-5E6 110

Figure 3.5 *bak* mRNA levels in HCT116 WT BAK cells expressing pEFIRES-5E6 in response to UVB 111

Figure 3.6 BAK protein levels in HCT116 WT BAK cells expressing pEFIRES-5E6 in response to UVB and proteasome inhibitors 113

Figure 3.7 Caspase-3 activation in HCT116 WT BAK cells expressing pEFIRES-5E6 in response to UVB 115

Figure 3.8 Mutation of BAK residue K113 to arginine 118

Figure 3.9 Expression of WT and K113R BAK by retroviral infection in HCT116 DKO cells 120

Figure 3.10 Calculation of BAK activation using Ab1 fluorescence by flow cytometry 121

Figure 3.11 Characterisation of HCT116 cells expressing K113R BAK compared to those expressing WT BAK 122

Figure 3.12 K113R BAK levels in HCT116 cells expressing pEFIRES-5E6 after UVB irradiation 126

Figure 3.13 Caspase-3 activation in HCT116 K113R BAK cells expressing HPV5 E6 in response to UVB 128

Figure 3.14 Dephosphorylation of BAK at Y108 in response to UVB in HCT116 WT BAK cells expressing HPV5 E6 130

Figure 3.15 Dephosphorylation of BAK at S117 in response to UVB in HCT116 WT BAK cells expressing HPV5 E6 131

Figure 3.16 p53 binding to BAK in response to UVB in HCT116 WT BAK cells expressing HPV5 E6 132

Figure 3.17 BAK activation in HCT116 WT BAK and HT1080 cells expressing HPV5 E6 in response to UVB 134

Figure 3.18 Temporal regulation of HPV5 E6-mediated BAK degradation in HCT116 WT BAK and HT1080 cells 136

Figure 3.19 Model of the BAK hydrophobic pocket and S117 139

Figure 3.20 BAK S117E levels in HPV5 E6 expressing HCT116 cells in response to UVB 140

Figure 3.21 Cytochrome *c* release in HCT116 WT BAK cells expressing HPV5 E6 upon UVB irradiation 142

Figure 4.1 siRNA screen of HECT domain involved in HPV5 E6-mediated BAK degradation in Saos2 cells 152

Figure 4.2 *herc1* mRNA knockdown in HCT116 and HT1080 cells 155

Figure 4.3 BAK levels in the presence of HPV5 E6 and HERC1 knockdown in HCT116 WT BAK cells 158

Figure 4.4 BAK levels in HPV5 E6-expressing cells with HERC1 knockdown by two individual siRNA oligos 160

Figure 4.5 BAK levels in HPV5 E6 expressing HEKa cells with *herc1* knockdown 162
Figure 4.6 PLISA assay 166
Figure 4.7 PLISA assay for an interaction between BAK and HERC1 168
Figure 4.8 HERC1 has a putative BH3 domain 174
Figure 4.9 HERC1 BH3 sequence binding to BAK and BAK S117E 176
Figure 4.10 Construction of the HERC1 mini-gene 179
Figure 4.11 HERC1 and E6AP C-terminus alignment 184
Figure 4.12 Purification of His-BAKΔC protein 189
Figure 4.13 Purification of MBP, GST-5E6, and GST proteins 191
Figure 4.14 Purification of MBP-HERC1 fusion proteins 193
Figure 4.15 Ubiquitination assay using His-BAKΔC protein 195
Figure 4.16 Ubiquitination assay using mitochondrial sub-cellular fractions 196
Figure 4.17 Schematic of HPV E6-mediated cell survival through BAK proteolysis 204
Figure 5.1 High-risk cutaneous HPV E6 proteins have a conserved C-terminal YHDW motif 207
Figure 5.2 Isolation of YHDW interacting proteins 209
Figure 5.3 Expression of HPV E6 transcripts in N-TERT cells 214
Figure 5.4 Western blot of N-TERT lysates expressing HPV E6 constructs for plaque, junctional and cytoskeletal proteins 217
Figure 5.5 Immunofluorescent staining of β_1-integrin and FAK levels in HPV E6-expressing N-TERT cells 221
Figure 5.6 Immunofluorescent β_1-integrin staining in the PM1 cell line expressing HPV5 E6 223
Figure 5.7 Integrin-β_1 immunofluorescence by saponin permeabilisation in N-TERT cells expressing HPV E6 constructs 225
Figure 5.8 Paxillin immunofluorescence in N-TERT cells expressing pLXSN HPV E6 constructs 227
Figure 5.9 Actin cytoskeleton in migrating N-TERT cells expressing HPV E6 constructs 229

Figure 5.10 Percentage wound closure in N-TERT cells expressing HPV E6 constructs 232

List of Tables

Table 1.1 Cancers attributable to infection with oncogenic HPV in developed and developing countries 30

Table 1.2 HPV E6 protein activities which may contribute to malignancy 47

Table 2.1 Components of RM+ media 68

Table 2.2 siRNA target sequences 72

Table 2.3 5x Laemmli buffer 75

Table 2.4 SDS-PAGE acrylamide gels 75

Table 2.5 Antibodies and working concentrations 76

Table 2.6 Peptide sequences 79

Table 2.7 Thermocycling protocol for reverse transcription reaction 85

Table 2.8 RT-QPCR primers 86

Table 2.9 Thermocycling RT-QPCR program 87

Table 2.10 Example calculation of relative mRNA knockdown by RT-QPCR 89

Table 2.11 Thermocycling program for Velocity polymerase 90

Table 2.12 Taq polymerase reaction primers 91

Table 2.13 Thermocycling program for Taq polymerase 91

Table 2.14 Cloning primer sequences 93

Table 2.15 Table of mutations generated and the primers used 94

Table 2.16 Sequencing primers 96

Table 4.1 OriGENE HuSH shRNA constructs against *herc1* 154

Table 4.2 HERC1 mini-gene construction primers 185

Table 5.1 Unique interacting proteins of the YHDW peptide 211

Abbreviations

6,4PPs	6,4 photoproducts
AIF	Apoptosis Inducing Factor
Apaf-1	Apoptosis protease activating factor 1
BCC	Basal cell carcinoma
BH	BCL-2 homology domain
BPV	Bovine papillomavirus
cDNA	Complementary DNA
CER	Complete early region
CIN	Cervical intraepithelial neoplasia
CPDs	Cyclobutane pyrimidine dimers
DDR	DNA damage response
DISC	Death inducing signalling complex
DLG	Discs large
DMEM	Dulbecco's Modified Eagle Medium
DMSO	Dimethylsulphoxide
ECM	Extracellular matrix
EV	Epideromdysplasia verruciformis
FCS	Foetal calf serum
FADD	Fas associated death domain
FAK	Focal adhesion kinase
FasL	Fas ligand
HA	Haemagluttinin
HCT116 DKO	HCT116$^{bak-/-bax-/-}$ cells (double knockout)
HDACs	Histone deacetylases
HECT	Homologous to E6AP C-terminal
HPV	Human papillomavirus
HRP	Horseradish peroxidase
IAP	Inhibitor of apoptosis protein
NCR	Non-coding region
MBP	Maltose binding protein
MMP	Matrix metalloprotease
MOMP	Mitochondrial outer membrane permeabilisation
NMSC	Non melanoma skin cancer
OMM	Outer mitochondrial membrane
PBS	Phosphate buffered saline
PCR	Polymerase chain reaction
PKC	Protein kinase C
PFA	Paraformaldehyde
PP2A	Protein phosphatase 2A

RT-QPCR	Real time quantitative PCR
SCC	Squamous cell carcinoma
SDS	Sodium dodecyl sulphate
TBST	Tris buffered saline 0.1% Tween-20
TRAIL	TNF related apoptosis inducing factor
UV	Ultraviolet
WT	Wild type

Chapter 1 Introduction

The Human papillomaviruses (HPV) infect both mucosal and cutaneous epithelial tissues. Infection of the cutaneous epithelium with β-HPV, in concert with UV irradiation, may contribute to the development of non melanoma skin cancer (NMSC). The viral life cycle is highly dependent on the terminal differentiation program of keratinocytes and keratinocytes at different stages of this process form the structure of the skin. In order to replicate, HPV must induce a replicative state in differentiating keratinocytes which have exited the cell cycle. In order to do this the HPV genome encodes two oncogenic viral proteins, E6 and E7 which disrupt the normal keratinocyte life cycle through a number of mechanisms, including alteration of protein stability through targeting of substrates for proteasomal degradation.

This thesis focuses on the contributions of the E6 oncoprotein towards the progression of NMSC, with emphasised interest in the interaction of the E6 protein with host cell proteins to inhibit cellular apoptosis and to disrupt cell adhesion complexes and migration.

1.1 Skin

1.1.1 Skin Structure and Function

The skin is the largest organ of the human body with a surface area of approximately 2 square metres and has numerous roles, predominantly protection of the underlying tissues and structures from insult. In addition, the skin has regulatory and homeostatic roles; temperature, absorption and waste excretion, sensing pressure and pain as well as a synthetic role; hormones (Slominski, 2005) and vitamin D (Holick et al., 1980). The skin is comprised of two main layers: the epidermis and the underlying dermis and appendages include hair, nails, and sweat and sebaceous glands.

The dermis houses the vasculature of the skin, as well as the immune and lymphatic system and hair follicles. It also houses the neural sensory Merkel cells. The dermis is usually 2-4mm thick and comprises fibroblasts, apocrine and immune cells as well

as extracellular matrix (ECM) elastic connective tissues. It sits above the subcutaneous tissues and is connected to the epidermis via the basement membrane.

The epidermis is the thinner of the two structures (approximately 150µm but varying with body site) and does not contain any blood vessels. The epidermis is formed primarily by keratinocyte cells undergoing a programme of terminal differentiation. For hair-bearing skin keratinocyte stem cells renew in the hair follicle niche and differentiate as they transit to the surface, leading to the renewal of the skin every 30 days. The differing phenotypes of keratinocytes at the varying stages of differentiation results in the formation of distinct epidermal sublayers: stratum corneum, stratum granulosum, stratum spinosum and the innermost stratum basale (shown in Figure 1.1).

1.1.2 Epidermal Structure and Keratinocyte Differentiation

Keratinocyte stem cells residing in the hair follicles (Pincelli and Marconi, 2010) have the ability to self renew and produce rapidly proliferating daughter cells known as transit amplifying cells. Transit amplifying cells have a limited proliferative capacity, undergoing a restricted number of divisions before withdrawing from the cell cycle and beginning the process of terminal differentiation (Jones and Watt, 1993, Jones et al., 1995). Whilst apoptosis and terminal differentiation share common features: nuclear destruction, DNA degradation and proteolytic activity, the two processes are distinct: terminal differentiation is a tissue wide process which does not result in rapid elimination of cells, instead these dead cells perform a barrier function taking weeks to be eliminated, rather than hours (Lippens et al., 2005).

In order to differentiate keratinocytes must undergo both architectural and transcriptional changes from the proliferative state of the transit amplifying cells in the stratum basale to the anucleated, lipid filled corneocytes of the stratum corneum (Radoja et al., 2006). One stimulus for this may be detachment of keratinocytes

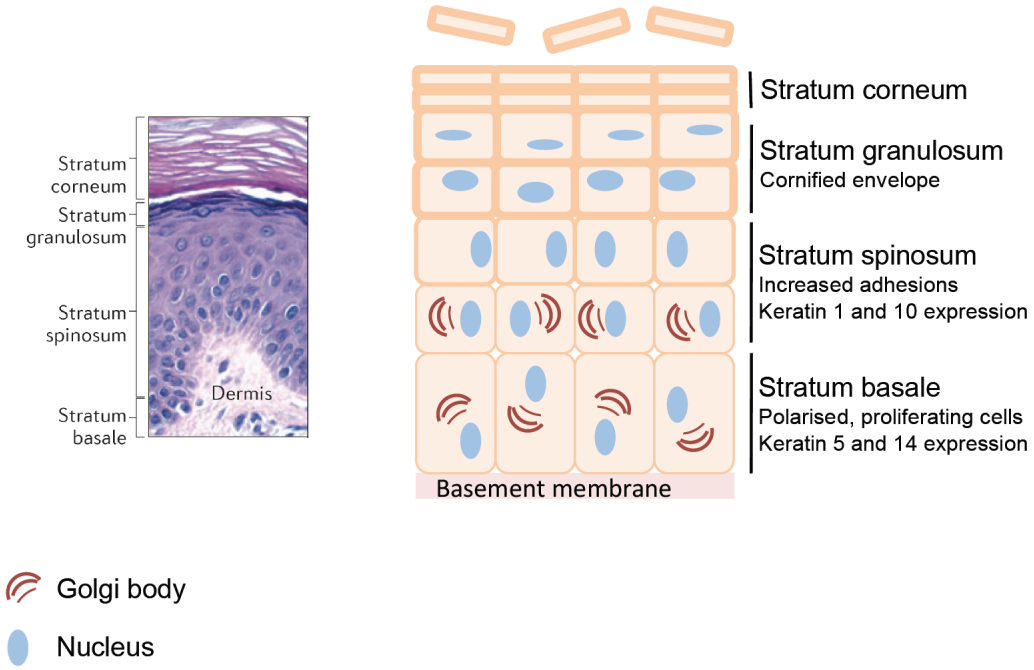


Figure 1.1 Structure of the epidermis

The epidermis is comprised of four strata which can be seen by eosin and haemotoxylin staining. Each strata is characterised by keratinocytes at differing stages of terminal differentiation. The proliferating cells in the stratum basale are attached to the basement membrane by integrin based adhesions. As these cells proliferate the daughter cells detach from the basement membrane changing their cytoarchitecture (junction and cytoskeletal components). As cells move towards the surface they lose cellular organelles and flatten to develop into corneocytes to form a protective barrier. At the stratum corneum cells slough off. Adapted from Simpson et al. (2011)

from the basement membrane. Keratinocytes adhere to the basal layer via integrin-mediated junctions (see chapter 1.1.3.1). The detachment of integrins from the basement membrane and their down-regulation may play a role in initiation of differentiation (Watt, 2002).

Another factor required for cell architectural changes observed during differentiation is calcium concentration, of which there is an increasing gradient of extracellular calcium from the stratum basale to the stratum corneum. Low calcium concentration therefore keeps cells in a proliferative state whilst higher concentrations stimulate differentiation, stratification, the formation of desmosome junctions and activity of the cross-linking transglutaminases (Fuchs, 1990). This calcium concentration across the epidermis may be maintained by the function of tight junctions and selective ion permeability (Kurasawa et al., 2011). As a result of architectural changes brought about by movement into areas of higher calcium concentration and membrane detachment, transcriptional changes may also be mediated through the Serum Response Factor, Notch signaling, p63 and its isoforms, and p300 (Watt et al., 2008, Simpson et al., 2011, Candi et al., 2006, Wong et al., 2010).

Transit amplifying cells constitute the stratum basale of the epidermis which sits on the basement membrane and the basement membrane forms contacts with the dermis. The transit amplifying cells attach to the basement membrane through hemidesmosome junctions which are predominantly composed of $\alpha_6\beta_4$-integrins (Fuchs and Raghavan, 2002). Furthermore the stratum basale houses Merkel cells and the pigment producing melanocytes.

Upon the decision to undergo differentiation, transit amplifying keratinocytes detach from the basement membrane, exit the cell cycle and alter their gene expression programme. The expression of one family of proteins subjected to tight regulation throughout terminal differentiation is that of keratins, the predominant keratinocyte cytoskeletal filaments providing cellular protection and mechanical resistance. The types of keratins expressed by keratinocytes vary dependent on body site, tissue type and epithelial strata according to the level of mechanical stress the cells are

exposed to. Cells which are not subjected to rigorous mechanical stress express very few keratins, whilst those cells closer to the skin outer surface express tougher and more densely bundled keratins more abundantly. Keratin expression is tightly regulated at different stages of cell differentiation, so much so that their expression can be used as markers of keratinocyte differentiation and recent work suggests that the differing keratin expression patterns may control keratinocyte proliferation and differentiation (Alam et al., 2011). Therefore upon beginning terminal differentiation keratinocytes switch off the genes encoding keratins 5 and 14 (Blanpain and Fuchs, 2009). These normally anchor the epidermis to the basement membrane via attachment to integrins in hemisdesmosome structures and so are markers of cells possessing proliferative potential. Production of the high molecular weight keratins 1 and 10 is then initiated, strengthening cell-cell junctions and providing resistance to mechanical stress. Keratinocytes at this stage of differentiation, along with melanocytes and Langerhans cells (immune surveillance cells), form the stratum spinosum.

Non-dividing keratinocytes then begin to flatten and, with the help of the production of the protein keratinohyalin, break down organelles and nuclei and produce additional structural filaments below the plasma membrane resulting in an impermeable barrier. These cells form the stratum granulosum of the epidermis where lipid bilayers are excreted into the extracellular space, waterproofing the skin, preventing pathogen entry and waterloss.

Finally the outer layer of the epidermis, the stratum corneum, is formed from approximately 30 sheets of keratinocytes that have completed the programme of terminal differentiation and are now known as corneocytes. They are strengthened by densely packed keratin filaments and surrounded by lipids. Corneocytes briefly form the outer protective layer of the skin before sloughing from the skin (desquamation) to be replaced by the differentiating cells below.

1.1.3 Junctions

Important structures for the maintenance of epithelial architecture, and consequently barrier and protective functions, are cell junctions. Cell junctional proteins mediate cell adhesion and communication to the extracellular matrix (ECM) and adjacent cells as well as mechanical strength. They also have a role in establishing cell polarity through lateral adhesion to other cells, apico-basal polarisation and adhesion to the extracellular matrix at the basal surface. They are therefore important in signalling, adhesion, proliferation, wound healing, regulation of cell differentiation and the epithelial mesenchymal transition and their modulation can impact tumour formation and metastasis (Shiozaki et al., 1994, Schipper et al., 1991).

Depending on the layer of the epithelium, keratinocytes express a selected pattern of cell junctions that is highly dynamic as keratinocytes progress through terminal differentiation as the layers migrate to the skin surface. Upon wound healing, the cell junction composition of cells may also change to result in a transient downregulation of adhesion, increasing proliferation.

The patterning of cell junctions within the keratinocytes of the epidermis changes with development but in the adult epidermis five main types of junction are found, each with a specific function and comprising specific proteins. These are outlined below and summarised in Figure 1.2. Generally, cell junctions comprise of a transmembrane component and plaque proteins acting as a linker to cellular filaments.

Gap Junctions

Gap junctions are intercellular transmembrane channels permitting the passive diffusion of nutrients, metabolites, ions and molecules for cellular communication. They are formed by connexin proteins which assemble into connexons. In the epidermis gap junctions are numerous and have a role in co-ordination of keratinocyte growth and differentiation (Salomon et al., 1994, Tada and Hashimoto, 1997).

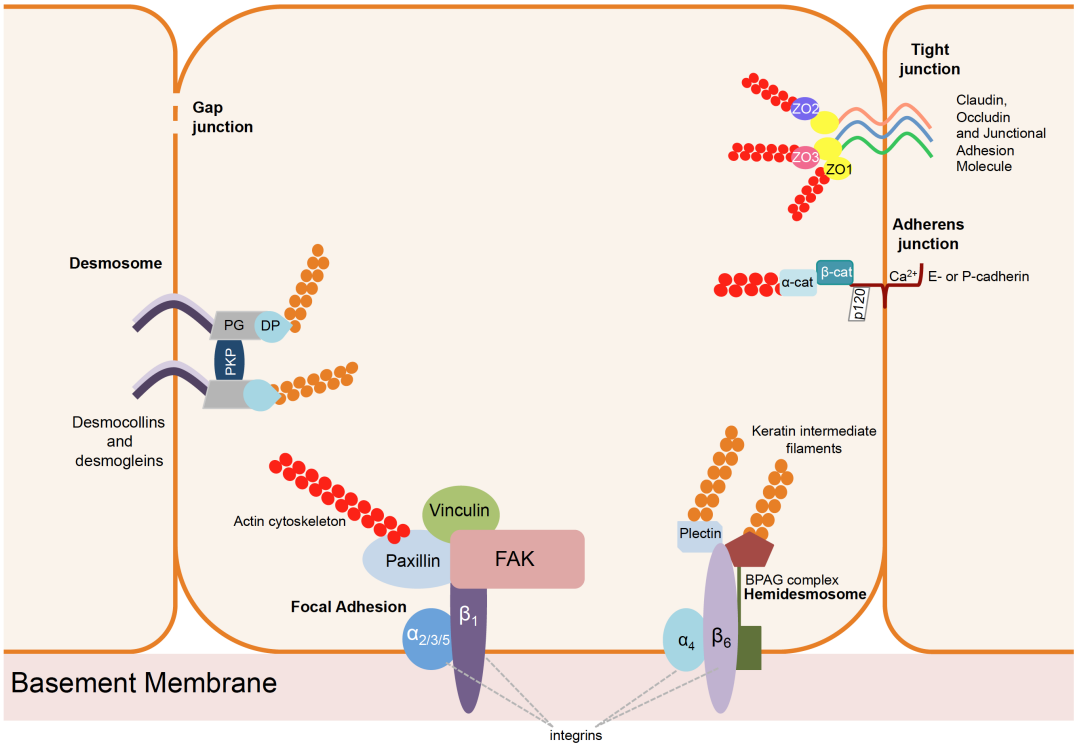


Figure 1.2 Schematic of epidermal cell junctions

Focal adhesions and hemidesmosomes are integrin-mediated junctions which adhere the cell to the basement membrane. Focal adhesions link to the actin cytoskeleton whilst hemidesmosomes link to keratin intermediate filaments. Adherens junctions and desmosomes form adjacent cell-cell contacts linking the actin or keratin filaments (respectively) of neighbouring cells. Tight junctions are apical junctions forming an additional barrier below the stratum corneum to prevent water loss. Gap junctions are open channels between cells allowing passive diffusion of small molecules.

PG; plakoglobin, PKP; plakophillin, DP; desmoplakin, ZO; zona occludin, cat; catenin.

Adapted from Simpson et al. (2011) and Blanpain and Fuchs (2009)

Tight Junctions

Tight junctions form a regulated permeability barrier to diffusion across the epithelium and separate the plasma membrane into basolateral and apical domains. They contain the transmembrane proteins occludins and claudins which connect to the cytoskeleton via proteins such as zona occludens-1 (ZO1). In the mammalian epidermis tight junctions are concentrated in the upper layers of the epidermis: stratum granulosum and stratum corneum (reviewed in Brandner, 2009).

Adherens Junctions

Adherens junctions in cells are located basal to tight junctions. They are an intercellular junction, acting as bridge to directly connect the actin cytoskeleton of adjacent cells. They are comprised of cadherin family proteins which act in a calcium dependent manner (reviewed in Simpson et al., 2011).

Epidermal cells have adherens junctions to connect the actin cytoskeleton but also have desmosomes. Desmosomes are similar to adherens junctions but connect the keratin intermediate filaments of cells as opposed to the actin cytoskeleton. Adherens junctions mediate intercellular adhesion in the metabolically active layers of epidermis and are involved in morphogenesis and cell positioning in epithelial tissues (Runswick et al., 2001).

1.1.3.1 Integrin Based Junctions

Integrins are heterodimeric transmembrane glycoproteins comprising an α and β subunit. They have a large extracellular ligand binding domain (~700 amino acids) and short cytoplasmic tail. Integrins are responsible for connecting cells to surrounding tissue: in the epidermis they tether basal keratinocytes to the basement membrane. The pairing of the differing α and β subunits to form dimers regulates the integrin receptor substrate specificity. Eleven integrin dimers have been identified in epidermal keratinocytes (Margadant et al., 2010). Integrins have no catalytic activity therefore they form the basis of junctions upon which other signalling proteins can be recruited (mainly to the cytoplasmic tail of the β subunit) to transmit external cues to cells, such as integrin-linked kinase (ILK) and focal

adhesion kinase (FAK). Integrins also function in an 'inside-outside' signalling manner to communicate the status of the cell to the surrounding environment (Harburger and Calderwood, 2009). Integrins crosstalk with receptors such as the epidermal growth factor receptor (EGFR) to induce proliferation in the stratum basale (Aplin and Juliano, 1999). As cells stratify, integrins are downregulated to allow cell cycle exit and differentiation. Unoccupied integrins may also signal for a cell to undergo anoikis (a form of apoptosis induced by cell detachment). Experimental keratinocyte suspension cultures have been used to show that β_1-integrins can upregulate BAX expression and mitochondrial damage to induce apoptosis (Mitra et al., 1997). It follows that expression of integrins in cells beyond the basal layers increases proliferation, delays differentiation and is consequently associated with increased risk of carcinogenesis, as shown in murine studies (Owens et al., 2003, Owens et al., 2005). Hemidesmosomes and focal adhesions are integrin-mediated junctions.

Hemidesmosomes

Hemidesmosomes are cell-matrix junctions mediating the anchorage of basal cells to the basement membrane. The transmembrane components comprise $\alpha_6\beta_4$-integrin heterodimers and link to keratin intermediate filaments through the plaque proteins plectin and dystonin. They provide mechanical strength to the base of the skin epidermis and attach undifferentiated epidermal stem cells to the basement membrane in the stratum basale of the epidermis (reviewed in 1999).

Focal adhesions

Focal adhesions also mediate cell-matrix adhesions, transmitting mechanical force. The transmembrane component is formed from $\alpha_2/\alpha_3\beta_1$-integrin heterodimers. Specific integrin heterodimers form receptors for specific ECM components. Integrin-$\alpha_2\beta_1$ binds to collagen, $\alpha_5\beta_1$-integrins bind fibronectin and $\alpha_3\beta_1$-integrins bind laminin 5 (reviewed in Huttenlocher and Horwitz, 2011). Integrin-β_1 levels are high in keratinocyte stem cells of the stratum basale to maintain their attachment to the basement membrane, as well as their proliferative and undifferentiated state.

Detached β_1-integrins signal for epidermal keratinocyte differentiation (Levy et al., 2000). The importance of β_1-integrin enrichment in basal keratinocytes is shown by the dramatic blistering due to epidermal detachment upon loss of β_1-integrin compared to loss of the α-integrins (Brakebusch et al., 2000). Integrins in focal adhesions mediate actin-myosin-driven processes such as migration and adhesion and connect focal adhesions to the ECM via the plaque proteins such as talin, α-actinin and paxillin. Attachment of integrins to the vinculin plaque protein link them to the actin in the cell cortex (Menkel et al., 1994).

Focal adhesions are enriched at the stratum basale and have diminished stability in migration: as cells move, they lay down immature connections to the ECM and, depending on the direction of migration, some are disassembled whilst others are matured. Cell matrix adhesions can be rapidly disrupted via endocytic removal of integrins from the cell surface which can then be recycled back to a different location of the plasma membrane to aid formation of new adhesion complexes (Caswell and Norman, 2006).

As previously mentioned, integrin signalling is mediated through the recruitment of other proteins, such as FAK. FAK is a non-receptor tyrosine kinase which localises to integrins through binding to the plaque proteins. FAK has been shown to be required for both focal adhesion assembly and dissembly (Ilic et al., 1995). Integrin binding to ECM ligands causes a conformational change in the β-integrin cytoplasmic tail to recruit FAK. FAK then autophosphorylates at tyrosine 397 to create a scaffold for Src kinase, causing a positive feedback loop to increase phosphorylation of FAK. Src and FAK activation then leads to phosphorylation of downstream proteins. FAK autophosphorylation also creates binding sites for other ligands, leading to effector protein signalling, such as the Rac and Rho GTPases and Arp2/3 complex, regulating actin organisation and polymerisation, cell polarisation and contractility (Schaller, 2010). Integrin signalling may also regulate the Jnk/NFKB, PI3K/AKT and MAPK/ERK pathways to confer survival and cell migration (for review on FAK see Mitra et al., 2005).

1.2 Apoptosis

The term ‘apoptosis’ was first coined in 1972 to describe a form of programmed cell death occurring in multicellular organisms (1972). Apoptosis is distinct from other forms of cell death such as autophagy, necrosis and terminal differentiation (for classifications of cell death see Kroemer et al., 2009) and is characterised by DNA fragmentation, controlled organelle breakdown and membrane blebbing which is executed by the caspase family of proteins.

Physiologically, apoptosis plays a key role in cell number homeostasis such as the removal of excess cells during development, such as finger webbing, the removal of self reactive B-cells in the immune system, tissue renewal, as well as the removal of virally infected or damaged cells (Vaux and Korsmeyer, 1999). Consequently apoptosis dysregulation can contribute to pathologies such as cancer and autoimmune and neurodegenerative diseases (Hanahan and Weinberg, 2011, Solary et al., 1996). Apoptosis can be initiated by two main pathways: the extrinsic and intrinsic pathways as outlined in Figure 1.3.

1.2.1 Extrinsic Pathway

The extrinsic pathway is initiated by the binding of ligands to cell surface death receptors. Cells in which apoptosis has been initiated in this way have often been targeted for death by cytotoxic T cells of the immune system. Binding of the ligands Fas Ligand (FasL; also known as CD95), Tumour Necrosis Factor α (TNFα) or TNF-related apoptosis inducing ligand (TRAIL) to their respective receptors (Fas, TNF receptor 1 and Death Receptors 4 and 5 respectively) causes the receptors to trimerise. The receptor cytoplasmic tails contain the so-called Death Domains which recruit Death Domain containing adaptor proteins, such as FADD (Chinnaiyan et al., 1995) for the Fas receptor and TRADD for the TNF receptor (Hsu et al., 1995). FADD and TRADD form a platform for the assembly of the death-inducing signalling complex (DISC; Kischkel et al., 1995). FADD contains a Death Effector Domain which can interact with that of the caspase-8 zymogen, concentrating several

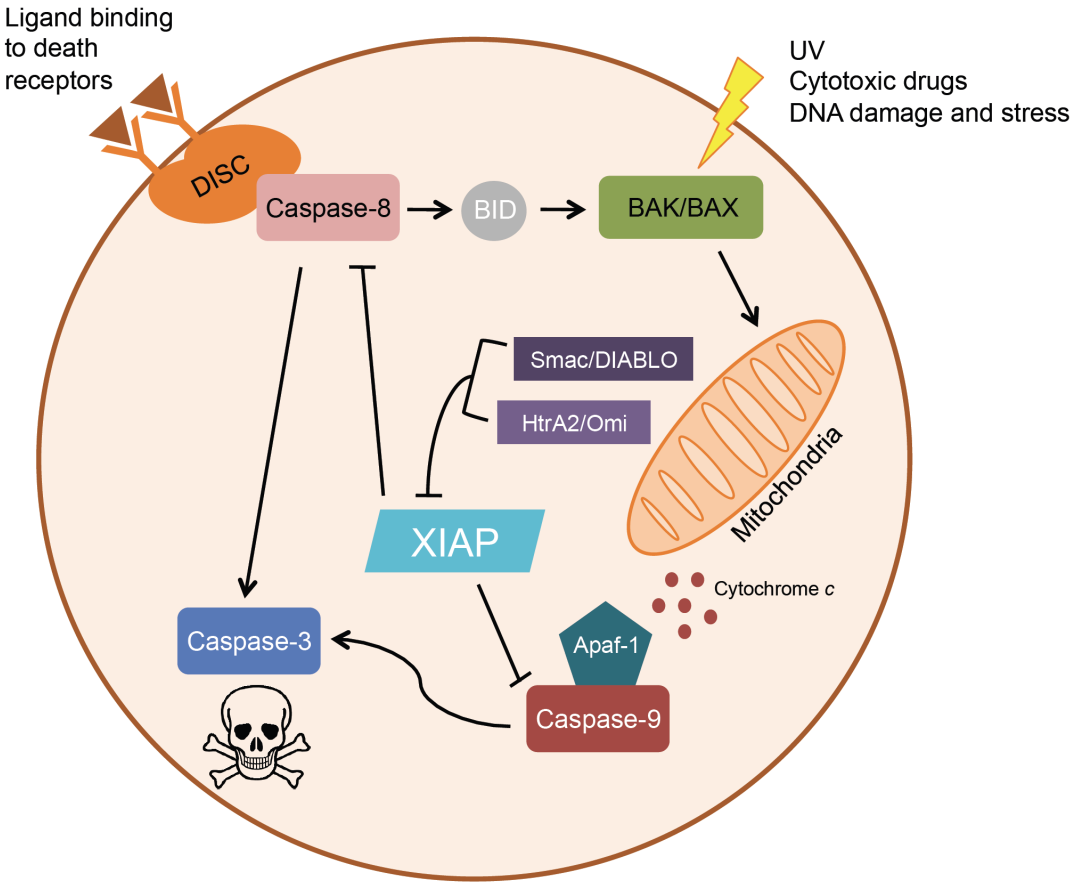


Figure 1.3 Apoptosis pathways

Apoptosis can be initiated via two pathways: the extrinsic and intrinsic pathways.

The extrinsic pathway is activated by ligand binding to death receptors. Adaptor binding to the cytoplasmic tail of the receptors initiates the formation of the death inducing signalling complex (DISC). This activates caspase-8 which can activate the effector caspase-3 to cleave cellular substrates and induce cell breakdown. If death receptor signalling is insufficient to stimulate apoptosis caspase-8 can cleave BID to an active form to initiate the intrinsic apoptosis pathway.

The intrinsic apoptosis pathway is regulated by BCL-2 proteins. Activation results in permeabilisation of the outer mitochondrial membrane by the BAK and BAX effector proteins. Mitochondrial factors are released, activating caspase-9 and subsequently effector caspases, such as caspase-3. Smac/DIABLO and HtrA2/Omi inhibit the IAP family of proteins (such as XIAP) to relieve caspase inhibition.

Adapted from Salvesen and Duckett (2002)

procaspase-8 molecules to the DISC (Muzio et al., 1996). Autocatalytic activation of procaspase-8 leads to the release of active caspase-8 initiating a cascade of downstream effector caspases, such as caspase-3, that are able to cleave cellular substrates to result in cell breakdown and death. This direct caspase-dependent mechanism of death receptor-mediated apoptosis is classed as type I extrinsic cell death (Scaffidi et al., 1998).

Initiation of mitochondrial apoptosis (see chapter 1.2.2) may be stimulated by activation of the death receptors. This death receptor activation of the intrinsic pathway is known as type II extrinsic cell death and occurs if the death receptor apoptotic stimulus is not sufficient to directly activate the effector caspase proteins. Initiation of mitochondrial apoptosis amplifies the apoptotic signal and is activated by caspase-8 cleavage of the BCL-2 family member BID into its truncated, active form, tBID (Luo et al., 1998).

1.2.2 Intrinsic Pathway

Integration of apoptotic stimuli resulting from internal cellular cues, such as DNA damage, nutrient starvation and oxidative stress, occurs at the mitochondria. Promotion of apoptosis at the mitochondria results in permeabilisation of the outer mitochondrial membrane (OMM), disrupting mitochondrial membrane potential and leading to the release of downstream apoptotic factors such as apoptosis inducing factor (AIF), Smac/DIABLO, HtrA2/Omi, EndoG and cytochrome *c*. Permeabilisation of the OMM is a key step in committing the cell to apoptosis and, once permeabilised, the release of cytochrome *c* is an 'all or nothing' response (Goldstein et al., 2000). Damaged or leaky mitochondria are physiologically removed by mitophagy, consequently a threshold amount of mitochondrial permeabilisation is required to compromise the integrity of sufficient mitochondria to release cytochrome *c* and commit the cell to apoptosis. This is achieved by the BCL-2 proteins BAK and BAX, discussed below.

Once released into the cytosol, cytochrome *c* binds the hub protein Apaf-1. Apaf-1 undergoes a conformational change permitting oligomerisation to form the

apoptosome. This initiates activation of procaspase-9 which activates the downstream effector caspases-3, -7 and -6 (Acehan et al., 2002). These caspases are usually inhibited by members of the Inhibitor of Apoptosis (IAP) family of proteins such as XIAP and survivin. XIAP is bound by HtrA2/Omi and Smac/DIABLO upon apoptosis induction, relieving XIAP inhibition of caspases.

1.2.2.1 The BCL-2 Family Proteins

The decision of whether to undergo apoptosis at the mitochondria in response to both pro- and anti-survival signals is regulated by the BCL-2 family of proteins (for review see Youle and Strasser, 2008). The founding member, BCL-2, was first identified in B Cell Lymphoma, a t(14;18) translocation placed the gene under the control of the IgG promoter, resulting in its over-expression and rendering cells more resistant to apoptosis, defining a new class of oncogene (Vaux et al., 1988). Subsequent members of the BCL-2 family have been identified by homology in BCL-2 domains (BH domains). These BH domains are not only tools for classification of BCL-2 family members but are also functionally used by the BCL-2 proteins to interact with, and regulate, each other.

BCL-2 family members can be classified as either anti- or pro-apoptotic (summarised in Figure 1.4). The anti-apoptotic members have four BH domains (1-4) and members include BCL-2, BCL_{XL} and MCL-1. Pro-apoptotic members can be further categorised according to the number of BH domains and function. BAK (BCL-2 antagonist killer) and BAX (BCL-2 associated X protein) have three BH domains (1-3) and are the effector BCL-2 proteins which permeabilise the OMM. The other group of pro-apoptotic BCL-2 proteins is the BH3 only proteins, so-called as they possess only the BH3 domain. These are sensors of apoptosis, relaying information from apoptotic stimuli to the mitochondria, and include the proteins BAD, BIK, BID, Harakiri, BIM, BMF, NOXA and PUMA (Youle and Strasser, 2008). It is the interplay between these pro- and anti-apoptotic members in response to diverse pro- and anti-apoptotic signals that ultimately determines the threshold for apoptosis

Figure 1.4 The BCL-2 proteins

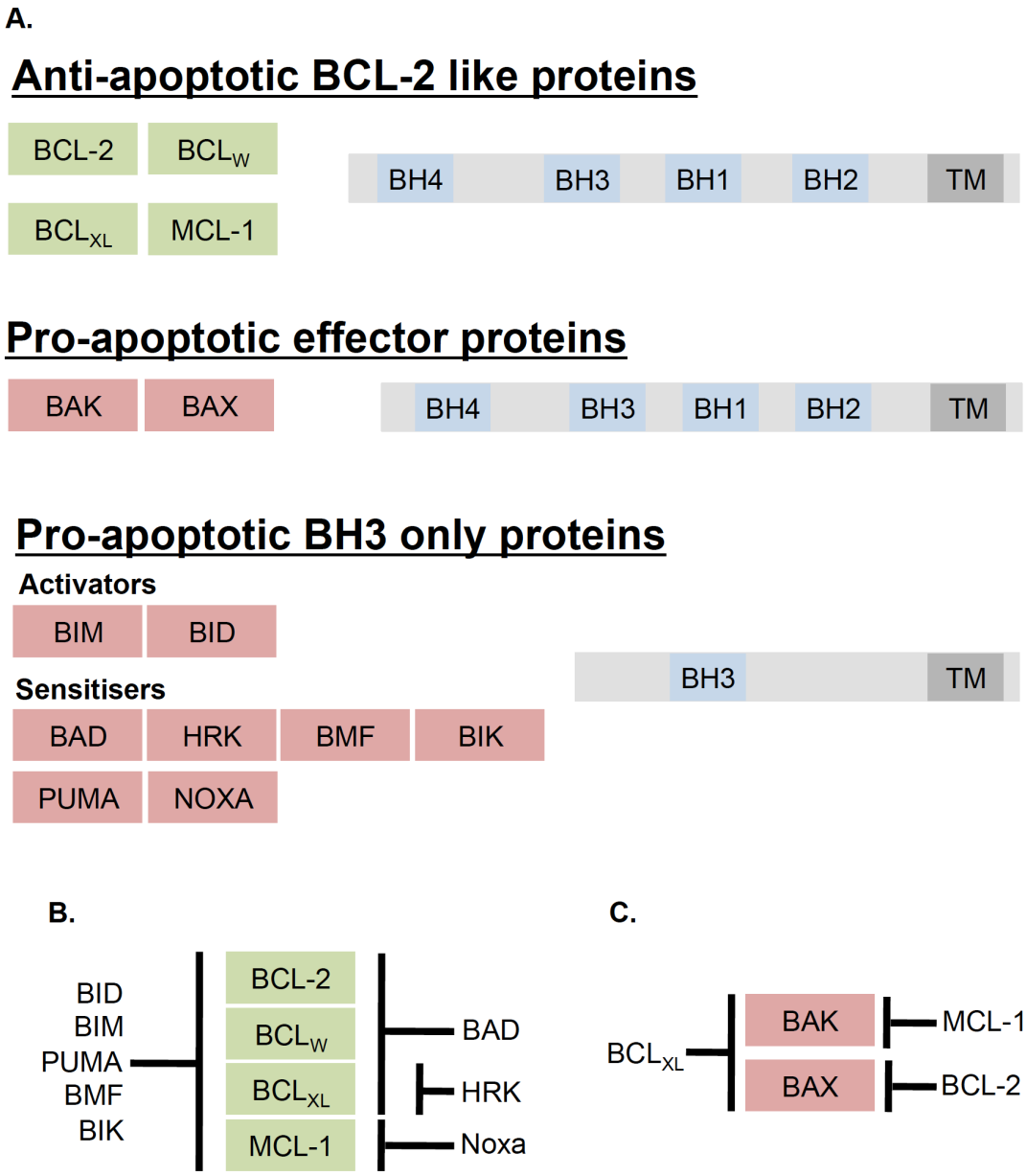


Figure 1.4 legend

A. The BCL-2 family of proteins regulate mitochondrial apoptosis. They include a number of BCL-2 Homology (BH) domains. They are classified as i) anti-apoptotic members which inhibit the pro-apoptotic family members, ii) the pro-apoptotic effector proteins BAK and BAX permeabilise the outer mitochondrial membrane, iii) the BH3 only family members retain only the BH3 domain. According to the model of indirect effector activation these family members are further categorised as activators, able to directly bind and activate BAK and BAX, or sensitisers which inhibit the anti-apoptotic family members. The interplay between the pro- and anti-apoptotic members determines the threshold for mitochondrial apoptosis. Family members are shown on the left-hand side of the diagram, whilst a generalised structure is shown on the right-hand side. TM; transmembrane domain.

B. The BH3 only proteins have specific binding preferences for the anti-apoptotic family members.

C. The anti-apoptotic BCL-2 proteins have preferential binding to the BAK and BAX effector proteins.

Adapted from Lessene at al. (2008)

---

induction, however exactly how these members interplay remains controversial (Chipuk et al., 2010). A key feature of the BAK and BAX effector proteins, as well as the anti-apoptotic BCL-2 proteins, involved in their interaction with the other BCL-2 family members, and consequently their activation, is a hydrophobic pocket which is able to bind the BH3 domains of other BCL-2 proteins (Chipuk et al., 2010).

Currently two models of how the BCL-2 family proteins regulate each other have been proposed: the ‘direct’ and ‘indirect’ models (summarised in Figure 1.5), however attempts to reconcile the two have recently been hypothesised (Llambi et al., 2011). In the ‘indirect’ model it is proposed that activation of BAK and BAX is prevented by their constitutive binding to the anti-apoptotic BCL-2 proteins. Upon an apoptotic stimulus the BH3 domains of the BH3 only proteins bind the BH3 domain binding hydrophobic pocket of the anti-apoptotic BCL-2 proteins. This relieves inhibition of the effector proteins permitting effector protein activation and subsequent mitochondrial outer membrane permeabilisation (MOMP; Willis et al., 2005, Willis et al., 2007, Uren et al., 2007). In the ‘direct’ model the BH3 only

proteins are further classified as ‘activators’ or ‘sensitisers’. The activators (tBID, BIM) directly bind BAK and BAX to induce activation (Kim et al., 2009) whilst the sensitisers bind and inhibit the activity of the anti-apoptotic BCL-2 proteins (Letai et al., 2002). Recent attempts to unify these models propose that anti-apoptotic BCL-2 proteins are able to sequester the direct activators of BAK and BAX (tBID and BIM) or the activated effectors, BAK and BAX, themselves. Each of these ‘modes’ have different sequestration efficiencies and kinetics of derepression in order to permit MOMP (Llambi et al., 2011). BAK and BAX activation can also occur by direct binding of p53 to a site independent of the hydrophobic pocket (Leu et al., 2004, Chipuk et al., 2004, Pietsch et al., 2008a).

Although the activation of BAK and BAX has the same result of MOMP, the activation mechanism and kinetics for the two proteins differ. BAX is an inactive monomer in the cytosol where the α9 helix occupies the BAX hydrophobic pocket (Suzuki et al., 2000). The α9 helix occupies the hydrophobic pocket in such a way as to expose polar residues to keep the protein soluble. Upon transient binding of BH3 only proteins, BAX undergoes a number of conformational changes to expose the α9 helix and a mitochondrial targeting sequence allowing it to homo-oligomerise and permeabilise the OMM (Lalier et al., 2007, Cartron et al., 2003, Kim et al., 2009).

In contrast to BAX, BAK is a mitochondrial membrane bound protein. This mitochondrial localisation means BAK activation kinetics are faster than those of BAX (Kim et al., 2009). Upon receipt of an activating signal, BAK is transiently bound by a BH3 only protein stimulating an N-terminal conformational change to expose a BH3 domain in a BAK monomer ('primed' BAK; Griffiths et al., 1999). This BH3 domain then binds the exposed hydrophobic pocket of another BAK monomer resulting in BAK dimer formation (Dewson et al., 2008). These dimers oligomerise to form homo-oligomers comprising at least 18 BAK molecules through an interface of α6 helices which permeabilise the OMM (Dewson et al., 2009, Oh et al., 2010b).

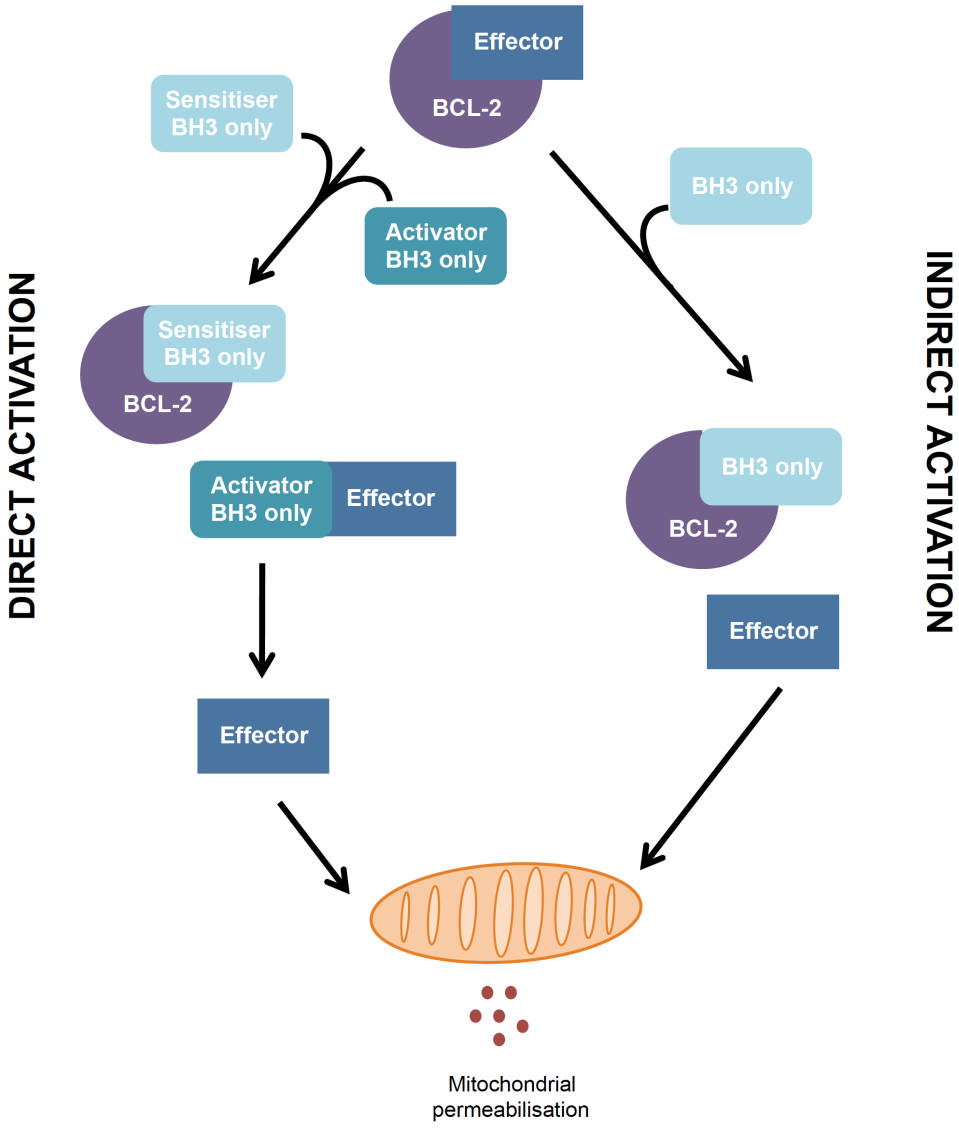


Figure 1.5 Schematic of the 'direct' and 'indirect' models of BCL-2 effector protein activation

It is proposed that in healthy cells the effector BCL-2 proteins, BAK and BAK, are sequestered and inactivated by binding to anti-apoptotic BCL-2 proteins. Upon apoptosis induction the 'indirect' model postulates that BH3 only proteins bind the anti-apoptotic proteins, relieving BAK and BAX inhibition, freeing the effector proteins to permeabilise the mitochondria.

For BAK and BAX activation to occur in the 'direct' model 'sensitiser' BH3 only proteins sequester the anti-apoptotic BCL-2 proteins but the free BAK and BAX must then be activated by transient binding to 'activator' BH3 only proteins, BIM and tBID, before mitochondrial permeabilisation can occur.

This results in dissipation of mitochondrial membrane potential and the release of apoptotic factors.

Through work with HPV and degradation of BAK by the E6 protein, this group developed an interest in the activation of BAK and has elucidated further regulatory steps required for its activation. BAK is a phospho-protein and, in healthy cells, membrane bound BAK is inactive as a result of phosphorylation at tyrosine residue 108 (Y108). Subsequent steps of BAK activation cannot progress without dephosphorylation at this residue by specific non-receptor protein tyrosine phosphatases (PTPN2, 5 and 23) in response to diverse apoptotic stimuli (Fox et al., 2010, Fox et al., 2011). Furthermore Azad et al. (2012) have shown that BAK is also phosphorylated at serine 117 (S117) and this residue is dephosphorylated by Protein Phosphatase 2 A (PP2A) upon apoptosis induction. This phosphorylation physically occludes the hydrophobic pocket and therefore regulates binding of the BH3 only proteins and BAK dimerisation. The ability of p53 to induce the BAK N-terminal conformational change is not affected by the phosphorylation status of the S117 residue.

It is noteworthy that BCL-2 proteins, including BAK and BAX, are required for the physiological maintenance of mitochondria (Perciavalle et al., 2012, Cleland et al., 2011, Karbowski et al., 2006), namely the processes of mitochondrial fission and fusion which regulate mitochondrial contiguity and length.

1.2.3 p53-Induced Apoptosis

p53 is a tumour suppressor protein which plays a major role in co-ordinating cellular response to diverse cellular stresses. p53 responds to DNA damage via execution of the DNA Damage Response (DDR; see chapter 1.3.1) through transcriptional and post-translational functions. Upon DNA damage, p53 undergoes a number of post-translational modifications (acetylation, phosphorylation, methylation and ubiquitination), stabilising p53 and modulating p53 function. p53 activation is able to arrest cells at G1/S and G2/M of the cell cycle to allow DNA damage repair and

upon failure to repair these lesions, p53 is able to induce the cell to undergo apoptosis.

p53 exerts its apoptotic effects through both transcription dependent and independent mechanisms. p53 apoptotic activity is largely through the intrinsic pathway and can directly transcribe apoptosis related genes (Yu et al., 1999, Sax and El-Deiry, 2003) which include the pro-apoptotic BCL-2 family members *bax* (Miyashita et al., 1994), *puma* (Nakano and Vousden, 2001), *noxa* (Oda et al., 2000) and *bid* (Sax et al., 2002) as well as upregulating effector machinery genes such as Apaf-1 (Kannan et al., 2001) and caspase-6 (MacLachlan and El-Deiry, 2002). p53 can also mediate the extrinsic pathway, upregulating transcription of the death receptors, such as *fas*, and their ligands (Owen-Schaub et al., 1995, Maecker et al., 2000) to reduce the apoptosis threshold. Through transcription p53 can also abrogate cellular pro-survival signalling pathways, for example, upregulation of the *pten* gene increases levels of the PTEN protein to negatively regulate the phosphatidylinositiol-3-kinase (PI3K) pathway inhibiting receptor tyrosine kinase signalling, such as that of the Insulin Growth Factor Receptor (Stambolic et al., 2001). p53 can also repress transcription of IAP genes, such as *survivin* (Hoffman et al., 2002). Survivin is over-expressed in many types of tumours (Ambrosini et al., 1997), possibly via recruitment of histone deacetylases (HDACs; Murphy et al., 1999).

Cells expressing p53 mutants which are able to bind DNA but are unable to activate transcription exhibit defects in apoptosis but not the complete elimination of p53-induced apoptosis (Haupt et al., 1995, Jimenez et al., 2000), suggesting that the role of p53 in apoptosis is not only transcription dependent. Indeed, p53 is able to translocate to the mitochondria and initiate apoptotic events before its transcriptional program occurs (Erster et al., 2004). The ability of p53 to translocate to the mitochondria correlates with efficacy of apoptosis induction at the mitochondria as exemplified by its codon 72 polymorphic variants where either proline or arginine is encoded. The p53 proline variant is less effective in

translocating to the mitochondria and induction of apoptosis compared with the arginine isoform (Dumont et al., 2003). At the mitochondria p53 interacts with the BCL-2 proteins to regulate their balance and promote apoptosis. p53 can stimulate BAX activity both directly and through counteracting the activities of the anti-apoptotic proteins BCL-2 and BCL_{xl} to release BID (Mihara et al., 2003, Chipuk et al., 2004). As previously discussed, p53 directly interacts with BAK disrupting the inhibitory interaction of BAK with MCL-1 and stimulating the N-terminal conformational change required for its oligomerisation (Leu et al., 2004, Pietsch et al., 2008a).

The p53 homologues, p63 and p73, share p53 functional domains and can compensate for some p53 activities in the absence of p53 (Stiewe and Putzer, 2000). Unlike p53, they have several isoforms and play a greater role in development. Some isoforms bind p53 response elements and subsequently their over-expression induces apoptosis and upregulates p53 target genes (Moll et al., 2001). However some isoforms lack the N-terminal transactivation domain (ΔNp73 and ΔNp63). These act in a dominant negative manner to abrogate the pro-apoptotic effects of p53 through direct binding of p53 or p53 response elements without activation (Murray-Zmijewski et al., 2006). p73 and p63 act as tumour suppressors, in cancers mutations in the proteins are rarely detected, however alterations in expression patterns, such as upregulation of N-terminal truncations, are observed (Pietsch et al., 2008b).

1.3 Non Melanoma Skin Cancer

NMSC is the most commonly diagnosed cancer in Caucasians. There are approximately 100,000 new cases each year in the UK. There are several different types of NMSC. The most common two are basal cell carcinoma (BCC; approximately 75% of NMSC cases) and squamous cell carcinoma (SCC; approximately 20% of NMSC diagnosed). Much rarer are Merkel cell carcinoma, most cases of which are associated with polyoma virus infection (Feng et al., 2008), Kaposi's sarcoma (often associated with HIV infection) and T cell lymphoma of the

skin. Focus will be given to SCC as these have been associated with HPV infection (discussed in chapter 1.4.2).

Basal cell carcinomas arise from the basal cells of the skin. They are slow growing, appear to have no precursor lesion and rarely metastasise. However, once an individual has developed one BCC they have an increased risk of developing additional BCC (Marcil and Stern, 2000). SCC arise from keratinocytes immediately superficial to basal cells and are cancers preceded by actinic keratoses (premalignant rough, thickened patches of skin). As for BCC, development of SCC predisposes to the development of further NMSC (Karagas et al., 1992). Some SCC may metastasise to other strata of the epidermis, less than 5% metastasise to lymph nodes however metastasis can be higher (upto 20% of cases) where one or more other risk factors are present: the lesion is large, deeply invasive, has vascularisation or the individual is immunosupressed (Veness, 2007).

Removal of BCC or SCC by surgery is usually the most successful course of action, and in a large number of cases, this is usually sufficient. If surgery is unsuitable or results in incomplete removal radiotherapy is used. Chemotherapy, photodynamic therapy or immunotherapy may also be used. Treatment of BCC and SCC is often successful, resulting in low mortality. However NMSC has a high morbidity owing to invasion of surrounding tissue and resultant damage from treatment. Subsequently treatment of BCC and SCC is a large burden on healthcare resources – the cost of care for NMSC in America is the 5th highest for all cancers (Housman et al., 2003, Nguyen and Ho, 2002). In England it is estimated that each case of NMSC costs the National Health Service approximately £1,000 (Morris et al., 2009, Vallejo-Torres et al., 2011).

Whilst genetic predisposition (Welsh et al., 2011), immunological status (DePry et al., 2011, Kovach and Stasko, 2009), environmental factors (such as exposure to chemical carcinogens) and infection by HPV may have contributing roles, the main aetiological cause of NMSC is the resultant DNA damage from prolonged exposure to ultraviolet light (UV). This is evidenced by an increased incidence of NMSC in

countries with higher UV indices, as well as higher levels of NMSC on sun-exposed body sites (backs of hands, face, neck and forearms). Differences in the densities of BCC and SCC at some locations have been noted: higher density of SCC on backs of hands compared to BCC suggesting a dose dependency for the differing types of cancer or differing susceptibilities to UV according to the differing nature of skin at different body sites (Armstrong and Kricker, 2001, van Dam et al., 1999, Rosso et al., 1996). BCC and SCC often occur in older people (over 50) and more commonly in men than women (due to a greater number of outdoor occupations) however they are presenting in younger females due to sunbed use (Wehner et al., 2012).

1.3.1 UV-induced DNA Damage and Repair

The skin has a very high exposure to terrestrial UV light. UV light has a wide spectrum that can be subdivided according to the range of the spectrum. The sun emits UVA (320 to 400 nm), B (290 to 320nm) and C (100 to 290nm). UVC is completely absorbed by stratospheric oxygen, ie. ozone. UVA penetrates into the deep layers of the skin and is therefore harmful to the basal layer keratinocytes. UVA is able to indirectly stimulate DNA damage in the form of single strand breaks via the formation of free radicals and reactive oxygen species as well as exhibiting immunosuppressive effects (Halliday et al., 2011, Cadet and Douki, 2011). Whilst UVB comprises only 5% of terrestrial UV, it permeates the epidermis and is particularly carcinogenic as, like UVA, it is able to oxidise DNA bases but is also able to directly induce new bonds between DNA bases, the repair of which is error-prone, leading to mutation in both mitochondrial and genomic DNA. These mutations are specific to UVB exposure and therefore UVB irradiation of DNA leaves a ‘signature’. Specifically, these mutations are C→T transitions at dipyrimidine sites and can include double CC→TT base changes.

Approximately 75% of UV-induced DNA lesions are in the form of cyclobutane pyrimidine dimers (CPD) and the remaining 25% are pyrimidine 6,4 photoproducts (6,4PPs) which result in covalent linkages between adjacent pyrimidine bases

The image originally presented here cannot be made freely available via ORA because of copyright. The original image can be sourced using the reference given below.

Figure 1.6 Formation of pyrimidine dimers upon UVB irradiation

Cyclobutane pyrimidine dimers are created by the formation of cyclobutane rings between the 5,6 bonds of two adjacent pyrimidine bases (thymine, cytosine or 5-methylcytosine) whilst 6,4 photoproducts result from bond rearrangement to result in a bond between position 6 and 4 of two adjacent pyrimidine bases.

Adapted from Li et al. (2006)

(Pfeifer and Besaratinia, 2012, Sinha and Hader, 2002). The structure of these lesions is shown in Figure 1.6. CPDs are created by the formation of cyclobutane rings between the 5,6 bonds of two adjacent pyrimidine bases (thymine, cytosine or 5-methylcytosine) whilst 6,4PPs arise from bond rearrangement to result in a bond between position 6 and 4 of two adjacent pyrimidine bases. These lesions alter DNA structure to prevent accurate base pairing during DNA replication and subsequently, if left unrepaired, become mutagenic. Although 6,4PPs have a greater ability to block DNA replication and transcription than CPDs (Batista et al., 2009), CPDs are considered to be much more mutagenic than 6,4PPs as they occur at much higher frequencies and have slower repair kinetics (Besaratinia et al., 2008).

In response to DNA damage cells initiate the DDR which, upon detection of DNA damage, can delay cell cycle progression, initiate repair mechanisms or induce the damaged cell to undergo apoptosis depending on the extent of the damage. Failure of the DDR may lead to the survival of genomically unstable cells. The DDR may be co-ordinated by p53, the 'guardian of the genome'. p53 is transcriptionally upregulated in response to UVB exposure (Dai and Gu, 2010) and co-ordinates a global cellular response to DNA damage (Lane, 1992). It can also stimulate the Nucleotide Excision Repair (NER) pathway.

The NER pathway is used to repair DNA lesions such as 6,4PPs and CPDs by resection of an approximately 30 base oligonucleotide, inducing single stranded DNA and repair by polymerases. If NER fails a single strand or double strand break maybe generated, activating the DNA damage signalling proteins ATM and ATR and other downstream repair pathways dependent on the cell cycle stage (Branzei and Foiani, 2008). The importance of NER in pyrimidine dimer repair and their contribution to skin cancer is highlighted by individuals with rare genetic defects such as xeroderma pigmentosum (XP). XP is characterised by mutation in one of 7 genes (*XPA-G*) coding for NER proteins and individuals exhibit hypersensitivity to UV light with a significantly increased incidence of all skin cancers (Cleaver, 2000).

1.3.2 Apoptosis and UV in Keratinocytes

Exposure of the skin to UV induces the formation of sunburn cells – apoptotic keratinocytes, predominantly in the basal layer (Qin et al., 2002). It has been shown that this apoptotic response is mediated by UV-induced DNA damage since introduction of the bacteria-derived DNA repair enzyme photolyase into a human keratinocyte cell line (HeLa cells) could abrogate cellular morphological changes associated with UV exposure (Stege et al., 2000, Kulms et al., 1999). Furthermore, Chinese Hamster Ovary cells deficient in NER are hypersensitive to UVC induced apoptosis (Dunkern et al., 2001) suggesting that the unresolved UV-induced DNA damage discussed in chapter 1.3.1 can stimulate the apoptosis pathway.

The execution of the apoptotic cascade in response to UV-induced DNA damage can, in part, be attributed to the activity of p53. In a p53-dependent manner, exposure to UV irradiation arrests cells in G1 to allow repair of damaged DNA prior to synthesis (Campbell et al., 1993). In the event of repair failure, p53 stimulates the cell to undergo apoptosis. p53 knock-out mice have significantly fewer sunburn cells and increased susceptibility to skin cancer compared to wild type counterparts (Jiang et al., 1999, Ziegler et al., 1994) highlighting the importance of p53 in UV-induced keratinocyte apoptosis and skin cancer prevention in mice.

However, in NMSC, the p53 gene (*TP53*) appears to be sensitive to UVB induced mutagenesis, exhibiting the UVB induced mutagenesis fingerprint C→T and CC→TT transitions. The p53 gene is known to have a number of DNA mutation hotspots (sites particularly sensitive to DNA damage), such as highly methylated CpG sites which are associated with C→T base changes (Pfeifer and Besaratinia, 2012, Pfeifer, 2000). Consequently p53 is found to be mutated and inactivated in at least 50% of human NMSC (Kraemer, 1997, Pfeifer and Besaratinia, 2012, Brash et al., 1991). Mutations in the p53 gene isolated from skin cancers often occur in the p53 DNA binding domain or introduce a premature stop codon (Ziegler et al., 1993, Giglia-Mari and Sarasin, 2003). Cells with p53 mutations may clonally expand to form ‘p53 patches’ in skin (Ziegler et al., 1994, Jonason et al., 1996). However the

contribution of p53 mutation to the progression of NMSC is unsure since p53 patches are found in healthy skin, have a morphologically normal appearance and exhibit very little, if any, pre-cancerous potential (Ren et al., 1996, Ren et al., 1997, Jonason et al., 1996). In addition, Li–Fraumeni patients, who have germline mutation of the p53 gene, have an increased risk of developing any soft tissue cancer with the exception of NMSC (Lustbader et al., 1992).

Tumourigenesis arising from cells with p53 mutations may be prevented by p53-independent apoptosis mechanisms, such as DNA damage induced activation of the intrinsic apoptosis pathway (Polager and Ginsberg, 2009). It has also been demonstrated that UVB can directly stimulate apoptosis at the cell membrane: through activation of the Fas death receptor in the absence of its ligand (FasL; Aragane et al., 1998). Expression of Fas and FasL can be induced in response to UVB and mice lacking active FasL have a reduced number of apoptotic keratinocytes and increased frequency of p53 mutation (Hill et al., 1999). Blocking of TNFα also partially inhibits UV-induced apoptosis (Schwarz et al., 1995) emphasising the importance of UV-induced extrinsic apoptosis pathway activation in keratinocytes in the event of p53 loss. Consequently both the DNA damage and death receptor response is required for efficient execution of apoptosis in response to UV (Kulms et al., 1999).

1.4 Human Papillomavirus

Papillomaviridae are a family of viruses which infect the epithelia of vertebrates. They are small double stranded DNA viruses and have a circular genome of ~8kb. Papillomaviruses have been classified into 29 genera according to homology of the gene encoding the L1 capsid protein (Figure 1.7). Papillomaviruses may infect a range of animals including reptiles, birds and bovids. The Alpha, Beta, Gamma, Mu and Nu genera papillomaviruses infect humans and these groups comprise approximately 120 types of papillomaviruses (Bernard et al., 2010). These HPV types infect the keratinocyte cells of mucosal and cutaneous epithelial tissues in

The image originally presented here cannot be made freely available via ORA because of copyright. The original image can be sourced using the reference given below.

Figure 1.7 Papillomavirus phylogenetic tree

The different papillomavirus groups are based on homology in the L1 gene nucleotide sequence of 189 human and animal papillomaviruses. Only the human papillomavirus types are shown here. Genus α papillomaviruses consists of both mucosal and cutaneous types. The β-, μ-, η- and γ-papillomavirus genera comprise human cutaneous types. β-genus papillomaviruses were previously referred to as EV types.

Adapted from Doorbar et al. (2012)

humans including those of the anogenital and oropharyngeal regions and skin to cause hyperproliferative lesions.

The μ-, η- and γ-HPV infect cutaneous tissues and are only rarely associated with cancer. The α-genus is the largest and comprises HPV infecting cutaneous and mucosal tissues which can be designated as high or low-risk depending on the probability of the lesion progressing to malignancy. The genus-α species 10 (α10) HPV6 and 11 are classified as low-risk mucosal HPV as infection results in benign hyperproliferative lesions which rarely progress to malignancy. α4 HPV2 and 57 are low-risk cutaneous HPV types associated with common warts. The high-risk mucosal HPV16 and 18 (α9 and 7 respectively) are established causative agents of the anogenital and cervical cancers, identified in ~70% of cervical cancers. HPV types from these same species have also been identified as carcinogenic in humans (including HPV31, 35, 58 and 59), consequently high-risk HPV have been identified in 99.7% of malignant cervical cancers worldwide (Walboomers et al., 1999, Munoz, 2000). The β-HPV have been linked to development of NMSC and are discussed further in chapter 1.4.2.

1.4.1 Cancer and α-HPV Epidemiology

HPV is transmitted by contact and, in the case of anogenital HPV, behaves as a sexually transmitted infection. The high-risk α-HPV are associated with cervical, vaginal, vulvar, and penile cancers (Watson et al., 2008), as well as there being a general trend towards an increasing incidence of HPV-associated head and neck cancers (Auluck et al., 2010, Chaturvedi et al., 2011, Furniss et al., 2007).

HPV has been identified as a necessary agent for the development of cervical cancer (Munoz, 2000). Cervical cancer is the 11th most commonly diagnosed cancer in women in the UK, and incidence and death appear to have declined over the past 40 years as a result of early diagnosis through Papanicolaou cervical smear screening (CRUK, 2010). However, HPV infection continues to play a large role in the causation of cancers in developing countries. This is highlighted in Table 1.1

The table originally presented here cannot be made freely available via ORA because of copyright. The original table can be sourced using the reference given below.

Table 1.1 Cancers attributable to infection with oncogenic HPV in developed and developing countries

The number of cases of cancer at the indicated sites and the number of those which are attributable to infection by oncogenic HPV (HPV16, 18, 31, 33, 35, 39, 45, 51, 52, 56, 58, 59 or 66), in the year 2002, are shown according to developed and developing countries.

AF; attributable fraction (fraction of the total number of cancers at a specific site associated with oncogenic HPV infection).

Adapted from Parkin (2006)

which shows that the percentage of all cancers attributable to HPV infection in developing countries is 7.7 whilst in developed countries this is only 2.2.

Lesions infected with α-HPV types 6, 11, 44 (α10); 40, 43 (α8); 42 (α1); 61, 72, 81 (α3) are associated with a low-risk for malignant progression (Munoz et al., 2003) where 90% of genital wart cases are attributable to infection with HPV6 and 11 (Castellsague, 2008).

HPV 51 (α5); 56, 66 (α6); 18, 39, 45, 59 (α7); 16, 31, 33, 35, 52, and 58 (α9) are classified as carcinogenic by the International Agency for Research on Cancer (Cogliano et al., 2005). HPV16 and 18 are most frequently detected in malignant lesions (Clifford et al., 2003, Munoz et al., 2004); approximately 50% of penile, vulvar and vaginal cancers (Watson et al., 2008) and HPV16 is detected in 50% of oropharyngeal cancers in America (Jayaprakash et al., 2011). However, HPV types tend to be transmitted together meaning several different HPV types can be identified in lesions (Schiffman et al., 2007).

Cervical intraepithelial neoplasia (CIN), the abnormal growth of squamous cells on the cervix, is a precursor for possible malignant transformation and is graded 1-3 according to severity (Schiffman et al., 2007). Fifty percent of CIN3 are caused by HPV16 and 18 (Smith et al., 2007b). Forty percent of CIN2 naturally regress over two years (Moscicki et al., 2010) however, the propensity to do this may be HPV type dependent. HPV16, 18 and 45 infected lesions show a lower likelihood of regression (Clifford et al., 2003, Castle et al., 2009). CIN regression may be the result of immune clearance of the virus (Kadish et al., 2002, Hopfl et al., 2000) and invasive cervical carcinoma may arise upon persistent HPV infection and viral protein expression, in part, through viral genome integration into that of the host cell. This is supported by an increased risk of anogenital HPV infection in immunosupressed individuals, such as those with human immunodeficiency virus (HIV; Ahdieh et al., 2000), and the observation that higher infection rates are observed in younger women, yet longer viral persistence and neoplasia is observed in older women (Ho et al., 1998).

1.4.2 NMSC and β-HPV

β-genus HPV have a cutaneous tropism and, analogous to the α-HPV, some are considered as potentially high-risk due to their isolation in SCC lesions. Specifically, these are HPV from the β1 and β2 species and include HPV 5, 8, 9, 12, 14, 15, 17, 19-25, 36-38, 47, and 50.

1.4.2.1 Epidermodysplasia Verruciformis

A link between β-HPV infection and NMSC was first postulated through studies of *Epidermodysplasia verruciformis* (EV) individuals who are predisposed to infection with the β-HPV identified above (originally termed EV-HPV types; Majewski and Jablonska, 1995) and the development of NMSC lesions (Orth et al., 1978). Seventy-five percent of EV individuals have mutations in either the EVER1 or EVER2 genes (Ramoz et al., 2002) and exhibit immune defects. The contribution of loss of these genes to pathogenesis remains to be elucidated with hypotheses including a role in HPV infection in keratinocytes, the immune response and zinc regulation (Majewski and Jablonska, 1995, Lazarczyk et al., 2008).

An association between sun exposure and NMSC progression in EV individuals has been noted. Approximately 30-70% of EV individuals develop SCC at sun-exposed sites starting as early as the age of 20. These lesions have been found to contain the DNA of common, low-risk α-HPV which, in the normal population, cause benign warts (such as HPV types 3 and 10) as well as β-HPV (de Villiers et al., 2004). β-types HPV5 and 8 have been identified in 90% of SCC from EV patients suggesting these carry the highest risk for malignant progression (Orth, 1986).

1.4.2.2 HPV Infection in the Immune Suppressed Population

As EV individuals show defects in cell-mediated immunity, susceptibility to HPV infection and NMSC development, it is noteworthy then that there is also an increased incidence of NMSC correlating with β-HPV infection and sun exposure in both the iatrogenically immune suppressed population (such as organ transplant recipients) and individuals with HIV. However, whilst individuals with HIV have a 3-fold increased incidence of NMSC compared to the immunocompetent population,

it is still 10-fold less than that of organ transplant recipients (Clifford et al., 2005). Whilst β-HPV have been identified in organ transplant recipients with and without a history of skin cancer (Proby et al., 2011), organ transplant recipients have an approximately 200-fold increased risk of SCC development compared to the immunocompetent population (Stockfleth et al., 2001, Hartevelt et al., 1990). Furthermore, SCC are more common than BCC in the immunocompromised population, in contrast to the immune competent population where BCC are more prevalent (Moloney et al., 2006, Pfister et al., 2003). In countries with higher UV indices, such as Australia, 70% of organ transplant recipients develop NMSC (Bouwes Bavinck et al., 1996), whilst approximately 40% of organ transplant recipients in countries with lower UV indices, such as the UK and Netherlands, develop NMSC (Wisgerhof et al., 2010), supporting a role for the virus as a co-factor with UV.

β-HPV DNA has been identified in 84% of SCC and 75% of BCC in iatrogenically immune suppressed individuals (Harwood et al., 2000). Like α-HPV, multiple cutaneous HPV are detected in single tumours from transplant recipients (Harwood et al., 2000), making epidemiological associations between specific HPV and malignancy difficult to delineate. However β-HPV associated with greatest risk for malignancy, such as HPV5, have been identified in the centre of a carcinoma, whilst other HPV types have been identified surrounding it (Pfister et al., 1983). Furthermore, the range of β-HPV identified in iatrogenically immune suppressed individuals is more diverse than that in EV individuals (Harwood et al., 1999), however a significant association between the concordant detection of both seropositivity and DNA for at least one type of β-HPV DNA in SCC has been noted (Proby et al., 2011). This study also noted a borderline significant association between SCC and infection with HPV5, 9, 24 and 36.

1.4.2.3 Immunocompetent Population

A link between HPV infection and skin disorder has been identified in the immunocompetent population (Iftner et al., 2003). In this study HPV DNA was

detected in 90% of benign warts and 60% of SCC in immunocompetent individuals. The identification of high-risk mucosal HPV type DNA (HPV16, 31, 35, 51) in lesions correlated with an increased risk of NMSC, suggesting that infection with high-risk mucosal HPV may have a role in the development of NMSC in the immunocompetent population (Iftner et al., 2003).

The DNA of β-HPV has also been detected in NMSC in the immunocompetent population (Masini et al., 2003, Bouwes Bavinck et al., 2010). β-HPV DNA has been identified in 50% of SCC in immunocompetent individuals (Asgari et al., 2008) whilst seropositivity to β-HPV, especially HPV5, 8 and 20 is also associated with risk of SCC (Karagas et al., 2006, Feltkamp et al., 2003). The highest risk for SCC is associated with infection by multiple HPV types. Individuals with tumours at sun-exposed sites were also found more likely to be seropositive for β-HPV types than individuals with SCC at other anatomic sites (Karagas et al., 2006). This correlates with a poor tanning ability, supporting a sun exposure component (Shamanin et al., 1996, Iannacone et al., 2012). Increased sun exposure appears to correlate with an increase in cutaneous HPV infection (Chen et al., 2008), possibly through UV-induced immune suppression (Ullrich, 2005).

The correlation between infection with β-HPV and BCC formation is less clear than that for β-HPV and SCC (Iftner et al., 2009): seropositivity to β-HPV and BCC formation did not show significant association (Karagas et al., 2006). Nevertheless HPV DNA (both α- and β-types) has been detected in approximately 37% of BCC in the immunocompetent population (Harwood et al., 2000).

Such discrepancies as to the presence of HPV in NMSC may be the result of differences in sampling sites and techniques. Hair follicles, biopsies from lesions, perilesional sites and normal skin are analysed for HPV DNA, however the prevalence and types may vary site to site for a single individual (Iftner et al., 2009). Whilst some groups investigate seropositivity and seroreactivity to viral proteins, others use PCR to detect viral DNA, however within these studies, variation in primers and PCR sensitivities may occur.

Doubts as to the role of β-HPV in the development of NMSC have been raised. These doubts arise from studies in which β-HPV can be detected in healthy skin showing no signs of pre-malignancy in the immunocompetent population (Alotaibi et al., 2006, Antonsson et al., 2003, Antonsson et al., 2000, Astori et al., 1998). Furthermore, β-HPV DNA is not ubiquitously detected in all NMSC and β-HPV DNA does not appear to persist in SCC: higher viral loads are detected in actinic keratoses compared to SCC (Pfister et al., 2003, Weissenborn et al., 2005). In addition, anogenital carcinomas contain at least one copy of the viral genome per cell and are detected in almost all cervical cancers whilst, in cutaneous cancers, HPV DNA is present in only 1 in 20-5000 cells (Weissenborn et al., 2005).

However these results may be interpreted so as to support a role for HPV in the early stages of cutaneous malignancy if the model does not require continued HPV infection, in contrast to anogenital malignancy. Considering the differences in viral proteins between α- and β-HPV (discussed in chapter 1.4.5) and the different tropisms of HPV from differing genera it is predicted that they may have diverse roles in the progression of malignancy.

It has been proposed that β-HPV have a 'hit and run' role in the early stages of the development of cancer. In this model, HPV infects a keratinocyte basal cell and, via expression of the oncogenic viral E6 and E7 proteins (chapters 1.4.5.4 and 1.4.5.5), alters the cell phenotype. Expression of the E6 protein inhibits apoptosis and DNA damage repair in response to UV whilst E7 expression drives increased cell proliferation, leading to increased genomic instability and loss of differentiation. Consequently, a cancer stem cell (Egawa, 2003) is formed which clonally expands as surrounding cells, competent for apoptosis, die. As the rate of keratinocyte proliferation increases, the viral genome is lost. This would present a contrasting model for the contribution of β-HPV to malignancy to that of the high-risk anogenital α-HPV where maintenance of E6 and E7 oncogene expression is required for continued tumourigenesis (Borgogna et al., 2012, Doorbar et al., 2012).

1.4.3 HPV Life Cycle

The HPV life cycle is tightly linked to the epithelial cell differentiation programme, infecting stem-like basal cells to maintain viral genomic DNA and using terminally differentiated cells to produce virion progeny (summarised in Figure 1.8).

It is thought that the virus must first infect the dividing basal cells of the epidermis in order to initiate viral replication and maintain infection, given the epidermal cell turnover. In order for the virus to reach these cells in the basal layers of the epidermis wounding must occur. Little is known as to the receptor for HPV and mechanism of entry but it has been hypothesised that virions reach the basal membrane through micro-abrasions, where it is believed they attach to the heparan sulphate proteoglycan and laminin 5 (Culp et al., 2006, Kines et al., 2009). As cells move during wound healing the virus transfers to α_6-integrin and heparan-sulphonated proteoglycans (Shafti-Keramat et al., 2003, Evander et al., 1997) on the keratinocyte surface and subsequently enters the cell by both clathrin or cavelolin dependent and independent mechanisms dependent upon the HPV type (Smith et al., 2007a, Day et al., 2003, Spoden et al., 2008, Bousarghin et al., 2003).

Upon entry into the cell the virus uncoats and the viral genomic DNA is transported to the nucleus in complex with the L2 capsid protein via the nexin 17 adaptor protein to facilitate endosomal escape (Bergant Marusic et al., 2012). The viral genome encodes eight proteins. The 'Early proteins' E1, E2, E4, E5 (not present in β-type HPV genomes), E6 and E7 and the 'late' proteins L1 and L2 (named according to the stage of the viral life cycle at which they are produced). Upon binding of cellular transcription factors to the promoter/enhancer region the E1 and E2 proteins are expressed at low level. Binding of cell specific transcription factors and cell specific control of the HPV non-coding region (NCR) may determine HPV tropism (Sen et al., 2004, Ottinger et al., 2009).

E1 is a DNA helicase/ATPase required for viral genome replication. E2, at low expression levels and its full length, is a transcription factor which promotes

The image originally presented here cannot be made freely available via ORA because of copyright. The original image can be sourced using the reference given below.

Figure 1.8 Comparison of the structure of uninfected and HPV-infected epithelium during the viral life cycle

HPV infect the basal keratinocytes when exposed through wounding. Upon infection viral genomes are replicated in the lower strata of the skin. As cells differentiate, the expression of the E6 and E7 proteins maintains keratinocytes, which would have exited the cell cycle, in a replicative state to promote viral amplification and preventing the formation of the protective granular and cornified strata. Newly synthesised viral particles are shed from the upper layers of the epithelium.

Adapted from Moody and Laimins (2010)

transcription of the viral early promoter. The viral genome is episomally amplified to 50-100 copies per cell in the non-productive, latent phase of the life cycle. Activation of the ATM and ATR DDR proteins upon viral protein expression, and the recruitment of repair proteins to the viral genome may be important for genome amplification (Reinson et al., 2012, Moody and Laimins, 2009, Gillespie et al., 2012).

As the basal cells detach from the basement membrane the oncoproteins E6 and E7 are expressed, stimulating the infected cells to enter into the cell cycle, overriding the cell cycle arrest associated with the onset of terminal differentiation and abrogating apoptotic responses. This results in an acceleration of the host cell life cycle required for that of the virus, promotion of the distribution of viral episomes so that a greater cell number amplify the viral genome and activation of the host cell DNA replication machinery required for amplification of the viral genome.

Little is known about the functions of the E4 and E5 proteins but they may be involved in genome amplification in the upper layers of epidermis (Peh et al., 2004, Genther et al., 2003). The L1 and L2 genes are activated during the later stages of the viral life cycle during host cell terminal differentiation. L1 and L2 encode major and minor capsid proteins respectively, which package the new viral genomes. Release of viral progeny occurs as the terminally differentiated host cells slough off, the non-lytic nature of the HPV infection meaning it escapes the host inflammatory response and immune surveillance.

Upon prolonged infection with high-risk α-HPV malignancy arises as a consequence of deviation from the ‘normal’ productive viral life cycle. The productive viral life cycle is dependent upon epidermal differentiation, therefore expression of the E6 and E7 proteins is normally balanced to promote a replicative environment whilst allowing completion of the productive life cycle. However, in malignancy, viral genome integration into that of the host cells has been observed (Arias-Pulido et al., 2006). Integration often leads to dysregulation of E2-mediated repression of the E6 and E7 promoter, leading to constitutive E6 and E7 expression, cell immortalisation and the

promotion of malignancy. Reintroduction of E2 represses E6 and E7 after integration and restores cellular control (Dowhanick et al., 1995, Francis et al., 2000).

1.4.4 HPV Genome Structure

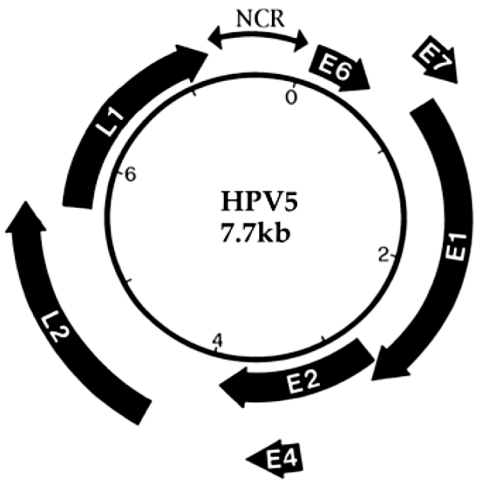
HPV are non-enveloped, icosahedral particles made up of 72 capsomers formed from the L1 and L2 capsid proteins which encloses the viral DNA (Modis et al., 2002).

The viral genome is circular and approximately 8,000 base pairs. The genome transcripts are polycistronic and contain two or more overlapping open reading frames meaning alternate splicing is required for gene expression. The genome can be divided into three sections: Early, Late and NCR. The Early region comprises approximately 50% of the genome and encodes the E1, E2, E4, E5, E6 and E7 genes. The Late region lies downstream of the Early region and encodes the L1 and L2 gene open reading frames. The NCR includes the origin of replication and transcription binding sites important for the regulation of HPV genome transcription. Whilst the genomes of α- and β-HPV are similar, the β-type HPV genomes do not encode the E5 gene, shown in Figure 1.9.

Figure 1.9 Genome organisation of β-HPV

The β-HPV genome comprises the early genes; E1, E2, E4 and E6 and the late genes; L1 and L2 which encode the viral capsid proteins.

The β-genus HPV genomes lack the gene coding for the E5 protein found in α-HPV genomes. NCR; non-coding region.



1.4.5 Virus-Encoded Proteins

The α- and β-HPV have similar genomes and encode similar proteins, with the exception of the α-HPV-only E5 protein. Overall, the same proteins encoded by different genera of HPV have the same function: the E1 and E2 proteins drive viral replication, E4 and E5 promote the later stages of the viral life cycle, E7 maintains a replicative cell state and E6 abrogates the cellular apoptotic response. However, as discussed below, the same proteins from HPV of different genera are structurally similar but vary in their surface charge and therefore interact with distinct proteins in order to disrupt the normal cellular environment. This may explain different tissue tropisms and risks for malignancy associated with different HPV.

1.4.5.1 L1 and L2

The L1 and L2 proteins are the viral capsid proteins required for new viral progeny assembly before shedding. L1/L2 transcription occurs only in differentiated cells due to the differentiation dependence of the HPV late promoter (Ozbun and Meyers, 1997).

The viral capsid is assembled from 72 pentameric capsomeres (each comprised of 5 L1 monomers) and 12 L2 minor capsid proteins. The L1 protein can assemble into viral capsids in the absence of the L2 protein but it is believed that L2 increases the efficiency of assembly (Stauffer et al., 1998, Zhou et al., 1993). L2 may also accumulate at promyelocytic leukaemia nuclear bodies, thought to be the site of virus replication (Swindle et al., 1999), to recruit the L1 protein (Spoden et al., 2008). L2 is also required for viral DNA escape from endosomes after uncoating upon cell entry (Kamper et al., 2006).

The L1 protein can bind keratinocyte cell surface proteins which may mediate transfer of viral particles from the ECM to the cell surface (Joyce et al., 1999). L1 alone can self assemble into virus like particles, is highly immunogenic (Kirnbauer et al., 1992) and, along with E1, is the most highly conserved protein across different virus types (Bernard et al., 2010). Subsequently the L1 protein forms the immunogen for the preventative HPV vaccines currently available. Gardasil is a

quadrivalent vaccine based on the L1 protein synthesised in yeast, protecting from the benign genital wart causing HPV6 and 11 as well as the high-risk mucosal HPV16 and 18, the causative agent in cervical cancers (previously discussed in chapter 1.4.1). Cervarix is a bivalent vaccine for which the HPV 16 and 18 L1 protein have been synthesised from insect cells. Implementation of the HPV vaccination programme will reduce the HPV associated healthcare, morbidity and mortality burden (Villa, 2011, Frazer et al., 2011).

1.4.5.2 E1 and E2

The E1 and E2 proteins are required in the basal layer of the epidermis to maintain the viral genome at low copy numbers and are involved in viral replication and partitioning of the viral genome between daughter cells. Together they recruit cellular factors to promote bidirectional replication of viral DNA.

The E1 protein is an ATP-dependent helicase (Hughes and Romanos, 1993) which initiates replication by binding to the viral origin of replication and unwinding the viral DNA. Recruitment of E1 to the origin is not an efficient process, however binding of the E2 protein to these sites results in cooperative binding of E1. E1 is a phospho-nuclear protein of 600-650 amino acids consisting of a N-terminal domain containing a nuclear import and export signal, a DNA sequence specific binding site, an oligomerisation domain and a helicase domain. The oligomerisation domain allows a double hexameric E1 ring to form around DNA to facilitate helicase activity (Wilson et al., 2002). As the helicase domain of E1 binds to the transcription activation domain of E2, dissociation of E2 from E1 after recruitment to the origin occurs. Efficient viral genome replication initiation by E1 requires interaction with the cell cycle replication factors cyclinA/E-cdk2 (Ma et al., 1999) and DNA replication machinery including Topoisomerase I and II, the DNA polymerase α-primase complex and replication protein A (Melendy et al., 1995, Kuo et al., 1994).

Viral integration may be mediated by the viral E1 protein which can bind DNA, and induce the DDR through double strand breaks (Fradet-Turcotte et al., 2011,

Sakakibara et al., 2011) resulting in recombinant integration as well as general genomic instability of HPV-infected cells (Kadaja et al., 2009).

The E2 protein is composed of approximately 360 amino acids and includes a transcription activation domain and DNA binding domain. The E2 protein, along with E1, is required for initiation of viral genome replication however, unlike E1, E2 is also required for the maintenance of replication. The E2 protein of β-genus HPV can also repress transcription of β-integrins (Oldak et al., 2004, Oldak et al., 2010), reducing keratinocyte adhesion to promote keratinocyte differentiation and viral amplification.

High and low-risk α-HPV E2 proteins bind the viral NCR at four highly conserved E2 binding sites. It is believed that this sterically hinders binding of cellular transcription factors such as Sp1 and TBP to these regions to therefore control the HPV genome early region promoter by repression (Dostatni et al., 1991, Dong et al., 1994, Hou et al., 2002). E2 can also recruit transcriptional repressors such as Brd4 (Wu et al., 2006).

Under low E2 expression levels, the E2 protein may promote weak activation of the HPV NCR promoter (Bouvard et al., 1994, Steger and Corbach, 1997). E2 interacts with basal transcription factors which may be required for E2 transcriptional activities (Rank and Lambert, 1995) as well as transcription co-factors such as p300/CBP (Lee et al., 2000a) and the histone acetyl transferase NuA4/TIP60 (Smith et al., 2010).

As well as genome replication, the Bovine papillomavirus 1 (BPV1) and HPV16 E2 proteins ensure equal segregation of the viral genome between daughter cells by acting as an adapter to tether viral genomes to host chromosomes via binding of Brd4, a protein associated with mitotic chromosomes (You et al., 2004, Bastien and McBride, 2000).

The E2 protein normally represses transcription of the E6 and E7 oncogenes (Baker et al., 1987). Integration of the cervical α-HPV genome into that of the host often disrupts the E2 open reading frame and therefore leads to the loss of E2 protein

expression. In episomally maintained HPV genomes, methylation of the HPV genome may occur, inhibiting binding of the E2 protein to DNA binding sequences (Thain et al., 1996, Kim et al., 2003). Consequently, loss of E2 protein activity by either of these mechanisms may lead to over-expression of the HPV oncogenes.

1.4.5.3 E4 and E5

The E4 and E5 proteins are believed to be involved in the later stages of the HPV life cycle and infection.

The E4 protein is synthesised as a fusion protein with part of the E1 protein (E1^E4). Recently it has also been identified as a fusion with 12 amino acids of E2, rather than the five amino acids of E1 (Tan et al., 2012a). As little is known about the function of the E2^E4 fusion, E1^E4 will be discussed here.

E1^E4 is expressed at low levels in early infection but becomes the most predominant viral product in late infection (Fang et al., 2006). E1^E4 is believed to be required for virus life cycle completion since deletion from the viral genome of HPV16, 18 and 31 leads to a defective life cycle via reduced genome amplification and loss of late viral gene expression (Nakahara et al., 2005, Wilson et al., 2005, Wilson et al., 2007).

HPV1 and 16 E1^E4 interacts with the cellular keratin network and, in the case of HPV16, results in disruption of the cellular keratin scaffolding (Doorbar et al., 1991, Roberts et al., 1993, McIntosh et al., 2010).

HPV1, 16 and 18 E1^E4 proteins can also modulate the cell cycle. These HPV E1^E4 proteins can bind and sequester the serine-arginine (SR)-specific protein kinase (SRPK1). This may affect SRPK1 activation and regulation of substrates which are linked to modulation of the cell cycle and RNA splicing (Bell et al., 2007). The HPV18 and HPV16 E1^E4 fusion proteins may also affect cell cycle regulation through induction of G2/M arrest which correlates with cytoplasmic cyclin-cdk sequestration. Though the purpose of this is not understood since HPV18 E1^E4 cyclin sequestration does not seem to contribute to the vegetative phase of the viral

life cycle for genome amplification and L1 protein production (Knight et al., 2011, Davy et al., 2006).

The E5 protein is only encoded by mucosal HPV genomes. The HPV16 E5 protein is 83 amino acids and it is a highly hydrophobic membrane bound protein. The function of the E5 protein is still ambiguous (possible activities have been reviewed in Venuti et al., 2011). However the E5 protein has the ability to oligomerise and localises to cellular membranes (such as the Endoplasmic Reticulum, Golgi apparatus and plasma membrane; Borzacchiello et al., 2010). The E5 protein has also recently been shown to exhibit channel-forming abilities, these data are consistent with the hypothesis that E5 may act as a viroporin to facilitate virion release (Wetherill et al., 2012).

Studies investigating HPV31 and HPV16 suggest that the E5 protein has a greater importance in the later stages of the HPV life cycle during genome amplification and gene transcription from the late promoter whilst maintaining cell mitosis following differentiation induced cell cycle arrest (Fehrmann et al., 2003, Genther et al., 2003). E5 may also subvert the immune response to viral infection (Suprynowicz et al., 2008, Gruener et al., 2007, Schapiro et al., 2000) and promote cell fusion (Hu and Ceresa, 2009, Hu et al., 2010).

The E5 protein has been shown to have transforming properties where E5 expression induced tumour formation (Leechanachai et al., 1992) and epithelial hyperproliferation, possibly through disruption of the proto-oncogene Epidermal Growth Factor Receptor (Genther Williams et al., 2005) and inhibition of both the intrinsic and extrinsic apoptosis pathways. E5-expressing cells have reduced levels of the cell surface FasL death receptor and compromised DISC formation upon receptor ligation (Kabsch and Alonso, 2002). Zhang et al. (2002) have shown that expression of the E5 protein protects keratinocytes from UV-induced apoptosis both through PI3K survival signalling and upregulation of the anti-apoptotic BCL-2 proteins. E5 can also degrade the pro-apoptotic effector protein BAX to protect from hydrogen peroxide stimulated death (Oh et al., 2010a).

1.4.5.4 E6

The E6 protein is approximately 18kDa and is one of the transforming proteins encoded by the HPV genome. It consists of two zinc binding domains formed by conservation of four CXXC motifs (Nomine et al., 2003) connected by a helical inter-domain linker and can self-associate through homodimerisation of the N-terminal zinc finger (Zanier et al., 2012). The high-risk HPV E6 mRNA exhibit splice variants encoding the first 42 or 44 amino acids of HPV16 E6 and HPV18 E6 respectively. The function of these splice variants (E6*) is currently ambiguous but may have a role in regulating the degradation of full-length E6 protein targets (Pim and Banks, 1999).

During HPV infection the E6 protein, along with E7, promotes proliferation of the infected cell population. As discussed below, E6 is able to contribute to cellular transformation in a number of ways but primarily, through abrogation of the apoptotic response to the transforming properties of the E7 protein (see chapter 1.4.5.5).

The HPV16 E6 protein has been detected in the nucleus and cytoplasm of cells (Masson et al., 2003, Vaeteewoottacharn et al., 2005). The E6 protein has no enzymatic activity and exerts its activity via binding to a large number of cellular substrates. The E6 proteins encoded by different HPV types have different physical and chemical properties, as exemplified by the differing surface charges: the surface charge of the high-risk cutaneous HPV5 E6 is more hydrophobic than the negatively charged surface of the high-risk mucosal HPV16 E6 protein (shown in Figure 1.10). This suggests the E6 proteins from the different HPV may have differing effects and interacting proteins (Nomine et al., 2006). Indeed, the E6 protein has been found to interact with many proteins (for review of E6 and E7 interacting proteins see Klingelhutz and Roman, 2012), the significance of only some of these interactions has been explored. The interactions of relevance here are summarised in Table 1.2.

Expression of the viral E7 protein drives the cells into unscheduled proliferation. The

Figure 1.10 Structure of the HPV E6 proteins

The image originally presented here cannot be made freely available via ORA because of copyright. The original image can be sourced using the reference given below.

Although the overall structure of the E6 proteins is conserved from different genera HPV, they vary in surface charge. The α-HPV E6 proteins are more polar whilst the β-genus E6 proteins have more hydrophobic amino acid residues on their surface to suggest that the same proteins encoded by different HPV may have differing interacting proteins. White; A, G, P, Green; R, K, H, Red; D, E, Yellow; N, Q, S, T, Purple; M, V, L, I, F, W, Y.

Adapted from Nominé et al. (2006)

normal cellular response to this is activation of the DDR and apoptosis, however the function of the E6 protein is to abrogate these responses. Expression of the E6 proteins can inhibit the DDR, not only through degradation of p53 (an activity, until recently, believed to be attributed to only certain high-risk α-HPV E6 proteins discussed in chapter 1.4.5.4.2) but also through p53 degradation independent mechanisms. The E6 proteins of HPV 1, 8 and 16 can directly bind the DNA repair protein XRCC1 to reduce the efficiency of single strand break repair (Iftner et al., 2002). Furthermore cells expressing HPV5 and 18 E6, but not that from HPV10 or 77 have a reduced ability to repair thymine dimers through degradation of p300 and the resultant decrease in the protein levels and activity of the DDR protein ATR (Wallace et al., 2012, Giampieri and Storey, 2004).

The β-HPV8, 17a and 38 E6 proteins can repress the Notch pathway to delay keratinocyte differentiation so that cells have suprabasal expression of integrins and

Table 1.2 HPV E6 protein activities which may contribute to malignancy

The E6 proteins from varying HPV types have different interacting proteins in order to disrupt host cell pathways. See text for further details.

Target	E6 types	Effect
p53	Predominantly high-risk α-HPV	Inhibit p53-mediated DDR, cell cycle arrest and apoptosis.
XRCC1	HPV1, 8, 16	Inhibit DNA Repair
p300	HPV5, 18, 16	Inhibit DDR and gene transcription
Mastermind 1	HPV8, 17, 38	Disrupts the Notch pathway required for cell differentiation
hTERT	HPV16	Increases cell lifespan
BAK	β-type HPV5, 8, 10, 20, 22, 38, 76, 92, and 96 α-type HPV16, 18, 77	Inhibit the intrinsic apoptosis pathway
BAX	High-risk α-HPV	
FADD	HPV16	Inhibit the extrinsic apoptosis pathway
Caspase-8	HPV16	
PDZ domain containing proteins	High-risk α-HPV with an ETQV/L motif	Disrupt cell polarity and adhesion. Such proteins include Scribble, the MAGI family, Dlg and MUPP1
E6AP	α-HPV	Used to target host cell substrates for degradation
Paxillin	BPV1 and HPV16	Disruption of focal adhesions
E6BP	High-risk α-HPV	Calcium binding protein
TSC2	High-risk α-HPV	Activation of mTOR signalling
MCM7	High and low-risk α-HPV	DNA replication
HIPK2	HPV23 and 38	Prevent p53 activation
TIP60	HPV8, 11, 16 and 18	Inhibit p53-dependent activation of apoptotic pathways

a basal keratinocyte phenotype. These E6 proteins can bind components of the Notch signalling pathway (Mastermind 1) to repress their activity and Notch transcriptional targets such as *hes1* and *hey1* (Tan et al., 2012b, Brimer et al., 2012). Loss of Notch signalling has been identified in skin, head and neck SCC (Agrawal et al., 2011, Stransky et al., 2011). Furthermore, loss of Notch signalling in response to UV radiation has been associated with tumour formation in the epidermis (Hu et al., 2012).

α-HPV, along with some β-HPV, E6 proteins are capable of activating telomerase. The high-risk α-HPV E6 proteins, such as HPV16 E6, show an upregulation of hTERT mRNA (Oh et al., 2001, Klingelhutz et al., 1996). Increased expression of this telomerase catalytic subunit, along with the cell cycle inhibitor pRb inactivation by E7, contributes to immortalisation of epithelial cells (Kiyono et al., 1998). The β-HPV E6 proteins are able to upregulate hTERT mRNA to varying degrees. HPV38 E6 shows the most significant hTERT mRNA upregulation through mechanisms similar to that of HPV16 E6 whilst HPV5 and 8 E6 have moderate activity towards hTERT and HPV20 E6 has none (Bedard et al., 2008).

The E6 proteins are also able to suppress the apoptotic response to unscheduled cell cycle entry. Disruption of p53 and BAK to affect the intrinsic apoptosis pathway is discussed in detail below but, with respect to the extrinsic pathway, HPV16 E6 has been shown to inhibit apoptosis induced by death receptor activation by FasL, TRAIL and TNFα ligation, via binding and degradation of the adaptor protein FADD, and caspase-8 (Garnett et al., 2006, Filippova et al., 2004). The β-HPV5 E6 protein is able to upregulate osteoprotegerin to confer protection from apoptosis via the extrinsic pathway in concert with Interleukin-6 to inhibit the intrinsic pathway in response to UV, elucidating how a small number of HPV-infected cells in the skin can confer protection to surrounding non-infected cells (Tomlins and Storey, 2010).

1.4.5.4.1 E6 and PDZ Proteins

A distinguishing difference between α- and β-HPV E6 proteins is the existence of a conserved ETQV/L motif at the very C-terminus of the α-HPV E6 proteins which is

not found in the β-types. This motif is known to bind PDZ domain containing proteins in host cells (the domain was originally identified in proteins PSD-95, Discs large [Dlg] and ZO-1) and result in PDZ protein degradation. Whilst the ability to promote degradation of PDZ proteins does not correlate with epidemiological risk classification or cell immortalisation (Muench et al., 2009), it has been shown that E6-mediated PDZ protein degradation is important for the ability of E6 to induce carcinogenesis (Simonson et al., 2005) and correlates with keratinocyte transformation (Watson et al., 2003). Furthermore deletion of the PDZ binding domain of E6 proteins reduces hyperplasia (Nguyen et al., 2003).

Only high-risk α-HPV E6 proteins, such as HPV16 and 18, are able to target PDZ domain containing proteins for proteasomal degradation. Such proteins are involved in the formation of cellular junctions, regulation of cell polarity, adhesion and proliferation, acting as tumour supressors (Banks et al., 2012, Massimi et al., 2004). These include members of the membrane-associated guanylate kinase inverted (MAGI) family (Thomas et al., 2002), MUPP1 (multi-PDZ domain protein 1; Lee et al., 2000b), Scribble (Nakagawa and Huibregtse, 2000) and Dlg (Gardiol et al., 1999). Reports investigating the requirement of the only known E6 associated E3 ligase, E6AP (discussed further in chapters 1.4.5.4.2 and 1.4.6), for E6-mediated ubiquitination and degradation of PDZ domain proteins are conflicting, not only between the PDZ domain protein investigated, but also in the experimental system used which may have contributed towards these differences (Massimi et al., 2008, Nakagawa and Huibregtse, 2000, Kuballa et al., 2007). This is discussed in further detail in chapter 4.1.

Recently Lazic et al. (2012) have shown that HPV8 E6, though it does not contain a PDZ binding motif, can regulate PDZ domain containing proteins, such as syntenin-2, by altering transcription. Loss of syntenin-2 is associated with increased cell proliferation and reduced differentiation. This highlights how the same protein from different genera of HPV has evolved to target key host cell defenses in different ways.

Binding of PDZ proteins may not only have implications for disruption of cell polarity but also significance for expression of the E6 protein. Loss of the PDZ binding motif in the HPV16 E6 protein resulted in higher proteasomal turnover of the E6 protein and correlated with the inability of genomes lacking the PDZ binding motif to be maintained as episomes (Nicolaides et al., 2011, Lee and Laimins, 2004).

1.4.5.4.2 E6 and p53

Targeting of the p53 protein for degradation is one of the best characterised functions of the E6 proteins (Scheffner et al., 1990). Degradation of p53 not only abrogates the cellular p53-dependent apoptotic response but also contributes to genomic instability by abrogation of the p53-mediated DDR. The proteasomal degradation of p53 was believed to be a function of only high-risk α-HPV E6 proteins (HPV16, 18 and 33) however recently the β3 HPV49 E6 protein has been shown to degrade p53 in retrovirally transduced human foreskin keratinocytes, albeit with lesser efficiency than observed for the α-HPV (Cornet et al., 2012).

In order to target p53 for degradation E6 leads to ubiquitination of p53. To do this E6 recruits the ubiquitin ligase E6AP, discussed further in chapter 4.1 (Huibregtse et al., 1991, Huibregtse et al., 1993a). Whilst some α-HPV E6 proteins, such as HPV11 and 36, are able to bind E6AP they do not target p53 for degradation (Kuballa et al., 2007). E6AP contains a well characterised high-risk HPV E6 docking motif (LXXLLG, also known as the L2G motif; Kuhne and Banks, 1998) which is used by both human and bovine papillomavirus E6 proteins to interact with a number of substrates such as paxillin, E6AP, E6BP, tuberous sclerosis complex 2 (TSC2) and MCM7 (Kuhne and Banks, 1998, Elston et al., 1998, Tong and Howley, 1997) identified by yeast two hybrid screen and peptides (Huibregtse et al., 1993b, Elston et al., 1998, Vande Pol et al., 1998). Huibregtse et al. (1991) showed that E6AP only targets p53 in the presence of E6 and Zanier et al. (2012) have recently shown that E6 needs to self-associate via its N-terminal domain to promote the polyubiquitination of p53 by E6AP (Figure 1.11 and discussed further in

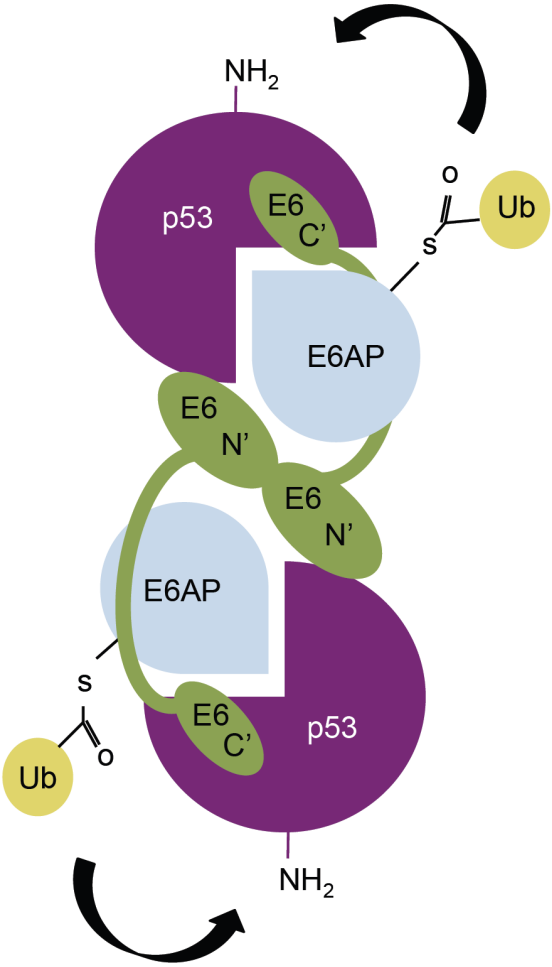


Figure 1.11 Model of high-risk α-HPV E6-mediated p53 degradation

Recent work suggests that the E6 protein binds p53 using its C-terminus (C'). The E6 protein then dimerises via its N-terminus (N') to mediate transfer of ubiquitin to the amino group of lysine residues (NH_2) on p53. Ub; ubiquitin.

Adapted from Zanier et al. (2012)

chapter 3.1). In the absence of E6, p53 turnover is regulated by several other ubiquitin ligases (reviewed in Lee and Gu, 2010). It is also noteworthy that p53 degradation by high-risk mucosal HPV E6 proteins can occur in E6AP null mouse embryonic fibroblasts, suggesting E6 associates with more than one E3 ligase to target p53 (Massimi et al., 2008).

In contrast to the high-risk α-HPV E6 proteins, cutaneous HPV E6 proteins, in general, do not interact with p53 or E6AP (Elbel et al., 1997, Rozenblatt-Rosen et al., 2012) and, along with other cutaneous HPV E6 proteins, do not generally target p53 for degradation (Jackson et al., 2000, Steger and Pfister, 1992). However, cutaneous HPV E6 proteins, along with α-HPV E6 proteins, can abrogate p53-dependent pathways independently of p53 degradation. β-HPV E6 proteins are able to aberrantly activate the p73 isoform ΔNp73 to inhibit the capacity of p53 to promote transcription of growth arrest and pro-apoptotic genes (Accardi et al., 2006). β-HPV can also disrupt the histone acetyltransferase p300 to abrogate p53 function (Muench et al., 2010). HPV5 and 8 E6 bind the p300 protein with greater affinity than that of HPV16 E6 to prevent the p300 association with the AKT protein.

Association with AKT normally stabilises p300, therefore E6 binding to p300 increases p300 turnover and disrupts DNA repair, cell growth and differentiation (Howie et al., 2011). High-risk α-HPV E6 proteins are also able to repress p53-dependent transcription through inhibition of p300-mediated acetylation (Thomas and Chiang, 2005). Both low and high-risk HPV E6 proteins (HPV 8, 11, 16 and 18) can mediate the degradation of the histone acetyltransferase TIP60 resulting in attenuation of p53-dependent activation of apoptotic pathways (Jha et al., 2010).

β-HPV E6 may also act by preventing p53 activation. p53 is phosphorylated by HIPK2 in response to UV damage to promote p53 stabilisation and acetylation by the transcriptional co-activator CREB Binding Protein (CBP) to promote transcription of apoptotic genes. To date, only the E6 proteins of β2 HPV (HPV23 and 38) have

been shown to interact with HIPK2, inhibiting HIPK2-mediated p53 phosphorylation. Interaction of HPV8 and 20 E6 (β1) and HPV16 E6 with HIPK2 could not be detected (Muschik et al., 2011).

1.4.5.4.3 E6 and the Intrinsic Apoptosis Pathway

In addition to inhibition of p53-dependent apoptosis pathways and the extrinsic apoptosis pathway discussed above, the E6 proteins of high-risk mucosal and cutaneous HPV target the intrinsic apoptotic response.

As noted in chapter 1.2.2, the effector proteins BAX and BAK are required for permeabilisation of the OMM. Conflicting reports exist as to whether the HPV E6 protein has evolved to inhibit BAX activity. Magal et al. (2005) report that the high-risk HPV E6 proteins target BAX for degradation and repress *bax* mRNA expression in cervical cancer. In addition, expression of the HPV5 and 8 E6 proteins has been observed to correlate with reduced BAX steady state levels (Struijk et al., 2008). Contrary to these reports, *in vitro* binding of BAX to the HPV16, 18 and 11 E6 proteins could not be detected and HPV16 E6 did not target BAX for degradation *in vivo* (Thomas and Banks, 1999). Interestingly, lower levels of BAX are expressed in the upper layers of the epithelia compared to BAK (Krajewski et al., 1994, Krajewski et al., 1996) and therefore there is no selective pressure for HPV to target BAX (Thomas and Banks, 1999).

The E6 proteins of both α- and β-HPV target the pro-apoptotic effector protein BAK for degradation in response to UV (Jackson et al., 2000, Underbrink et al., 2008) to preserve mitochondrial integrity (Leverrier et al., 2007) and prevent release of pro-apoptotic factors which may contribute to the reduced apoptotic levels observed in SCC (Jackson et al., 2002). Since p53 acts on BAK to initiate its apoptotic effects, this is another way by which E6 proteins unable to target p53 for degradation can abrogate the p53-dependent apoptotic effects.

Despite the well established links between the mucosal E6 proteins, E6AP and p53 degradation there is controversy surrounding the E3 ubiquitin ligase used by E6 to degrade BAK, this is expanded upon further in chapter 4.1.

1.4.5.5 E7

The E7 protein, along with E6, is able to transform keratinocytes (Munger et al., 1989). Figure 1.12 summarises how the E6 and E7 proteins function as oncogenes.

In normal infection the function of the E7 protein is to induce a replicative state in post-mitotic cells in the upper layers of the epithelium. E7 levels are controlled by degradation of the protein using the ubiquitin-proteasome system (Reinstein et al., 2000, Oh et al., 2004) and the HPV E2 protein can control the promoter of E7 through repression. It is thought that loss of E2 repression of E7 (see chapter 1.4.5.2) and the subsequent over-expression of E7 contributes to immortalisation (Stoler et al., 1992, Thierry, 2009).

The best characterised way in which the high-risk HPV E7 proteins can disrupt cell cycle control is to degrade the tumour suppressor protein retinoblastoma (pRb; Gonzalez et al., 2001, Munger et al., 1991, Huh et al., 2007). Hypo-phosphorylated pRb binds and inactivates the E2F family of transcription factors, therefore the E7-mediated degradation of pRb releases E2F to transcribe genes required for DNA synthesis driving cells into S-phase, summarised in Figure 1.13. A LXCXE motif in the E7 protein is required for pRb binding (Wang et al., 2001, Gonzalez et al., 2001). The E7 proteins use the Cullin 2 ubiquitin ligase complex to degrade pRb (Huh et al., 2007). Whilst β-HPV E7 proteins also interact with pRb the strength of the interaction is much weaker (Schmitt et al., 1994), only leading to transformation in conjunction with the activated H-Ras oncogene (Yamashita et al., 1993). Recently HPV5 E7 has been shown to degrade pRb in Saos2 co-transfection experiments, however this did not correlate *in vivo* where bioengineered skin expressing HPV5 E7, grafted onto the backs of nude mice, did not show pRb degradation (Buitrago-Perez et al., 2012). In contrast, primary human keratinocytes in monolayer culture expressing the HPV8 E7 gene have lower levels of pRb, correlating with cell cycle defects and increased proliferation (Akgul et al., 2007).

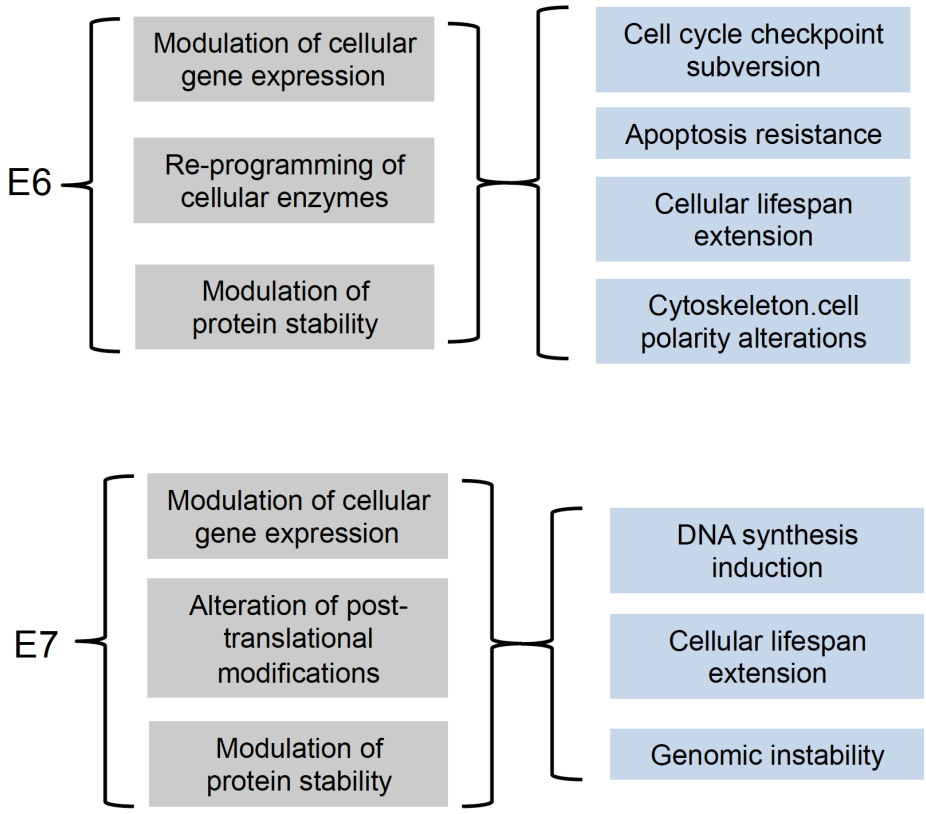


Figure 1.12 Summary of the function of HPV E6 and E7 proteins

Mechanisms the proteins use are shown in grey boxes. Blue boxes show the altered ongogenic cell phenotype as a result of expression of the proteins.

Adapted from Mclaughlin-Drubin and Munger (2009)

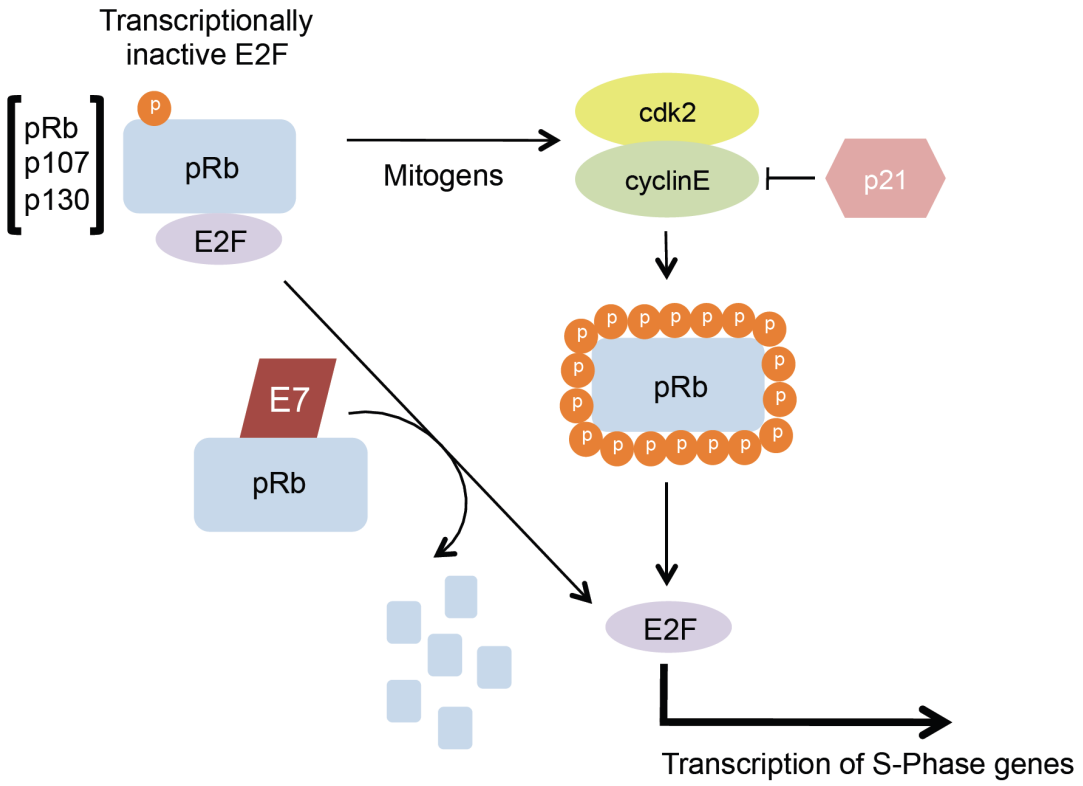


Figure 1.13 Disruption of the cell cycle by the E7 protein

Hypo-phosphorylated pRb, or the related pocket proteins p107 and p130, bind the E2F transcription factor to inhibit transcription of S-phase genes. Upon receipt of a proliferation signal cyclin-cdk complexes phosphorylate pRb. CyclinE-cdk2 has been identified as the main kinase for this activity. p21 is a cyclinD/E-kinase inhibitor. Expression of the E7 protein targets pRb for degradation, permitting constitutive expression of S-phase genes by the E2F transcription factor.

Adapted from Gil and Peters (2006)

E7 is also able to overcome cell cycle arrest controls mediated by other pRb family member pocket proteins such as p107 and p130 (Helt and Galloway, 2003). The ability to target p130 is shared by both low and high-risk HPV E7 proteins as both HPV6 and HPV16 E7 can target p130 for degradation. The HPV6 E7 protein however was unable to target p107 or pRb, unlike the high-risk α-HPV (Zhang et al., 2006). p130 acts at the G0/G1 cell cycle commitment point in differentiated cells whilst p107 is more abundant in proliferating cells and acts at the G1/S and G2/M check points (Cobrinik, 2005). Therefore E7 can disrupt cell cycle control, disturbing the differentiation process, as cells progress through the epithelium.

The proliferative capacity of E7 can also be attributed to pRb and pocket protein binding independent mechanisms (Caldeira et al., 2000). E7 has been shown to bind and inhibit other cell cycle inhibitors such as the Cip/Kip family proteins p21 and p27 (Zerfass-Thome et al., 1996). The high-risk HPV16 E7 protein can block the p21 interaction with cyclinA and E associated kinases, leading to increased cdk2 activity (Jones et al., 1997). HPV16 E7 expression also disrupts p21 activity through association with Miz-1 to inhibit UV-induced expression of p21 (Morandell et al., 2012).

The HPV16, 18 and 31 E7 proteins can directly interact with cdk2-cyclinA and E complexes to increase kinase activity (Tommasino et al., 1993, McIntyre et al., 1996, He et al., 2003). The E7 protein of β-HPV types 5 and 8 can also overcome the effects of cell cycle inhibitors, namely p16 (Westphal et al., 2009). These proteins also play a role in the DDR, their disruption by E7 therefore contributes to genomic instability as well as driving proliferation. The E7 proteins of high-risk HPV can also induce genomic instability, as exhibited by abnormal centrosome numbers and mitotic abnormalities in HPV-infected lesions (Duensing et al., 2000).

Expression of the E7 protein can also alter cell transcription control, in part this is mediated through degradation of pRb which normally recruits HDACs to chromatin in order to repress gene transcription (Brehm et al., 1998). E7 can also mediate transcriptional control independently of pRb destruction. HPV31 E7 is able to

upregulate transcription of E2F by blocking the interaction of HDACs with the E2F promoter (Longworth et al., 2005) whilst HPV16 E7 interacts with HDACs indirectly through binding to Mi2, a component of the NuRD chromatin remodeling complex (Brehm et al., 1999).

The E7 protein may also have a role in host cell immune system suppression where the HPV8 E7 protein suppresses expression of the CCL20 chemoattractant, required for Langerhans cell migration in immunesurveillance of the skin (Sperling et al., 2012).

1.4.6 The Proteasome

An important ability of the cell is to be able to destroy unwanted protein whether it be misfolded or damaged or for signalling purposes. However aberrant loss of proteins or accumulation, through degradation failure, can have detrimental consequences for a cell. This can be exploited by number of viruses, including adenoviruses, Epstein-Barr virus as well as HPV, which use the proteasome to promote a cellular environment conducive to their survival and replication as exemplified by the HPV E6 and E7 proteins described above.

Cells can degrade proteins via two main pathways. The lysosomes contain a number of hydrolytic enzymes which non-selectively degrade proteins. Alternatively, cells can selectively target proteins to the proteasome for degradation, largely, by conjugation of the small protein ubiquitin. The proteasome is a 'barrel shaped' protein complex that mediates the ATP dependent degradation of proteins into small peptides which can then be further broken down into their constituent amino acids. The proteasome can exist in different forms but the most common is known as the 26S proteasome consisting of a 20S core capped by two 19S regulatory subunits. It is the 19S regulatory units which recognise ubiquitin chains on proteins and subsequently target substrates to the 20S catalytic core for proteolysis (Murata et al., 2009).

Ubiquitin is a 8.5kDa protein consisting of 76 amino acids. It is conjugated to the ε-NH_2 group of lysine residues on cellular proteins to be degraded via the ubiquitin

C-terminal glycine (G76). Proteins may be monoubiquitinated or, alternatively, undergo polyubiquitination whereby ubiquitin chains are formed. These chains are formed by sequential conjugation of ubiquitin moieties to substrate-conjugated ubiquitin molecules via the seven internal lysine residues of ubiquitin. Dependent upon whether a protein is monoubiquitinated, polyubiquitinated and the structure of the ubiquitin chain, ubiquitination of proteins can have a number of effects. Monoubiquitination can alter membrane transport and regulate histones (Hicke, 2001), formation of polyubiquitin chains via conjugation to lysine residue 63 of ubiquitin may signal for DNA repair and transcription factor activation whilst polyubiquitin chain formation through lysine 48 signals for proteasomal degradation (Weissman, 2001).

The control of protein activity and levels by ubiquitination (through both degradation and non-degradative inactivation) is exemplified in the control of the onset of apoptosis (reviewed in Jesenberger and Jentsch, 2002, Broemer and Meier, 2009). Although protein ubiquitination is reversible, degradation is not. Therefore ubiquitination allows for sensitive regulation of apoptosis proteins to determine whether a cell survives. This is in contrast to the cleavage and degradation of substrates by activation of caspases, for example, upon apoptosis execution where substrate degradation is more widespread.

Ubiquitination of proteins involves a series of enzymes which mediate the activation and transfer of ubiquitin to substrates through conjugation of ubiquitin to active site cysteine residues. Firstly an E1 enzyme activates ubiquitin by formation of a thioester with the carboxyl group of G76 in an ATP-dependent manner. An E2 enzyme mediates the transfer of the activated ubiquitin and association with the E3 ubiquitin ligase enzyme which subsequently determines the substrate specificity for ubiquitination (Pickart, 2001). Whilst there are only two E1 enzymes to mediate ubiquitin activation, there are predicted to be around 40 E2 enzymes and over 600 E3 ligases in the human genome (Li et al., 2008, van Wijk et al., 2009). While E2 enzymes can associate with multiple E3 enzymes, there are restrictions and

preferences in the associations. The E3 enzymes are broadly classified as either RING (really interesting new gene) or HECT domain (homologous to E6AP C-terminal; Huibregtse et al., 1995) which mediate transfer of ubiquitin to substrates using different mechanisms (summarised in Figure 1.14). RING E3 ligases do not covalently bind ubiquitin but associate with the E2 enzyme and substrate for ubiquitination and the ubiquitin is directly transferred from the E2 to the substrate. RING finger E3 ligases may act as monomers, dimers or multisubunit complexes (such as the Cullin family of RING E3 ligases).

HECT domain E3 ligases are characterised by a 350 amino acid conserved C-terminus which includes a conserved active cysteine residue. This active site cysteine in the HECT domain forms a transient thioester bond with ubiquitin and catalyses the formation of the isopeptide bond between ubiquitin and substrate.

Both RING and HECT domain ligases are important for regulation of apoptotic proteins. For example, E3 ligases have been shown to regulate apoptosis through control of BAX (Johnson et al., 2012), MCL-1 (Zhong et al., 2005), IAPs (which have an intrinsic E3 ligase activity themselves; Schile et al., 2008, Garrison et al., 2011) and death receptors (Christian et al., 2011).

Despite this classical view of the requirement of ubiquitin conjugation to substrates for degradation some proteins have been identified as being targeted for proteasomal degradation in the absence of ubiquitin conjugation (Jariel-Encontre et al., 2008). Other proteins, such as the cell cycle regulator p21, bypass the requirement for substrate internal lysine residues by conjugating ubiqutin to the α-NH_2 group of the N-terminal residue (Ciechanover and Ben-Saadon, 2004).

1.4.6.1 HPV and the Proteasome

Viral proteins almost always intercept the normal proteasome targeting process at the substrate recognition step involving the E3 ligases (Banks et al., 2003). Viruses may encode their own E3 ligase, such as the Herpes Simplex Virus type-1 E3 Ligase ICP0 (Hagglund et al., 2002, Hagglund and Roizman, 2002), or alter the activity and specificity of host cell E3 ligases.

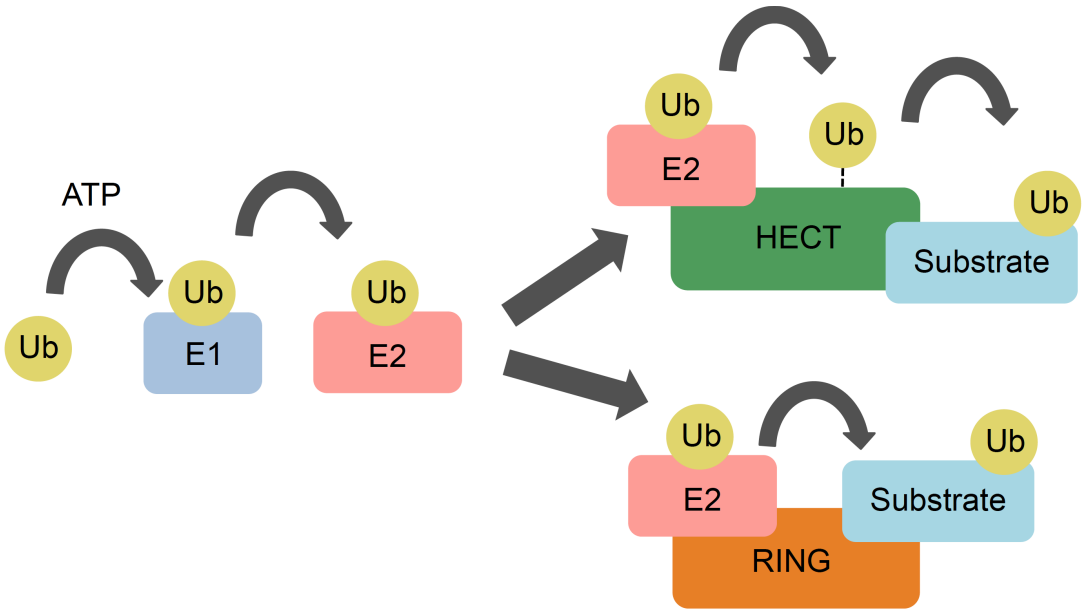


Figure 1.14 Schematic of HECT domain and RING finger E3 ligase-mediated ubiquitination

For E3 ligase-mediated ubiquitination, ubiquitin (ub) is first activated by formation of a thioester bond with the E1 enzyme using ATP. Ubiquitin is then transferred to the E2 carrier enzyme.

For HECT domain ligase-mediated ubiquitination of substrates the ubiquitin conjugated E2 enzyme associates with the HECT domain ligase and the ubiquitin protein forms a transient thioester bond with an active cysteine in the HECT domain. The HECT domain ligase then selectively binds the substrate for ubiquitintion and mediates transfer of the ubiquitin residue to the substrate.

In RING E3 ligase-mediated ubiquitination the RING protein binds the ubiquitin carrying E2 enzyme and the substrate. The ubiquitin protein is then transferred directly to the substrate from the E2 enzyme.

Whilst the levels of HPV proteins E6 and E7 themselves are regulated by proteasomal degradation (Wang et al., 2001, Stewart et al., 2004, Reinstein et al., 2000) the E6 and E7 proteins alter the activity of host cell ligases to promote a replicative environment. The E7 protein recruits the Cullin 2 ubiquitin ligase and acts as an adaptor to promote pRb degradation (Huh et al., 2007). The cutaneous HPV8 E7 protein may associate with a different E3 ligase in order to lower cellular pRb levels (Akgul et al., 2007).

With respect to the E6 protein, the most studied association with an E3 ligase is that with E6AP. E6AP was first identified via the association with E6 (E6 Associated Protein) and the degradation of p53 (Scheffner et al., 1990, Huibregtse et al., 1991, Huibregtse et al., 1993a). E6AP was the founding member of the HECT domain E3 ligases (Lee et al., 2012). Despite p53 regulation by a number of ligases including the RING ligase MDM2 and the HECT E3 ligase MULE (Lee et al., 2012), E6 alters the specificity of E6AP to that of p53. E6AP is encoded by the *ube3a* gene and exists in three isoforms (90-100kDa; Yamamoto et al., 1997) differing at the N-termini, generated by differential mRNA splicing. Upon interaction of HPV16 E6, E6AP dimerises and auto-ubiquitinates (Kao et al., 2000, Nuber et al., 1998). E6AP is also regulated by the E3 ligase EDD in the presence of HPV18 E6 (Tomaic et al., 2011). Mutation or loss of the E6AP protein results in Angelman syndrome, a neurodevelopmental disorder characterised by mental retardation, movement and balance disturbance and limitations in speech and language (Kishino et al., 1997).

Although the use of E6AP by the high-risk mucosal HPV E6 proteins to target p53 for degradation is well established, there are known host cell substrates targeted for degradation by both cutaneous and mucosal HPV E6 proteins for which an E3 ligase has not been identified (Jha et al., 2010, Howie et al., 2011). The involvement of E6AP in the degradation of BAK by the high-risk mucosal and cutaneous HPV E6 proteins is controversial and is discussed further in chapter 4.1.

1.4.7 Models of HPV Infection and Cancer

In order to study the effect of high-risk α-HPV in carcinogenesis, transgenic mice expressing the HPV16 E6 and/or E7 proteins or complete HPV16 genome under differing promoters have been generated. Depending on the promoter, varying malignancies at differing sites, including the stomach and salivary glands, are observed with high penetrance (Searle et al., 1994, Sasagawa et al., 1994). Expression of the HPV16 genome or HPV16 E6/E7 from the keratin-14 promoter directs expression to stratified epithlia and leads to, predominantly, skin hyperplasia and aberrant epidermal differentiation with high penetrance (Arbeit et al., 1994, Kim et al., 2004). However, treatment of these mice with estrogen leads to the exclusive development of cervical and vaginal squamous cell carcinomas (Arbeit et al., 1996). Lower dose estrogen treatment directs this carcinogenesis to the cervical transformation zone, the site of human cervical cancer (Elson et al., 2000). Treatment with estrogen increases proliferation of HPV16 cervical epithelia (Arbeit et al., 1996) and growth of the tumours is dependent on continued presence of estrogen since withdrawal resulted in reduced incidence and tumour volume (Brake and Lambert, 2005).

In this model, expression of the HPV16 E7 protein is the more potent oncogene required for cervical and vaginal carcinogenesis (Arbeit et al., 1996, Riley et al., 2003, Song et al., 2000). However, in the skin, HPV16 E7 expression from the keratin-14 promoter led to formation of benign tumours whilst E6 expression contributed to malignant conversion (Herber et al., 1996, Song et al., 2000).

For the β-HPV E7 and E6 oncogenes the previously described activities (cell cycle checkpoint overrides, inhibition of apoptosis, prevention of differentiation, the compromise of genome integrity) may contribute to the promotion NMSC. However a large proportion of these studies have been carried out in monolayer cell culture whilst the skin comprises several layers of keratinocytes at differing stages of differentiation to which the viral life cycle is tightly coupled. Subsequently organotypic ‘raft’ cultures have been used to investigate the contribution of the HPV

E6/E7 genes to disruption and differentiation of keratinocytes in a model mimicking the epidermal structure. In these raft cultures, primary human epithelial keratinocytes retrovirally infected with the E6/E7 genes of HPV5, 12, 15, 17, 20 and 38 were seeded on collagen scaffold which promotes terminal differentiation at the air/medium interface. The E6/E7 genes of HPV5 and 12 showed the greatest extent of differentiation disruption and delay of the HPV investigated whilst the HPV15 and 17 E6/E7 genes appeared to promote the greatest basal cell proliferation, however no invasive phenotype was observed (Boxman et al., 2001). In contrast to these data, using organotypic cultures generated on a deepidermalised dermis scaffold as a better model of basement membrane composition, keratinocyte invasion into the basement membrane was detected, accompanied by over-expression of matrix metalloproteinases (Akgul et al., 2005a).

These data were supported in mouse models where increased expression of matrix metalloproteinases was detected in tumours from transgenic mice expressing the complete early region of HPV8 (CER; E1, E2, E4, E6 and E7) under a keratin-14 promoter (Akgul et al., 2006). Here, 91% of these mice also spontaneously developed tumours, 6% of which progressed to SCC without additional insult (Schaper et al., 2005). Mice transgenically expressing only the HPV8 E6 proteins also spontaneously developed tumours, 6% of which progressed to malignancy, comparable with those mice expressing the CER to suggest E6 as the major oncogene required for malignancy in this system. However, UV irradiation caused a striking increase in papilloma formation. Increased papilloma formation was also observed with wounding to suggest that an inflammatory infiltrate may also have a role (Marcuzzi et al., 2009). Examination of culture supernatants of primary human keratinocytes expressing the HPV8 early genes showed a downregulation of Interleukin-8. This effect was also seen by expression of HPV8 E6 and HPV5 E6 alone to the greatest extent and by HPV1, HPV20, HPV38 and HPV16 E6 proteins to lesser extent. Interleukin-8 is an inflammatory cytokine, released after UV-induced damaged and therefore its downregulation in the NMSC precursor actinic keratoses

lesions may reduce the inflammatory response to UV-induced damaged, facilitating the persistence of cells harbouring UV-induced mutations (Akgul et al., 2010).

Expression of the HPV8 E2 protein alone *in vitro* promoted anchorage independent growth (Iftner et al., 1989). Investigation of the ability of the HPV8 E2 protein to induce tumour formation was also investigated using mice transgenically expressing the HPV8 E2 protein using the keratin-14 promoter. K14-E2 mice demonstrated severe dysplasia which significantly increased after a single UV dose (Pfefferle et al., 2008), however this was less severe than observed for the mice expressing the HPV8 CER. Again, expression of the HPV8 E2 protein may also act through upregulation of matrix metalloproteinases (Akgul et al., 2011). HPV8 is associated with malignant transformation in EV individuals, therefore these models support a role for β-HPV in NMSC progression and provide useful information to allow investigation of the interplay of many different factors in the skin to clarify how they may contribute to HPV-infected malignancy.

Transgenic mouse models for other β-HPV types have also allowed the exploration of the role of HPV in NMSC progression in co-operation with UV exposure. The high level of infection in malignant actinic keratoses suggests HPV infection has a role in the early stages of tumour development (Weissenborn et al., 2005). In agreement with this mice expressing the HPV38 E6 and E7 genes under a keratin-14 promoter showed reduced cell cycle arrest and p21 accumulation, development of actinic keratoses, a proportion of which progressed to SCC, in response to chronic UV exposure whilst wild type animals did not (Dong et al., 2005, Viarisio et al., 2011). The co-operation of HPV with UV in NMSC progression has also been studied in mice transgenically expressing the E6 and E7 proteins of the α-HPV 27 (associated with benign wart formation) or β-HPV20 (an EV type prevalent in SCC). Expression of these proteins in the suprabasal compartment in conjunction with chronic UV exposure led to the development of SCC, upon cessation of UV irradiation only HPV20 expressing mice continued to show hyperproliferation and loss of differentiation. Given that β-HPV genome promoters can be activated in response to

UV (Akgul et al., 2005b), these data support a co-factorial role of the β-HPV with UV exposure in the development of NMSC.

1.5 Summary and Aims

In the epidermis, keratinocyte stem cells give rise to progenitor cells which undergo a tightly regulated programme of cell cycle exit and terminal differentiation. Upon infection of these basal stem cells with HPV during wounding, the physiological program of keratinocyte differentiation is disrupted. This is achieved through the activities of the HPV oncogenes E7 and E6. Whilst the β-HPV viral proteins may have differing mechanisms to the α-HPV, both target similar pathways to maintain keratinocytes in a replication competent state whilst abrogating the resultant apoptotic cellular response to promote cell survival for completion of the viral life cycle. The differences between the α- and β-HPV proteins, life cycle and in the physiology of the sites they infect, along with the wide ranging pathologies they result in, from benign warts to malignancies, suggests that models for the contribution of β-HPV to NMSC are different from that of the high-risk α-HPV in the development of cervical cancer.

The mechanism and requirement of high-risk α-HPV in the progression of cervical cancer is well understood. In contrast a role for the β-HPV in cutaneous malignancies remains to be elucidated since a large proportion of the population are infected with these HPV without apparent pathology. However, a model by which β-HPV, through the E6 protein, act to inhibit the apoptotic response to UV damage, to which the skin is frequently exposed, may explain how β-HPV act as a co-factor with UV in NMSC development. In this model β-HPV infect the basal proliferating keratinocytes to form a HPV-infected ‘cancer stem cell’ (Egawa, 2003), possibly in the hair follicle niche where high HPV loads are found (Weissenborn et al., 2012, Boxman et al., 1997) allowing the persistence of infection via production of virus infected daughter cells. The expression of the E7 protein uncouples terminal differentiation from exit from the cell cycle leading to cells with an increased proliferative capacity. Expression of the E6 protein abrogates the apoptotic response

to both the effects of unscheduled S-phase entry and DNA damage in response to UV exposure. Consequently, in response to UV exposure, uninfected apoptosis-competent keratinocytes die, leaving apoptosis-compromised HPV-infected cells to survive, accumulating further genomic instability with increasing UV exposure.

Given that cutaneous HPV E6 proteins inhibit the cellular apoptotic response to UV damage, in part, through targeting the pro-apoptotic protein BAK for proteolysis, the main aim of this thesis was to investigate the mechanism of this process. Specifically, the aims were to:

- investigate at which stage of the BAK activation process the E6 protein targets BAK for proteolysis.

- elucidate the role of a novel cutaneous HPV E6-associated E3 ligase, HERC1, in HPV5 E6-mediated BAK degradation.

Additionally, this thesis aimed to probe the binding partners of a C-terminal motif, YHDW, conserved amongst some cutaneous HPV E6 proteins in order to further understanding of how the HPV E6 proteins may contribute to NMSC progression.

Chapter 2 Materials and Methods

2.1 Mammalian Cell Culture

2.1.1 Media

Dulbecco's Modified Eagle's Medium (DMEM)

500ml High glucose, L-Glutamine DMEM (#11965-092, Gibco, Life Technologies) supplemented with 50ml Foetal Calf Serum (FCS, #A15-151, PAA).

EpiLife Media

500ml EpiLife Media (#MEPI500CA, Gibco, Life Technologies) supplemented with 5ml Human Keratinocyte Growth Supplement (#S0015, Gibco, Life Technologies).

Rheinwald Media (RM+)

3:1 (vol/vol) DMEM Ham's F12 media (US Biologicals, #D9811-14D), high bicarbonate, pH 7.5 with 10% FCS (#FB-1001, Biosera) supplemented with RM+ supplement to give the final concentrations listed in Table 2.1.

Table 2.1 Components of RM+ media

An RM+ concentrated supplement was prepared so that upon 100-fold dilution in media gave the final concentrations indicated below.

Component	Final Concentration in Media
Hydrocortisone	0.4µg/ml
Cholera toxin	10^{-10}M
Transferrin	5µg/ml
Liothyronine	2 x 10^{-11}M
Insulin	5µg/ml
Epidermal Growth Factor (EGF)	10ng/ml

2.2 Cell Lines and Maintenance

2.2.1 Cell Lines

HCT116$^{bak-/-bax-/-}$ (Edlich et al., 2011) hereby referred to as HCT116 Double Knockout (HCT116 DKO), HT1080, PT67 and 293T cells maintained at 37^{o}C, 10% CO_2 in DMEM + 10% FCS.

N-TERT (Dickson et al., 2000) and Adult Human Epidermal Keratinocytes cells (HEKa, Life Technologies) were maintained in an undifferentiated state in EpiLife media at 37°C, 5% CO_2.

N-TERT cells, when differentiation was to be assessed, and PM1 cells (Proby et al., 2000) were cultured in RM+ media at 37°C, 10% CO_2.

All cell lines used are adherent, therefore for passage the media was aspirated and cells washed with Phosphate Buffered Saline (PBS). The cells were detached using a volume of 1x Trypsin-EDTA solution in PBS (from 10X stock, #15400-054, Life Technologies) sufficient to cover the flask surface. Once cells were detached the trypsin was neutralised with an equal volume of DMEM + 10% FCS. A fraction of this was then resuspended in the relevant growth media. Specific cell densities were acquired by counting live cells using a haemocytometer.

2.2.2 Mycoplasma Testing

Cell lines were periodically tested for mycoplasma using the PCR based Venor GeM kit. The primers provided are specific to the 16S rRNA coding region in the mycoplasma genome. Internal control primers are also included as a positive control for the PCR reaction.

Testing was performed according to the manufacturer's instructions. Briefly, cell culture supernatant was heated at 95°C for 5 minutes and cell debris pelleted by centrifugation. Two microlitres of this supernatant, water as a negative control or positive control DNA was added to a 25µl PCR reaction and the PCR reaction performed as described by the manufacturer. PCR products were analysed on a 2% agarose gel, loading 10µl of the PCR reaction. A PCR product of 191bp indicated a successful PCR reaction and a product of 270bp indicated mycoplasma contamination.

2.2.3 UVB Irradiation of Cells

Cells were seeded in 60mm-150mm dishes at approximately 70% confluence. Sixteen to twenty-four hours later the media was removed and cells washed in PBS.

Cells were then irradiated with indicated doses using either a UVP CL-1000 Ultraviolet Crosslinker (F875 bulbs, spectral peak at 312nm) or a calibrated lamp (UV source MRL 58 lamp). Fresh media was then added and cells incubated for the indicated time points.

2.2.4 Cyclohexamide Treatment

Inhibition of protein synthesis was achieved by treatment with cyclohexamide. The cell culture media was replaced with that containing 100µg/ml InSolution Cyclohexamide (Merck Chemicals) for the indicated times.

2.2.5 Storage and Recovery of Cell Lines

Cells were detached using trypsin and neutralised with DMEM + 10% FCS as described above (chapter 2.2.1). Cells were pelleted by centrifugation at 1,000rpm for 5 minutes (Heraeus Biofuge Primo), resuspended in FCS + 10% dimethylsulphoxide (DMSO) at a density of 10^6/ml and 1ml aliquoted to cryovials. Vials were wrapped in 5 layers of tissue paper and frozen at -80^{o}C. They were later transferred to liquid nitrogen for long term storage.

To revive from liquid nitrogen cells were rapidly thawed at 37^{o}C and diluted in 5ml of DMEM + 10% FCS and pelleted by centrifugation at 1,000rpm for 5 minutes (Heraeus Biofuge Primo). The media was aspirated to remove the DMSO, the cell pellet resuspended in appropriate culture media and transferred to a 75cm^2 flask for culture.

2.3 Transfection of Mammalian Cells

2.3.1 DNA Transfections

Fugene

HT1080 and PT67 cells were seeded at 5x10^4 cells in a 6 well plate. Twenty-four hours later cells were transfected using XtremeGene 9 (Roche). Transfection reagent (3:1 transfection reagent [µl] to DNA [µg]) was diluted to a total volume of 100µl using serum free media. One to two micrograms of DNA were added and mixed by pipetting. After incubation at room temperature for 15 minutes the mixture was added to 2ml of culture media on cells.

Turbofect

HCT116 cells were transfected using Turbofect (Fermentas). Cells were seeded at $2x10^5$ in a 6 well plate. One to two micrograms of DNA was diluted in 100µl of serum free media and Turbofect was added in a ratio of 3:1 transfection reagent (µl) to DNA (µg). Due to transfection reagent toxicity, the transfection media was removed after 4 hours and replaced with culture media.

2.3.2 siRNA Transfections

Dharmafect

HCT116 cells were seeded at $3x10^5$ in 60mm dishes at least 16 hours before transfection. To transfect with 50nmoles of siRNA oligonucleotide 75µl of a 2µM siRNA solution (non-target control; Silencer Select siRNA negative control 1 Ambion, E6AP duplex; Dharmacon, HERC1 SMARTpool; Dharmacon, see Table 2.2 for sequences) was mixed with 75µl of serum free DMEM. For mock transfections the siRNA oligo was replaced with the same volume of 1x siRNA buffer (#B-002000-UB-100, Dharmacon). In a separate tube 2µl of Dharmafect4 transfection reagent (Dharmacon) was mixed with 148µl of serum free DMEM and incubated at room temperature for 5 minutes. Both mixes were combined and incubated at room temperature for 20 minutes. The cell culture media was removed and replaced with 2.7ml of fresh DMEM + 10% FCS and the transfection mixture added to result in a total volume of 3ml on the cells. Sixteen hours later the transfection media was removed and replaced with new culture media. Cells were analysed for mRNA knockdown 48-72 hours after transfection.

HiPERFECT

In order to transfect HEKa cells with siRNA oligonucleotides the HiPERFECT transfection reagent was used (Qiagen). HEKa cells were seeded at $2x10^5$ on a 35mm dish. A volume of 2µM working stock of oligonucleotide, to give the final concentration in 1ml of culture media indicated, was diluted in a total volume of 50µl serum free media. Six microlitres of HiPERFECT transfection reagent was added and the mixture vortexed and incubated at room temperature for 10 minutes. The oligonucleotide was added to 1ml of culture media on the cells and incubated at

37°C for 4 hours. An additional 3ml of culture media was then added and the cells incubated overnight. The transfection mixture was then replaced with new culture media and the cells left for the indicated amount of time before treatment or harvesting to check for knockdown.

Table 2.2 siRNA target sequences

The HERC1 and E6AP (*ube3a* gene) siRNA oligonucleotides were purchased from Dharmacon.

siRNA	Catalogue number	Target mRNA sequence (5'→3')
siHERC **06**	J-007181-**06**	GCACCGACCUUAUUGUGUA
siHERC **07**	J-007181-**07**	UAGAUUAGCUUCUGAGUUG
siHERC **08**	J-007181-**08**	CCACAGGUCCUAUUACUAA
siHERC **09**	J-007181-**09**	GAACAAAGGAACCACUUGA
E6AP (*ube3a*) i	Custom	AGAUGUGACUUACUUAACA
E6AP (*ube3a*) ii	Custom	CAACUCCUGCUCUGAGAUA

2.3.3 Retrovirus Production and Transduction

In order to re-introduce wild type and various BAK mutants into HCT116$^{bak-/-bax-/-}$ double knockout cells (Edlich et al., 2011) and HPV E6 expression into keratinocyte lines, which have a low transfection efficiency, cells were retrovirally transduced with recombinant viruses encoding the genes of interest using the pLXSN vector (Clontech). pLXSN also contains a neomycin resistance gene enabling selection of transduced cells with G418. The plasmids were transfected into the viral packaging cell line PT67 ($1x10^5$ cells per well of a 6 well plate) using XtremeGene9 (Roche, see chapter 2.3.1). Twenty-four hours after transfection cells were selected using 500µg/ml G418. Cells were maintained in G418 selection and passaged until untransfected control cells were dead. Selected cells were grown to confluence in T180 flasks. Sixteen millilitres of fresh media was added and cells maintained overnight at 32°C to package RNA into replication incompetent retroviral particles.

Media containing the viral particles was collected in 4ml aliquots and frozen at -80^{o}C.

For infection, cells were seeded 24 hours previous at 1x10^{5} cells per well of a 6 well plate. The culture media was aspirated and cells incubated with 2ml serum free DMEM containing 5µg/ml polybrene (Hexadimethrine bromide) previously mixed in glass (as polybrene adheres to plastic) for 10 minutes at 37^{o}C then removed by aspiration. Polybrene was added to viral supernatant to a final concentration of 5µg/ml and 2ml added to each well of cells. Cells were centrifuged with the viral supernatant for 1 hour at room temperature at 350rpm (Beckamn Coulter, AllegraX-12R) to increase efficiency of infection. The supernatant was removed and fresh media added to the cells. Twenty-four hours later 500µg/ml G418 selection was added to the cells and cells were passaged to sufficient number under G418 selection. Primary human epidermal keratinocytes were selected with 100µg/ml G418 for 3 days.

2.4 Protein Techniques

2.4.1 Whole Cell Extracts

The media was removed from cells which were washed once with PBS on ice. Cells were then scraped into microcentrifuge tubes and washed once with PBS. Cells were pelleted by microcentrifugation at 4,000rpm for 5 minutes at 4^{o}C and the PBS removed. Unless indicated otherwise microcentrifugation at 4^{o}C was performed using an Eppendorf centrifuge 5415R. Pellets, if not immediately lysed, were snap frozen on dry ice for 10 minutes and stored at -80^{o}C.

For lysis, frozen cell pellets were first thawed on ice. Pellets were resuspended in 80-200µl (dependent on pellet size) of appropriate lysis buffer and incubated on ice for at least 30 minutes with occasional vortexing. Samples microcentrifuged at 4^{o}C at 13,000rpm for 5 minutes to pellet cell debris. The protein lysate supernatant was transferred to a clean microcentrifuge tube and the protein content quantified by NanoDrop at A_{280}.

2.4.1.1 Protein Extraction Buffers

Triton lysis buffer: 10mM Tris-HCl pH 8.0, 150mM NaCl, 10% glycerol, 1% Triton X-100, 0.5% sodium deoxycholate, 0.1% Sodium Dodecyl Sulphate with complete EDTA free protease inhibitor cocktail (Roche).

RIPA buffer: 20mM Tris-HCl pH 7.5, 1mM EDTA, 150mM NaCl, 1% Triton X-100, 0.5% sodium deoxycholate, 0.1% SDS, 1 x protease inhibitors.

2.4.2 Sodium Dodecyl Sulphate Polyacrylamide Gel Electrophoresis

Protein lysates containing 1x Laemmli sample buffer (5x stock given in Table 2.3) were denatured at 90^{o}C for 4 minutes and run on 10 or 12% acrylamide gels depending on the size of the proteins to be analysed. 1.5mm thick gels were used for transfer to membrane for western blotting. For coomassie staining, 1.0mm thick gels were used. Gels were cast (gel compositions are given in Table 2.4) and run using standard equipment. Gels were electrophoresed in SDS-PAGE running buffer (25mM Trizma base, 192mM glycine, 0.1% SDS) at 35mA. Proteins were transferred to Hybond C Nitrocellulose membrane (GE Healthcare) in transfer buffer (25mM Tris-base, 192mM glycine, 20% [v/v] methanol) for 2 hours at 150mA.

For SDS-PAGE of samples to be analysed for HERC1 the Life Technologies NuPAGE system was used. Samples were run on precast 1mm 3-8% NuPAGE Tris-Acetate gels in Tris-Acetate SDS Running Buffer using the XCell SureLock system (Life Technologies) according to manufacturer's instructions. Proteins were then transferred to Hybond C Nitrocellulose membrane, again using the SureLock system with NuPAGE Transfer Buffer according to manufacturer's instructions.

Table 2.3 5x Laemmli buffer

5x Laemmli buffer was diluted to 1x in protein lysates for SDS-PAGE separation.

Component	**Concentration in 5x stock**
Tris-HCl pH 6.8	625mM
Sodium Dodecyl Sulphate	5%
Glycerol	25%
β-mercaptoethanol	100mM
Bromophenol blue	0.025%

Table 2.4 SDS-PAGE acrylamide gels

The resolving mix was made and APS and TEMED added immediately before use and poured into a 10x8cm gel cast (1.0 or 1.5mm thick). The gel was covered by a thin layer of isopropanol to ensure even setting. The isopropanol was removed by rinsing with water. The stacking gel was then poured.

Volume per gel	3ml	10ml	
Component	4% stacking	10% resolving	12% resolving
Distilled water (ml)	2.1	4	3.3
30% acrylamide (ml)	0.5	3.3	4
1.5M Tris pH 8.8 (ml)	-	2.5	2.5
1M Tris pH 6.8 (ml)	0.38	-	-
10% SDS (ml)	0.03	0.1	0.1
10% APS (ml)	0.03	0.1	0.1
TEMED (ml)	0.005	0.006	0.006

2.4.3 Western Blotting

Unless otherwise stated, nitrocellulose membranes were blocked in 10% fat free milk (w/v) TBST (50mM Tris-base, 150mM NaCl, pH 7.5, 0.1% Tween-20) overnight at 4^{o}C. Primary antibodies were incubated with the membrane in 0.1% milk TBST for 1 hour at room temperature at the concentrations described in Table 2.5.

The primary antibody solution was discarded and membranes washed three times for at least 5 minutes with TBST before incubating with appropriate goat anti-rabbit or rabbit anti-mouse secondary horseradish peroxidise conjugated antibody used at 1/2000 in 0.1% milk TBST for 1 hour at room temperature. Membranes washed as previous and developed by the addition of electrochemical luminescence reagent (GE Healthcare, #RPN2106). Membranes exposed to X-ray film (Fuji Super RX) or Amersham Hyperfilm ECL for higher sensitivity detection (GE Healthcare #28906837) and the films were developed using X-ray developers (Xograph Imaging).

Table 2.5 Antibodies and working concentrations

The antibodies and dilutions used in western blots and immunoprecipitations are indicated in the table. All antibodies were monoclonal except where indicated otherwise.

Antibody	Company and catalogue number	Dilution and application	Species
BAK [Y164], total BAK	Abcam, ＃32371	1/1000	Rabbit
Ab1 [TC-100], BAK	Calbiochem, ＃AM03	1/250 WB	Mouse
Ab2 [TC-102], BAK	Calbiochem, ＃AM04	1/250 WB	Mouse
FLAG M2	Sigma, ＃F1804	1/1000 WB	Mouse
GAPDH [6C5]	Millipore, ＃MAB374	1/5000 WB	Mouse
α-Tubulin	Calbiochem, ＃CP06	1/1000 WB	Mouse
E6AP	Bethy Laboratories, ＃A300-352A	1/1000 WB	Rabbit polyclonal

HERC1	Bethyl laboratories, ＃A301-904A	1/1000 WB	Rabbit polyclonal
Phospho-BAK S117	Anti-sera against the peptide TKIAT-pS-LFESG. Biogenes, Berlin, Germany	25µl/IP	Rabbit polyclonal
Phospho-BAK Y108	Anti-sera against the peptide TAENApYEYFTK. Biogenes, Berlin, Germany	8µl/IP	Rabbit polyclonal
Paxillin	BD Bioscience, ＃612405	1/1000 WB & IF	Mouse
β-Actin [AC15]	Abcam, ＃Ab6276	1/1000 WB	Mouse
F-actin [NH3]	Abcam, ＃Ab205	1/1000 WB	Mouse
ZO1 (mid)	Life Technologies, ＃40-2200	1/1000 WB & IF	Rabbit
Desmoplakin	Serotec, ＃AHP320	1/1000 WB	Rabbit
Vinculin, clone SPM227	Abcam, ＃AB18058	1/1000 WB	Mouse
Integrin-β_1, P5D2	Covance, ＃MMS-472R	1/100 WB & IF	Mouse
Focal Adhesion Kinase	Cell signalling, ＃3285	1/1000 WB & IF	Rabbit
P53 (DO1)	CRUK	1/5000 WB	Mouse
Rabbit immunoglobulin fraction	DAKO, ＃X0903	IP	Rabbit
Mouse IgG control	Beckton Dickson, ＃349040	1µg/ml IP	Mouse

2.4.4 Immunoprecipitation (IP)

Cells were seeded on 150mm dishes and grown to 80% confluence. After treatment the media was removed and the cells washed twice with cold PBS and cells harvested by scraping. Unless immunoprecipitation was performed from mitochondrial enriched fractions (see chapter 2.4.7), whole cell extract lysates were prepared by lysis on ice with the appropriate buffer (indicated below). Protein concentrations were determined by NanoDrop A_{280} and equal amounts of protein in the lysate (1-2mg) were used per IP. The total reaction volume was kept constant (100-400µl) using excess buffer and incubated with 1-2µg of antibody overnight with

rotation at 4°C. Fifty to seventy microlitres of 50% slurry of appropriate beads (Protein A or G sepharose, Sigma) were washed 3x in lysis buffer by microcentrifugation at 3,000rpm for 1 minute and added to the IP mixture for 90 minutes. The beads were pelleted, the supernatant discarded and beads washed three times as previously described. Bound proteins were eluted with 25µl 2x Laemmli buffer (20% glycerol, 10% β-mercaptoethanol, 4.6% SDS, 0.025% Bromophenol blue, 62.5mM Tris-HCl pH 6.8) and heating at 90°C for 4 minutes. Samples were separated by SDS-PAGE and western blotted as described in chapters 2.4.2 and 2.4.3. Antibodies indicated in Table 2.5.

2.4.4.1 Immunoprecipitation Buffers

1% CHAPS lysis buffer: 10mM Tris-HCl pH 7.5, 100mM NaCl, 2mM EDTA pH 8.0, 1% 3-[(3-Cholamidopropyl)dimethylammonio]-1-propanesulfonate (CHAPS), 1/100 phosphatase inhibitor cocktail 1 and 2 (Sigma), complete EDTA free protease inhibitor cocktail (Roche).

Assay: Phospho-serine 117 IP, p53 and BAK co-IP. HERC1 IP and E6AP IP using 0.3% CHAPS.

Triton Lysis Buffer: As previously described in chapter 2.4.1.1 with the addition of 1/100 phosphatase inhibitor cocktail 1 and 2 (Sigma).

Assay: Phospho-BAK Y108 IP.

2.4.5 Peptide Pull-Down Assay

N-TERT cells were harvested using Accutase (Millipore) and washed twice in PBS. Cells were lysed using 3 volumes of TAP lysis buffer (20mM Tris-HCl pH 8, 0.3M KCl, 5mM $MgCl_2$, 10% glycerol, 0.1 Tween-20, 10mM β-mercaptoethanol, protease inhibitors [Roche]) and 2 freeze/thaw cycles. The lysate was incubated for 30 minutes at 4°C with rotation and microcentrifuged at 13,000rpm for 30 minutes at 4°C. The supernatant was removed and centrifuged again for 10 minutes. The lysate protein content was quantified by NanoDrop A_{280}. Fifty microlitres of anti-HA agarose beads (#A2095, Sigma) were washed three times in TAP lysis buffer and incubated

with the supernatant for 45 minutes at 4°C with rotation to reduce any none specific binding proteins. Beads were precipitated by microcentrifugation at 5,000rpm for 1 minute and the supernatant removed and added to a new aliquot of washed beads with 150nmoles of the YHDW peptide or the control peptide lacking the YHDW motif (sequences in Table 2.6). The HA-tagged peptides were synthesised by K. di Gleria (Weatherall Institute of Molecular Medicine, Oxford). Beads, peptides and lysate were incubated together overnight at 4°C with rotation. The beads were precipitated as previously described and washed 5 times with TAP lysis buffer for 5 minutes each time with agitation. Binding proteins were eluted with 20µl of 2x Laemmli buffer, separated by SDS-PAGE (NuPAGE 4-8% Tris-Acetate gels, Life Technologies) and analysed by silver staining (FOCUS FASTsilver, G-Biosciences) according to the manufacturer's instructions. Unique bands pulled down using the YHDW peptide and corresponding areas from the control peptide were cut from the gel, in-gel digested with trypsin and the resulting peptides were analysed by LC-MS/MS to identify interacting proteins (B. Kessler, Henry Wellcome Building for Molecular Physiology, Oxford).

Table 2.6 Peptide sequences

A peptide comprising a HA-tag (bold), a flexible gly-ser-ser repeat linker region and the YHDW motif was synthesised by K. di Gleria of the WIMM Peptide Synthesis Facility. The purity was checked by HPLC. A control peptide lacking the YHDW motif was synthesised as a control.

Peptide	Peptide sequence
YHDW	**YPYDVPDYA**GSSGSSGSSYHDW
Control peptide	**YPYDVPDYA**GSSGSSGSS

2.4.6 BH3 Peptide Pull-Down

Peptides were synthesised and purified by HPLC by K. di Gleria of the peptide synthesis facility, Weatherall Institute of Molecular Medicine. BH3 peptide binding assays were performed as described previously (Gallenne et al., 2009). Briefly, equal amounts of extract were prepared in 1% CHAPS buffer (10mM HEPES, pH 7.5, 150mM NaCl, 1% CHAPS, supplemented with EDTA-free protease inhibitor cocktail and phosphatase inhibitor cocktail). Lysates were incubated with 10μM biotinylated peptide for 4 hours with agitation at 4°C. Thirty microlitres of avidin-agarose beads were added and incubated overnight at 4°C. Beads were pelleted, washed three times in CHAPS buffer and resuspended in 2x loading buffer and analysed for BAK binding by western blot.

2.4.7 Mitochondrial Fractionation

Mitochondria were prepared from cells using a method that preserves mitochondrial integrity. Cells were collected and washed with ice-cold PBS. Mitochondria were isolated by Dounce homogenisation in HIM buffer (20mM HEPES-KOH pH 7.5, 10mM KCl, 1.5mM $MgCl_2$, 250mM sucrose, 1mM EGTA, pH 7.4 supplemented with protease inhibitor cocktail) using a protocol described previously (Jiang et al., 2006). Briefly, homogenates were microcentrifuged at 1,000rpm for 5 minutes at 4ºC to remove debris. The supernatant was collected and microcentrifuged again at 10,000rpm for 20 minutes at 4°C to obtain cytosolic and mitochondrial-enriched fractions. The pellet containing mitochondria was then resuspended in HIM buffer. The protein concentration was measured by Bradford assay and equal amounts used in immunoprecipitations.

2.4.8 BAK Dimerisation Assay

Mitochondrial fractionation was performed as in chapter 2.4.7. One hundred micrograms of mitochondria was resuspended in HE buffer (10mM HEPES pH7.5, 1mM EDTA supplemented with protease inhibitor cocktail) and incubated with 10mM bis(maleimido)ethane (BMOE, Pierce), a short-armed protein sulphydryl-sulfhydryl cross-linker, at 37°C for 1 hour to cross-link BAK dimers. The reactions were

microcentrifuged at 12,000rpm for 10 minutes (Heraeus Biofuge Pico) and pellets mixed in 25µl of 2x SDS buffer and subjected to NuPAGE 4-12% gradient gel separation and western blotted against rabbit human anti-BAK antibody (Y164, Abcam).

2.4.9 Expression of Fusion Proteins in *E. coli*

In order to assess whether HERC1 could directly ubiquitinate BAK, an *in vitro* ubiquitination assay was attempted using His-tagged BAKΔC, GST-HPV5 E6 and a Maltose Binding Protein (MBP) fused HERC1 protein expressed from a 'mini-gene' (see chapter 4.3.6) expressed in the *E. coli* strain Rosetta (F^- ompT $hsdS_B(R_B^- m_B^-)$ gal dcm λ(DE3 [lacI lacUV5-T7 gene 1 ind1 sam7 nin5]) pLysSRARE (Cam^R)).

Specific protocols for isolation of His-tagged BAKΔC, GST-HPV5 E6 and the MBP-HERC1 protein are given below. However, initially these constructs were transformed into *E. coli* BL21 (F- *dcm ompT hsdS*(r_B- m_B-) gal $[malB^+]_{K-12}(\lambda^S)$) according to chapter 2.5.4.1. A single clone was selected and used to inoculate 10ml bacterial cultures that were grown overnight at 37°C. These cultures were then amplified in 20ml of Terrific Broth with 100µg/ml ampicillin selection and grown to an OD_{600} of 0.6 using a spectrophotometer. The starter cultures were then added to 800ml of media and cultures allowed to grow for 2-3 hours or until an OD_{600} of 0.6 was achieved. Protein expression was induced using isopropyl β-D-1-thiogalactopyranoside (IPTG), added to a final concentration of 1mM and cultures incubated for 3 hours at 25°C. Bacterial pellets were collected by centrifugation at 6,000x *g* for 15 minutes at 4°C.

2.4.9.1 Purification of GST-HPV5 E6 from Bacteria

The HPV5 E6 GST fusion protein was encoded by the pGEX-2T-5E6 vector expressed in the BL21 strain. GST protein was also purified similarly. During induction of bacteria expressing the GST-HPV5 E6 protein, a final concentration of 100µM zinc chloride was added to stabilise zinc finger folds in the HPV5 E6 protein.

To extract the GST proteins bacterial pellets derived from 800ml cultures were suspended in 40ml of GST binding buffer (25mM Tris pH7.5, 150mM NaCl, 1mM

EDTA, 1mM DTT, protease inhibitors) on ice. Sarkosyl (Sodium Lauroyl Sarcosinate) was added to a final concentration of 1% and bacterial lysis achieved by three cycles of freeze/thaw on dry ice, followed by sonication until reduced viscosity was observed. Debris was pelleted at 16,000rpm using a Beckman centrifuge in a JA25 rotor for 10 minutes at 4°C. Triton X-100 was added at a final concentration of 1% to the clarified supernatant and incubated with 1ml glutathione conjugated sepharose beads (Glutathione SuperGlu Resin, Generon), pre-washed in GST binding buffer, at 4°C overnight with rotation. Beads were pelleted by centrifugation at 1,000rpm (Beckman Coulter, Allegra X-12R) for 3 minutes and washed three times for 15 minutes in 40ml of GST binding buffer containing 0.1% NP40. GST protein purity and quantity checked in a 20µl sample of the non-bound fraction and each of the three wash steps, and by elution from a 30µl sample of the beads with an equal volume of 2x Laemmli buffer and analysed by SDS-PAGE and gel fixing in 10% methanol, 10% acetic acid and staining with InstantBlue coomassie dye (Expedeon). The remaining fusion protein was eluted from the beads by 10 minute incubation at room temperature with one bead volume of 50mM Tris (pH8.0), 20mM reduced glutathione, 5% glycerol. Three elution fractions were collected and 20µl samples from each checked by SDS-PAGE and coomassie stain as above. The fractions were dialysed against 50mM HEPES pH8.0, 100mM NaCl, 10% glycerol overnight at 4°C using tube-o-dialyser 4K molecular weight cut off (#786-141-4K, G Biosciences) and then concentrated to ~1µg/µl using Spin X UF concentrators 5K molecular weight cut off (#431477, Corning) and quantified by Bradford assay. Proteins were stored at -80°C.

2.4.9.2 Purification of His-BAKΔC from Bacteria

The BAK protein used for substrate was fused to a 6xHis-tag in the pQE9 vector (Qiagen) available in the lab. The BAK construct lacked the hydrophobic C-terminal transmembrane domain of 21 amino acids through the introduction of a premature stop codon (designated His-BAKΔC) to increase solubility.

BL21 bacteria from an 800ml culture expressing the His-BAKΔC construct were suspended in 40ml PBS (where the NaCl concentration has been adjusted to 0.5M) containing 5mM β-mercaptoethanol. Lysis achieved by three cycles of freeze/thaw on dry ice, followed by sonication until reduced viscosity was observed. Debris was pelleted at 16,000rpm using a Beckman centrifuge in a JA25 rotor for 10 minutes at 4^{o}C. Imidazole was added to a final concentration of 5mM to minimise non-specific binding of bacterial proteins. His-Select Nickel affinity gel (Sigma) was then added to the supernatant and proteins bound overnight at 4^{o}C with rotation. Beads were pelleted and washed three times with binding buffer. The His-BAKΔC protein was eluted in three fractions by incubation in buffer containing 200mM imidazole. Eluted proteins were dialysed, concentrated and stored as described above for GST proteins.

2.4.9.3 Purification of HERC1 Mini-gene MBP Fusion Proteins

MBP, the wild type HERC1 and mutant C859A HERC1 mini-gene fusion proteins were encoded by the pMAL-2C vector (New England Biolabs).

Protein was purified from bacterial pellets as previously described by Riggs (2001). Bacterial pellets were resuspended in 40ml MBP buffer (20mM Tris-HCl, pH7.4, 200mM NaCl, 500mM EDTA, 10mM β-mercaptoethanol) and lysed using three freeze/thaw cycles followed by sonication. The lysate was cleared by centrifugation in a JA25 rotor at 16,000rpm for 30 minutes at 4^{o}C. The lysate was then incubated with 1ml of amylose beads (New England Biolabs) pre-washed in MBP buffer at 4^{o}C overnight with rotation. The amylose beads with the bound MBP fusion proteins were pelleted and washed three times for 30 minutes each in MBP buffer. The fusion proteins were then eluted from the beads using MBP buffer containing 10mM maltose. The proteins were then dialysed, concentrated and stored as described above. Samples retained at different stages of purification were analysed by SDS gel electrophoresis.

2.4.10 *In Vitro* Ubiquitination Assay

An *in vitro* ubiquitination assay was performed in order to assess whether a HERC1 protein expressed from a mini-gene construct could ubiquitinate BAK using proteins purified in chapter 2.4.9. The *in vitro* ubiquitination assay was performed according to previous experiments investigating ubiquitination of other proteins, such as p53 (Li et al., 2003, Okamoto et al., 2009, Woelk et al., 2006).

100ng of E1 ubiquitin activating enzyme (recombinant human Ube1, # E-305-025, Boston Biochemicals), 150ng of the UbcH5a E2 ubiquitin conjugating enzyme (recombinant human, #E2-616-050, Boston Biochemicals), 5µg of ubiquitin (recombinant human, #U-100H-10M, Boston Biochemicals), were mixed in a 20µl reaction with 2µl 10x reaction buffer (Boston Biochemicals), His-BAKΔC, GST alone or the GST-HPV5 E6 protein and MBP, the wild type MBP-HERC1 or the HERC1 C859A mutant. Further detail of the amounts of the bacterially expressed proteins used in the reactions are given in chapter 4.3.7. The reaction volume was made to 18µl with water and reactions initiated by addition of 2µl Mg^{2+}-ATP solution (from ubiquitination reaction kit #SK10, Boston Biochemicals). Alternatively, 5µl (~ 40µg) of purified mitochondria isolated from HCT116 BAK cells that had been UV-irradiated was substituted for the His-BAKΔC substrate. Reaction mixtures were incubated at 37^{o}C for 1 hour and then stopped with an equal volume of 2x Laemmli buffer and heating to 90^{o}C for 4 minutes. The reaction was separated by SDS-PAGE and western blotted for BAK using the monoclonal rabbit BAK antibody. In previous experiments with other substrates, ubiquitinated species have been identified as either a smear (multi-ubiquitinations) or proteins with an increased molecular weight of 8kDa (indicating monoubiquitinated proteins).

2.5 Molecular Biology Techniques

2.5.1 Polymerase Chain Reaction

2.5.1.1 RNA Isolation from Cells

RNA longer than 200 nucleotides was extracted and purified from cell pellets (less than 1x10^{7} cells) using the Qiagen RNeasy mini kit spin protocol (Qiagen). Briefly,

cells were removed from the plate by trypsinisation as previously described and excess media removed by washing with PBS. Cells were lysed with appropriate amount of RLT lysis buffer, which contains guanidine-thiocyanate to inactivate RNases, according to protocol. One volume of 70% ethanol was added and the mixture was placed in the RNeasy spin column. Columns were centrifuged for 1 minute at 8,000x *g* to allow binding of RNA to the silica column under high salt conditions and the flow through was discarded. Contaminants were removed by washing as per manufacturer's instructions. The flow through was again discarded and the column spun for an additional minute to remove any residual buffer. Thirty microlitres of water was placed on the column and incubated at room temperature for 1 minute. RNA was eluted in water by centrifugation as above.

2.5.1.2 Reverse Transcription of RNA

Reverse transcription reaction was performed using Finnzymes Dynamo Sybr Green 2 Step RT-QPCR kit (Thermo Scientific, #F430) to generate complementary DNA (cDNA) templates from mRNA.

In a 20µl reaction: 10µl 2x Reverse Transcriptase Buffer, 1µl random hexamers, 2µl M-MuLV RNase H+ reverse transcriptase containing RNase inhibitor, 7µl RNA eluted as chapter 2.5.1.1. The PCR program is described in Table 2.7.

Table 2.7 Thermocycling protocol for reverse transcription reaction

mRNA was reverse transcribed using the program below.

Step	Temperature	Time
Primer extension	25°C	10 minutes
cDNA synthesis	37°C	30 minutes
Termination	85°C	5 minutes
Cooling	4°C	4 minutes

2.5.1.3 Real Time Quantitative Polymerase Chain Reaction

A real time quantitative Polymerase Chain Reaction (RT-QPCR) was used to measure the mRNA levels of target genes. mRNA was extracted as described in chapter 2.5.1.1 and cDNA generated by reverse transcription as described in chapter 2.5.1.2 using random hexamers. The cDNA templates were used in RT-QPCR reactions with primers against the target gene designed to span exon junctions in order to quantitate only mRNA, and not contaminating genomic DNA (Table 2.8). The same cDNA templates were also used in control reactions with primers against a reference gene (β-glucuronidase; *gus*) in order to control for DNA loading and quality. RT-QPCR was performed using a DNA Engine Opticon 2 Continuous Fluorescence Detector (MJ Research) and the Finnzymes Dynamo Sybr Green 2 Step QRT-PCR kit (Thermo Scientific, #F430).

In a 20µl reaction: 10µl 2x mastermix, 0.5µM forward primer, 0.5µM reverse primer and 0.5µg cDNA, water to 20µl.

Table 2.8 RT-QPCR primers

Primers were designed to amplify small (~200bp) gene fragments. The forward and reverse primers spanned exon junctions so only mRNA was amplified in the reactions.

Primer name	**Sequence (5'→3')**
HERC1 Fwd	ATGCGGTCACCCATAAAGAG
HERC1 Rve	GCAGGGTCACTTTCTTCAGC
GUS Fwd	AAACGATTGCAGGGTTTCAC
GUS Rve	CTCTCGTCGGTGACTGTTCA
BAK Fwd	TTTCCGCAGCTACGTTTTT
BAK Rve	GGTGGCAATCTTGGTGAAGT

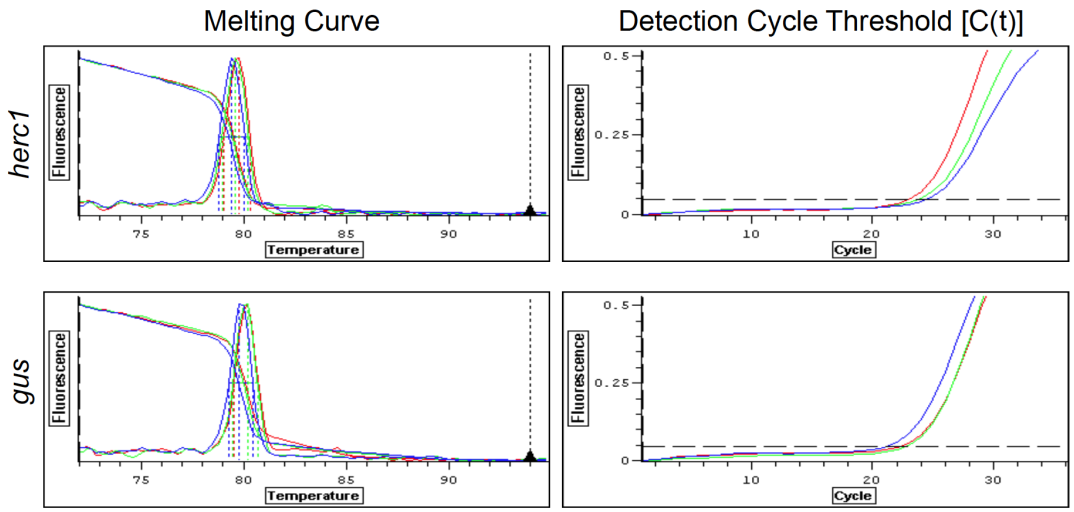
The reaction plates were sealed and centrifuged to remove any air bubbles. The reaction program is shown in Table 2.9.

The reaction specificity was checked by the melting curve, with a narrow, single peak, overlaying curves indicating a specific reaction product. The PCR cycle number at which the fluorescence signal reaches the threshold [cycle threshold; C(t)] was manually set to be just at the exponential phase of detection before the PCR reaction efficiency becomes variable across the reactions. The C(t) for the target gene was normalised to that of *gus* for the same cDNA sample to account for differences in cDNA template loading. In order to determine relative quantification of a target gene between a siRNA knockdown sample and untransfected control, thereby inferring the relevance of differences in C(t) values for a gene, the $2^{-\Delta C(t)}$ method was used to calculate the linear change ratio. In order to do this, the change in C(t) value between the sample and the untreated control was calculated. The change in C(t) was then linearised, giving the relative expression. This was subtracted from 1 and multiplied by 100 to represent percentage mRNA knockdown relative to the control. An example is shown in Figure 2.1 and Table 2.10.

Table 2.9 Thermocycling RT-QPCR program

The RT-QPCR program below was used to amplify the genes of interest. After each amplification cycle the reaction fluorescence was measured.

Step		**Temperature**	**Time**	**Number of cycles**
1	Initial Denaturation	95°C	15 minutes	1
2	Denaturation	94°C	10 seconds	44
3	Annealing	55°C	30 seconds	
4	Extension	72°C	30 seconds	
5	Plate read			
6	Final extension	72°C	5 minutes	1
7	Melting Curve	72°C to 95°C	0.2°C/sec ramp	
8	Reannealing	72°C	5 minutes	1



Red; mock, **Green**; non-target, **Blue**; *herc1* siRNA pool

Figure 2.1 Example raw RT-QPCR data

RT-QPCR reactions are performed using cDNA templates with primers against a target gene (*herc1*) and reference gene (*gus*). Melting curves show the specificity of the reaction. The C(t) for each sample is calculated by setting the detection threshold for fluorescence at the beginning of the exponential amplification phase (indicated by the dotted line). After normalisation to *gus*, a higher C(t) value indicates later amplification, therefore a lower expression level.

	Primer target gene	Raw C(t) Value	Normalised *gus* values (sample/ mock)	C(t) *herc1* normalised to *gus*	ΔC(t) (sample-mock)	$2^{-\Delta C(t)}$	% mRNA knockdown relative to mock $[1-2^{-\Delta C(t)}]*100$
Mock	*herc1*	23.00		23.00	0.00	1.00	0
Non-targeting	*herc1*	23.74		23.27	0.27	0.83	17
HERC1 siRNA sample	*herc1*	24.36		25.64	2.64	0.16	84
Mock	*gus*	22.32	1.00				
Non-targeting	*gus*	22.79	1.02				
HERC1 siRNA sample	*gus*	21.20	0.95				

Table 2.10 Example calculation of relative mRNA knockdown by RT-QPCR

The C(t) for the target gene is normalised to the *gus* reference gene.

$\Delta C(t) = C(t)_{sample} - C(t)_{mock}$

Relative expression of the gene in the sample compared to the control = $2^{-\Delta C(t)}$

% mRNA knockdown in sample = $[1-2^{-\Delta C(t)}]*100$

2.5.1.4 High Fidelity Polymerase Chain Reaction

For high fidelity PCR (cloning) Velocity Polymerase (Bioline, #BIO-21098) was used.

In a 50µl reaction: 10µl 5x reaction buffer, 1µl 10mM dNTP (Promega), 0.5µM forward primer, 0.5µM reverse primer, 10ng template DNA, 0.7µl Velocity polymerase, water to 50µl. Cycling conditions detailed in Table 2.11.

Table 2.11 Thermocycling program for Velocity polymerase

Amplification of genes using the Velocity polymerase was performed using the cycling program below.

Step		Temperature	Time	Number of cycles
1	Initial Denaturation	98°C	2 minutes	1
2	Denaturation	98°C	30 seconds	30
3	Annealing	5°C lower than lowest T_m of primer pair	30 seconds	
4	Extension	72°C	15-30 seconds/kb	
5	Final extension	72°C	10 minutes	1
6	Cooling	4°C	4 minutes	1

2.5.1.5 Taq Polymerase Chain Reaction

Where high sequence fidelity was not required, such as confirmation of E6 expression in cell lines, recombinant Taq polymerase (Fermentas, #EP0402) was used to amplify genes using the thermocycling program indicated in Table 2.13.

In a 50µl reaction: 5µl 10x Taq buffer with $(NH_4)_2SO_4$, 1µl 10mM dNTP (Promega), 0.2µM forward primer, 0.2µM reverse primer, 1.5µM $MgCl_2$, 10ng DNA template, 1.25 units of Taq Polymerase, water to 50µl.

Table 2.12 Taq polymerase reaction primers

Primers were designed in order to detect cellular expression of the indicated genes by PCR.

Primer	Sequence (5'→3')
GAPDH Fwd	GAGTCAACGGATTTGGTCGT
GAPDH Rve	TTGATTTTGGAGGGATCTCG
HPV5 E6 Fwd	ATGGCTGAGGGAGCCGAACACC
HPV5 E6 Rve	TTACCAATCATGATAAAAATGC
HPV8 E6 Fwd	ATGGACGGGCAGGACAAGGC
HPV8 E6 Rve	TTACCAATCATGATACAAAT
HPV20 E6 Fwd	ATGGCTACACCTCCTTCTTCAG
HPV20 E6 Rve	TTATTGAAAATGCTTACACAGC

Table 2.13 Thermocycling program for Taq polymerase

Amplification of gene products using the Taq polymerase was performed using the thermocycling program outlined below.

Step		Temperature	Time	Number of cycles
1	Initial Denaturation	95°C	2 minutes	1
2	Denaturation	95°C	30 seconds	30
3	Annealing	5°C lower than lowest T_m of primer pair	30 seconds	
4	Extension	72°C	1 minute/kb	
5	Final extension	72°C	10 minutes	1
6	Cooling	4°C	4 minutes	1

2.5.1.6 Agarose Gel Electrophoresis

DNA products (PCR and plasmids) were typically separated on a 1% agarose mini gel (30ml) at 70V in 1x TBE buffer (0.4nM EDTA, 18mM Boric acid, 18 mM Tris Base pH 8.2) until adequate resolution was achieved. DNA was loaded in dye (6x, Fermentas) and stained using Webgreen DNA stain (WebScientfic). Markers used were O'Gene Ruler 100bp or 1kb (Fermentas, #SM0241 and #SM0312 respectively).

2.5.2 Vector Construction

2.5.2.1 Restriction Digest and Ligation

2.5.2.1.1 Restriction Enzyme Digests

PCR products were amplified according to chapter 2.5.1.4 using primers encompassing the indicated restriction sites (Table 2.14). The PCR products were cleaned using the Qiagen PCR purification kit according to manufacturer's instructions to remove excess primers and nucleotides.

Digestion of vector (1-2µg) and PCR products was carried out in 50µl reactions using the indicated enzymes (New England Biolabs) and compatible buffer according to the New England Biolabs double digest finder[1]. Digestions were performed at 37^{o}C for 1 hour. The vector was dephosphorylated by addition of 6µl of calf intestinal alkaline phosphatase 10x buffer, 3µl of water and 1µl of calf intestinal alkaline phosphatase for 10 minutes at 37^{o}C after digestion to reduce self annealing (Promega, #M1821). The vector was then gel purified using the Qiagen MinElute Gel Extraction kit (Qiagen). Briefly, the vector was electropheresed by agarose gel (as described in chapter 2.5.1.6) and the linearised vector extracted using a 312nm emission light box and processed according to manufacturer's instructions. The PCR product and gel extracted vector were phenol/chloroform purified to remove digested fragments and protein from the sample as described below.

---

1 http://www.neb.com/nebecomm/DoubleDigestCalculator.asp#.T3DSpsXOy5I

Table 2.14 Cloning primer sequences

The primers below were used to amplify the indicated gene products, adding the noted restriction sites. Restriction enzyme recognition sequences are indicated in bold.

Primer	Sequence (5'→3')
pEFIRES HPV5 E6 cloning *Nhe1* Fwd	TAT**GCTAGC**ATGGCTGAGGGAGCCGAAC
pEFIRES HPV5 E6 cloning *NotI* Rve	CCG**GCGGCCGC**TTACCAATCATGATAAAAA

2.5.2.1.2 Phenol Chloroform Purification

After digestion, to remove small digested fragments and enzymes, the DNA solution was diluted to 100µl with 2x TNE buffer (20mM Tris-HCl, 400mM NaCl, 2mM EDTA pH 7.4). One hundred microlitres of phenol:chloroform solution was added and the mixture vortexed followed by centrifugation at 13,000rpm for 3 minutes at room temperature (Heraeus Biofuge Pico). The supernatant was removed to a clean microcentrifuge tube and an equal volume of chloroform was added, vortexed and centrifuged for 1 minute at 13,000rpm (Heraeus Biofuge Pico). The supernatant was removed to a new microcentrifuge tube and 1/10 volume of 3M sodium acetate pH 5.2 added. Mixture was vortexed and twice the volume of absolute ethanol was added. The solution was vortexed and frozen on dry ice for 20 minutes. The DNA was thawed and centrifuged at 13,000rpm for 10 minutes (Heraeus Biofuge Pico). The DNA pellet was then washed once with 70% ethanol, and pelleted by centrifugation as above. Excess supernatant was discarded and pellet left to dry at 40^{o}C.

2.5.2.1.3 Ligations

To ligate PCR fragments into the digested vector, after phenol/chloroform purification, the vector and PCR product were each suspended in 10µl of water and the DNA concentration quantified by NanoDrop A_{260}. The vector and PCR fragment were mixed at a ratio of 1:5. Two microlitres of 10x T4 DNA ligase buffer and 1µl T4 DNA ligase were added. The reaction volume was then made up to 20µl with water. The reaction was left at room temperature for a minimum of 1 hour. Ten microlitres

of the reaction was then transformed into bacteria and single colonies screened for successfully ligated vector with PCR product by diagnostic restriction digests and subsequently, sequencing.

2.5.3 Mutagenesis

Codon changes in vector sequences to result in amino acid mutations were performed using the QuikChange II XL Site Directed Mutagenesis Kit (Stratagene) according to the manufacturer's protocol. Briefly, forward and reverse primers were designed containing the desired mutation with at least 14 bases complementary to the original sequence spanning either side of the mutation, ending with cytosine or guanosine in order to maximise primer annealing (see Table 2.15). In the presence of the template plasmid the primers are extended using a DNA polymerase to generate the mutated plasmid. Treatment of the reaction mixture with *DpnI* endonuclease digests methylated and hemimethylated DNA and is therefore specific for the digestion of parental DNA template. Ten microlitres of the remaining mutated

Table 2.15 Table of mutations generated and the primers used

Mutagenic primers were designed to alter nucleotides and result in codon changes. The mutagenised nucleotides are indicated in bold.

Parental Vector	Mutation	Sequence (5'→3')
pLXSN WT BAK	BAK K113R Forward	GCCTATGAGTACTTCACCA**G**GATTGCCACCAGC CTGTTTG
	BAK K113R Reverse	CAAACAGGCTGGTGGCAATC**C**TGGTGAAGTAC TCATAGGC
pLXSN HPV5 E6	HPV5 E6 D156A Forward	GTAAGCATTTTTATCATG**C**TTGGTAAAGAGGTC
	HPV5 E6 D156A Reverse	GACCTCTTTACCAA**G**CATGATAAAAATGCTTAC
	HPV5 E6 W157A Forward	CATTTTTATCATGAT**GC**GTAAAGAGGTCACC
	HPV5 E6 W157A Reverse	GGTGACCTCTTTAC**GC**ATCATGATAAAAATG

DNA was transformed into XL-10 Gold Ultracompetent cells (as described in chapter 2.5.4.1). The DNA of surviving colonies was isolated using the Qiagen Mini Prep kit as described in chapter 2.5.4.2 and sequenced to screen clones for the mutation.

2.5.4 Plasmid DNA Preparation

2.5.4.1 Bacterial Transformation

Fifty microlitres of DH5α *E. coli* subcloning efficiency competent bacteria (Life Technologies) were aliquoted into pre-chilled microcentrifuge tubes on ice. For some bacterial strains (SURE2 supercompetent, XL-10 Gold Ultracompetent, Stratagene), 1µl of β-mercaptoethanol was added and incubated for 10 minutes on ice with occasional agitation. Upto 10µl of ligation or mutagenesis reactions or 10ng of DNA were added and incubated for 30 minutes on ice. Bacteria were subsequently heat shocked for 20 seconds at 42^{o}C and then cooled on ice for 2 minutes. Five hundred microlitres of Luria Bertani (LB) media with 2% glucose was added and the bacteria were incubated with agitation at 37^{o}C for 1 hour before plating on selective agar plates containing the appropriate antibiotic.

2.5.4.2 Plasmid Purification

Four millilitres of LB medium with selection was inoculated with a single bacterial colony and grown in a shaking incubator at 37^{o}C overnight. 1.5ml of the 4ml bacterial culture was pelleted by centrifugation at 16,000x *g* for 2 minutes. The plasmid was extracted according to manufacturer's instructions using the QIAprep Spin Miniprep Kit (Qiagen).

For plasmid amplification, after 8 hours of incubation, 200µl of the 4ml starter culture was used to inoculate a larger 200ml culture which was incubated overnight. Two hundred millilitre bacterial cultures were pelleted by centrifugation at 6000x *g* for 15 minutes at 4^{o}C. Pellets were either frozen at -80^{o}C or the plasmid extracted immediately using the Qiagen Plasmid Maxi Kit (#12163) according to manufacturer's instructions. Briefly, the Qiagen Plasmid DNA Isolation protocols lyse bacteria under alkaline conditions with SDS and RNase A to solubilise the cell membrane, denature proteins and DNA and to digest any RNA. Addition of acidic

potassium sulphate precipitates chromosomal DNA, proteins and debris and re-natures in-solution plasmid DNA. The insoluble debris is removed by centrifugation. The plasmid DNA is extracted from the supernatant by binding to a silica membrane under high salt conditions. Following washing the plasmid DNA is eluted with distilled water.

2.5.4.3 DNA Sequencing

DNA sequencing was performed in-house by the Weatherall Institute Human Immunology Unit Sequencing Service. The primers indicated in Table 2.16 were used to sequence vector constructs and genes. Normally, only sequencing of one vector or PCR strand was performed. Sequencing data was analysed by Finch TV.

Table 2.16 Sequencing primers

Primers were designed upstream of the multiple cloning site of vector constructs. The HERC1 mini-gene sequencing primers (HERC1 MG seq1-8) were designed at ~300bp intervals.

Primer	**Sequence (5'→3')**
pLXSN Sequencing Forward	CCCTTGAACCTCCTCGTTCGAC
pEFIRES Sequencing Forward	CCACTTTGCCTTTCTCTCCA
pcDNA seq fwd	GCGTGTACGGTGGGAGTCTA
HERC1 MG seq1	CAGACAAAGGGGCCAAACTA
HERC1 MG seq2	TTGGCTACAAGTGGCAATGA
HERC1 MG seq3	GCTACAGCCTGGTCAGGAGA
HERC1 MG seq4	AAGTGGGACCCTACAGGTCA
HERC1 MG seq5	AATCAAATTGCCAGGATGGA
HERC1 MG seq6	CAACCAGAGGACGGAAGTGT
HERC1 MG seq7	GCACAAAGAAGCCTCTGGAC
HERC1 MG seq8	ACTGGAGCAGATGGTGTGTG

2.6 Flow Cytometry

2.6.1 BAK N-terminal Conformation Change Assay

BAK undergoes a number of stages of activation during which an epitope at the N-terminus is exposed. This epitope is recognised by the BAK antibody Ab1 (#AM03,

Calbiochem), using a fluorophore conjugated secondary antibody, the amount of BAK that has undergone the N-terminal conformational change in cells can be measured by flow cytometry. This method has previously been published (Fox et al., 2010, Griffiths et al., 1999).

After treatment, the media was removed and cells washed once with PBS. The PBS was removed and cells fixed in 0.25% paraformaldehyde (PFA) in PBS for 10 minutes on ice. Cells were harvested by scraping and pelleted by microcentrifugation at 9,000rpm for 1 minute at 4^{o}C and resuspended in 100µl PBS. Cells were pelleted as previous and resuspended in 100µl PBS/0.01% saponin for 5 minutes to permeabilise the plasma membrane. Cells were pelleted and resuspended in 100µl BAK Ab1 primary antibody diluted 1/50 in PBS/0.01% saponin which binds to BAK which has undergone the N-terminal conformational change, or 100µl mouse IgG1 (BD Pharmingen) diluted 1/30 with PBS/0.01% saponin as a control for non-specific binding. Cell and antibody reactions were then incubated at 4^{o}C for 30 minutes with rotation. Cells were pelleted as above and washed in 100µl PBS/0.01% saponin for 3 minutes. Cells were pelleted and incubated in 100µl rabbit anti-mouse phycoerythrin [RPE conjugated rabbit anti-mouse Affinity-isolated F(ab')$_2$, Dako, #R0439] diluted 1/30 with PBS/0.01% saponin for 30 minutes at 4^{o}C with rotation. Cells were pelleted and resuspended in 500µl PBS for analysis. All flow cytometry analysis was performed using a CyAn ADP flow cytometer (Beckman) detecting phycoerythrin fluorescence.

Example data analysis is given in chapter 3.3.8. BAK activation is calculated in arbitrary units by subtracting the median fluorescence of the cell line IgG control from each test sample. The median value is then multiplied by the percentage of Ab1 positive cells as determined by the IgG control to give the Ab1 BAK specific fluorescence of each sample (BAK activation).

2.6.2 Active Caspase-3

Caspase-3 is synthesised as an inactive pro-enzyme. Caspase-3 is cleaved to an active form by caspase-8 in response to the extrinsic apoptosis pathway activation

and by caspase-9 in response to activation of the intrinsic apoptosis pathway. Caspase-3 is an effector caspase, cleaving other caspases and cellular substrates during the later stages of apoptosis. The active form of caspase-3 can be specifically recognised by a primary antibody directly conjugated to the fluorophore fluorescein isothiocyanate (FITC; excitation 495nm, emission 521nm) and subsequent detection by flow cytometry.

After treatment, the media from the cells was collected and stored to capture detached cells which may be positive for active caspase-3. Cells were then washed with PBS and the PBS collected and mixed with the media, again to capture any detached cells. Adherent cells were then detached with Accutase (Millipore), added to the media/PBS and pelleted by centrifugation at 1,500rpm for 5 minutes at 4^{o}C (Beckman Coulter, Allegra X-12R). The supernatant was removed and the cell pellet washed with 500µl PBS and transferred to a microcentrifuge tube. Cells were re-pelleted by microcentrifugation at 4,000rpm for 1 minute at 4^{o}C and fixed in 100µl 0.25% PFA in PBS on ice for 10 minutes. Cells were pelleted by microcentrifugation at 9,000rpm for 1 minute at 4^{o}C and washed with PBS. Cells were permeabilised with 100µl 0.1% saponin/PBS for 5 minutes and stained with anti-caspase-3 FITC conjugated antibody (BD Pharmingen, #550480) in a total volume of 100µl, 1 in 20 in 0.1% saponin/PBS by incubation in the dark at room temperature for 30 minutes with agitation. Cells were pelleted again by microcentrifugation at 9,000rpm for 1 minute at 4^{o}C and resuspended in 500µl PBS for analysis detecting FITC fluorescence. The percentage of cells positive for active caspase-3 above control cells is recorded. Data analysis shown in chapter 3.3.6.

2.6.3 Cytochrome *c* Release

Flow cytometric analysis of cytochrome *c* release was performed as described previously (Waterhouse and Trapani, 2003). After treatment adherent cells and non-adherent cells were pooled and the plasma membrane permeabilised with 0.05% digitonin in PBS with 100mM KCl before fixation with 4% PFA/PBS. Cells were washed three times with PBS to remove cytosol and any cytosolic cytochrome

c. Cells were then incubated with FITC conjugated anti-cytochrome *c* antibody (#NB100-78347; Novus Biologicals) in 3% BSA/PBS with 0.05% saponin overnight at 4°C. Cells were washed and resuspended in PBS for analysis. Approximately 10,000 cells were analysed per sample.

2.7 Immunocytochemistry

Cells were seeded on coverslips and, after treatment, the media was removed and cells were washed once with PBS. Cells were fixed with 4% PFA for 10 minutes at room temperature, permeabilised as indicated and blocked with 3% BSA blocker for 30 minutes. Cells were incubated with the indicated antibody for 1 hour (1/1000 in 1% BSA blocker/PBS) at room temperature (antibodies listed in Table 2.5). Any unbound primary antibody was removed by washing three times for 5 minutes with PBS. All secondary antibodies were used 1/2500; rabbit anti-mouse Alexafluor488 or goat anti-rabbit Alexafluor568 (Life Technologies), in 1% BSA/PBS and cells were incubated in the dark for 1 hour at room temperature. Unbound secondary antibody was removed with 3x 5 minute washes with PBS. Coverslips were then mounted on glass slides using Fluoromount-G (SouthernBiotech, #0100-01) containing DAPI (1µg/ml) and visualised using Carl Zeiss Axioskop 2 plus or Zeiss LSM 510 META confocal microscope as indicated.

For double staining, such as β_1-integrin and FAK, cells were first stained for FAK as above (using the goat anti-rabbit secondary antibody) and sequentially stained, after re-blocking, for β_1-integrin (using a rabbit anti-mouse secondary antibody).

For F-actin staining cells were permeabilised with 0.5% Triton X-100, blocked as above and incubated with the F-actin specific toxin phalloidin which was directly conjugated to Alexafluor635 (Life Technologies, #A34054). The stock solution of phalloidin conjugate (6.6µM) was diluted 1/100 in 1% BSA blocker/PBS for 30 minutes in the dark before washing three times with PBS and immediate mounting with fluoromount, containing DAPI, as above.

2.7.1 Proximity Ligation *In Situ* Assay

Cells were seeded on coverslips and after treatment the media was removed. Cells were washed once in PBS and then fixed for 10 minutes in cold 4% PFA in PBS at room temperature. Cells were washed once with PBS and stored in PBS at 4^{o}C. Cells permeabilised in 0.01% saponin/PBS and blocked in 10% horse serum with 0.2% fish skin gelatin/PBS for 30 minutes at room temperature then incubated with BAK Ab1 and HERC1 (Bethyl laboratories, ♯A301-904A) antibodies for 1 hour at room temperature. Cells were washed three times with PBS and interaction detected using Duolink II fluorescence (OLINK Bioscience) according to manufacturer's protocol. Briefly, secondary antibodies conjugated with complementary oligonucleotides were incubated with the cells. The two oligonucleotides, if in proximity, are ligated. In a rolling circle amplification reaction, if the oligonucleotides are ligated, fluorescently labelled oligonucleotides are incorporated to provide a distinct fluorescent spot indicating the two proteins are in proximity. Fluorescence detected using Carl Zeiss Confocal Laser Scanning Microscope 510.

2.8 Cell Migration Assays

EssenBio ImageLock 24 well plates were coated with 15µg/ml rat tail collagen I (collagen diluted in PBS with 127µM NaOH according to manufacturer's instructions) and air dried. Cells were seeded on the plates at 2x10^{5} cells/well and grown to confluence in RM+ media. Cells were treated with 10µg/ml mitomycin C for 1 hour at 37^{o}C to inhibit cell proliferation. The mitomycin C media was then removed and a scratch created in the confluent cell monolayer using a 10µl tip. Any detached cells were removed by washing with PBS and new culture media added. Cells were then monitored for migration using the Incucyte live cell imaging system (EssenBio). Images at three distinct points of each wound were taken at 2 hour intervals for a total of 10 hours. The Incucyte software then calculated the average percentage relative wound closure for each well at each time point.

2.9 Statistics

Statistics were calculated by unpaired t-test, one way or two way ANOVA where indicated. Bonferroni post-hoc test was used to compare means after ANOVA tests were performed. In all cases significance was taken to be less than 5% ($p \leq 0.05$). Calculations were performed using GraphPad Prism software.

Chapter 3 Investigation Into the Mechanism of HPV E6 Targeting of BAK Following DNA Damage

3.1 Introduction

The mechanism of how β-HPV may contribute to the progression of NMSC is unclear. Expression of the α- and β- type HPV E6 proteins can protect cells from apoptosis in response to UVB irradiation (Jackson and Storey, 2000, Struijk et al., 2008) by targeting both the intrinsic and extrinsic apoptosis pathways as previously discussed in chapter 1.4.5.4.

One of the ways in which E6 can act to prevent execution of the intrinsic apoptosis pathway in response to apoptotic stimuli is through targeting of the pro-apoptotic protein BAK. Activation of BAK, along with that of BAX, to result in MOMP is a key point in the decision of a cell to undergo apoptosis. As discussed in chapter 1.2.2, upon receipt of an apoptotic stimulus BAK undergoes dephosphorylation at Y108 (Fox et al., 2010). Binding of p53 or the BH3 only proteins, such as BID and BAD, then causes BAK to undergo an N-terminal conformational change involving exposure of a BH3 domain (Leu et al., 2004, Griffiths et al., 1999, Wei et al., 2000). Dephosphorylation of S117 by PP2A then exposes a hydrophobic pocket on the BAK molecule (Azad et al., 2012) which allows binding of the BH3 domain of another BAK monomer, permitting BAK to dimerise in a symmetric manner (Dewson et al., 2008). These BAK dimers assemble into oligomers which are believed to form pores that permeabilise the OMM (Figure 3.1), leading to the release of apoptotic factors, such as cytochrome *c*, and downstream apoptotic events. Therefore E6 expression preserves mitochondrial integrity and prevents release of apoptotic factors in response to UV (Leverrier et al., 2007), contributing to the survival of DNA damaged, HPV-infected cells that may contribute towards tumour formation (Jackson et al., 2002). Reviewed in Storey (2002).

The β-HPV5 E6 protein has evolved to upregulate Interleukin-6 expression whose downstream signalling cascade suppresses BAK function (Tomlins and Storey,

2010). The E6 proteins of both α- and β-HPV can also target BAK directly for proteasomal degradation (Underbrink et al., 2008, Jackson et al., 2000).

For a large number of proteins, targeting to the proteasome requires conjugation of a ubiquitin moiety to a substrate lysine residue through the recruitment of an E3 ubiquitin ligase. The high-risk α-HPV E6 proteins recruit the E3 ligase E6AP to constitutively target p53 for ubiquitination and degradation (Scheffner et al., 1993, Huibregtse et al., 1993b). For the high-risk α-HPV E6 proteins to degrade p53, E6 must first be stabilised by binding an L2G motif within E6AP, promoting a conformational change in the E6 protein (Ansari et al., 2012). E6 then self-associates via the N-terminus and binds the p53 core region, targeting p53 for degradation (Zanier et al., 2012, Li and Coffino, 1996). However the mechanism of BAK degradation due to β-HPV expression is less clear.

Previous work from this lab suggests that not all BAK in HPV5 E6 infected cells can be targeted for degradation. In addition, BAK degradation only occurred in HPV5 E6-expressing cells after UVB irradiation (Jackson et al., 2000) in contrast to some previous reports indicating that BAK was constitutively degraded (Du et al., 2004, Struijk et al., 2008).

3.2 Aim

The first aim of this work was to demonstrate the requirement of lysine residues for proteolysis of BAK after targeting by the E6 protein and to delineate the effects of a BAK lysine point mutation on E6-mediated BAK degradation and cell survival.

The second aim was to investigate the BAK activation process in cells expressing the HPV5 E6 protein. Given that not all BAK is targeted for degradation by the E6 protein, the aim was to determine at which stage of the activation process E6 targets BAK for degradation.

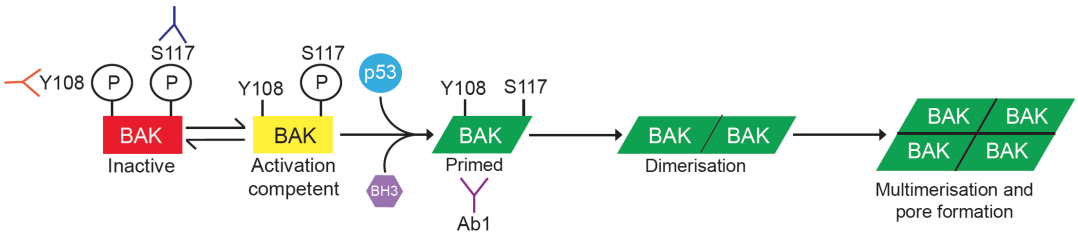


Figure 3.1 Schematic of BAK activation

The different conformations and modifications of BAK during its activation process can be recognised by antibodies. Antibodies against a phospho-Y108 BAK peptide and a phospho-S117 peptide are available. The commercially available Ab1 antibody from Calbiochem recognises an N-terminal epitope of BAK which is only exposed after BAK has been induced to undergo the N-terminal conformational change by transient binding of p53 or BH3 only proteins.

3.3 Results

3.3.1 Construction of pEFIRES vector expressing the HPV5 E6 sequence

Previous work surrounding HPV E6-mediated degradation of BAK has predominantly been carried out in the fibrosarcoma H1080 and p53 null Saos2 osteosarcoma cell lines. This showed that E6-mediated BAK degradation is cell type independent and suggested that E6-mediated degradation uses cellular machinery common to different cell types. The BAK and BAX null HCT116 cell line was chosen (HCT116$^{bak-/-bax-/-}$, gifted by R. Youle, hereby referred to as HCT116 double knockout cells [HCT116 DKO]) so that effects on BAK can be determined independently of BAX and permitting analysis of BAK mutants in subsequent experiments. Wild type (WT) *bak* was reintroduced by retroviral transduction as described in chapter 2.3.3 using the pLXSN vector (previously described in Fox et al., 2010). Successfully transfected cells were selected using G418 and cell line pools established.

The β-HPV5 E6 protein was chosen since targeting of BAK by HPV5 E6 is E6AP independent as it is a cutaneous viral protein, UV damage is therefore physiologically relevant. The HPV5 E6 gene was cloned into the pEFIRES vector which contains a bicistronic transcriptional unit that allows for transcription of a

puromycin selection cassette (allowing selection compatible with that of G418) along with the target sequence on a single transcript (Hobbs et al., 1998). The vector map is shown in Figure 3.2A. Primers were designed to amplify the HPV5 E6 gene from a pcDNA template vector with the *Nhe1* and *NotI* restriction sites on the forward and reverse primers respectively (sequences given in Table 2.14). The PCR was performed at two different annealing temperatures (66 and 70^{o}C) to determine which gave greatest yield and specificity and a fraction of the product examined by agarose gel electrophoresis. Figure 3.2B shows successful amplification of a product of the expected size (474bp) using the Velocity polymerase (Bioline) which has 5'-3' DNA polymerase and 3'-5' proofreading exonuclease activities. The use of this polymerase reduces the probability of mutations being induced for cloning.

Use of 66^{o}C for annealing gave a higher yield but both annealing temperatures gave a specific product. Therefore both PCR reactions were pooled and excess template DNA, primers and nucleotides removed using QIAquick PCR clean up (Qiagen). Both the pEFIRES vector and HPV5 E6 product were digested with the *NheI* and *NotI* restriction enzymes and phenol extracted to inhibit the enzymes and remove proteins. The phenol was removed by subsequent chloroform extraction. The HPV5 E6 insert was ligated into the pEFIRES vector and transformed into DH5α *E. coli* and selected on ampicillin plates. Colonies were grown and screened by test restriction digests on small preparations of DNA purified using QIAprep Spin Miniprep (Qiagen). DNA from colonies showing successful insertion of the HPV5 E6 sequence were confirmed by DNA sequencing. A clone with the correct sequence was amplified and DNA extracted by Qiagen Plamid Maxi kit (Qiagen). The pEFIRES vector encoding the HPV5 E6 gene is henceforth referred to as pEFIRES-5E6.

3.3.2 Generation of HCT116 DKO stable cell lines expressing pEFIRES and pEFIRES-5E6

The HCT116 DKO cells retrovirally transduced to express wild type BAK and selected using G418 (herein referred to as HCT116 WT BAK) were seeded at 1x10^{5}

A. *The image originally presented here cannot be made freely available via ORA because of copyright. The original image can be sourced using the reference given below.*

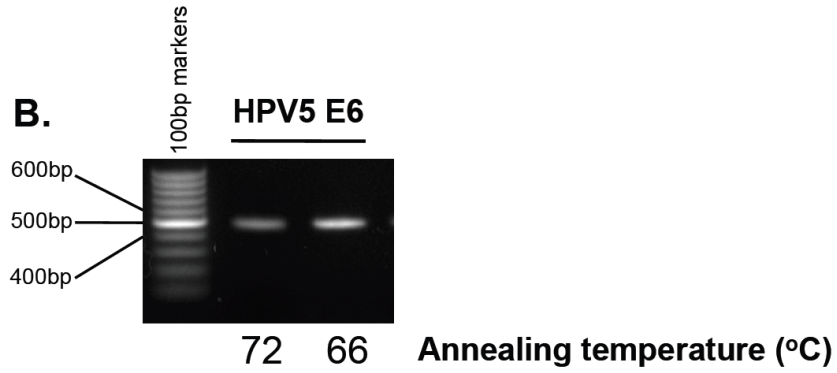


Figure 3.2 Construction of pEFIRES vector encoding the HPV5 E6 gene

A. The pEFIRES vector has a human elongation factor 1α promoter (pEF-1a), a chimeric intron (INTRON), a multiple cloning site with unique restriction sites indicated (MCS), an internal ribosomal entry site (IRES), a modified *pac* gene encoding puromycin N-acetyl transferase (pac), SV40 terminator/poly(A) signal (SV40 PA), phage f1 origin (f1) and ampicillin resitence gene (AmpR). Adapted from Hobbs et al. (1998)

B. The HPV5 E6 gene sequence was amplified from a vector to introduce the *NheI* and *NotI* restriction sites at the 5' and 3' ends respectively. The annealing step of the PCR was performed at 72°C and 66°C to optimise specificity and yield and the PCR products run on a 1% agarose gel. This product (474bp) was cloned into the pEFIRES vector using these restriction sites. The final HPV5 E6 encoding vector was confirmed by sequencing.

cells/well of a 6 well plate and transfected with 2µg of the pEFIRES or pEFIRES-5E6 vector using the Turbofect transfection reagent at a 3:1 ratio (Turbofect volume [µl] to DNA mass [µg]). The transfection reagent proved toxic if left for prolonged periods of time and the transfection media was therefore removed and replaced with culture medium after 4 hours. Successfully transfected cells were selected 24 hours after transfection by treatment with 0.4µg/ml puromycin for 7 days.

Successful selection was determined by complete cell death in untransfected HCT116 WT BAK cells and detection of HPV5 E6 transcripts from cell mRNA extracts. Briefly, mRNA was extracted from cell pellets and a reverse transcription reaction performed using a reverse transcriptase with random hexamers to generate a complementary DNA (cDNA) template. A PCR reaction using the Taq polymerase

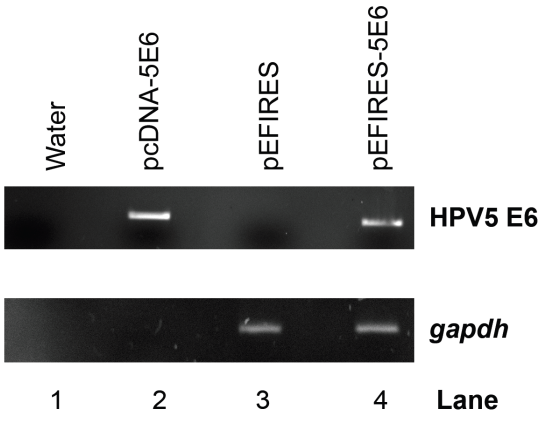


Figure 3.3 pEFIRES-5E6 expression in HCT116 WT BAK cells

mRNA was extracted using the Qiagen RNeasy kit from cell line pools of HCT116 WT BAK cells transfected with the pEFIRES or pEFIRES-5E6 vectors. cDNA was generated by reverse transcription and used in PCR reactions with the Taq polymerase and primers specific to the HPV5 E6 sequence (474bp product) or the house keeping gene *gapdh* (261bp product). Products were analysed by agarose gel electrophoresis. Lane 1 and 2; water or 10ng of the pcDNA vector encoding the HPV5 E6 gene was used in place of the cDNA template respectively, Lane 3 and 4; template cDNA generated from HCT116 WT BAK cells transfected with pEFIRES or pEFIRES-5E6, respectively.

with primers specific to the HPV5 E6 sequence or the cell housekeeping gene glyceraldehyde 3-phosphate dehydrogenase (*gapdh*) was then performed and the products analysed by agarose gel electrophoresis. Figure 3.3 shows that the HPV5 E6 transcript could only be detected in those cells transfected with the pEFIRES-5E6 vector and *gapdh* could be detected in both reactions using the cDNA template generated from cell mRNA extracts. A negative control reaction performed using water in place of cDNA showed there was no contamination of the reactions and the PCR performed using pcDNA vector encoding the HPV5 E6 gene (positive control) showed the primers could anneal to the HPV5 E6 sequence. Cell line pools were then established since high levels of E6 expression can be toxic to cells. The cell line pools were expanded to 80% confluence in 2 x T150cm^2 flasks, detached by trypsinisation and stocks frozen in 10% DMSO/FCS and stored in liquid nitrogen.

3.3.3 Effects on BAK levels in HCT116 WT BAK cells expressing HPV5 E6 following UVB irradiation

Having established HCT116 WT BAK cell lines expressing HPV5 E6 using the pEFIRES vector, it was necessary to characterise the activity of the HPV5 E6 protein towards BAK in this system as previous work has been performed in keratinocytes, Saos2 and HT1080 cell lines. Firstly the UVB dose required to stimulate BAK degradation in the HPV5 E6 expressing HCT116 WT BAK cell line, and its accumulation in the HCT116 WT BAK cells expressing the pEFIRES vector, was determined. The HCT116 WT BAK pEFIRES cell lines were seeded in 60mm dishes at 3x10^5 cells and irradiated with 2 or 5mJ/cm^2 UVB. As previous work from this lab has shown that BAK stabilisation in response to UVB can be detected upto 24 hours after irradiation (Jackson et al., 2000), cells were harvested in RIPA buffer 24 hours after treatment and lysates western blotted for total BAK levels using a rabbit monoclonal antibody. Figure 3.4A shows that BAK levels were increased in pEFIRES-expressing cells at both 2 and 5mJ/cm^2 UVB and, consistent with previous reports, BAK levels were reduced at both UVB doses in cells expressing pEFIRES-5E6. Here, initial levels of BAK are higher in HPV5 E6-expressing cells, compared to cells expressing the empty vector. Since 5mJ/cm^2 gave the greatest

stabilisation in pEFIRES-expressing cells and the greatest reduction in BAK levels in pEFIRES-5E6-expressing cells, 5mJ/cm^2 was used in subsequent in experiments.

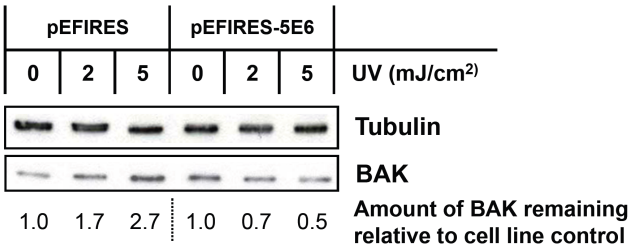
3.3.4 Levels of p53 and E6AP in response to UVB in HCT116 WT BAK cells expressing HPV5 E6

To check that expression of the HPV5 E6 protein in this cell system did not alter p53 behaviour and that the dose of UVB determined in Figure 3.4A caused sufficient DNA damage to stimulate the DDR, involving upregulation of p53, HCT116 WT BAK cells expressing pEFIRES or pEFIRES-5E6 were seeded as before and exposed to 5mJ/cm^2 UVB. Cells were lysed in RIPA buffer 24 hours later and lysates western blotted for p53, BAK and E6AP. This confirms that BAK levels are reduced upon UVB exposure in HPV5 E6-expressing cells, though initial BAK levels in HPV5 E6 cells are higher than pEFIRES-expressing cells, and that p53 levels are increased in both empty vector and HPV5 E6-expressing cells in response to UVB (Figure 3.4B). Western blotting for E6AP, the E3 ligase associated with α-HPV E6 protein degradation of p53, demonstrates that E6AP levels were unchanged in both cell lines and is unaffected by UVB in this system. Therefore, these results show that HPV5 E6 does not target p53 for degradation as previously reported for other systems. They also suggest that these cells make a useful experimental system in which to investigate BAK activity.

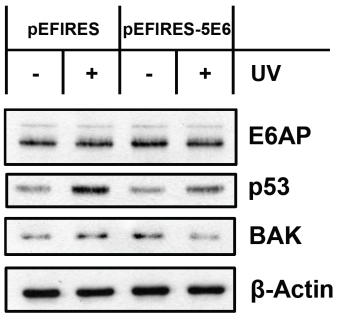
3.3.5 BAK is targeted to the proteasome by HPV5 E6 in HCT116 WT BAK cells

Expression of the cutaneous E6 proteins, through modulation of transcription regulatory proteins such as the histone acetyl transferases p300 and TIP60, and exposure to UVB are known to alter cellular gene expression (Howie et al., 2011, Jha et al., 2010, Crish and Eckert, 2008, Weinkauf et al., 2012). Therefore to ensure that the decrease in BAK levels in HPV5 E6-expressing cells in response to UVB was not an alteration of gene transcription or mRNA levels by the E6 protein, or UV itself, real time quantitative PCR (RT-QPCR) was performed. mRNA was extracted from HCT116 WT BAK cells expressing pEFIRES or pEFIRES-5E6 16 hours after exposure to 5mJ/cm^2 UVB using the Qiagen RNAeasy kit. A cDNA template was

A.



B.



	Amount of protein remaining relative to untreated cell line control			
	pEFIRES		pEFIRES-5E6	
UV	**-**	**+**	**-**	**+**
E6AP	1.0	1.1	1.0	1.0
p53	1.0	3.1	1.0	2.0
BAK	1.0	1.5	1.0	0.6

Figure 3.4 Levels of BAK, p53 and E6AP in response to UVB in HCT116 WT BAK cells expressing pEFIRES-5E6

A. Western blot of total BAK levels (~28kDa) in HCT116 WT BAK cells expressing pEFIRES or pEFIRES-5E6 24 hours after irradiation with 2 or 5mJ/cm^2 UVB.

B. Western blot of p53 (53kDa), E6AP and total BAK levels 24 hours after treatment with 5mJ/cm^2 UVB in HCT116 WT BAK cells expressing pEFIRES or pEFIRES-5E6. Changes in protein levels were quantified relative to the amount of protein in the unirradiated cell line control for this blot (shown in the adjacent table).

NB. Three N-terminal splice variants of E6AP exist (predicted to be ~90, 98 and 100kDa) which are visible on the blot.

Antibodies: Total BAK; Abcam ＃ab32371, p53; CRUK DO1, E6AP; Bethyl Laboratories ＃A300-352A

ImageQuant software was used to quantitate protein levels. Protein intensities were normalised to the β-actin loading controls. The normalised protein intensity was divided by that of the untreated cell line control to give the amount of protein remaining relative to cell line control.

Experiment performed three times. A representative image is shown.

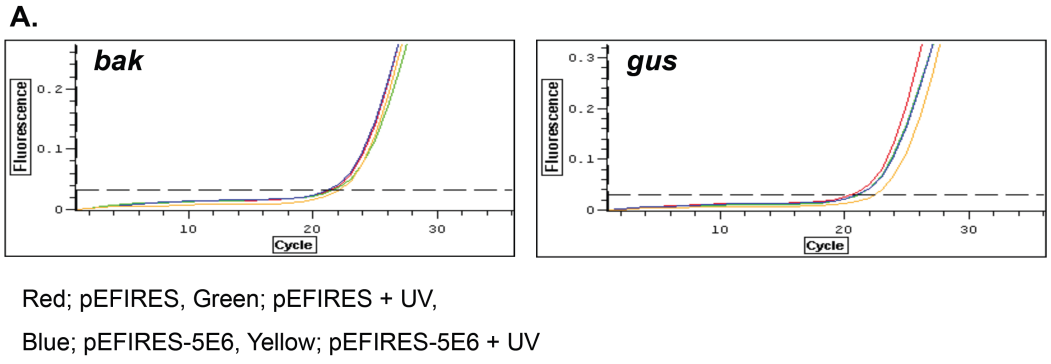


Figure 3.5 *bak* mRNA levels in HCT116 WT BAK cells expressing pEFIRES-5E6 in response to UVB

A. RT-QPCR for *bak* was performed on cDNA generated from mRNA prepared from HCT116 WT BAK cells expressing pEFIRES or pEFIRES-5E6 16 hours after exposure to UVB.

B. Example RT-QPCR curves. The C(t) is the point at which the amplified products (coloured lines) cross the threshold (dashed line).

C. The mean number of PCR cycles normalised to the housekeeping gene *gus* required for the *bak* fluorescence to reach the detection threshold [C(t)] is shown. n=3, mean ± SEM.

D. Agarose gel electrophoresis of example real time PCR products from (A). PCR product for *bak* is 248bp, that for *gus* is 190bp.

PCR reactions performed three times.

generated according to manufacturer's instructions using the reverse transcriptase DyNAmo SYBR Green 2-Step RT-QPCR Kit. This was then used in a RT-QPCR reaction using the same kit with primers for *bak* and *gus* (β-glucuronidase; reference gene to control for cDNA loading). The PCR cycle number at which the fluorescence signal reaches the threshold [cycle threshold; C(t)] was manually set to be just at the exponential phase of detection before the PCR reaction efficiency becomes variable across the reactions (Figure 3.5A). The C(t) for *gus* of each sample was normalised to the pEFIRES control and the C(t) for *bak* normalised to that of the equivalent *gus* reference gene, accounting for variation in difference of cDNA template loading. Figure 3.5B demonstrates that all samples had similar normalised C(t) values for *bak* indicating that *bak* transcription is unaffected by HPV5 E6 expression and UVB irradiation in these cells. The PCR products from the reactions were analysed by agarose gel electrophoresis to ensure that the primers were specific, examples are shown Figure 3.5C. These data suggest that the changes in BAK protein levels observed in Figure 3.4 are not due transcriptional changes, rather post-translational modifications.

To confirm that the HPV5 E6 protein affects BAK protein levels by targeting to the proteasome the HCT116 WT BAK cell lines were irradiated with 5mJ/cm^2 and treated with three different proteasome inhibitors (50μM lactacystin, 37.5μM MG115 or 10μM MG132, all purchased from Sigma) for 2 hours prior to harvesting, a total of 18 hours after UVB irradiation. Lysates were western blotted for total levels of BAK. Figure 3.6 shows that that some decrease in BAK levels could be detected in HCT116 WT BAK cells expressing pEFIRES in response to UVB, this may be the result of some natural BAK turnover or an increase in cell death. In pEFIRES-5E6-expressing cells BAK levels were reduced to a much greater extent than that observed by the pEFIRES-expressing cells upon UVB irradiation, again higher initial levels of BAK are observed in HPV5 E6-expressing cells compared to those expressing the empty vector. The different proteasome inhibitors have different mechanisms of action and some are more specific to the proteasome than others

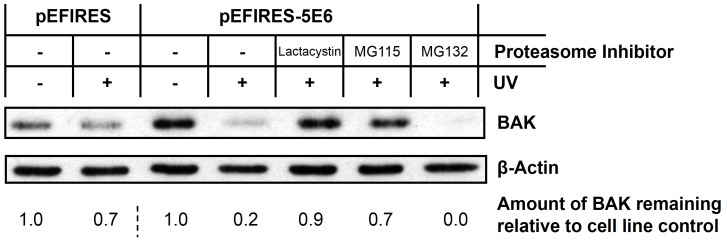


Figure 3.6 BAK protein levels in HCT116 WT BAK cells expressing pEFIRES-5E6 in response to UVB and proteasome inhibitors

Western blot of BAK levels in HCT116 WT BAK cells 18 hours after exposure to UVB. HPV5 E6-expressing cells were treated with 3 different proteasome inhibitors for 2 hours prior to harvesting: 50μM lactacystin, 37.5μM MG115 or 10μM MG132.

Blot performed three times. Representative image shown.

(Kisselev and Goldberg, 2001). Lactacystin is a very specific proteasome inhibitor and treatment of UVB irradiated HPV5 E6-expressing cells with lactacystin rescued BAK levels. Treatment with MG115 also rescued BAK levels, though to a slightly lesser extent than lactacystin, however treatment with the proteasome inhibitor MG132 failed to stabilise BAK levels after UVB irradiation. Since lactacystin is regarded as the 'gold standard' proteasome inhibitor and MG115 has a lower specificity for the proteasome but was also able to rescue BAK levels, these data suggest that HPV5 E6 in this cell system is targeting BAK to the proteasome to give the observed reduced levels of BAK in response to UVB. MG132, though widely used as a proteasome inhibitor, also has lower specificity for the proteasome and failure to rescue BAK levels here might be the result of cell specific effects.

3.3.6 Caspase-3 activation in HPV5 E6 expressing HCT116 WT BAK cells in response to UVB

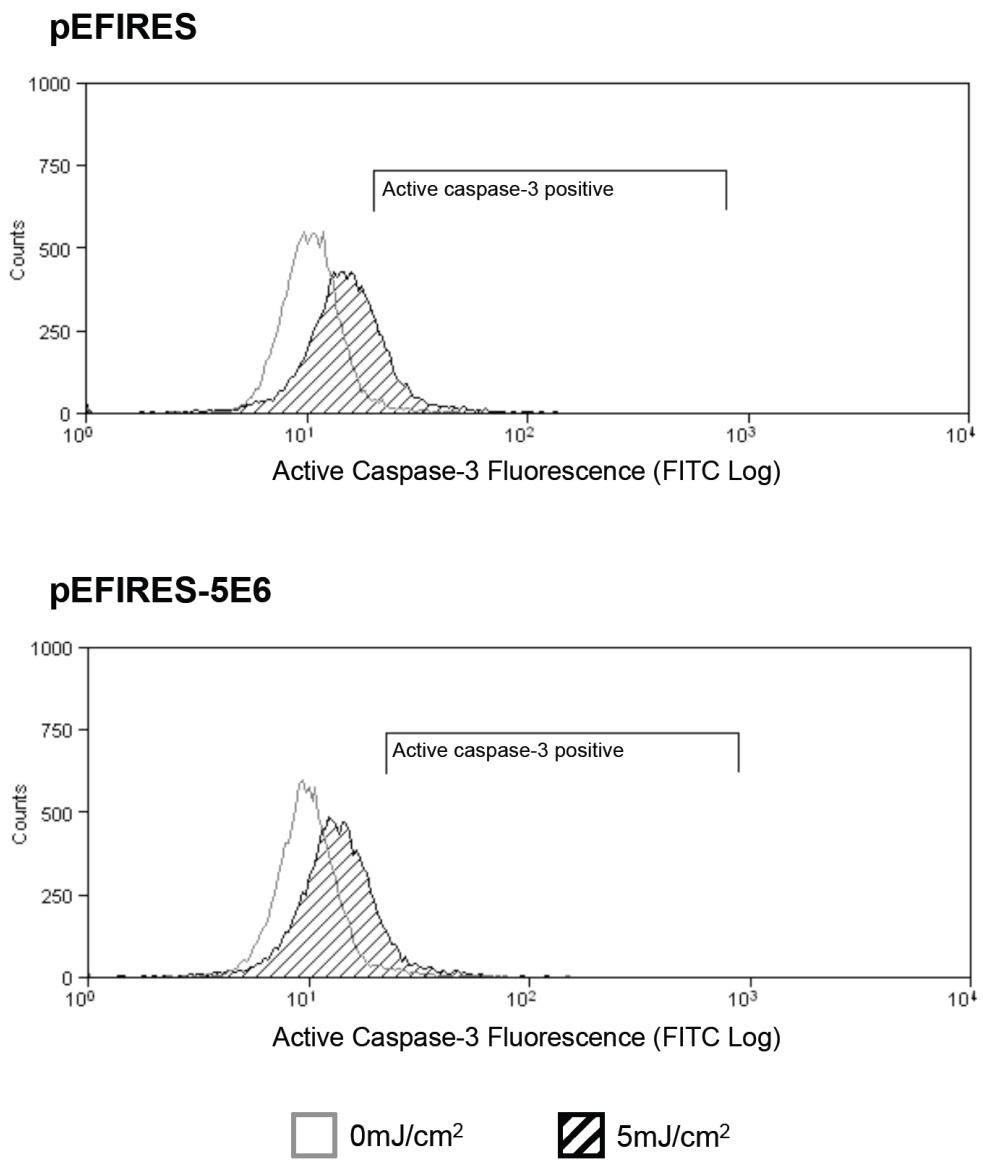
To further characterise the HPV5 E6 protein activity in HCT116 WT BAK cells a UVB dose response was performed on pEFIRES and pEFIRES-5E6-expressing cells to determine if expression of the HPV5 E6 protein can protect these cells from apoptosis. A flow cytometry assay using an antibody conjugated to FITC recognising the cleaved, and therefore active, form of the downstream apoptosis effector caspase-3 was used as a marker of apoptosis induction.

HCT116 WT BAK cells expressing pEFIRES or pEFIRES-5E6 were irradiated with 0, 2, 5 or 10mJ/cm^2 UVB and analysed for staining of active caspase-3 24 hours later. Figure 3.7A shows example traces of the FITC fluorescence for both pEFIRES and pEFIRES-5E6-expressing cells with and without UVB irradiation. The gate for baseline active caspase-3 staining was set to 3% of the untreated control as it is assumed that the majority of cells in the untreated samples should not have any active caspase-3 and, in addition, only the most brightly stained cells are investigated. Each untreated cell line control was then gated to this baseline percentage of cells positive for active caspase-3 of 3% and the change in the percentage of cells positive for active caspase-3 upon UVB measured so as to reflect changes in caspase-3 activation only in response to UVB exposure. Upon treatment with UVB a shift in the peak for active caspase-3 staining (FITC fluorescence) is observed. The percentage of cells falling within the gate was recorded (Figure 3.7B).

Figure 3.7C shows that only a small increase in the percentage of cells positive for active caspase-3 was observed for both pEFIRES and pEFIRES-5E6-expressing cells when irradiated with 2mJ/cm^2 UVB compared to untreated cells. This suggests that this dose of UVB is insufficient to stimulate caspase-3 activation. Upon irradiation with 5 and 10mJ/cm^2 UVB both pEFIRES and pEFIRES-5E6-expressing cell lines had a significant increase in the percentage of cells positive for active caspase-3 compared to each untreated cell line control. However, comparison of the percentage of cells positive for active caspase-3 between pEFIRES and pEFIRES-5E6-expressing cell lines at each UVB dose in Figure 3.7D by two way ANOVA shows that upon irradiation with 5mJ/cm^2 UVB there was a significantly lower percentage of pEFIRES-5E6-expressing cells that were positive for active caspase-3 compared to pEFIRES-expressing cells irradiated with the same dose. A similar observation is made at 10mJ/cm^2 irradiation however the lower percentage of pEFIRES-5E6-expressing cells positive for active caspase-3 compared to pEFIRES-

Figure 3.7 Caspase-3 activation in HCT116 WT BAK cells expressing pEFIRES-5E6 in response to UVB

A.



B.

Cell line	% of cells positive for active caspase-3	
	0mJ/cm^2	**5mJ/cm^2**
pEFIRES	3.31	31.33
pEFIRES-5E6	3.18	10.15

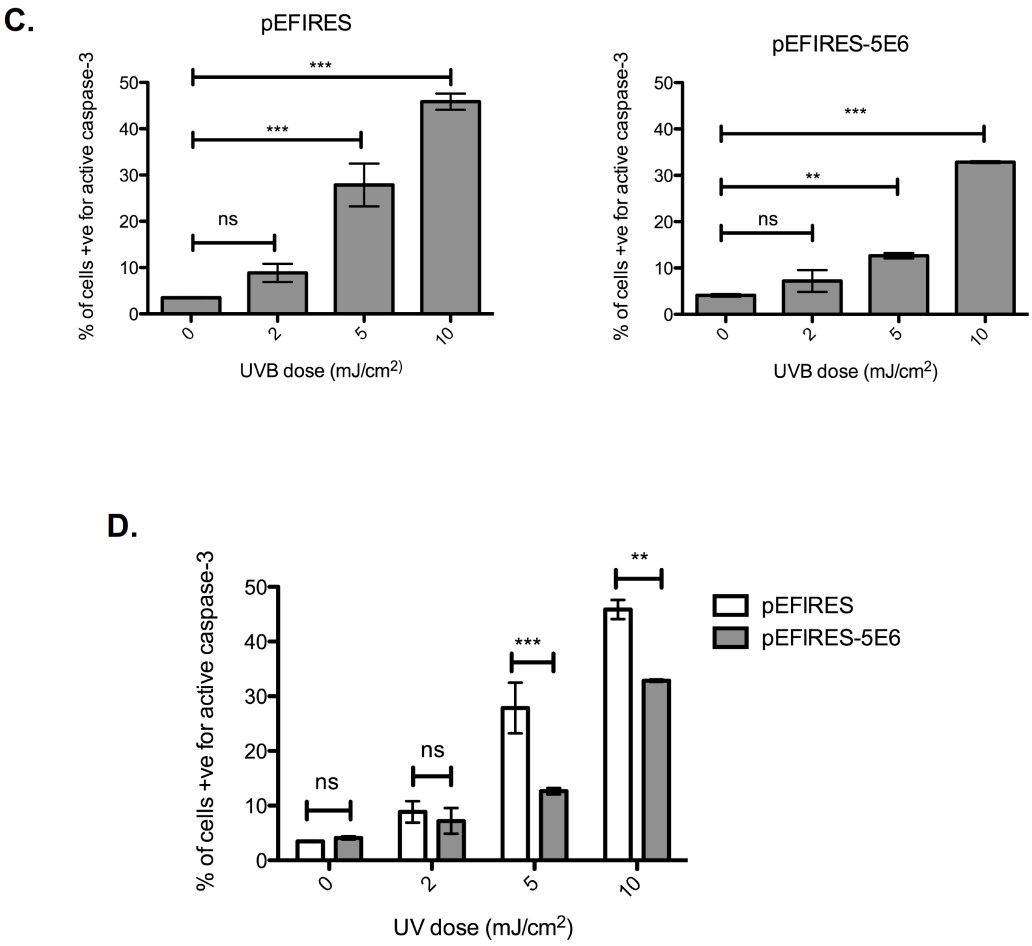


Figure 3.7 legend

A. Example traces of active caspase-3 measurement by flow cytometry in HCT116 WT BAK pEFIRES and pEFIRES-5E6 cell lines after exposure to UVB. Gates were set at 3% for each unirradiated cell line. The percentage of cells within that gate after UVB irradiation was recorded as shown in (B).

B. Table showing figures for the example trace in (A). Each experimental condition was performed in triplicate and the average percentage of cells positive for active caspase-3 calculated.

C. HCT116 WT BAK cells expressing HPV5 E6 were irradiated with 2, 5 or 10mJ/cm^2 UVB. Twenty-four hours later the levels of active caspase-3 were analysed by flow cytometry using an antibody conjugated to FITC recognising only the cleaved form of caspase-3. n=3 ± SEM. Statistical significance calculated using one way ANOVA and compared to 0mJ/cm^2 control.

D. To compare effects at each UVB dose across cell lines the data in (C) was analysed using two way ANOVA. ** p≤0.01, *** p≤0.001.

Flow cytometry analysis performed three times.

expressing cells is less marked than upon irradiation with 5mJ/cm^2. These data suggest that the HPV5 E6 protein cannot completely abrogate the apoptotic response to UVB irradiation at higher UV doses, as measured by caspase-3 activation. The small increase observed may be the result of the extrinsic apoptosis pathway activity. These data also show that the HPV5 E6 protein is able to reduce caspase-3 activation most efficiently over a narrow range of UVB doses, particularly at 5mJ/cm^2 as used for previous studies.

3.3.7 Generation of a BAK lysine mutant

In order to investigate the requirement of a lysine residue in E6-mediated BAK turnover, the 211 amino acid sequence of BAK was analysed revealing it possesses only two lysine residues. Proteins usually contain many lysine residues making this task more difficult, however the BAK lysine residues were identified at positions 113 and 210. Since K210 is positioned at the very C-terminus of BAK, close to the transmembrane domain (residues 188-205; Lazarou et al., 2010) on the internal side of the OMM it is unlikely to be accessible for ubiquitination. Consequently, K113 was identified as the most likely candidate for ubiquitination as it is located on the BAK surface. It is also on the same α4 helix as Y108 and S117, residues implicated as being important for activation, suggesting that this is a notable regulatory region (Figure 3.8A). To investigate the role of K113 in HPV5 E6-mediated BAK degradation, this amino acid was mutated to another positively charged amino acid, arginine (K113R), a strategy frequently used to determine ubiquitination sites in other proteins (Rodriguez et al., 2000, Batonnet et al., 2004, Tan et al., 2008).

Figure 3.8B suggests that this mutation does not alter the overall structure of BAK. Codon mutation of AAG to AGG was performed using the QuikChange II XL Site-Directed Mutagenesis Kit (Stratagene) according to chapter 2.5.3 using the primers given in Table 2.15. Mutagenised plasmids were transformed into bacteria, plated onto selective plates and the DNA from single colonies extracted and screened by sequencing to check for correct mutants. A correct clone was isolated

Figure 3.8 Mutation of BAK residue K113 to arginine

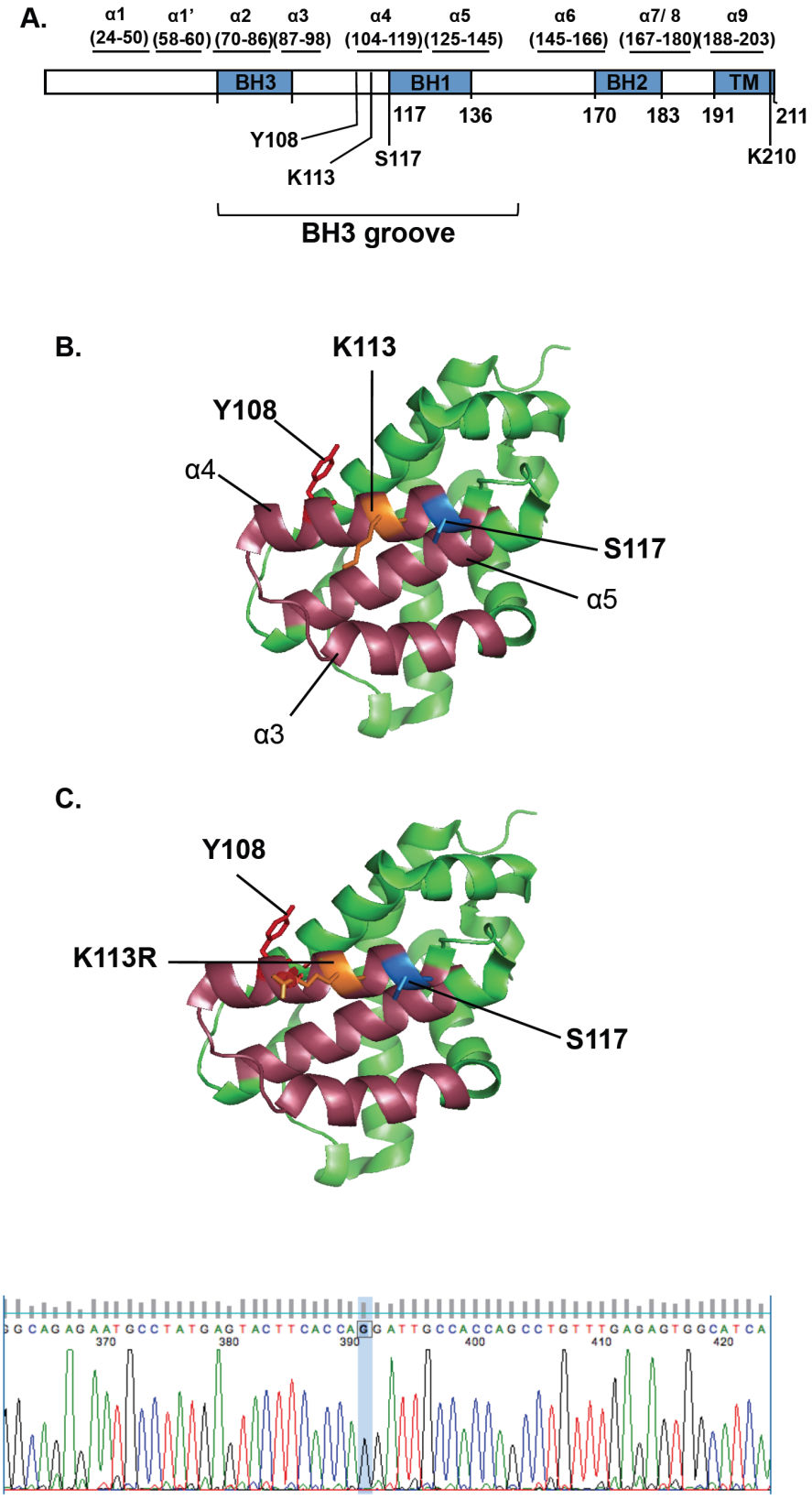


Figure 3.8 legend

A. Schematic showing the lysine residues in BAK.

B. Model of BAK structure showing the location of K113 (orange) in the same α helix as Y108 (red) and S117 (blue) suggesting this is an important regulatory region. The three magenta helices (α3, α4 and α5) form the hydrophobic groove. This model lacks the C-terminus. Modeled in PyMOL using Protein Data Bank file 2IMS.

C. Lysine 113 in WT BAK was mutated to arginine (K113R).

D. Sequencing trace showing successful mutation of the nucleotide, changing the codon from AAG to AGG.

---

and the DNA plasmid amplified and extracted (the sequence trace showing the mutation is given in Figure 3.8C). The pLXSN-K113R BAK vector was retrovirally transduced into HCT116 DKO cells and selected as previously described for WT BAK in chapter 3.3.1 (hereby referred to as HCT116 K113R BAK). Lysates were prepared from parental HCT116 DKO cells, and those selected for expression of WT BAK and K113R BAK, and western blotted for BAK to check that mutation of K113 in BAK did not prevent expression of the protein. Figure 3.9 shows that K113R BAK is expressed in HCT116 cells, albeit at a reduced level compared to WT BAK.

3.3.8 Characterisation of the BAK K113R mutant

Before investigating the effect of mutation of K113 to arginine on activity of E6 towards BAK it was necessary to investigate whether the mutation affected BAK activity. In order for BAK to become activated to result in pore formation and MOMP, BAK undergoes an N-terminal conformational change. Upon doing so an epitope recognised by the BAK antibody Ab1 is exposed (Griffiths et al., 1999). By exposure of this epitope the amount of BAK undergoing the N-terminal conformational change can be investigated using a flow cytometry assay using the Ab1 antibody. Figure 3.10A shows an example trace of BAK staining by flow cytometry with Ab1 and an increase in staining in response to UVB in HCT116 WT BAK cells. Figure 3.10B shows an example of how the data is manipulated to quantify BAK activation

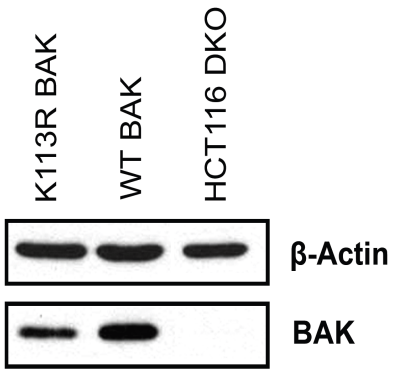


Figure 3.9 Expression of WT and K113R BAK by retroviral infection in HCT116 DKO cells

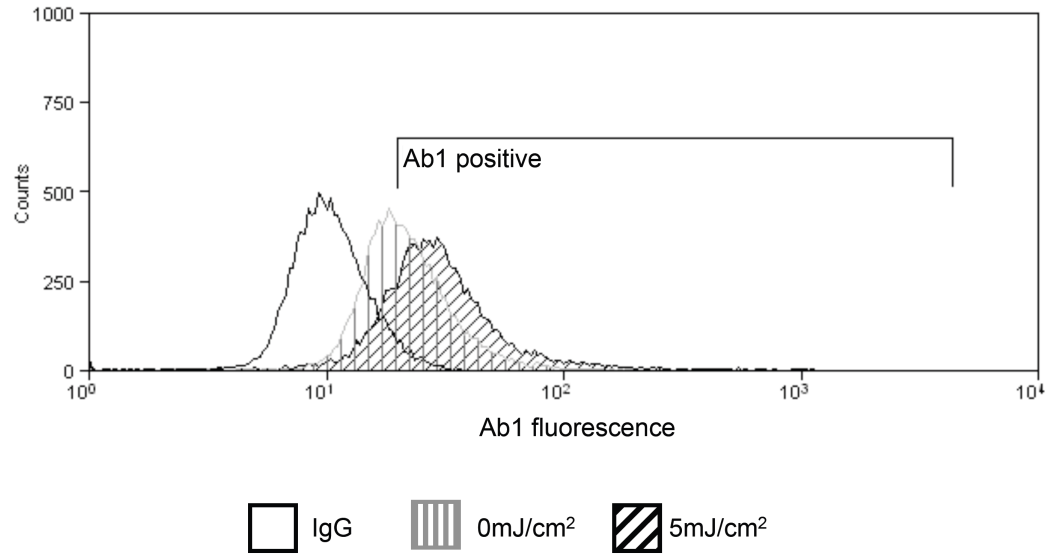
The pLXSN vector encoding K113R or WT BAK was transduced into HCT116 DKO cells and a cell line pool established. Lysates of the selected cells were western blotted for expression of BAK.

(as previously published Griffiths et al., 1999, Fox et al., 2010). Briefly, the median BAK-associated fluorescence was determined by subtracting the median fluorescence of the cell line IgG control from each test sample. The median value was then multiplied by the percentage of Ab1 positive cells as determined by the IgG control to give the Ab-1 BAK specific fluorescence of each sample (BAK activation).

Figure 3.11A shows the calculated BAK activation values for HCT116 WT BAK and BAK K113R cells in response to the indicated doses of UVB 8 hours after treatment. These data show that the amount of BAK K113R that undergoes the N-terminal change increases in a UVB dose dependent manner. Furthermore, the assay suggests that mutation of lysine 113 to arginine does not affect the ability of BAK, when compared to WT BAK, to undergo the N-terminal conformational change stage of its activation process.

In order to effectively permeabilise the OMM through pore formation, BAK must dimerise and subsequently multimerise. The ability of BAK to multimerise can be assessed through the use of protein cross-linkers and analysing the presence of the higher molecular weight structures by western blotting. It has been previously

A.



B.

	Median	Median – IgG Median	% cells Ab1 positive	BAK activation (arbitrary)
0mJ/cm^2	20.8	10.7	57.0	609.9
5mJ/cm^2	28.8	18.7	80.8	1511.0

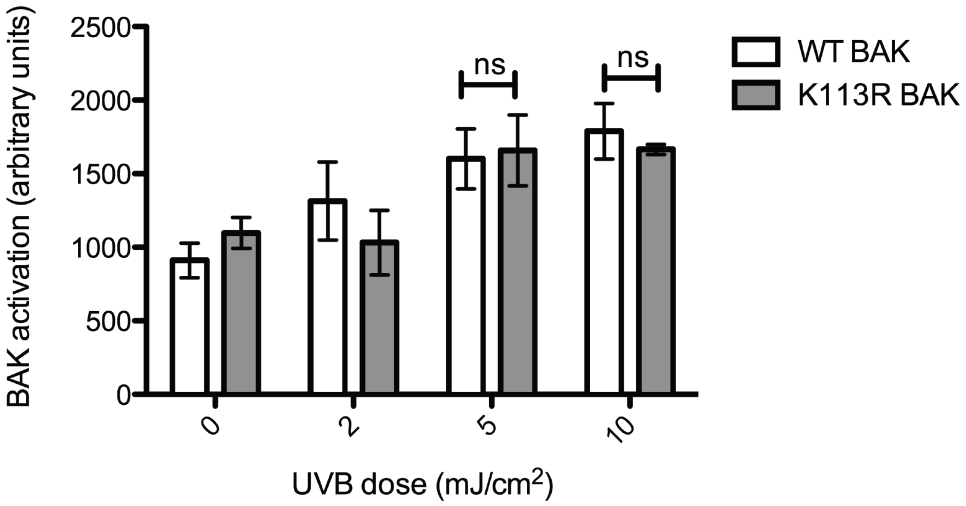
IgG median = 10.1

Figure 3.10 Calculation of BAK activation using Ab1 fluorescence by flow cytometry

A. Example trace of Ab1 staining by flow cytometry (#AM03, Calbiochem). An IgG control is used to gate for basal, non-specific staining. Staining with the Ab1 antibody, recognising an epitope in BAK only exposed once BAK has undergone its N-terminal conformational change, gives a right shift in Ab1 fluorescence upon UVB irradiation.

B. Table showing manipulation of the flow cytometry data to give BAK activation. Arbitrary units are used. Ab1 positive cells are gated on 5% of the IgG as a background reading. The sample median and percentage within the Ab1 positive gate is recorded. The IgG median is subtracted from the sample median. The resulting median is multiplied by the percentage of Ab1 positive cells.

A.



B.

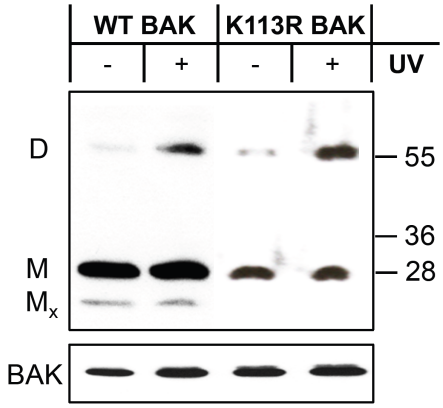


Figure 3.11 Characterisation of HCT116 cells expressing K113R BAK compared to those expressing WT BAK

A. HCT116 K113R BAK and HCT116 WT BAK cells were exposed to the indicated doses of UVB. After 8 hours cells were fixed in PFA, permeabilised with saponin and stained using the Ab1 BAK antibody which binds to BAK that has undergone the N-terminal conformational change. The amount of BAK activation is quantified by flow cytometry analysis. n=3 ± SEM, statistical significance calculated using two way ANOVA, ns; $p \geq 0.05$ was taken as not significant. Flow cytometry analysis performed three times.

B. HCT116 WT BAK and HCT116 K113R BAK cells were irradiated with 10mJ/cm^2 UVB. Eight hours later the amount of dimerised BAK was measured by cross-linking mitochondria enriched fractions using BMOE and western blotting for BAK. The bands at 28kDa represent monomeric BAK (M) and those at 55kDa represent dimerised BAK (D). M_x indicates intra-molecularly cross-linked BAK.

C.

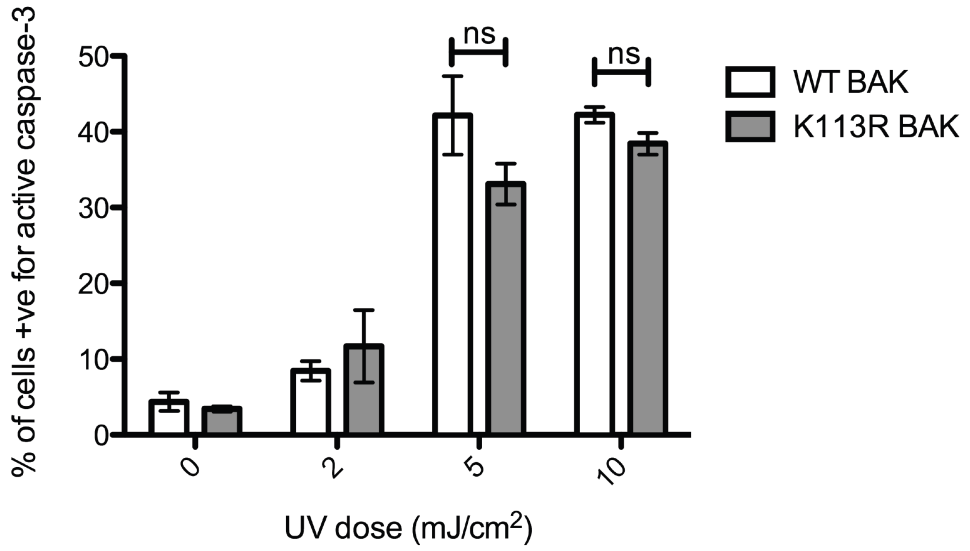


Figure 3.11 continued

C. HCT116 K113R BAK and HCT116 WT BAK cells were exposed to the indicated dose of UVB. Twenty-four hours later cells were fixed with PFA and stained with an antibody recognising the cleaved (active) form of caspase-3. The percentage of cells positive for active caspase-3 was analysed by flow cytometry. The baseline percentage of cells positive for caspase-3 was set to 3% for WT BAK and all other samples analysed using this gate. n=3 ± SEM, significance calculated by two way ANOVA, ns; $p \geq 0.05$ was taken as not significant.

Flow cytometry analysis performed three times.

published that BAK multimerisation can be detected 8 hours after irradiation with 10mJ/cm^2 UVB (Azad et al., 2012). Consequently, HCT116 WT or K113R BAK-expressing cells were seeded on 150mm dishes and irradiated. The samples were harvested and then enriched for the mitochondrial fraction (see chapter 2.4.7). BAK dimers in the mitochondrial fraction were cross-linked using a short-armed sulfhydrl-sulfhydryl protein cross-linker, BMOE. BMOE only detects dimers and not higher order structures (Dewson et al., 2008).

Figure 3.11B shows that, upon separation by SDS-PAGE and western blotting for BAK, 8 hours after 10mJ/cm^2 UVB exposure higher order complexes of approximately 55kDa, consistent with that of BAK dimers, could be recognised upon irradiation in both HCT116 WT and K113R BAK cells. It is perhaps noteworthy that the ratio of higher order complexes to monomer for the BAK K113R mutant is higher than that of WT BAK. As BAK dimerisation is analysed using the mitochondria enriched cell fraction, these data suggest that the K113R BAK mutant is able to localise to the mitochondria and dimerise and is therefore able to induce MOMP.

Finally, to confirm that the ability to undergo apoptosis in BAK K113R-expressing cells is not compromised, caspase-3 activation was measured using the active caspase-3 flow cytometry assay previously described. HCT116 WT and K113R BAK were irradiated with the indicated doses of UVB and analysed 8 hours later. Figure 3.11C shows that no significant difference in the percentage of cells positive for active caspase-3 was detected between cells expressing WT and K113R BAK at all doses of UVB. Together, these data suggest that mutation of K113 to arginine on BAK does not affect the ability of BAK to be activated in response to UV damage and to induce apoptosis.

3.3.9 Requirement of K113 for HPV5 E6-mediated degradation of BAK

Having established that BAK K113R behaves comparably with WT BAK in the Ab1 flow cytometry, multimerisation and caspase-3 activation assays, cell lines stably expressing the HPV5 E6 protein were generated by transfection with the pEFIRES or pEFIRES-5E6 vectors and selection with puromycin as previously described.

After selection mRNA was extracted, cDNA generated using a reverse transcription reaction and expression of HPV5 E6 mRNA verified using a PCR reaction with primers recognising the HPV5 E6 sequence, along with *gapdh* to monitor cDNA quality, as previously described. Figure 3.12A shows that HPV5 E6 transcripts could only be detected in HCT116 K113R BAK cells transfected with the pEFIRES-5E6 plasmid. K113R BAK degradation induced by the HPV5 E6 protein expression was then investigated in these cells.

The HCT116 WT BAK and K113R cells stably expressing pEFIRES or pEFIRES-5E6 were seeded at $2x10^5$ cells in 60mm dishes and left untreated or irradiated with 5mJ/cm^2 UVB. Twenty-four hours later the cells were harvested and lysed in RIPA buffer and BAK levels analysed by western blot. Figure 3.12B shows that after UVB irradiation the relative levels of K113R BAK to untreated cell line controls in cells expressing pEFIRES increased by 50%. In pEFIRES-5E6-expressing cells the levels of the K113R mutant BAK remained approximately the same after irradiation. As previously shown, WT BAK levels were stabilised in pEFIRES-expressing cells upon UVB irradiation but decreased in HCT116 WT BAK cells expressing pEFIRES-5E6 upon UVB exposure. These data show that the HPV5 E6 protein cannot mediate degradation of K113R BAK in response to UVB.

3.3.10 Caspase-3 activation in response to UVB in HCT116 K113R cells expressing HPV5 E6

Having shown that the HPV5 E6 protein is unable to target BAK K113R for degradation it was of interest to determine whether the HPV5 E6 protein could protect cells expressing this mutant form of BAK from apoptosis, as measured by capase-3 activation. HCT116 WT and K113R BAK cells expressing pEFIRES or pEFIRES-5E6 were seeded in 60mm dishes and remained either untreated or were irradiated with 5mJ/cm^2. Twenty-four hours later the cells were analysed for caspase-3 activation as before using flow cytometry.

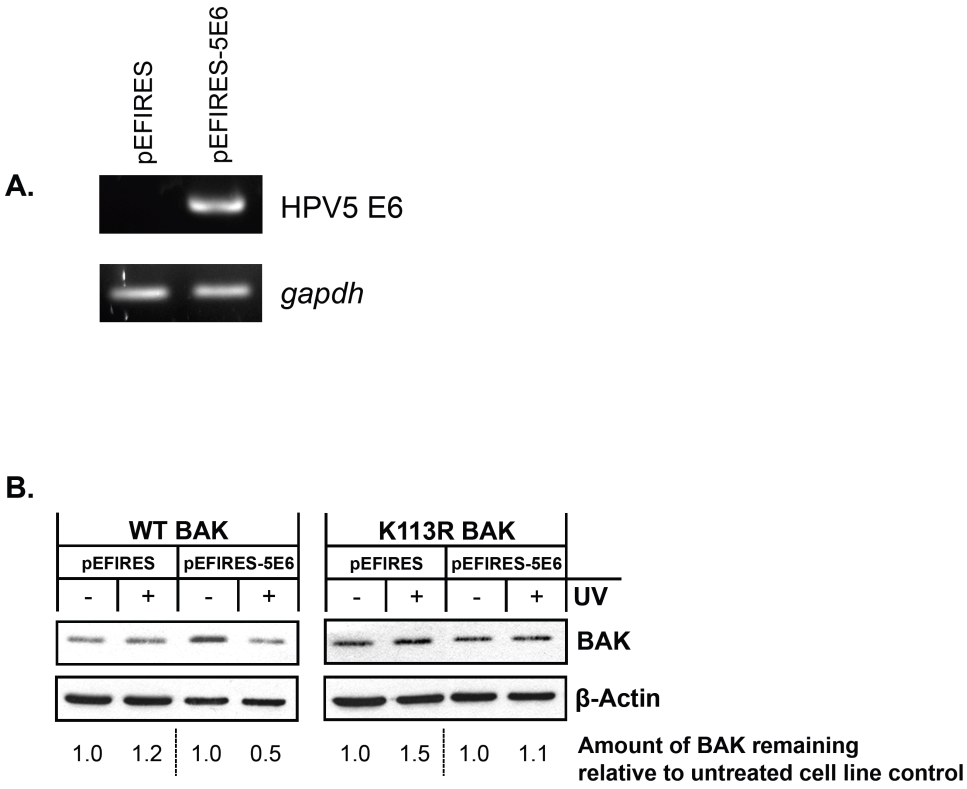


Figure 3.12 K113R BAK levels in HCT116 cells expressing pEFIRES-5E6 after UVB irradiation

A. An agarose gel showing expression of HPV5 E6 mRNA in HCT116 K113R BAK cells transfected with the pEFIRES or pEFIRES-5E6 vector using primers specific to the HPV5 E6 gene (474bp) in a PCR reaction using template cDNA generated from the K113R BAK-expressing cell lines. Primers to *gapdh* used as control (261bp).

B. HCT116 cells expressing K113R or WT BAK ± HPV5 E6 were irradiated ± 5mJ/cm^2. Twenty-four hours later BAK protein levels were analysed by western blot. Blots perfomed three times.

Figure 3.13A shows the data analysed by setting the flow cytometry gate to a baseline of 3% of cells positive for active caspase-3 for HCT116 WT BAK cells expressing pEFIRES and this was used for all cell lines. Analysing the data in this manner highlights differences in the percentage of cells positive for caspase-3 activation between the unirradiated cell lines. It can be seen that the percentage of HCT116 K113R BAK cells expressing pEFIRES that were positive for active caspase-3 is slightly lower than those cells expressing WT BAK and the pEFIRES vector. This may be a result of the lower expression levels of K113R BAK observed (Figure 3.8).

The percentage of cells positive for active caspase-3 in unirradiated HCT116 K113R BAK pEFIRES-5E6-expressing cells is seen to be higher than that of HCT116 K113R BAK cells expressing pEFIRES, this may be attributed to cellular stress as a result of E6 expression as a similar observation is made for cells expressing WT BAK. Whilst HCT116 K113R cells expressing pEFIRES still exhibit an increase in the percentage of cells positive for active caspase-3 upon UVB irradiation, the percentage of HCT116 K113R BAK pEFIRES cells positive for active caspase-3 upon UVB irradiation was less than those expressing WT BAK pEFIRES exposed to UV. However treatment of HCT116 K113R BAK pEFIRES-5E6-expressing cells with UVB leads to a significantly higher ($p \leq 0.001$) percentage of cells positive for active caspase-3 compared to irradiated HCT116 K113R BAK pEFIRES cells. This may be a result of the differences in starting percentages of cells positive for active caspase-3 accounted for by differences in expression of WT and K113R BAK (previously shown in Figure 3.9) and, as noted above, by the effects of E6 expression. To address this the data was also analysed by normalising the baseline percentage of cells positive for active caspase-3 to 3% for each of the unirradiated control cell lines, showing only the increase in the percentage of cells positive for active caspase-3 in response to UVB irradiation. These data are shown in Figure 3.13B. Analysing the data in this way shows that cells expressing K113R

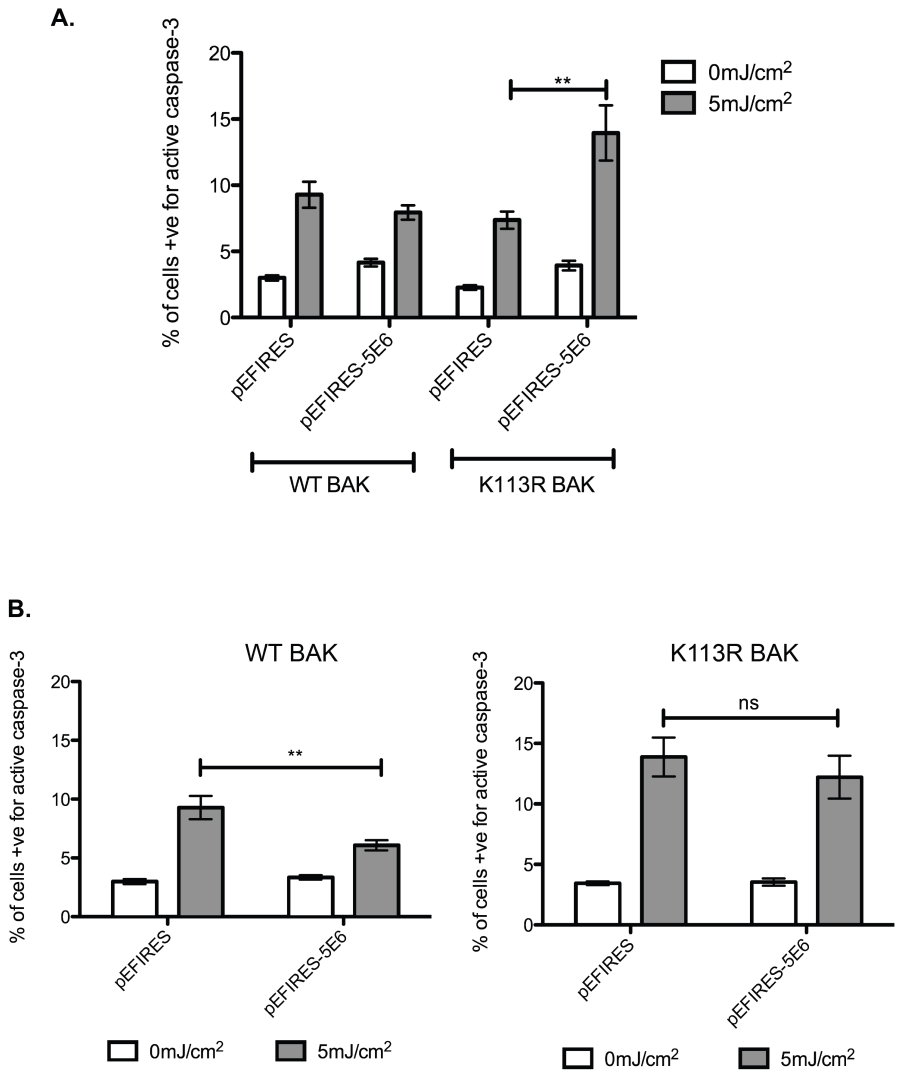


Figure 3.13 Caspase-3 activation in HCT116 K113R BAK cells expressing HPV5 E6 in response to UVB

A. HCT116 WT or K113R BAK cells ± HPV5 E6 were irradiated ± 5mJ/cm^2 UVB. Twenty-four hours later cells were stained for cleaved (active) caspase-3 as a marker of apoptosis and the percentage of cells positive for cleaved caspase-3 was measured by flow cytometry. The baseline gate was set to 3% for the WT pEFIRES cell line and all other data sets were analysed using this gate. **p≤0.01, by two way ANOVA.

B. The same data as in (A) was analysed by setting the baseline gate to 3% for each cell line so only the change in caspase-3 activation in response to UVB is represented. n=3, mean ± SEM, ns; p≥0.05 was taken as not significant, **p≤0.01, by two way ANOVA.

Flow cytometry analysis performed three times.

BAK and pEFIRES are able to activate caspase-3 to a greater extent than that of cells expressing WT BAK and pEFIRES in response to UVB. Consistent with previous data, there is a significantly lower ($p \leq 0.001$) percentage of HCT116 WT BAK pEFIRES-5E6-expressing cells positive for active caspase-3 compared to those expressing only pEFIRES upon UVB irradiation, as analysed by two way ANOVA. In contrast, there is no significant difference in the percentage of cells positive for active caspase-3 between HCT116 K113R BAK cells expressing pEFIRES or pEFIRES-5E6 in response to UVB irradiation, implying that cells expressing the HPV5 E6 protein are no longer able to limit the activation of caspase-3 in response to UVB in K113R BAK cells.

3.3.11 Phosphorylation status of Y108 in response to UVB in HCT116 WT BAK cells expressing HPV5 E6

Consistent with previous observations from the lab, E6-mediated degradation of BAK occurs only in response to UVB and is incomplete (Figure 3.4 and Figure 3.6). These findings suggest that only a proportion of BAK molecules undergo activation to reach a particular conformation and that it is only these molecules that are targeted for degradation. Our lab has shown that for BAK to be activated it must be dephosphorylated at Y108 by protein tyrosine phosphatases to result in an 'activation competent' form of BAK (Fox et al., 2010) that can then go on to undergo the conformational change and multimerise. Levels of BAK dephosphorylated at Y108 can be investigated by immunoprecipitating BAK using anti-sera generated against a phospho-Y108 BAK peptide (as previously described in Fox et al., 2010).

To begin to explore which conformation of BAK is targeted by E6, HCT116 WT BAK cells were seeded in 150mm plates and treated with 10mJ/cm^2 UVB and harvested 8 hours later since pilot data had previously shown that BAK dephosphorylation could not be detected in control cells using 5mJ/cm^2. Lysates were prepared using Triton X-100 based buffer which were then incubated with the anti-sera for phospho-BAK Y108 and Protein G sepharose beads. The precipitated proteins were

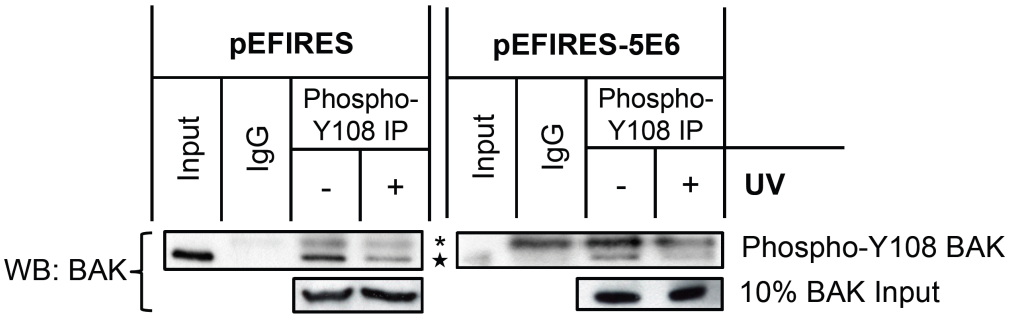


Figure 3.14 Dephosphorylation of BAK at Y108 in response to UVB in HCT116 WT BAK cells expressing HPV5 E6

BAK was immunoprecipitated from HCT116 WT BAK cells 8 hours after exposure to 10mJ/cm^2 UVB using anti-sera specific to the phospho-Y108 form of BAK and western blotted for total BAK using the BAK Ab1 antibody.

Experiment performed three times.

* Indicates non-specific IgG band. ★ Indicates BAK band.

then analysed by western blot. Figure 3.14 shows that the amount of BAK precipitated with the phospho-BAK Y108 anti-sera decreased in both control and HPV5 E6-expressing cells after irradiation. This suggests that the first stage of BAK activation in cells expressing HPV5 E6 can proceed normally.

3.3.12 Phosphorylation status of S117 in HCT116 WT BAK cells expressing HPV5 E6 in response to UVB

In order to proceed through its activation process BAK undergoes an N-terminal conformational change to expose a BH3 domain. The N-terminal conformational change can be stimulated by two pathways: binding of BH3 only proteins such as BID and BIM to the hydrophobic grove of BAK or by binding of p53 to an area distinct from that of the hydrophobic pocket. Binding of the BH3 only proteins requires exposure of the BH3 domain binding hydrophobic pocket on BAK which this lab has shown is occluded in inactive BAK by phosphorylation of S117 (Azad et al., 2012). By immunoprecipitation of BAK using anti-sera against a phospho-S117

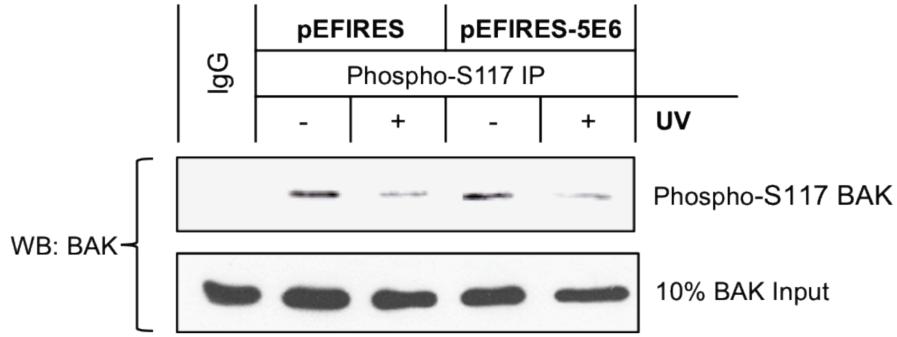


Figure 3.15 Dephosphorylation of BAK at S117 in response to UVB in HCT116 WT BAK cells expressing HPV5 E6

BAK was immunoprecipitated from mitochondria enriched HCT116 WT BAK cell lysates 8 hours after exposure to 10mJ/cm^2 UVB using anti-sera specific to the phospho-S117 form of BAK and then western blotted using an antibody recognising total BAK.

Experiment performed twice.

peptide, the ability of S117 to be dephosphorylated in response to UVB in HCT116 WT BAK cells expressing pEFIRES-5E6 was examined.

As previously noted for phospho-BAK Y108, pilot data suggested that S117 dephosphorylation could not be detected in response to 5mJ/cm^2 in control cells. Therefore HCT116 WT BAK cells expressing pEFIRES or pEFIRES-5E6 were irradiated with 10mJ/cm^2 UVB and harvested 8 hours later. As the anti-sera to phospho-BAK S117 was not as good as that for phospho-BAK Y108, BAK was precipitated from mitochondrial enriched cell fractions prepared by Dounce homogenisation as previously described. The mitochondrial fraction was then lysed with 1% CHAPS buffer and incubated with anti-sera against phospho-BAK S117 overnight at 4^{o}C, precipitated the next day with Protein G sepharose and western blotted for BAK (previously described by Azad et al., 2012). Dephosphorylation of BAK at S117, as shown by reduced levels of BAK immunoprecipitated by the anti-sera, could be detected in HCT116 WT BAK cells expressing both pEFIRES and pEFIRES-5E6 in response to 10mJ/cm^2 UVB irradiation 8 hours after treatment

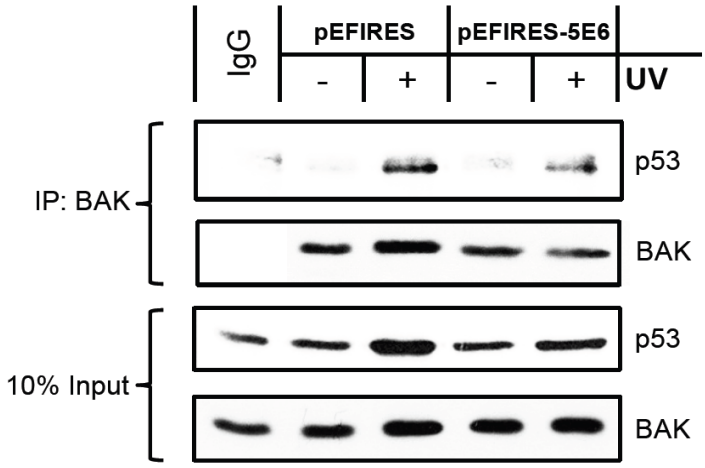


Figure 3.16 p53 binding to BAK in response to UVB in HCT116 WT BAK cells expressing HPV5 E6

HCT116 WT BAK cells expressing HPV5 E6 were irradiated with 10mJ/cm^2 UVB. Eight hours later mitochondrial extracts were prepared and then solubilised in 1% CHAPS buffer. BAK was immunoprecipitated using the rabbit BAK antibody (Abcam). The immunoprecipitates were western blotted for p53 (DO1) and BAK (Ab2 antibody). The untreated pEFIRES extract was used for the IgG control.

(Figure 3.15). This suggests that exposure of the hydrophobic pocket of BAK, to which BH3 only proteins can bind, is unaffected by expression of the HPV5 E6 protein.

3.3.13 Binding of p53 to BAK in HCT116 WT BAK cells expressing HPV5 E6 in response to UVB

Binding of p53 to BAK to stimulate its N-terminal conformational change involves translocation of p53 to the mitochondria. In previous experiments performed by this group, p53 mitochondrial localisation has been detected in HCT116 cells 2-4 hours after treatment with an apoptotic stimulus. Upon translocation to the mitochondria, p53 can bind BAK, independently of S117 status, at a site distinct from that of the hydrophobic pocket involving residues E24, E25 and R160 (Pietsch et al., 2008a). It is noteworthy that translocation of p53 to the mitochondria is dependent on p53 binding to the E24/E25 residues in BAK in HCT116 cells (Azad et al., 2012). The ability of p53 to translocate and bind to BAK was probed by the ability of p53 to be co-precipitated with BAK in untreated and irradiated pEFIRES and pEFIRES-5E6

expressing HCT116 WT BAK cells. As shown in Figure 3.16, p53 could only be detected when BAK was immunoprecipitated from cells which had received UVB treatment showing that p53 binding to BAK is unaffected by expression of the HPV5 E6 protein.

3.3.14 Investigation of the BAK N-terminal conformational change in response to UVB irradiation in HCT116 WT BAK and HT1080 cells expressing the HPV5 E6 protein

To determine if the amount of BAK undergoing the N-terminal change in response to UVB was altered in HPV5 E6-expressing cells HCT116 WT BAK pEFIRES and pEFIRES-5E6 cells were irradiated with 5mJ/cm^2 and 8 hours later fixed in 4% PFA for analysis by Ab1 flow cytometry. Figure 3.17A shows example raw flow cytometry data for this assay where an increase in the amount of BAK that has undergone the N-terminal conformational change has increased in both cells expressing both pEFIRES and pEFIRES-5E6. However, showing the mean raw BAK activation as biological replicates is difficult as the status of the cells may vary, subsequently the ability of BAK to undergo the N-terminal conformational change calculated by the fold change relative to the unirradiated cell line control for three independent experiments is shown in Figure 3.17B. This demonstrates that HCT116 WT BAK cells expressing pEFIRES-5E6 are able to undergo the N-terminal conformational change in response to 5mJ/cm^2 UVB to the same extent as those expressing pEFIRES. The lower dose of UVB was used here as the flow cytometry assay is more sensitive than that of the protein techniques used previously. HT1080 cells have been used extensively to investigate the targeting of BAK for degradation by the E6 protein (Jackson et al., 2000, Jackson and Storey, 2000, Leverrier et al., 2007), the ability of BAK in these cells to undergo the N-terminal conformational change was therefore also investigated using the Ab1 flow cytometry assay.

Stable cell line pools expressing HPV5 E6 were generated by transfecting the HT1080 parental cell line with the pcDNA vector or pcDNA encoding the HPV5 E6 gene using Fugene 6 (Roche) and selecting with 500µg/ml G418 until untransfected

Figure 3.17 BAK activation in HCT116 WT BAK and HT1080 cells expressing HPV5 E6 in response to UVB

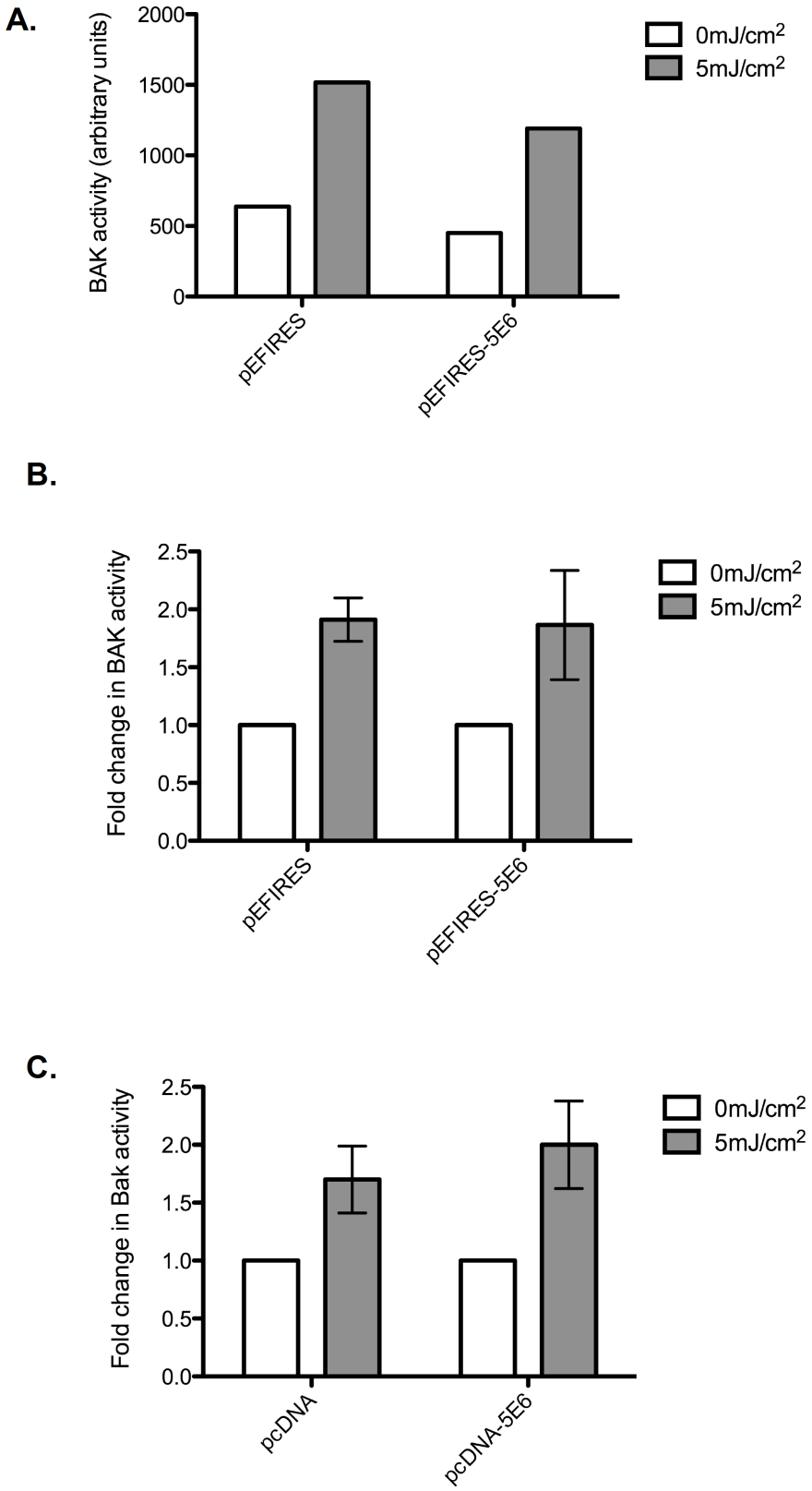


Figure 3.17 legend

A. Example raw data from Ab1 flow cytometry analysis of BAK activation in response to UVB in HCT116 WT BAK cells expressing pEFIRES or pEFIRES-5E6, n=1

B. Graphs showing the fold change in BAK activity using the Ab1 flow cytometry assay 8 hours after 5mJ/cm^2 UVB irradiation in HCT116 WT BAK cells expressing pEFIRES-5E6, n=3 ± SEM

C. Fold change in BAK activity using the Ab1 flow cytometry assay 8 hours after 5mJ/cm^2 UVB irradiation in HT1080 cells expressing pcDNA-5E6, n=3 ± SEM.

---

parental controls were dead as previously described (Jackson and Storey, 2000). These cell lines were seeded at 2x105 cells in 60mm dishes and irradiated with 5mJ/cm2 UVB and stained for Ab1 flow cytometry analysis 8 hours later as previously described. The data in Figure 3.17C shows that BAK is also able to undergo the N-terminal conformational change in response to UVB in HT1080 cells expressing either empty vector or HPV5 E6 in a similar manner to that in the HCT116 WT BAK cell lines (fold changes in response to UVB shown). As the N-terminal conformational change cannot proceed without dephosphorylation of Y108, dephosphorylation of S117 or p53 binding, Figure 3.17 implies that these modifications are likely to proceed normally in HT1080 cells expressing the HPV5 E6 protein.

Taken together the dephosphorylation, p53 translocation and N-terminal conformational change assays indicate that E6 does not interfere with the early steps of the BAK activation process. Furthermore, experiments using the BAK K113R point mutant suggest that the K113 residue in BAK is important for E6-mediated BAK turnover and prevention of caspase-3 activation in E6-expressing cells.

3.3.15 Temporal regulation of BAK degradation in HPV5 E6 expressing HCT116 WT BAK and HT1080 cells

In order to better understand the temporal regulation of E6-mediated degradation of BAK the WT BAK pEFIRES and pEFIRES-5E6 cell lines were subjected to cyclohexamide chase ± UVB irradiation and harvested at the indicated time points.

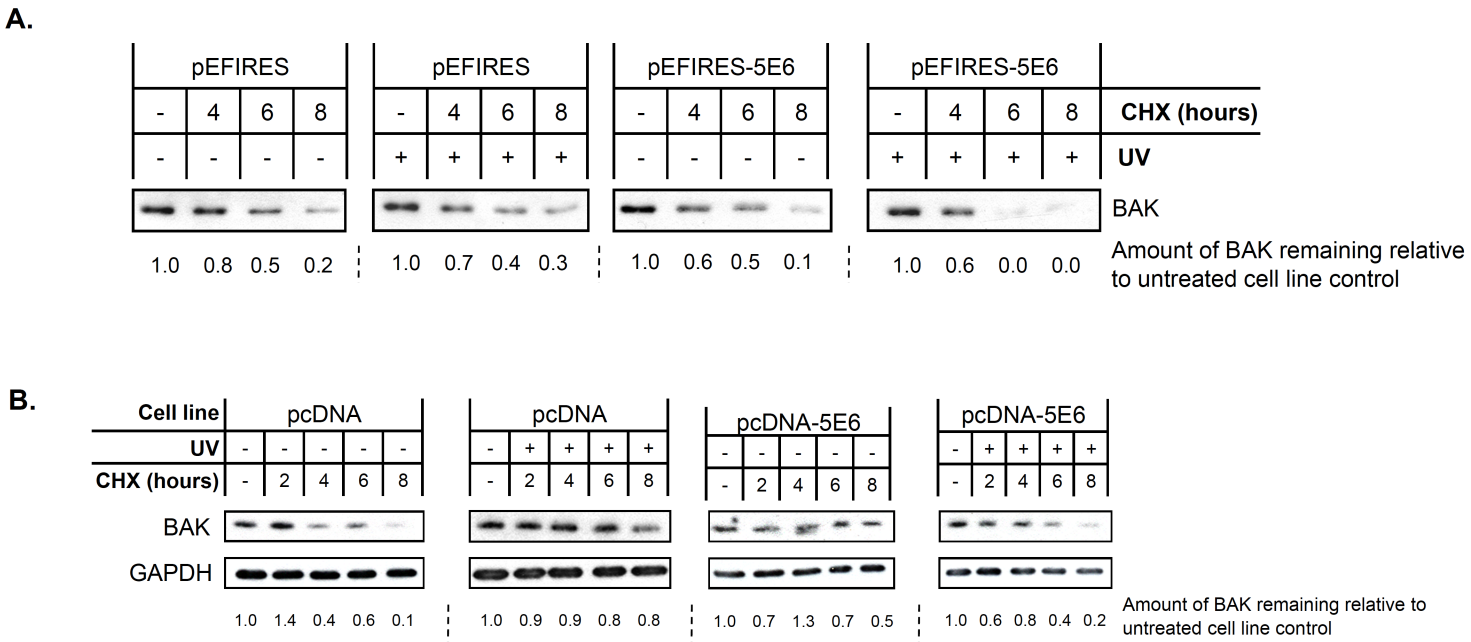


Figure 3.18 Temporal regulation of HPV5 E6-mediated BAK degradation in HCT116 WT BAK and HT1080 cells

A. HCT116 WT BAK cell expressing pEFIRES of pEFIRES-5E6 were treated with 100µg/ml cyclohexamide ± 5mJ/cm^2 UVB for the indicated time points. Cells were harvested in RIPA buffer and western blotted for BAK. Experiment performed twice with consistent results.

B. The same experiment as in (A) was performed using HT1080 cells expressing pcDNA or pcDNA-5E6. CHX; cyclohexamide. Data from a single experiment.

Total levels of BAK were analysed in the lysates by western blot and are shown in Figure 3.18A. The level of BAK relative to the untreated cell line controls in the pEFIRES cells at each of the time points was consistent in both unirradiated and UVB exposed samples with BAK still detectable 8 hours post UV treatment. The same degree of BAK turnover was observed in the unirradiated HPV5 E6-expressing cells. However, in response to UVB irradiation HPV5 E6-expressing cells had undetectable levels of BAK at 6 hours. Data in this chapter suggest that the E6 protein targets BAK after it has undergone the N-terminal conformational change into its 'primed' conformation. Given that BAK turnover in HPV5 E6 cells in response to UV is consistent with that of the empty vector cells at 4 hours suggests that BAK is not targeted immediately by E6 following UVB irradiation supporting previous observations that BAK must first undergo the post-translational modifications associated with the early steps of BAK activation.

BAK turnover by cyclohexamide chase was also investigated in HT1080 pcDNA and pcDNA-5E6-expressing cell lines. The experiment was performed as described for the HCT116 cell lines and the results are shown in Figure 3.18B. Similar to HCT116 cells, a reduction in BAK levels is observed after 4 hours in untreated cells

expressing pcDNA and continues to decrease 8 hours after cyclohexamide treatment. Upon UVB irradiation the levels of BAK are stabilised over the 8 hour time course. Conversely in non-irradiated HPV5 E6-expressing cells the half-life of BAK is prolonged whilst, when treated with UVB, the levels of BAK begin to be reduced after 6 hours of cyclohexamide and UVB treatment and continue to reduce after 8 hours of treatment. As the level of BAK at 0 hours in empty vector and HPV5 E6-expressing cells is equivalent, this data supports the idea that HPV5 E6 is targeting an active conformation of BAK which is induced by UVB treatment. Further investigation is required to determine if the same molecular mechanisms are used to degrade BAK in the untreated empty vector cells compared to irradiated HPV5 E6-expressing cells.

3.3.16 Targeting of a BAK mutant unable to expose the hydrophobic pocket for degradation by the HPV5 E6 protein

Previous data suggests that BAK is targeted by the E6 protein in the later stages of the BAK activation process. To further probe the point in the activation process at which BAK is targeted by E6, a BAK construct with a point mutation of S117 to glutamic acid was available in the lab (S117E). The glutamic acid residue places a negative charge to block access to the hydrophobic groove on BAK (Figure 3.19). This mutant has previously been characterised where it was shown that the mutant prevents the binding of BH3 peptides, preventing BAK dimer and multimer formation (Azad et al., 2012). However the mutant is still able to bind p53 and can therefore undergo the N-terminal conformational change (Azad et al., 2012). It follows that HCT116 DKO cell lines were generated expressing BAK S117E (HCT116 BAK S117E) and pEFIRES or pEFIRES-5E6 as previously described for WT BAK and K113R BAK.

HCT116 BAK S117E pEFIRES ± HPV5 E6 cell lines were seeded at $3x10^5$ cells in 60mm dishes and irradiated with 5mJ/cm^2 UVB. Eight hours later the cells were fixed with PFA and analysed for Ab1 antibody staining by flow cytometry to check that, in the presence of the E6 protein, this BAK mutant could undergo the N-terminal conformational change. Figure 3.20A shows that in response to UVB both WT BAK and BAK S117E underwent an increase in activation to a similar degree.

Subsequently the ability of E6 to induce degradation of BAK S117E was investigated. HCT116 WT BAK and S117E BAK cells expressing pEFIRES or pEFIRES-5E6 were irradiated with 5mJ/cm^2 UVB and cultured in media containing cyclohexamide to prevent further protein synthesis for 0, 4 or 6 hours before harvesting. Cyclohexamide was used as before since E6 appears to target only BAK at a specific point, which may be a small amount of the total BAK levels in the cell and can therefore be difficult to detect. BAK levels were then analysed by western blot as before. Figure 3.20B shows that cells expressing WT BAK and HPV5 E6 had

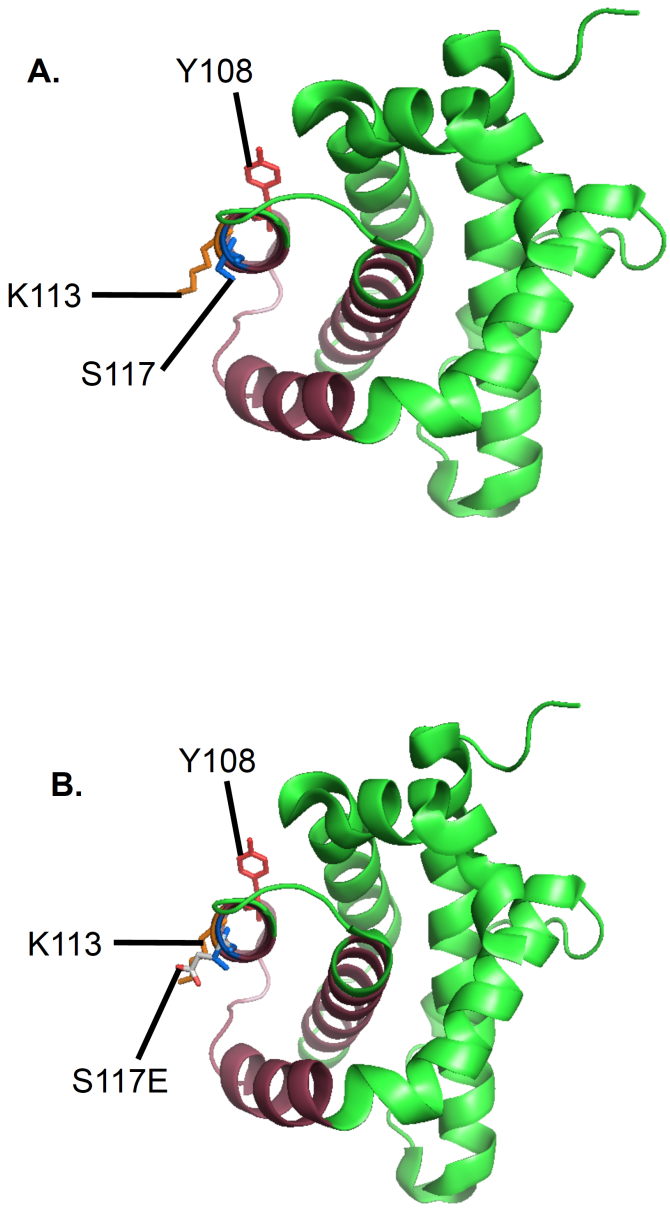


Figure 3.19 Model of the BAK hydrophobic pocket and S117

A. Model showing the structure of the BAK hydrophobic pocket (magenta) and the position of tyrosine 108, lysine 113 and serine 117 in relation to it.

B. Model showing mutation of serine 117 to glutamic acid. The negative charge of glutamic acid blocks access to the pocket of proteins that use a BH3 domain.

Modeled in PyMOL using Protein Data Bank file 2IMS.

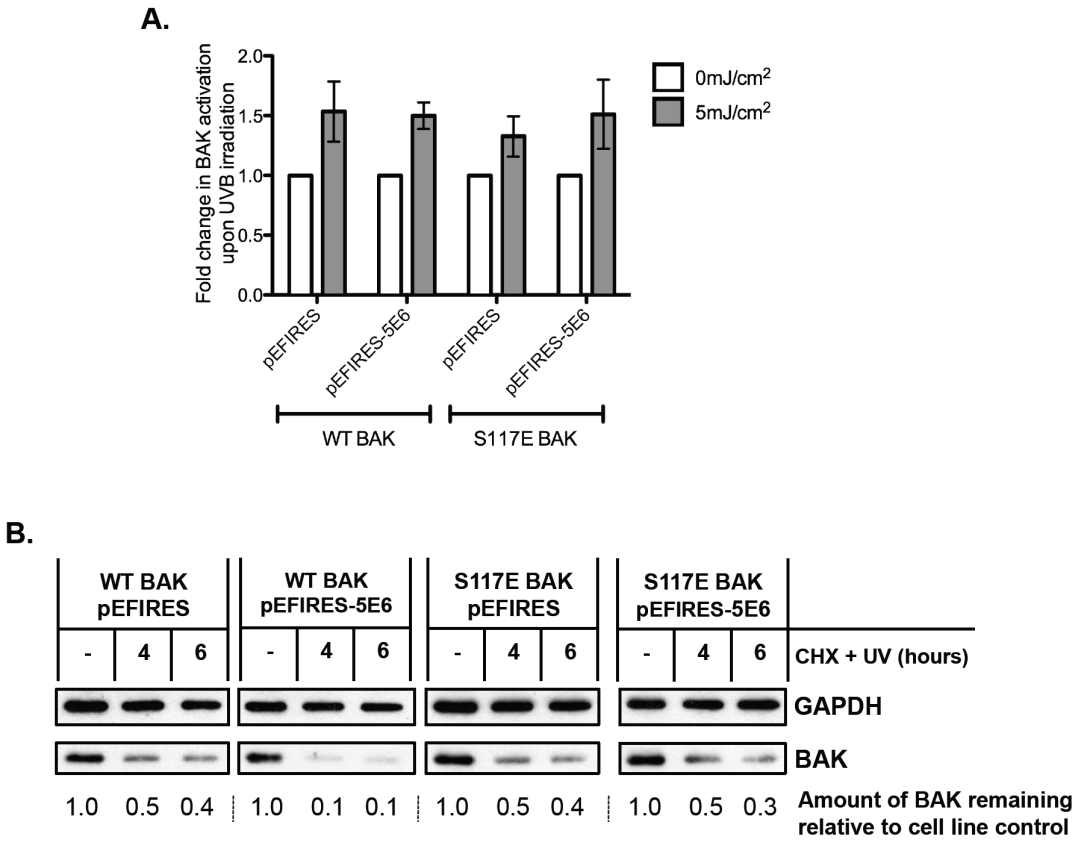


Figure 3.20 BAK S117E levels in HPV5 E6 expressing HCT116 cells in response to UVB

A. HCT116 S117E BAK cells expressing pEFIRES or pEFIRES-5E6 were irradiated ± 5mJ/cm^2. Eight hours later cells were stained with the Ab1 antibody and used to measure the amount of BAK in the N-terminal conformational change by flow cytometry. Fold changes in BAK activity in response to UVB are shown to remove baseline variability accounted for by differences in expression levels of WT BAK and S117E BAK. n=3 ± SEM.

B. HCT116 WT or S117E BAK cells expressing pEFIRES or pEFIRES-5E6 were irradiated ± 5mJ/cm^2 UVB and treated with cyclohexamide for the indicated time points. Lysates were then western blotted for total BAK levels and β-actin loading control.

Blots performed three times.

barely detectable levels of BAK 4 and 6 hours after UVB and cyclohexamide treatment whilst approximately half the control amount of BAK persisted at 4 and 6 hours in HCT116 WT BAK cells expressing pEFIRES. HCT116 S117E BAK cells, regardless of E6 expression, had similar relative levels of BAK 4 and 6 hours after UVB and cyclohexamide treatment to HCT116 WT BAK pEFIRES cells showing that HPV5 E6 cannot promote degradation of the BAK S117E mutant. Therefore it was hypothesised that, in order to be degraded, BAK must undergo the N-terminal conformational change and that, since S117 dephosphorylation proceeds normally in E6-expressing cells, exposure of the hydrophobic pocket might be required for E6-mediated degradation of BAK.

3.3.17 Investigation of outer mitochondrial membrane integrity in response to UVB in HCT116 WT BAK pEFIRES-expressing cells

The data above (Figure 3.17) provides evidence that the early stages of BAK activation are unaffected in HPV5 E6-expressing cells and suggest that HPV5 E6 targets BAK for degradation after it has undergone the N-terminal conformational change and that dephosphorylation at S117 is required for a reason distinct from just that of promoting the N-terminal conformational change. To further probe the point at which BAK is targeted, the ability of the cells to release cytochrome *c* was measured. As there is no BAX in this system, cytochrome *c* release is a direct downstream effect, and indicator, of permeabilisation of the OMM by BAK oligomerisation. HCT116 WT BAK pEFIRES or pEFIRES-5E6-expressing cells were irradiated with 5mJ/cm^2 UVB. Twenty-four hours later the cell plasma membranes were permeabilised with digitonin and fixed with PFA. Any cytosol containing cytochrome *c* as a result of MOMP was washed out. The mitochondrial membranes are permeabilised using saponin and any remaining cytochrome *c* stained using a FITC conjugated anti-cytochrome *c* antibody. The percentage of cells positive for cytochrome *c* is quantified by flow cytometry. Figure 3.21 demonstrates that the percentage of HPV5 E6-expressing cells which are able to release cytochrome *c* in response to UVB is not significantly different to those left unirradiated whilst in

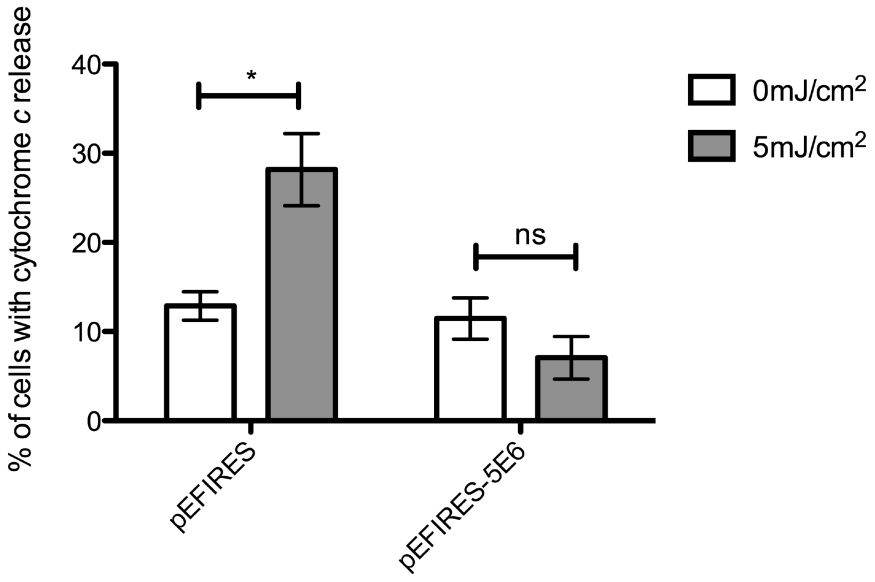


Figure 3.21 Cytochrome *c* release in HCT116 WT BAK cells expressing HPV5 E6 upon UVB irradiation

HCT116 WT BAK cells expressing pEFIRES or pEFIRES-5E6 were irradiated with 5mJ/cm^2 UVB. Twenty-four hours later cells were fixed, and the plasma membrane permeabilised using digitonin. Cytosolic cytochrome *c* was washed out and the cells then stained using an anti-cytochrome *c* antibody conjugated to FITC with saponin. The percentage of cells with cytochrome *c* remaining within the mitochondria was analysed by flow cytometry and the percentage of cells with cytochrome *c* loss plotted. n=3, ± SEM. *p≤0.05 calculated by unpaired t-test. ns; p≥0.05 was taken as not significant.

Flow cytometry analysis performed three times.

response to UVB approximately 30% of cells release cytochrome *c*. The lack of MOMP suggests that the HPV5 E6 protein targets BAK before it is able to form pores and permeabilise the OMM.

3.4 Discussion

β-HPV types inhibit apoptosis, in part through the E6 protein-mediated proteolysis of BAK. Conjugation of ubiquitin to lysine residues of substrates is the signal for proteins to be sent to the proteasome for degradation. In these experiments, through mutational analysis, K113 has been identified as being required for E6-mediated degradation of BAK and that the BAK K113R mutant reduces HPV5 E6-mediated apoptosis inhibition, as measured by caspase-3 activation. Furthermore, given that, in response to apoptotic stimuli BAK undergoes a complex series of post-translational and conformational modifications it was of interest to uncover at which stage of the BAK activation process targeting by E6 occurs. This work demonstrates that the earlier stages of BAK activation appear to be unaffected by the presence of the HPV5 E6 protein in HCT116 and HT1080 cells. This includes the ability to undergo dephosphorylation at both Y108 and S117 residues, binding to p53 and subsequent N-terminal conformational change enabling BAK to reach the 'primed' conformation. However cytochrome *c* release, a direct consequence of BAK multimerisation in this system, is prevented in HPV5 E6-expressing cells, implying that E6 targets BAK after it has reached its 'primed' conformation but before it is able to multimerise to form pores in the OMM. A cyclohexamide chase revealed that, in the HCT116 system used here, BAK is not targeted until approximately 6 hours after treatment with UVB correlating with the time scale for BAK activation where Y108 dephosphorylation can be detected 4 hours after apoptotic stimulus (though via a different apoptotic stimulus, Fox et al., 2010) and dimerisation approximately 6-8 hours after apoptotic stimulus (Azad et al., 2012).

To characterise E6 activity towards BAK a system was established in HCT116 DKO cells in which BAK and HPV5 E6 constructs could be expressed. In this system degradation of WT BAK could only be detected in response to UVB irradiation of

which 5mJ/cm^2 was found to be most effective 16-24 hours later. In this sytem BAK degradation is not constitutive as some previous reports have suggested (Struijk et al., 2008, Du et al., 2004). In contrast, here the level of BAK in untreated HPV5 E6-expressing cell lines was higher than that of cells expressing the empty vector (Figure 3.4, Figure 3.6 and Figure 3.12). Whilst previous reports have shown reduced BAK levels in HPV5 E6-expressing cells at similar time points in response to damage, higher doses of UVB were required (Jackson et al., 2000). Differences may be attributed to the use of different cell lines which have lower sensitivity to UVB than the HCT116 cell line here or calibration of the UVB lamp. Further differences observed in this system are that, although lower levels of BAK were detected in HPV5 E6-expressing cells after UVB irradiation compared to unirradiated cells, BAK degradation by HPV5 E6 was not complete. This may be due to the stable expression of BAK from a vector, expressing higher levels of the protein in the cells than are normally found. It may also suggest that not all BAK in the cell is in a conformation in which it can be recognised by E6 for degradation, as discussed below. It is also noteworthy that expression of the HPV5 E6 protein could not completely abrogate caspase-3 activation in Figure 3.7. This may be the result of direct activation of death receptors by UVB, resulting in activation the extrinsic apoptotic pathway which is mediated by caspase-8 cleavage of caspase-3.

Not investigated here is the ability of E6 to target BAK for degradation in response to other apoptosis inducing agents. Previous reports suggest expression of the E6 protein can protect from staurosporine-induced apoptosis (Steller et al., 1996). However epidemiological data suggests a specific interaction between UV-induced DNA damage and HPV infection in the development of NMSC. Subsequently, the rate of onset, amount and type of DNA damage (determining the apoptosis threshold) induced by other apoptotic stimuli may be important in the ability of E6 to target BAK. This may be emphasised in Figure 3.7 where inhibition of apoptosis upon expression of the HPV5 E6 protein was reduced upon irradiation of cells with 10mJ/cm^2 UVB compared to those treated with 5mJ/cm^2. This suggests that the

DNA damage incurred upon exposure to 10mJ/cm^2 was too severe for expression of E6 to promote cell survival as efficiently as upon exposure to 5mJ/cm^2 UV.

Proteasomal degradation, in the majority, requires the attachment of ubiquitin chains to lysine residues on substrates. Here K113 was identified in the BAK amino acid sequence as a likely candidate for ubiquitination. K113 is located on the α4 helix of the BAK surface and its mutation to arginine had no significant effects on BAK structure as modelled by PyMol (Figure 3.8). Furthermore, the K113R mutant BAK behaved comparably to the WT BAK protein in assays measuring the ability of K113R BAK to undergo the N-terminal conformational change. This suggests that BAK K113R is able to undergo the early stages of the activation process involving dephosphorylation at Y108 and binding of p53 and BH3 only proteins. K113 is located at the interface of BAK dimerisation (Figure 3.8A), it was therefore important to check that mutation did not affect the ability of BAK to dimerise. Dimerisation of BAK K113R could be detected, since dimerisation is a prerequisite for multimerisation and MOMP, this suggests cells expressing BAK K113R are able to execute the intrinsic apoptosis pathway. This is supported by comparable caspase-3 activation to that of cells expressing WT BAK in response to UVB, although this might include a component derived from activation of the extrinsic apoptotic pathway activation (Figure 3.11).

Although BAK K113R appeared to act in a way comparable to that of WT BAK in the absence of the HPV5 E6 protein, BAK K113R was not targeted for degradation in HPV5 E6-expressing cells in response to UVB exposure. Furthermore, reduced caspase-3 activation in response to UVB was no longer observed in the presence of the HPV5 E6 protein in cells expressing BAK K113R (Figure 3.12). It is tempting to speculate that this lack of degradation is the result of an inability of the E6 protein to mediate ubiquitination of BAK on the lysine residue and it follows that the inability to degrade BAK restores the ability to undergo apoptosis in these cells. However further work is required to elucidate how the K113R mutation disrupts E6-mediated BAK degradation. Whilst it is unknown how BAK, E6 and the E3 ligase interact, it is

possible that the mutation disrupts an E3 ligase or E6 recognition sequence in BAK to prevent ubiquitination and/or degradation, therefore interaction studies would contribute to our understanding of this (explored in Chapter 4). Furthermore investigation of the ability of BAK K113R to permeabilise the OMM by measurement of cytochrome *c* release or membrane depolarisation in the presence of E6 would broaden understanding of the contribution of the inability of the E6 protein to degrade BAK K113R to cell death induction, rather than the more downstream measurement of caspase-3 activation which may also incorporate some degree of extrinsic apoptosis activation.

There have been examples of lysine independent ubiquitination of proteins (Kravtsova-Ivantsiv and Ciechanover, 2012), examination of the ubiquitination status of WT BAK and K113R BAK by *in vitro* or *in vivo* ubiquitination assays would further elucidate why mutation of K113 would prevent degradation. Were BAK K113R to be ubiquitinated, it may prove to be lysine independent or indicate involvement of K210, though how E6 would mediate this is hard to envision as it has been not reported that E6 proteins, albeit those of α-HPV, localise to mitochondria (Masson et al., 2003). A failure of K113R BAK ubiquitination however would not clarify how the K113R mutation results in ubiquitination failure, that is, whether ubiquitin is directly conjugated to the lysine residue, or the lysine is a component of a recognition motif required for BAK ubiquitination.

Of further interest would be an assessment of the requirement of K113 for normal BAK turnover in the absence of E6. In these experiments there appeared to be lower expression levels of BAK K113R compared to that of WT BAK when re-introduced into cells. This may be the result of a failure of the mutated protein to pass through the cell protein quality control. However, the comparable activation of K113R BAK to WT BAK would suggest the protein structure is not compromised to a great extent. Alternately, it could be hypothesised that K113 is required for normal BAK protein turnover and therefore cells expressing high levels of the mutant are more sensitive to death. Although this is not observed in Figure 3.13A where a lower

percentage of unirradiated HCT116 K113R BAK cells expressing pEFIRES are observed compared to WT BAK, again this may be a result of the lower expression of the protein.

With respect to investigation of the conformation of BAK targeted, dephosphorylation of BAK at Y108 and S117 by western blot could not be detected using 5mJ/cm^2 UVB irradiation. However, the N-terminal conformational change can be detected in HCT116 WT BAK pEFIRES-5E6-expressing cells using 5mJ/cm^2 UVB. This would suggest that Y108 dephosphorylation, p53 binding and/or S117 dephosphorylation to permit BH3 protein binding to the hydrophobic groove to stimulate the N-terminal conformational change also occur at 5mJ/cm^2, but cannot be observed due to insufficient sensitivity of the assays. Although the use of 10mJ/cm^2 was required to observe the dephosphorylation steps, it was shown in Figure 3.7 that E6 still exerts its protective effect at 10mJ/cm^2 but with less efficacy than 5mJ/cm^2. Similarly, although the BAK activation process is quick and p53 translocation to the mitochondria has previously been detected within 4 hours, the longer time points used here are in order to allow enough modified protein in the cell pools to accumulate to be at levels sufficient for detection.

That BAK must undergo post-translational and conformational changes in order for it to be targeted for degradation by HPV5 E6 is in interesting contrast to the maintenance of low cellular p53 levels, regardless of modification, by the α-HPV E6 proteins. Evidence presented here suggests that the HPV5 E6 protein targets only BAK which has become activated and is capable of mitochondrial fragmentation in response to apoptotic stimuli. It is noteworthy that BAK is also required for normal mitochondria dynamics of fusion and fission, consequently complete removal of BAK may be detrimental to the cell, undermining the effects of the E6 protein to promote cellular survival.

These data suggest that BAK must undergo the N-terminal conformational change in order to be degraded, but that it is targeted before it is able to permeabilise the OMM as this is a key commitment point of intrinsic apoptosis. As BAK S117E is able

to undergo the N-terminal conformational change through p53 binding, the inability of the HPV5 E6 protein to degrade BAK S117E suggests that access to the hydrophobic groove of BAK, or a conformation of BAK downstream of S117 dephosphorylation which BAK S117E cannot achieve, is required for E6-mediated degradation. Given the proximity of K113 to the hydrophobic pocket and S117, this is an interesting finding which is discussed further in Chapter 4. To confirm requirement of the two dephosphorylating steps for BAK degradation, pre-treatment with a tyrosine phosphatase inhibitor, such as sodium stibogluconate, or PP2A inhibitor, such as okadaic acid, should prevent E6-mediated degradation upon UVB irradiation. Furthermore, to confirm the requirement of Y108 dephosphorylation a Y108E BAK mutant available in the lab which cannot proceed through the activation process (placing a constitutive negative charge in place of the phosphorylated tyrosine residue, Fox et al., 2010) would be predicted to not be degraded via the E6 protein activity.

Overall these data suggest that K113 is important for HPV5 E6-mediated turnover of BAK and that mutation of this residue affects E6 activity towards BAK and E6-mediated cell survival. However further work is required to delineate the mechanism of this effect. It is also hypothesised that the conformation of BAK targeted for degradation must be either the S117 dephosphorylated monomer or dimerised BAK, correlating with the cyclohexamide chase time frame. Targeting of the BAK dimer would suggest that dephosphorylation of S117 is required only to permit BAK dimer formation whilst targeting of the monomer may imply a requirement of the hydrophobic pocket for another purpose in the degradation process. Since oligomerisation of BAK leads to rapid MOMP it seems unlikely that BAK oligomers would be targeted by the E6 protein. Taken together these data further understanding of E6-mediated BAK proteolysis in response to UV-induced apoptosis.

Chapter 4 Investigation of a novel E6 associated E3 ubiquitin ligase

4.1 Introduction

E6AP was the first identified E3 ubiquitin ligase to be associated with the α-HPV E6 proteins. The first substrate identified to be targeted by the E6 proteins using this ligase was p53 (Scheffner et al., 1990, Huibregtse et al., 1991, Huibregtse et al., 1993a). p53 is not a substrate for E6AP in the absence of E6 indicating that the E6 protein is able to change the substrate specificity of E6AP. E6 proteins can recognise host cell proteins via a L2G motif and using this motif E6 first binds E6AP (Elston et al., 1998, Grm and Banks, 2004) causing E6 to undergo a conformational change (Ansari et al., 2012) allowing the E6 N-terminal to dimerise (Zanier et al., 2012) and bind p53, mediating the transfer of ubiquitin from E6AP.

The E6 proteins are known to target a number of host cell proteins for degradation, some of these have been reported to be E6AP independent, including TIP60 (Jha et al., 2010). The dependence of PDZ protein degradation on the presence of E6AP is unclear. The degradation of MUPP1 is suggested to be E6AP independent (Scheffner and Whitaker, 2003) whilst the degradation of Scribble (Nakagawa and Huibregtse, 2000), Dlg (Kuballa et al., 2007, Massimi et al., 2008, Pim et al., 2000) and MAGI-1 (Kuballa et al., 2007, Grm and Banks, 2004) can be both dependent on and independent of E6AP. This may be reflective of the different experimental systems used. Further, in E6AP null MEFS, p53 has also been shown to be targeted for degradation in an E6AP-independent manner (Massimi et al., 2008). These data raise the possibility of the E6 proteins interacting with other E3 ligases.

The HECT domain E3 ligases HERC2 and EDD have been shown to interact with the α-HPV E6 proteins (White et al., 2012, Tomaic et al., 2011), however they have only been associated with the regulation of E6AP activity, both in the presence and absence of the E6 protein. EDD over-expression prevented degradation of p53 and the PDZ domain proteins MAGI2 and Dlg (Tomaic et al., 2011), proteins previously

associated with E6AP-mediated degradation. HERC2 has been reported to have no effect on the E6-mediated degradation of p53 (Kuhnle et al., 2011) and therefore an E6-associated ligase involved in the degradation of E6 substrates targeted for degradation independently of E6AP has not been identified since the discovery of E6AP some years ago.

E6AP has been associated with targeting of BAK for proteolysis both in the absence of HPV and in the presence of the α-HPV18 E6 protein (Thomas and Banks, 1998), as well as the β-HPV8 E6 protein (Underbrink et al., 2008). However, the β-HPV5 E6 protein can promote degradation of BAK in E6AP null MEFS (Simmonds and Storey, 2008) and an interaction between the HPV5, HPV8 and 38 E6 proteins with E6AP has not been found (Elbel et al., 1997, Howie et al., 2011, Rozenblatt-Rosen et al.). As yet no β-HPV E6 protein associated E3 ligase has been identified for any other β-HPV E6 protein substrates, such as p300 and TIP60, raising the question of which E3 ligase do β-HPV E6 proteins use to target BAK?

There are more than 600 E3 ligases encoded in the genome (Li et al., 2008). E6AP is the founding member of the HECT domain family of E3 ubiquitin ligases. Targeting of p53 for degradation by the high-risk mucosal E6 proteins using E6AP, association of the α-HPV E6 proteins with HECT domain ligases EDD and HERC2 (via E6AP), combined with studies showing that a specific point mutation in HPV5 E6 changed targeting specificity of the protein from BAK to p53 for degradation in an E6AP independent manner (Simmonds and Storey, 2008) suggested that the β-HPV E6 proteins may also utilise a HECT domain ligase to target BAK.

A functional siRNA screen of the 28 HECT domain E3 ligases was performed in Saos2 cells by a previous member of the group (M. Simmonds, PhD Thesis, University of London). Each of the 28 ligases was individually knocked down using siRNA pools, and cells were then transiently transfected with HPV5 E6 and haemagglutinin tagged BAK (HA-BAK) and harvested a further 24 hours later. The levels of BAK were detected by western blot using an anti-HA antibody (Figure 4.1). In this screen siRNA knockdown of E6AP (*ube3a*) did not recover the levels of BAK

in the presence of the HPV5 E6 protein, in agreement with previous observations. However the ubiquitin ligase HERC1 (HECT domain and Regulator of Chromosome Condensation 1-like domain-containing protein 1) was identified as a potential candidate, as knockdown of this mRNA recovered BAK levels in HPV5 E6-expressing cells. HERC1 is a protein of 532kDa and has been identified as a guanine nucleotide exchange factor for the ARF1 GTPase and Rab proteins, suggesting it is involved in protein trafficking, and is localised to inner cell membranes (Rosa et al., 1996). It is also known to interact with, and destabilise, tuberous sclerosis complex 2 (TSC2), an inhibitor of the mammalian target of rapamycin pathway (mTOR; Chong-Kopera et al., 2006).

HERC1 has not been identified in previously published E6 protein interaction studies (Howie et al., 2011, Rozenblatt-Rosen et al., 2012, Tan et al., 2012b, Thomas et al., 2013). Reasons for this may be a result of the large size of HERC1, a transient interaction with E6 proteins or the membrane localisation and instability of HERC1 complexes upon extraction.

4.2 Aim

The aims of these experiments were to elucidate the role of HERC1 in β-HPV E6-mediated degradation of BAK and to investigate the molecular basis of the interaction between BAK and HERC1, along with the requirement of E6.

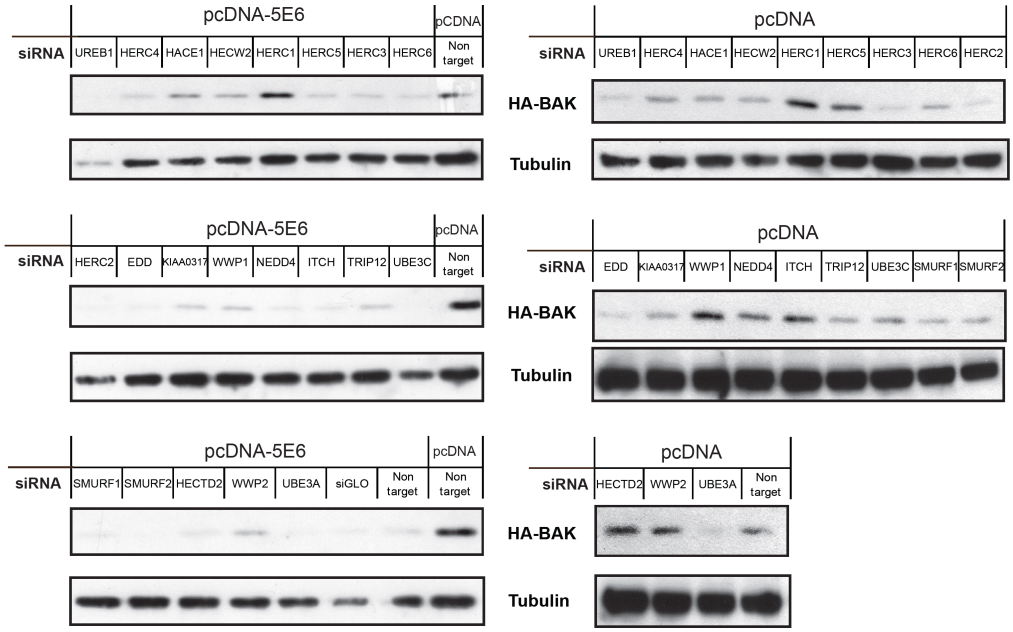


Figure 4.1 siRNA screen of HECT domain involved in HPV5 E6-mediated BAK degradation in Saos2 cells

Saos2 cells were transfected with a siRNA oligo pool against each of the HECT domain E3 ligases. Forty-eight hours later they were transiently transfected with HA-tagged BAK ± HPV5 E6. A further 24 hours later cells were harvested in RIPA buffer and western blotted for anti-HA and tubulin. The gene *ube3a* codes for E6AP. Experiment performed by Mark Simmonds.

4.3 Results

4.3.1 *herc1* knockdown in HCT116 DKO cells

Knockdown of HERC1 expression by siRNA implicates this E3 ligase as being involved in HPV5 E6-mediated proteolysis of BAK in a transient transfection experimental system in p53 null Saos 2 cells. As the ability of E6 to target BAK for proteolysis has been reported to be cell type independent, strategies to knockdown *herc1* in HCT116 DKO cells were investigated. As previously described, the use of HCT116 DKO cells reconstituted for BAK expression affords the opportunity to investigate BAK mutants with defined phenotypes allowing specific steps in the BAK activation process to be investigated. Ideally a cell line with stable *herc1* knockdown would be useful for consistent *herc1* knockdown for culture of a large number of cells, avoiding repetitive, transient and inconsistent *herc1* knockdown with expensive siRNA oligos. In order to achieve this vectors encoding 29mer small hairpin RNAs (shRNA) against *herc1* were obtained (OriGENE). shRNA vectors encode a RNA sequence which, when expressed, forms a tight hairpin RNA which leads to interference of the expression of the target gene RNA. Two control vectors are provided (pRS; empty vector, pRS-GFP; a non-targeting control against GFP) and four constructs each encoding a different shRNA against *herc1* (sequences given in Table 4.1).

Each of the vectors was transfected into HCT116 DKO cells using the Turbofect transfection reagent and selected using puromycin. Cell line pools were established and mRNA was extracted from each of the selected cell lines. A cDNA template was synthesised using random hexamers and RT-QPCR used to quantify *herc1* mRNA levels using primers designed to amplify a ~500 base pair region of *herc1*, spanning two exons so that any contaminating genomic DNA is not amplified (see Table 2.8). Expression of the gene *gus* was used as a reference. C(t) values were obtained for each gene in the different cell lines and those for *herc1* normalised to those for the

Table 4.1 OriGENE HuSH shRNA constructs against *herc1*

Vectors encoding shRNA against *herc1* were obtained from Origene.

HuSH	Product number	HERC1 HuSH shRNA target gene sequence (5'→3')
HuSH **25**	TI349925	AAGCAGTGTGGCATTGCTTCATAAACATC
HuSH **26**	T1349926	GTGGTAACCTCTATCACAATGGAGAACAG
HuSH **27**	T1349927	TACCTCGGTGCTATGAAGTCACTTAGTGC
HuSH **28**	T1349928	CAGAGGACAGTGAATCTATTGCTACAAGA
HuSH **pRS-GFP**	TR30003	TGACCACCCTGACCTACGGCGTGCAGTGC

gus controls. The $2^{-\Delta C(t)}$ method was then used to calculate the percentage knockdown of *herc1* for each HuSH vector as described in chapter 2.5.1.3. The percentage knockdown of *herc1* mRNA in each of the HuSH vector cell lines relative to the pRS cell line was calculated, shown in Figure 4.2A. HuSH vectors 25 and 28 had the greatest efficacy in *herc1* mRNA knockdown, resulting in approximately 20-50% knockdown relative to control. Vectors 26 and 27 had no discernable effect on *herc1* knockdown from the GFP non-targeting control. To increase efficiency of *herc1* knockdown, vectors 25 and 28 were transfected into a single cell line to gain an additive effect and cell line pools generated. RT-QPCR was performed as previously described but no increase in *herc1* mRNA knockdown could be detected compared to the control non-effective GFP vector cell line (Figure 4.2B). Loss of *herc1* has been shown to be lethal during development (Mashimo et al., 2009), it may also be that prolonged or dramatic *herc1* knockdown is lethal in cell lines.

herc1 knockdown in the Saos2 HECT E3 ligase screen had been previously achieved using a pool of siRNA oligos (Ambion). Therefore, four individual oligonucleotides targeting the *herc1* mRNA were obtained (Dharmacon; sequences given in Table 2.2) to achieve transient knockdown of *herc1* in HCT116 cells. A siRNA pool was generated and transfected into HCT116 WT BAK cells to a final concentration of 30nM (each oligonucleotide at a final concentration of 7.5nM).

Figure 4.2 *herc1* mRNA knockdown in HCT116 and HT1080 cells

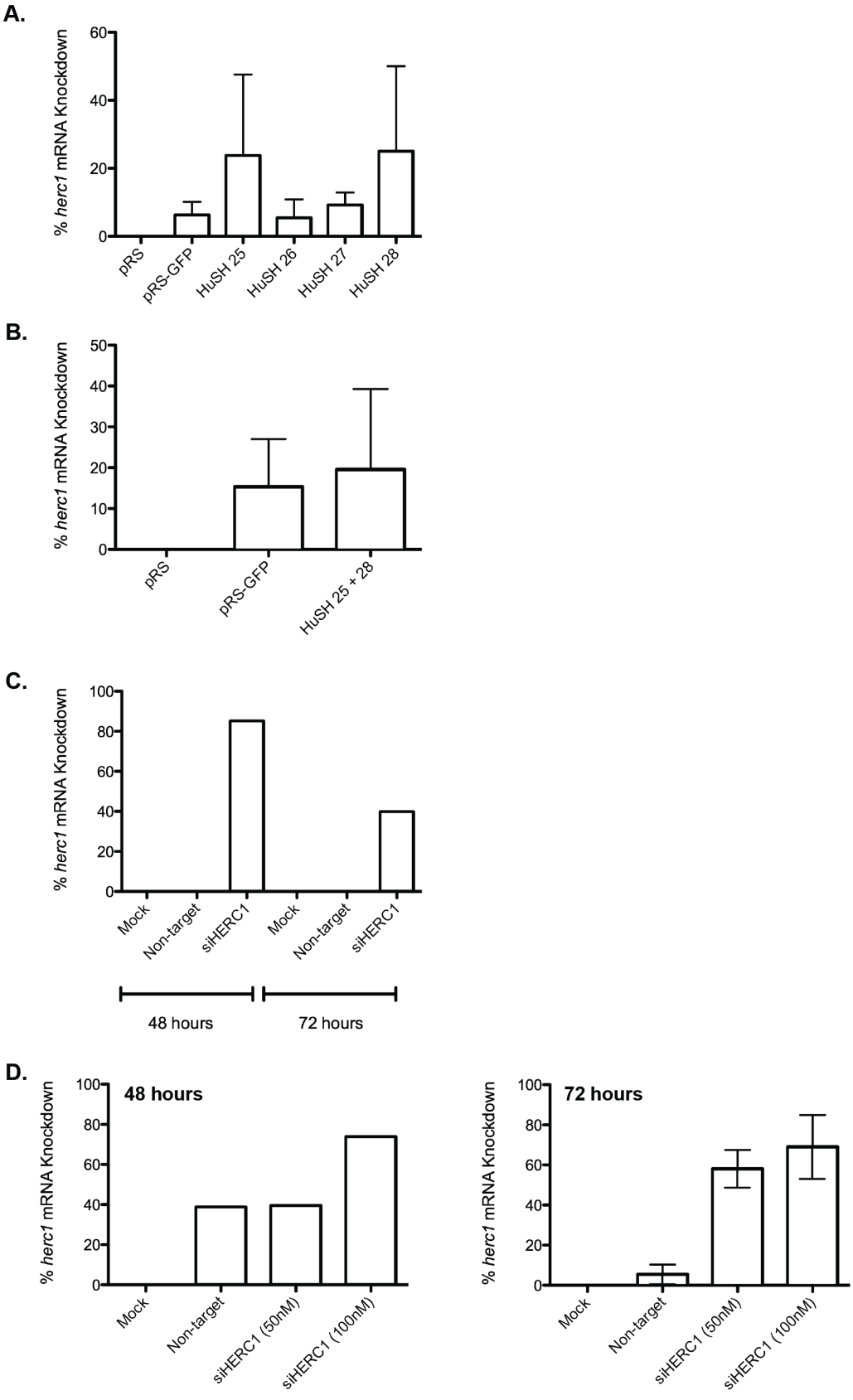


Figure 4.2 legend

A. HCT116 DKO pools stably expressing vectors encoding shRNA against *herc1* were generated. Percentage *herc1* mRNA knockdown, relative to the pRS control, in these cell lines was quantitated using RT-QPCR. pRS; empty vector, pRS-GFP; non effective control, Hush 25-28; vectors encoding different shRNA against *herc1*. n=3, mean percentage knockdown ± SEM

B. A HCT116 DKO pool stably expressing shRNA vectors 25 and 28 were generated and the percentage *herc1* mRNA knockdown quantitated by RT-QPCR. n=3, mean percentage knockdown ± SEM

C. Percentage *herc1* mRNA knockdown, relative to the mock transfection, in HCT116 DKO cells using 30nM Dharmacon siRNA pool of 4 oligonucleotides against *herc1* 48 and 72 hours after transfection compared to mock (no oligonucleotide) and non-targeting siRNA transfections. n=1

D. Percentage *herc1* mRNA knockdown, relative to the mock transfection, in HT1080 cells using 50nM or 100nM of the HERC1 oligonucleotide pool. mRNA knockdown was measured 48 and 72 hours after transfection by RT-QPCR. Forty-eight hours; n=2, 72 hours; n=3 ± SEM.

Transfection with 30nM of a non-targeting oligonucleotide (Silencer Select Negative Control No.1, Ambion) or a mock transfection, replacing the siRNA with only siRNA buffer, were used as controls. mRNA was extracted 48 or 72 hours later and RT-QPCR performed as previously described to assess *herc1* mRNA knockdown using the mock transfection as the untreated control. Figure 4.2C shows that approximately 20% of *herc1* mRNA remained after knockdown using the HERC1 siRNA pool 48 hours after transfection. A further 24 hours later (a total of 72 hours after transfection) the siRNA efficacy had reduced so that 60% of *herc1* mRNA, relative to the mock transfection, was detectable. Although Figure 4.2C shows only a single RT-QPCR of *herc1* knockdown in HCT116 cells, *herc1* knockdown using the siRNA pool had previously been performed in the HT1080 cell line during pilot work, before the HCT116 cell line was chosen for the reasons previously outlined. Knockdown of *herc1* mRNA, quantified by RT-QPCR relative to the mock transfected cells, in HT1080 cells using 50 or 100nM of the HERC1 siRNA pool 48 or 72 hours after transfection is shown in Figure 4.2D. The data show that 48 hours

after transfection both the non-targeting and 50nM HERC1 siRNA had a similar effect on *herc1* mRNA levels suggesting that the transfection may have affected *herc1* mRNA levels. However, 72 hours after transfection the effect of the non-targeting siRNA on *herc1* mRNA knockdown appears to have dissipated and 50-90% *herc1* mRNA knockdown is measured using 50 or 100nM HERC1 siRNA oligonucleotide. Consequently the *herc1* knockdown observed in Figure 4.2C in HCT116 cells was consistent with this *herc1* knockdown time frame, hence the following experiments using *herc1* knockdown by siRNA were performed 48-72 hours after siRNA transfection in HCT116 cells. For each experiment, *herc1* mRNA or protein knockdown was monitored.

4.3.2 Investigation of HERC1 involvement in HPV5 E6-mediated degradation of BAK in HCT116 cells

Having established a method to knockdown *herc1* in HCT116 cells, to test whether HERC1 was involved in HPV5 E6-mediated BAK degradation in this cell line, HCT116 WT BAK cells expressing pEFIRES or pEFIRES-5E6 were seeded in 60mm dishes at $3x10^5$ cells. Cells were then transfected with a final concentration of 50nM of either non-targeting siRNA (Ambion) or 50nM of the Dharmacon siRNA pool against *herc1* (each of the 4 siRNA oligonucleotides at a final concentration of 12.5nM). Cells were trypsinised and re-seeded at $1x10^5$ cells in a 60mm dish to obtain equal siRNA transfection efficiency for all samples 16 hours post-transfection. Following a further 48 hours, cells were treated with cyclohexamide for 8 hours with or without $5mJ/cm^2$ UVB irradiation, before harvesting in RIPA lysis buffer (a total of 72 hours after transfection). Equal amounts of protein (200μg) of the untreated non-target and HERC1 siRNA transfected lysates were then western blotted for HERC1 and E6AP. Cells transfected with the HERC1 siRNA pool had efficient HERC1 protein knockdown and the HERC1 siRNA had no effect on the levels of E6AP, which remained unaltered across the transfections (Figure 4.3A). BAK levels in all the samples were then analysed by western blot, with remaining BAK levels, relative to the untreated cell line control, calculated as previously described (Figure 3.4).

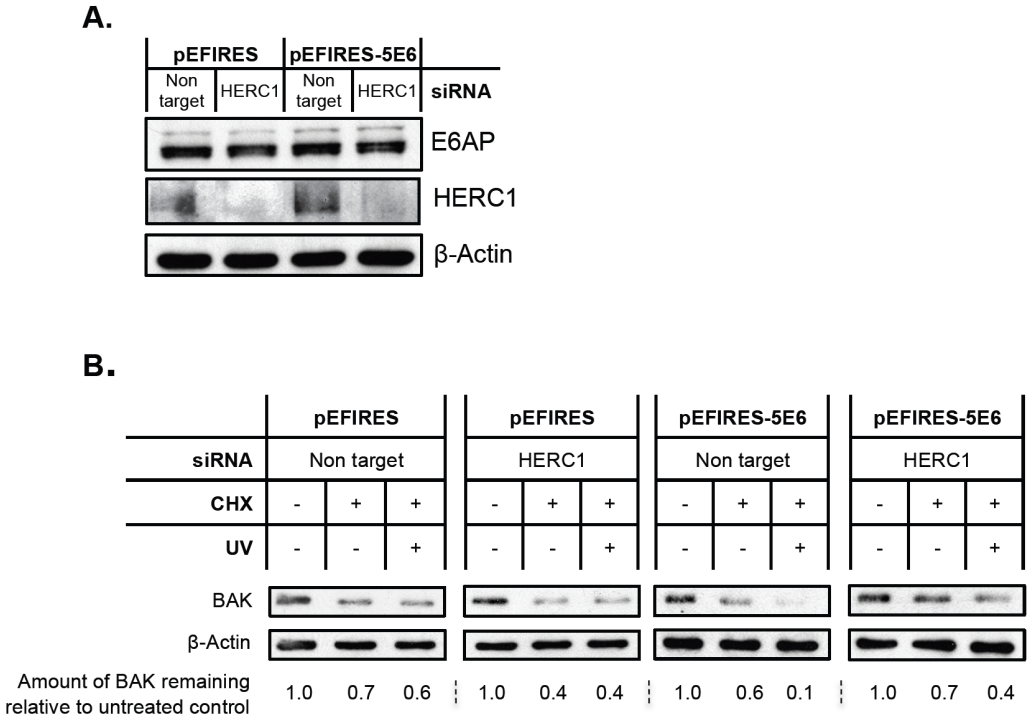


Figure 4.3 BAK levels in the presence of HPV5 E6 and HERC1 knockdown in HCT116 WT BAK cells

A. Western blot of HERC1 (532kDa) and E6AP in HCT116 WT BAK cells expressing pEFIRES or pEFIRES-5E6 72 hours after transfection with a non-targeting siRNA or a siRNA pool targeting *herc1*.

E6AP was analysed by SDS-PAGE on a 10% acrylamide gel. HERC1 was analysed by SDS-PAGE on a 3-8% Tris-Acetate gel using the SureLock system (Life Technologies) and western blotted by incubation with Bethyl Laboratories antibody ♯A301-904A in 0.1% milk/TBST for 1 hour at room temperature.

E6AP has three N-terminal splice variants predicted to be 90, 98 and 100kDa. The three observed bands may correspond to these (Yamamoto et al. 1997). β-actin was used as a loading control.

B. HCT116 WT BAK cells expressing pEFIRES or pEFIRES-5E6 were transfected with 50nM non-targeting siRNA or HERC1 siRNA pool. Sixty-four hours after transfection cells were treated ± 100µg/ml cyclohexamide ± 5mJ/cm^2 UVB and harvested a further 8 hours later. Lysates were western blotted for BAK and β-actin loading control.

Blots performed three times.

Figure 4.3B shows that BAK turnover was unaffected in pEFIRES cells both by treatment with UVB alone or HERC1 knockdown in combination with UVB. In pEFIRES-5E6-expressing cells transfected with the non-targeting siRNA BAK levels were almost undetectable 8 hours after UVB irradiation with cyclohexamide treatment, whilst the relative level of BAK in those cells treated with only cyclohexamide was comparable to that in pEFIRES cells. This suggests that E6 does not target BAK in the absence of DNA damage, supporting previous findings in Chapter 3. In contrast, UVB irradiated pEFIRES-5E6-expressing cells with HERC1 knockdown had higher relative levels of BAK (40% remaining) than those transfected with the non-targeting siRNA (10% remaining). The relative amount of BAK remaining in the HPV5 E6-expressing cells transfected with the HERC1 siRNA and treated with UVB was comparable to that of the pEFIRES cells transfected with the non-targeting siRNA. These data suggest that HERC1 is involved in the increased proteolysis of BAK observed in HPV5 E6-expressing cells in response to UV damage in a cell type independent manner.

To confirm that the HERC1 siRNA pool, and subsequently the observed effects, were specific to HERC1 knockdown, the HERC1 pool was resolved by transfecting HCT116 WT BAK cells with 30nM of each of the individual oligos to *herc1* (06, 07, 08 and 09) and harvesting 72 hours later. HERC1 protein levels were examined by western blot (Figure 4.3A). siRNAs 06 and 07 gave the greatest level of HERC1 knockdown and the experiment in Figure 4.3C was repeated using these two siRNAs individually at a concentration of 30nM. Figure 4.4 shows that BAK turnover in pEFIRES and pEFIRES-5E6-expressing cells appeared to be relatively consistent with no greater BAK degradation observed in HPV5 E6-expressing cells. This may be a result of using a single 8 hour timepoint where natural BAK turnover has reached a plateau with E6-mediated BAK degradation. A shorter time point may have elucidated differences in the degree of BAK turnover between the two cell lines. However for the pEFIRES line, all transfections gave a 70-90% reduction in

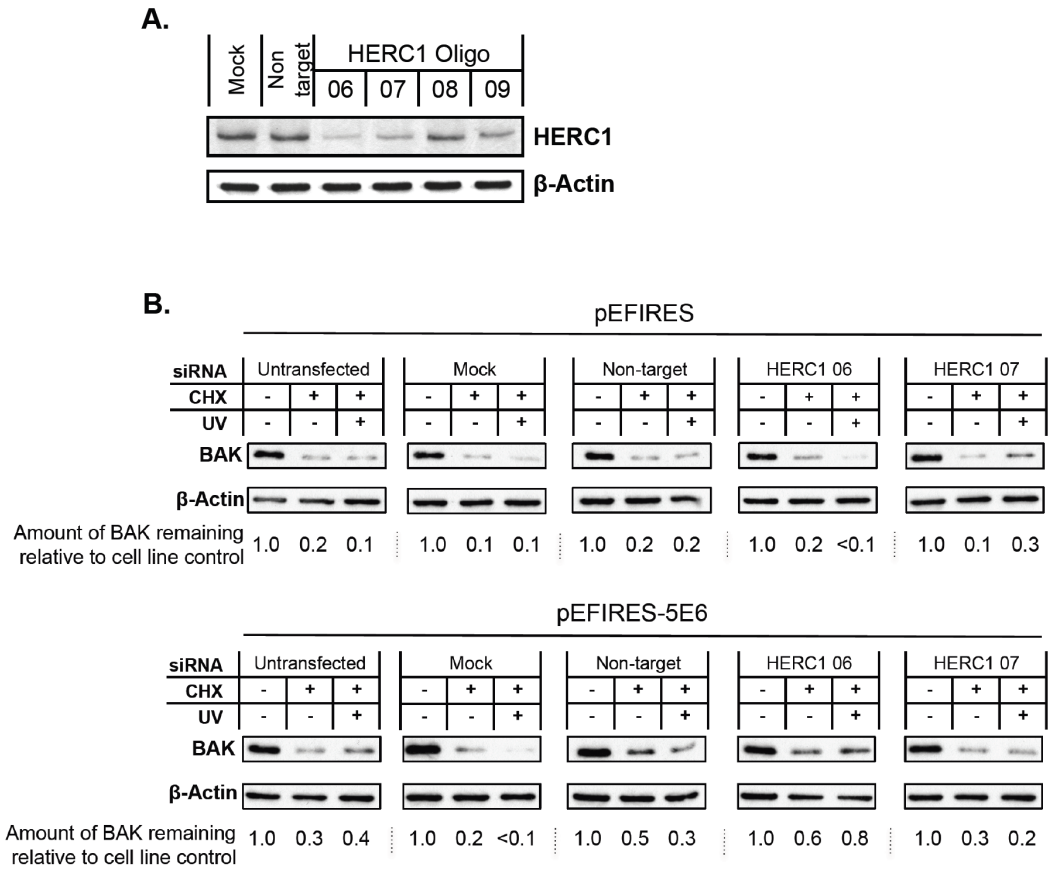


Figure 4.4 BAK levels in HPV5 E6-expressing cells with HERC1 knockdown by two individual siRNA oligos

A. Western blot of HERC1 levels in HCT116 WT BAK cells 72 hours after transfection with 30nM of the 4 individual oligonucleotides against HERC1 comprising the HERC1 siRNA pool. Mock; no oligonucleotide, non-targeting; transfection with a non-targeting siRNA, HERC1 06-09; individual HERC1 siRNA oligonucleotides.

B. Sixty-four hours after transfection with the indicated siRNA cells were treated ± 100μg/ml cyclohexamide ± 5mJ/cm^2 UVB for 8 hours. Lysates were western blotted for BAK and β-actin loading control.

Experiment performed three times.

BAK levels relative to the untreated control upon treatment with UVB and cyclohexamide. For the HPV5 E6-expressing cells, 60-100% reductions in BAK levels were observed for UVB and cyclohexamide treated samples in untransfected, mock and non-target samples. However HERC1 knockdown using oligo 06 in conjunction with UVB and cyclohexamide treatment shows a rescue of BAK levels (a 20% reduction in BAK levels compared to the untreated control). Oligo 07 gave no rescue of BAK levels, however Figure 4.4A shows that transfection with oligo 07 resulted in less HERC1 knockdown than that of oligo 06, therefore there may be sufficient HERC1 remaining to mediate BAK degradation.

4.3.3 Requirement of HERC1 for HPV5 E6-mediated BAK degradation in HEKa cells

Having investigated the involvement of HERC1 in E6-mediated BAK degradation in Saos2 and HCT116 cells it was important to assess the role of HERC1 in primary human epidermal keratinocytes (HEKa), the virus host cell. Firstly siRNA transfection optimisation of the keratinocytes was performed using a siRNA transfection indicator (siGLO red, #D-001630-02 Dharmacon). HEKa cells were seeded at $1.5x10^5$ cells in a well of a 6 well plate and cells were then transfected using HiPERFECT transfection reagent (Qiagen, see chapter 2.3.2). As HiPERFECT in pilot experiments had been observed to be toxic, 4 hours later the transfection media was either removed and replaced with new culture media or diluted with 3ml new culture media.

Transfection efficiency was examined by fluorescence microscopy 24 hours later. Little difference could be observed in transfection efficiencies and cell death between the two methods (Figure 4.5A) therefore the dilution protocol was chosen as this would provide a greater window for siRNA uptake by the cells. To assess whether this transfection efficiency was sufficient to cause a decrease in *herc1* mRNA expression, HEKa cells were transfected with 25nM of the HERC1 siRNA pool (Dharmacon) or non-targeting siRNA. Cells were harvested 72 hours post-transfection for RNA extraction and RT-QPCR performed using *gus* as a reference

Figure 4.5 BAK levels in HPV5 E6 expressing HEKa cells with *herc1* knockdown

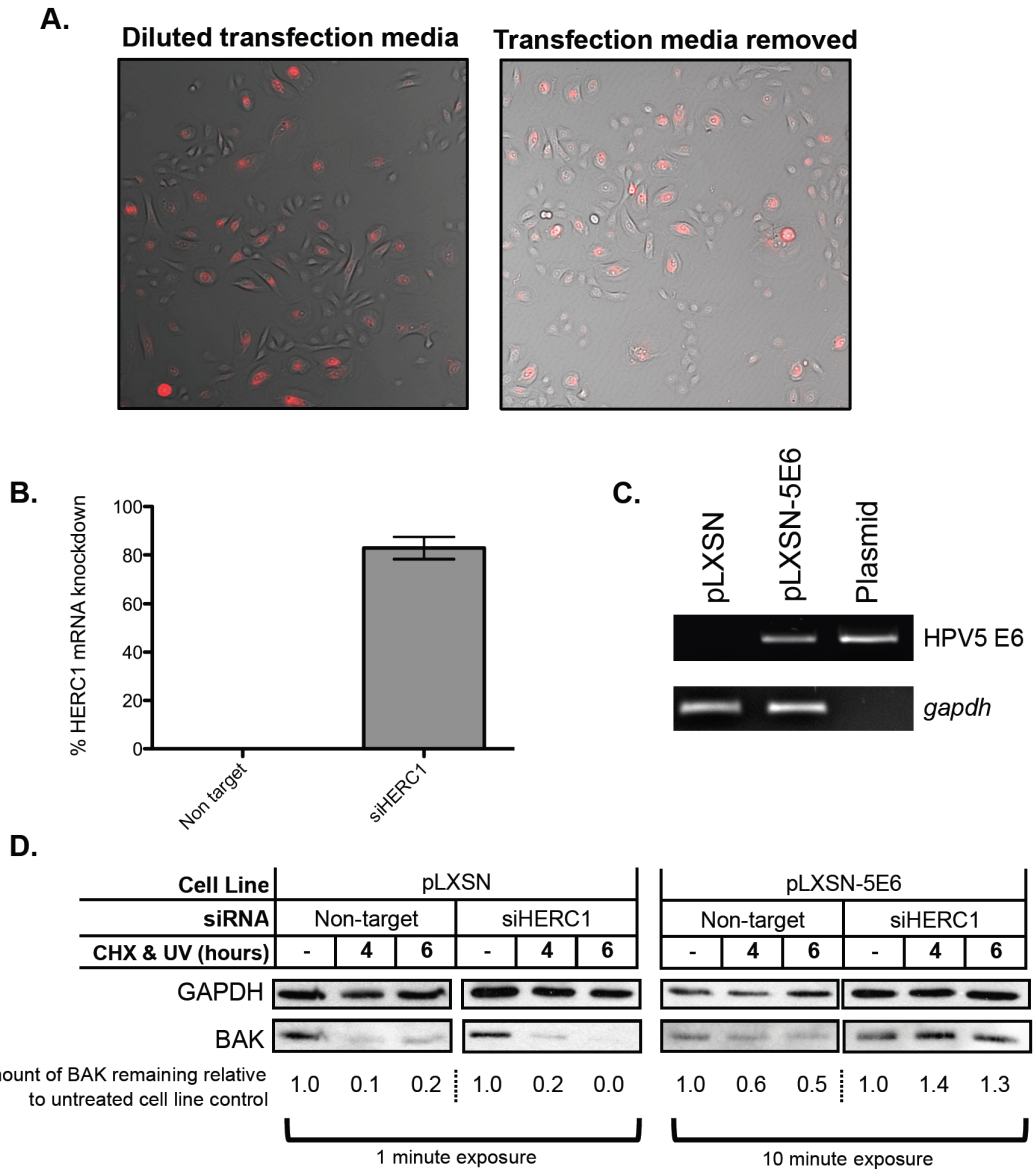


Figure 4.5 legend

A. siRNA transfection of HEKa cells was optimised using HiPERFECT transfection reagent with 25nm siGLO red. Four hours after transfection the transfection media was either diluted 1 in 4 with culture media or removed and replaced with culture media. The transfection efficiency was analysed 24 hours later by live cell fluorescence microscopy.

B. HEKa cells were transfected using HiPERFECT and 25nM HERC1 siRNA pool or a non-targeting siRNA. Seventy-two hours after transfection the mRNA was extracted and the percentage knockdown of *herc1* mRNA quantitated by RT-QPCR.

C. HEKa cells expressing HPV5 E6 by retroviral infection using the pLXSN vector were selected by resistance to G418. mRNA was extracted from the cell lines, cDNA templates synthesised and the expression of HPV5 E6 tested in pLXSN and pLXSN-5E6 cell lines by PCR using primers to HPV5 E6 (474bp product) and *gapdh* (261bp product). A pcDNA plasmid encoding the HPV5 E6 gene was used as a positive control.

D. HEKa cells expressing pLXSN or pLXSN-5E6 were transfected with a non-targeting siRNA or a siRNA pool against *herc1*. Cells were irradiated with 5mJ/cm^2 UVB and treated with 100µg/ml cyclohexamide 4 or 6 hours before harvesting a total of 72 hours after transfection. Lysates were western blotted for BAK (rabbit monoclonal [Y164]) and GAPDH as a loading control.

---

gene. The percentage *herc1* mRNA knockdown was calculated as previously described, using the non-target siRNA transfection as the untreated reference. Figure 4.5B shows that this gave approximately 80% knockdown in *herc1* mRNA expression compared to the non-targeting siRNA. Previous experiments in other cell lines suggest this degree of knockdown was sufficient to prevent E6-mediated BAK degradation.

To establish HPV5 E6-expressing cells HEKa cells were seeded at 2x10^5 cells in a 6 well plate and retrovirally transfected with pLXSN vector or pLXSN encoding HPV5 E6 as previously described (Tomlins and Storey, 2010). Twenty-four hours later transfected cells were selected using 100µg/ml G418 for 3 days. After selection HPV5 E6 mRNA expression was assessed by cDNA synthesis and PCR reaction as previously described (Figure 4.5C). The cells were expanded and immediately seeded at 1.5x10^5 in 35mm dishes. Some cells were harvested for mRNA extraction to assess HPV5 E6 mRNA expression, with the remainder being transfected with

the HERC1 siRNA pool or non-targeting siRNA using HiPERFECT transfection reagent 24 hours later. Cells were irradiated with 5mJ/cm^2 UVB and treated with 100µg/ml cyclohexamide for 4 or 6 hours before harvesting, a total of 72 hours post-transfection. Levels of BAK in the samples were analysed by western blot. Figure 4.5D shows that BAK levels were almost undetectable 4 hours after UVB irradiation with cyclohexamide treatment in pLXSN expressing HEKa cells cultured in EpiLife media and transfected with HERC1 or non-targeting siRNA pool. HEKa cells expressing pLXSN-5E6 transfected with a non-targeting siRNA showed a 50% reduction in BAK levels 6 hours after treatment with UVB and cyclohexamide. This is in contrast to previous cell systems where E6-mediated BAK turnover is more rapid than that in control cells. However, most interestingly, upon HERC1 knockdown in HPV5 E6 expressing HEKa cells BAK levels were stabilised 6 hours after UVB and cyclohexamide treatment showing a 30-40% increase in BAK levels compared to the untreated control, suggesting that HPV5 E6-mediated BAK degradation is dependent on HERC1 in keratinocytes.

Non-E6-mediated turnover of BAK has been previously observed in the HCT116 system (Figure 4.3 and Figure 4.4). As BAK was over-expressed in that system, the turnover observed in the HEKa cells may be similar but the decrease may be more apparent due to lower initial levels of endogenous BAK in the cells. Another difference may be that pLXSN-expressing cells appear to have higher starting levels of BAK compared to HPV5 E6-expressing cells, therefore a greater difference in BAK turnover is apparent by lower exposure times (1 minute). In contrast HPV5 E6-expressing cells had a lower level of BAK, requiring a longer exposure time (10 minutes) allowing lower levels at 4 and 6 hours to be observed.

4.3.4 Interaction of HERC1 with BAK *in vivo*

Having identified HERC1 as a novel ligase involved in E6-mediated BAK degradation, the next step was to investigate whether an interaction between BAK and HERC1 could be detected in cells. In contrast to the α-HPV constitutive targeting of p53, data previously presented suggests that HPV5 E6 only targets a

small amount of BAK in a specific, transitory conformation after UV damage. Therefore it was speculated that the interaction between BAK and HERC1, that is promoted by E6, may be transient. Furthermore, considering the large size of HERC1 and that HERC1 and BAK are likely to be membrane bound proteins, protein extraction preserving an association would be difficult. These factors may explain why HERC1 has not been identified in previously published E6 interactor studies (Howie et al., 2011, White et al., 2012, Tan et al., 2012b).

Although the domains of HERC1 which interact with BAK are unknown, in order to ubiquitinate a substrate, the active cysteine of the E3 ligase must be in proximity to the substrate lysine. Therefore, in attempts to preserve the interaction, lysates were incubated with an amine-sulfhydrl protein cross-linker (SPDP, #21857, ThermoScientific) however, using this approach, BAK could not be detected by western blot. Cross-linking may have compromised the BAK antibody epitope and subsequently this technique failed to show an interaction between BAK and HERC1 (data not shown).

In a different approach, the interaction between BAK and HERC1 was examined using a proximity ligation *in situ* assay (PLISA). PLISA uses primary antibodies against the proteins of interest from different species. Two secondary antibodies recognising the different species are then used, each conjugated to oligonucleotides with complementary sequences that enable them to hybridise. If in a proximity of <40nM, in subsequent reactions, the complementary oligonucleotides are ligated and a rolling circle amplification incorporates fluorescently labelled oligonucleotides to generate a fluorescent spot. This can be observed via fluorescence microscopy where a discrete focus indicates a single protein-protein interaction (summarised in Figure 4.6). This technique therefore allows for detection and localisation of single interactions between two proteins *in vivo* using antibodies against the proteins of interest, especially as the interaction between HERC1, BAK and E6 is likely to be transitory. As earlier data suggests that E6 is targeting BAK after it has undergone

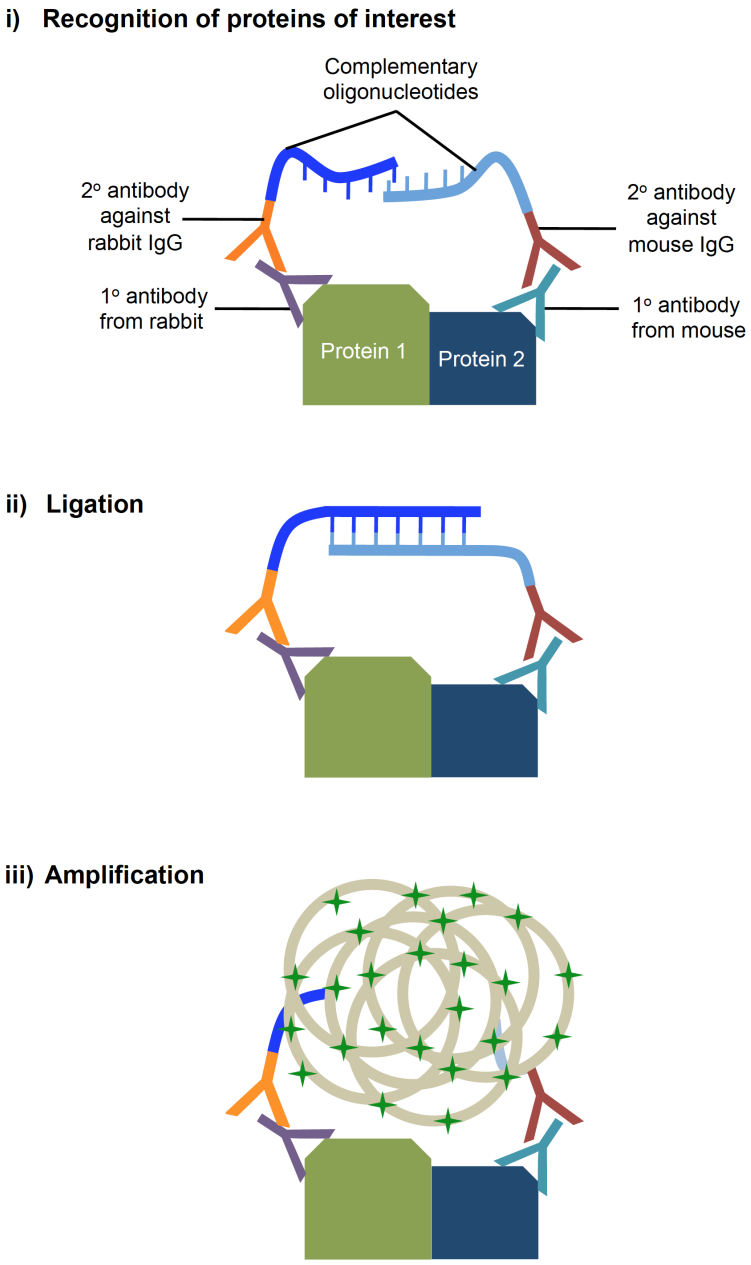


Figure 4.6 PLISA assay

i) Cells are fixed and stained with antibodies against the two proteins of interest, each antibody is raised in a different species. Cells are then incubated with two secondary antibodies, each recognising the primary antibodies from the different species and each conjugated to a complementary oligonucleotide.

ii) If in proximity of <40nm, the oligonucleotides are ligated.

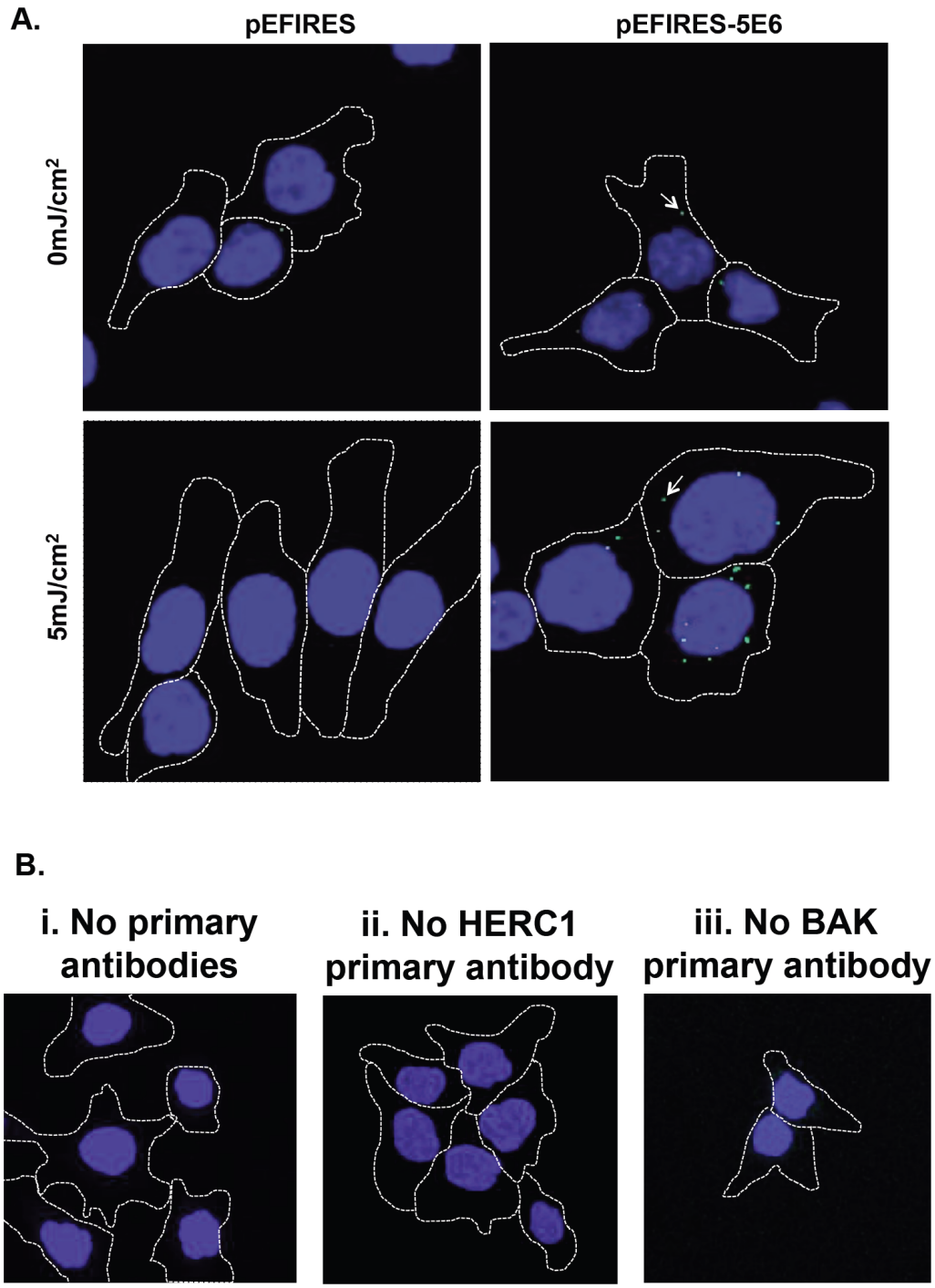
iii) After ligation, a rolling circle amplification is performed using the ligated oligonucleotides as a template, incorporating fluorescently labelled nucleotides.

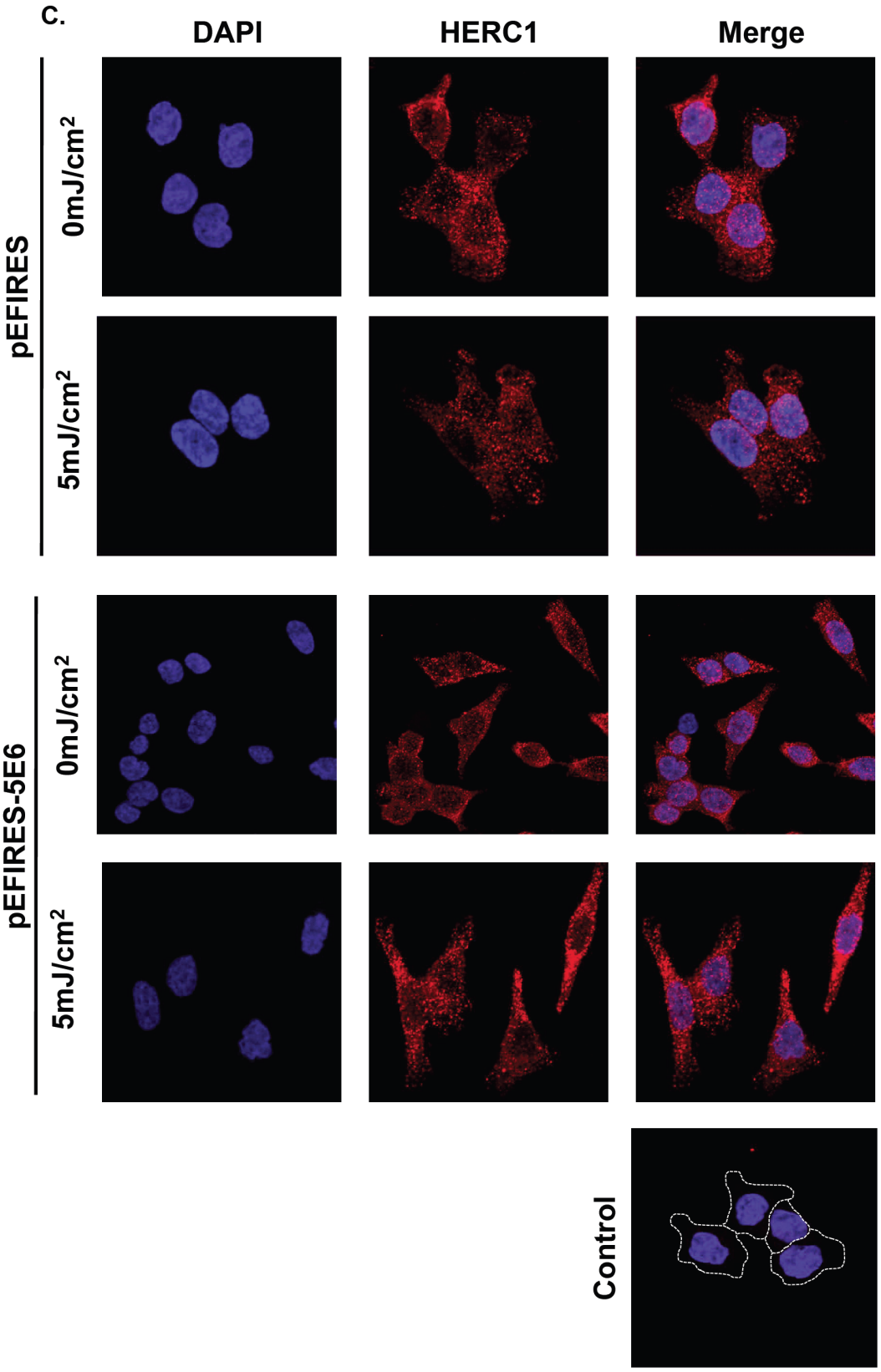
the N-terminal change, in this assay the BAK Ab1 antibody was used, therefore only the interaction of HERC1 with BAK molecules that have undergone the N-terminal conformational change are detected.

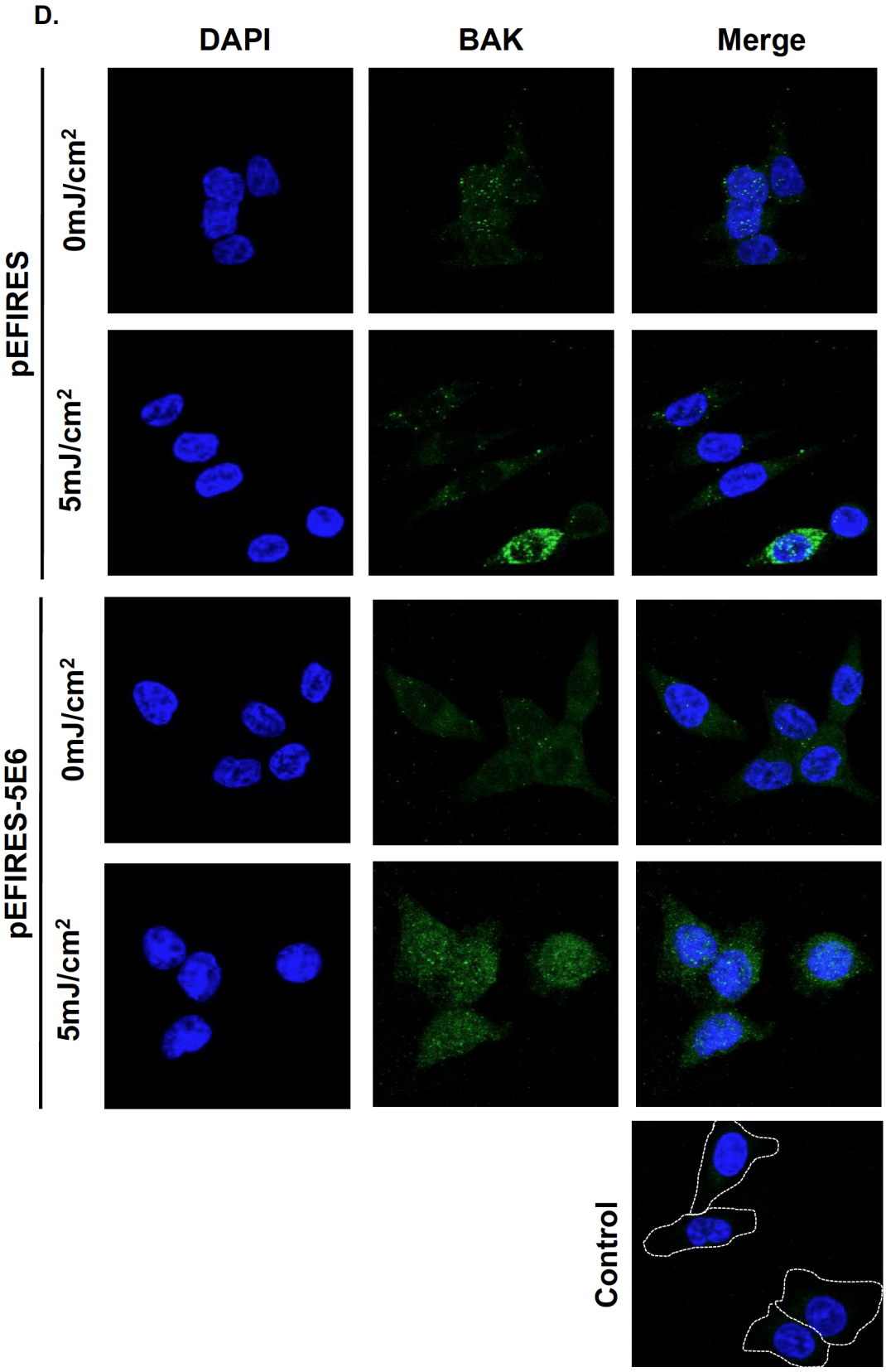
Figure 4.7 shows a proximity ligation assay performed in HCT116 WT BAK pEFIRES or pEFIRES-5E6-expressing cells which were seeded on coverslips and 24 hours later irradiated with 5mJ/cm^2 UVB for 4 hours. This time point was chosen as BAK degradation is observed approximately 6 hours after UVB irradiation, therefore an interaction between HERC1 and BAK is most likely to occur within this time window. Cells were fixed in PFA, permeabilised with saponin and the PLISA assay performed according to manufacturer's instructions. Sample images are shown in Figure 4.7A. PLISA control reactions omitting the primary antibodies are shown in Figure 4.7B to show that foci are specific to the presence of the antibodies. Figure 4.7C and D show single colour staining of HERC1 and BAK (Ab1), respectively, with the primary antibodies detected using fluorescently conjugated secondary antibodies to demonstrate the presence of the target proteins. These images show that HERC1 could be detected in both irradiated and non-irradiated cells expressing the empty vector and pEFIRES-5E6. The HERC1 staining shows a cytoplasmic localisation throughout the cell and is excluded from the nucleus. A significant difference in HERC1 staining is not observed between pEFIRES or pEFIRES-5E6-expressing cells with or without UVB irradiation.

The BAK staining is weak in unirradiated cells expressing pEFIRES or pEFIRE-5E6, as expected as there is likely to be only a small number of BAK molecules undergoing the activation process and is therefore recognised by the Ab1 antibody. Upon UVB irradiation the majority of pEFIRES-expressing cells stained weakly for Ab1, like the unirradiated cells, however some brightly staining cells could be observed suggesting these were apoptotic cells in which BAK had undergone the N-terminal conformational change. Upon irradiation of pEFIRES-5E6-expressing cells, BAK Ab1 staining appeared brighter compared to unirradiated cells but weaker

Figure 4.7 PLISA assay for an interaction between BAK and HERC1




C.
DAPI
HERC1
Merge
pEFIRES
0mJ/cm²
5mJ/cm²
pEFIRES-5E6
0mJ/cm²
5mJ/cm²
Control


D.
DAPI
BAK
Merge
pEFIRES
0mJ/cm²
5mJ/cm²
pEFIRES-5E6
0mJ/cm²
5mJ/cm²
Control

E.

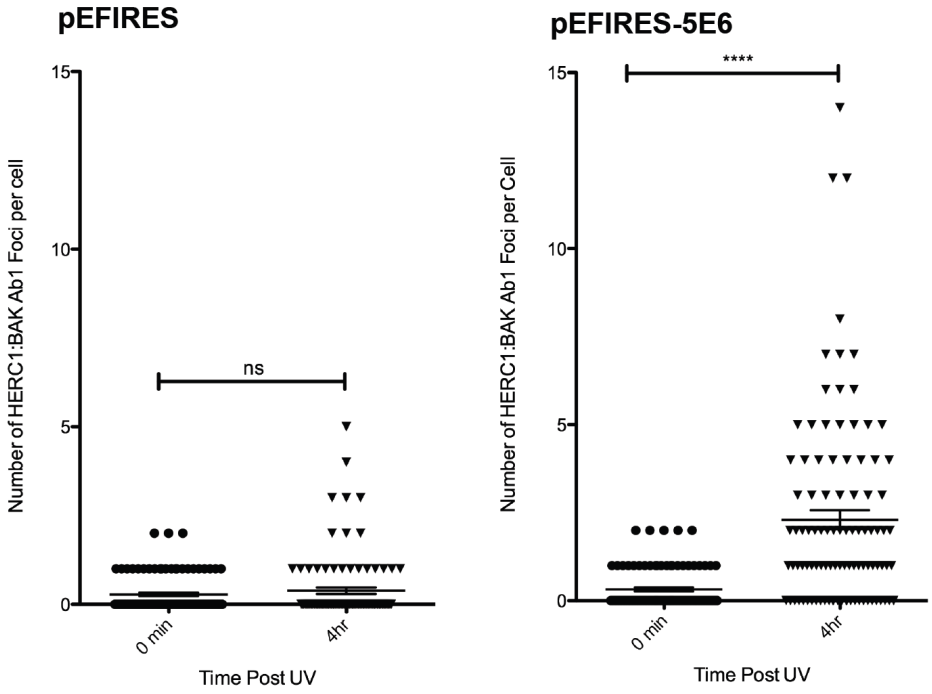


Figure 4.7 legend

HCT116 WT BAK cells expressing pEFIRES or pEFIRES-5E6 were seeded on coverslips and irradiated with 5mJ/cm^2. Four hours later cells were fixed, permeabilised using saponin and the HERC1/BAK interaction assessed using the proximity *in situ* ligation assay using a rabbit anti-HERC1 (Bethyl Laboratories, #A301-904A) and mouse anti-BAK (Ab1, #TC-100, Calbiochem) antibody.

A. Representative compressed Z-stack images of the PLISA assay. Blue; nuclear DAPI staining, green; HERC1/BAK foci. Dashed white lines indicate cell boundaries. Arrows indicate example foci showing a single interaction between BAK and HERC1.

B. Control PLISA reactions were performed to show specificity of the foci by performing the PLISA reactions omitting i. both the HERC1 and BAK primary antibody, ii. only the HERC1 primary antibody, iii. only the BAK primary antibody. Blue; nuclear DAPI staining. Dashed white lines indicate cell outline.

C. HCT116 WT BAK cells expressing pEFIRES or pEFIRES-5E6 were seeded on coverslips and irradiated with 5mJ/cm^2 for 4 hours. Cells were fixed and permeabilised using saponin. HERC1 single colour staining performed using an anti-rabbit HERC1 polyclonal antibody (Bethy Laboratories, #A301-904A) and AlexaFluor568 conjugated goat anti-rabbit secondary antibody. Control staining was performed by omission of the primary antibody (control).

D. HCT116 WT BAK cells expressing pEFIRES or pEFIRES-5E6 were seeded on coverslips and irradiated with 5mJ/cm^2 for 4 hours. Cells were fixed and permeabilised using saponin. Staining for BAK was performed using an anti-mouse BAK antibody recognising only BAK that has undergone the N-terminal conformational change (Ab1, #TC-100, Calbiochem) and AlexaFluor488 conjugated rabbit anti-mouse secondary antibody. Control staining was performed by omission of the primary antibody (control). Blue; nuclear DAPI staining, green; BAK.

E. The number of foci per cell were counted for 100 cells for each sample (50 cells from two experimental repeats). n=100 ± SEM, ns; p≥0.05 was taken as not significant, **** p≤ 0.0001 calculated by unpaired two tailed t-test to test the effect of UV within cell lines.

---

than that of the brightly staining cells observed for irradiated pEFIRES-expressing cells. These may be cells captured in an earlier stage of BAK activation and apoptosis induction. In UV-irradiated pEFIRES-5E6-expressing cells, there appeared to be fewer of the very brightly stained cells observed for UV-irradiated control cells. The BAK single colour staining highlights that BAK activation is not a synchronous event across a cell population and supports the use of the PLISA assay in detecting the likely transient interaction between HERC1 and BAK as BAK asynchronously reaches a conformation in which it can be targeted by the E6 protein in individual cells.

The number of foci per cell for 100 cells for each cell line (50 cells from two experimental repeats) was recorded and shown in the plots in Figure 4.7E. In non-irradiated pEFIRES and pEFIRES-5E6 cells only a minimal number (maximum of two) HERC1:BAK foci could be detected per cell. After 4 hours of UVB exposure in pEFIRES-expressing cells, compared to the untreated control, there was a small, but not significant, increase in the number of HERC1:BAK foci per cell. In contrast, 4 hours after irradiation of pEFIRES-5E6-expressing cells the number of HERC1:BAK foci increased significantly (p≤0.001) compared to the untreated control with up to 14 foci detected in one cell. This data suggests that HERC1 and BAK interact *in vivo* and that the interaction is significantly greater in cells expressing HPV5 E6 after exposure to UVB irradiation.

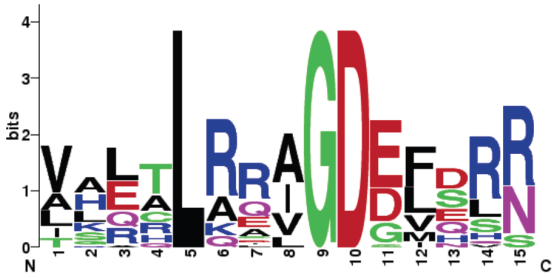
4.3.5 Investigation of a putative HERC1 BH3 sequence

Having generated evidence supporting that an interaction between BAK and HERC1 can occur, further studies were initiated in order to elucidate the mechanism of how the association between the two proteins may occur. MCL-1 is an anti-apoptotic BCL-2 protein which binds and inactivates BAK by inserting a BH3 domain into the hydrophobic pocket on a BAK monomer. This BH3 domain interaction with the hydrophobic pocket is a common mechanism used by BCL-2 family proteins to associate. Furthermore, MCL-1 is ubiquitinated by the HECT E3 Ligase MULE (MCL-1 Ubiquitin Ligase E3, also called UREB1) which similarly uses a BH3 domain to insert into the hydrophobic pocket of MCL-1 to interact (Zhong et al., 2005, Warr et al., 2005). Therefore the possibility that HERC1 could use a similar mechanism to interact with BAK was investigated. Since earlier data in this thesis showed BAK proteolysis could be blocked by the BAK S117E mutant (Figure 3.20), this suggests that exposure of the BAK hydrophobic pocket may be a requirement for HERC1 to associate with BAK.

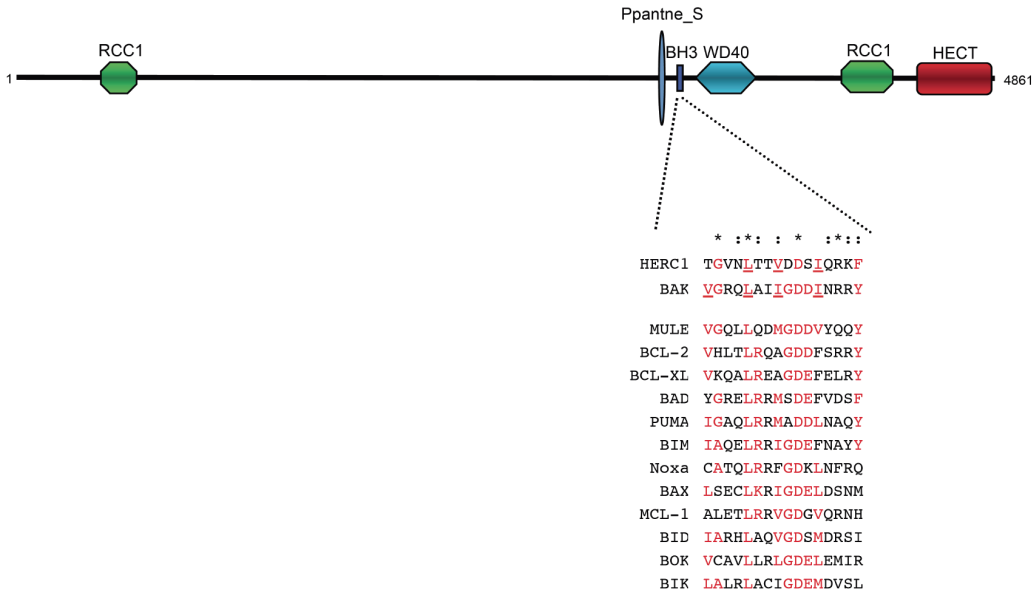
Using the T-Coffee alignment programme, global alignment of the entire HERC1 and BAK amino acid sequences revealed a region of the HERC1 protein that had homology to the BAK BH3 sequence, suggesting that this region of HERC1 may also function as a putative BH3 sequence. Comparison of this putative HERC1 BH3 sequence with BH3 sequences from other BCL-2 proteins showed that the putative HERC1 BH3 sequence had greatest sequence homology to that of the BAK protein (Figure 4.8A and B). BH3-only proteins, such as BID, are known to bind BAK at the hydrophobic surface. Four hydrophobic amino acids of the BAK BH3 sequence (V^{74}, L^{78}, I^{81} and I^{85}, underlined in Figure 4.8B) are required for insertion into the hydrophobic pocket of BCL_{XL} (Sattler et al., 1997, Dewson et al., 2008). In the putative BH3 sequence of HERC1, three of these four key amino acids are conserved, or conserved substitutions (L, V, I; underlined in Figure 4.8B). Helix

Figure 4.8 HERC1 has a putative BH3 domain

A.



B.



C.

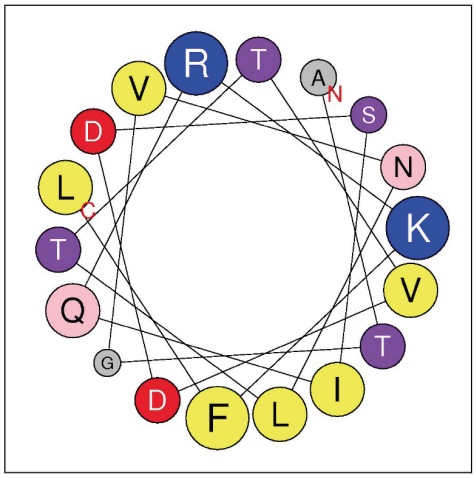


Figure 4.8 legend

A. The BH3 consensus sequence taken from http://prosite.expasy.org/PS01259

B. A putative BH3 domain in HERC1 was identified. This BH3 sequence has greatest homology to that of BAK. The underlined residues in the BAK BH3 sequence insert into the hydrophobic binding pocket of BAK for dimerisation. Three of these residues are conserved in the BH3 sequence identified in HERC1. Alignment performed using T-Coffee, http://www.ebi.ac.uk/Tools/msa/tcoffee/. * identical, : conserved substitution

C. The HERC1 BH3 sequence is predicted to form a helix, which would be required to bind the hydrophobic pocket of BAK. grey; small, blue; positive, yellow; hydrophobic, red; negative charge, pink; large polar, purple; small polar. Structure predicted using HeliQuest using the sequence **ATGVNLTTVDDSIQRKFL.**

---

formation software (HeliQuest) also predicted that this putative BH3 sequence in HERC1 could form a helix with a largely hydrophobic face required to insert into the BAK hydrophobic binding pocket (comprising F, L, I, T, V; where T is polar; Figure 4.8C).

Despite the identification of a BH3 consensus sequence, BH3 sequences are difficult to predict: the BH3 consensus shown in Figure 4.8A suggests glycine must occur at position 9 of the sequence, however the established BH3 sequences of BAD and PUMA have serine or alanine, respectively, at this position. Furthermore a hierarchy of interactions between the BCL-2 family members exists where preferential binding to certain family members and not others occurs for each of the proteins (Certo et al., 2006, Kim et al., 2006), consequently the requirement of this putative BH3 sequence in HERC1, and of the hydrophobic pocket on BAK, for the interaction between these two proteins was tested.

The experiment performed was similar to that previously used to identify the MULE BH3 domain binding to MCL-1 via peptide binding (Zhong et al., 2005). First the ability of the HERC1 BH3 sequence to bind BAK was tested. Biotinylated peptides were synthesised corresponding to the BH3 sequence of BAK, BID, HERC1 and MULE (used as a control) to test the specificity of binding of the peptides (sequences shown in Figure 4.9A). Mutant peptides of the BH3 domains were also

A.

Name	BH3 peptide amino acid sequence
BAK	TMGQVGRQLAIIGDDINRRYDSEFQT
BAK 4E	TMGQEGRQEAIEGDDENRRYDSEFQT
BID	IIRNIARHLAQVGDSMDRSIPPGGLV
BID 4E	IIRNEARHEAQEGDSEDRSIPPGGLV
HERC1	ISAATGVNLTTVDDSIQRKFLPSFLR
HERC1 4E	ISAAEGVNETTEDDSEQRKFLPSFLR
MULE	MTQEVGQLLQDMGDDVYQQYRSLTRQ
MULE 4E	MTQEEGQLEQDEGDDEYQQYRSLTRQ

B.

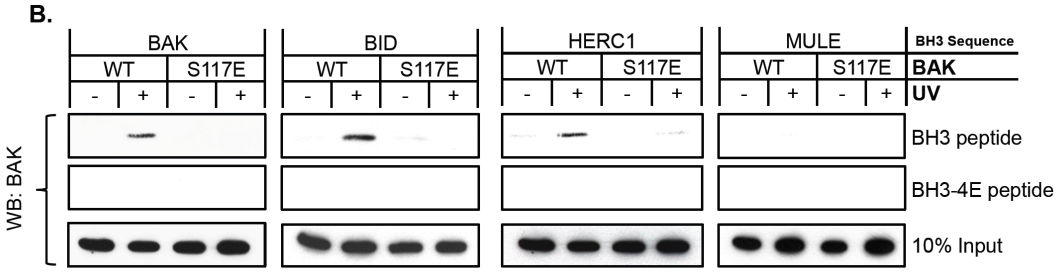


Figure 4.9 HERC1 BH3 sequence binding to BAK and BAK S117E

A. Biotinylated peptides corresponding to the BH3 domain sequences of BAK, BID, HERC1 and MULE were synthesised. Corresponding 4E mutant peptides were also synthesised where the 4 conserved amino acids known to bind the hydrophobic grove of BAK were mutated to glutamic acid (highlighted in red).

B. HCT116 WT or S117E BAK cells were irradiated ± 10mJ/cm^2 for 8 hours. Cell lysates were prepared and incubated with biotinylated peptides corresponding to the BH3 domain sequence of BAK, BID, HERC1 and MULE or with corresponding BH3-4E peptides in which the conserved amino acids in these BH3 sequences known to insert into the hydrophobic pocket of BAK were mutated to glutamic acid. The peptides were precipitated with avidin agarose beads and the pull-downs western blotted for BAK (rabbit monoclonal [Y164]).

Experiment performed twice.

synthesised where the four hydrophobic residues inserting into the hydrophobic pocket of BAK were replaced with glutamic acid (BH3-4E) as negative controls. Single mutation of these sites is known to destroy the BH3:groove interaction (Dewson et al., 2008, Sattler et al., 1997). HCT116 WT BAK or S117E BAK cells were seeded on 150mm dishes and 24 hours later were either left untreated or irradiated with 10mJ/cm^2 UVB to induce dephosphorylation of S117, and exposure of the hydrophobic pocket, and cells were harvested 8 hours later. Cell lysates were prepared and incubated with the specified peptide for 4 hours. Avidin-agarose beads were then added and incubated overnight. The beads were pelleted and the associated proteins that had been pulled down were western blotted for BAK.

Figure 4.9B shows that none of the mutant peptides were able to bind to either WT or S117E BAK regardless of whether the cells had been exposed to UVB irradiation. The peptide corresponding to the BH3 domain of BAK or BID could pull-down BAK but only if the cells had been irradiated as this stimulates removal of the inhibitory phospho-moiety by PP2A, as previously shown (Azad et al., 2012). The peptide corresponding to the BH3 sequence of HERC1 could also pull-down BAK once the cells had been exposed to UVB, whilst the MULE peptide not bind BAK under any conditions tested. This is in accordance with previous studies detailing interactions amongst BCL-2 family proteins (Kim et al., 2006). These data suggest that the putative BH3 sequence of HERC1 is able to bind BAK and requires exposure of the hydrophobic pocket on BAK in order to do so.

4.3.6 Construction of a HERC1 mini-gene

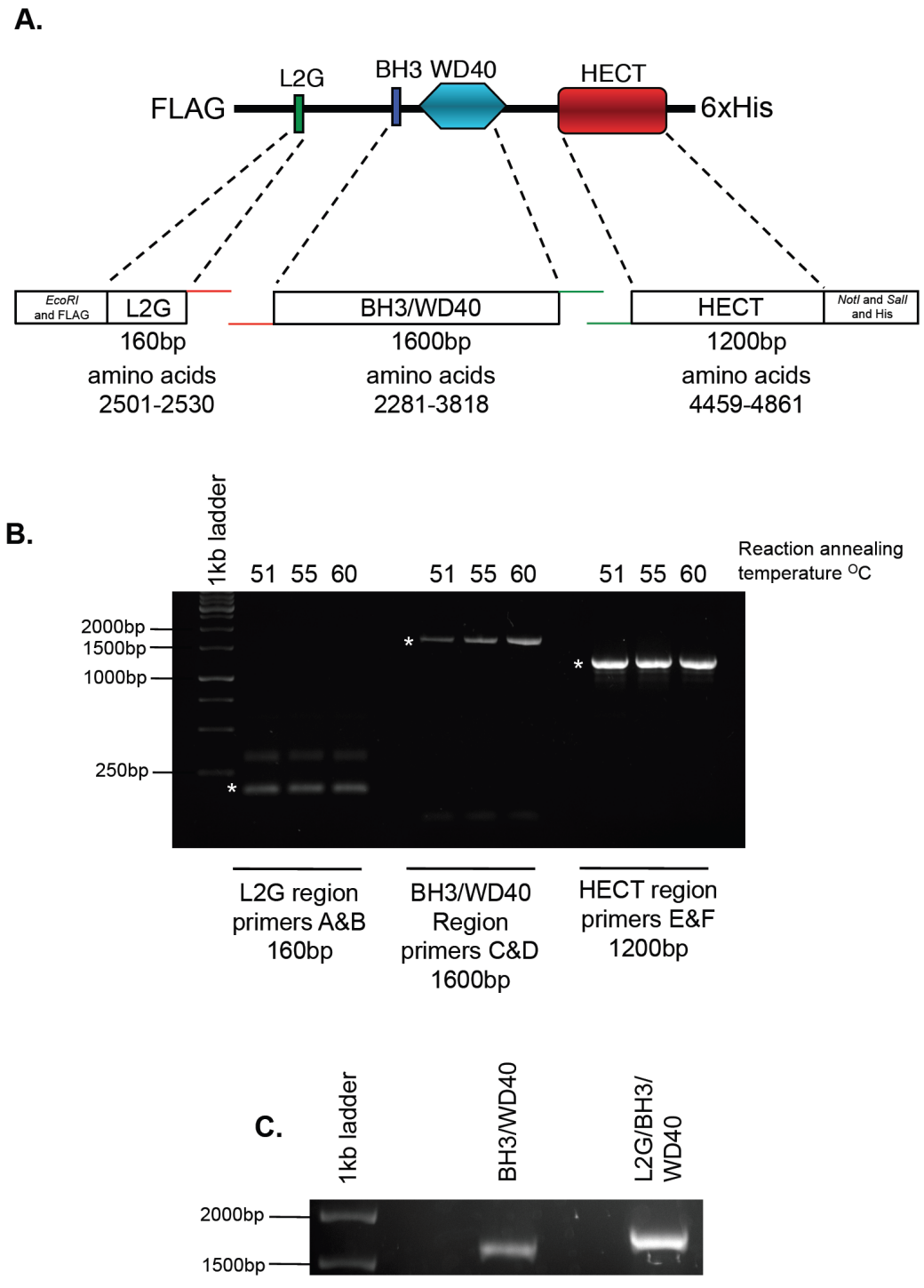
Following the previous work in this thesis suggesting that HERC1 and BAK can interact it was important to attempt to establish whether HERC1 could ubiquitinate BAK directly. Working with the full length HERC1 proved challenging for use in ubiquitination assays to assess its requirement for BAK ubiquitination. Previously ubiquitination experiments have been performed using only the C-terminal HECT domain of E3 ligases (Pandya et al., 2010). The involvement of only the HERC1 HECT domain has also been used to investigate HERC1-mediated TSC2 turnover

(Chong-Kopera et al., 2006), however such experiments lack substrate specificity recognition and it was important here to investigate the requirement of the putative BH3 domain identified in HERC1.

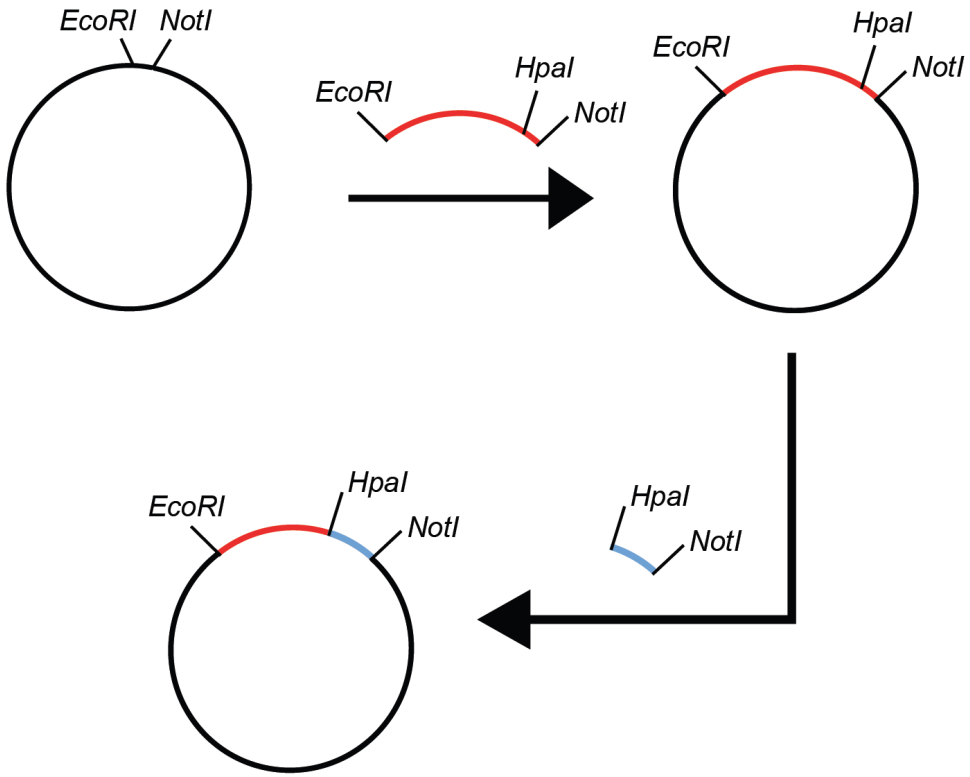
Consequently a HERC1 'mini-gene' was synthesised for use in an *in vitro* BAK ubiquitination assay (summarised in Figure 4.10). The mini-gene comprised only the regions of interest in order to reduce its size (Figure 4.10A). These were an L2G motif, required for the recognition of host cell interactors by some E6 proteins (amino acids 2501-2530 of full length HERC1; L2G region), the HERC1 putative BH3 domain and directly adjacent WD40 domain as it was hypothesised that these would be required for interaction with BAK (amino acids 2281-3818 of the full length HERC1 protein; BH3/WD40 region) and HECT domain comprising the active cysteine residue required for mediation of ubiquitin transfer (4459-4861 of the full length HERC1 protein; HECT region). Alignment of the HERC1 and E6AP C-terminal HECT domains and active cysteine is shown in Figure 4.11.

In order to construct the mini-gene the three fragments of interest were amplified by PCR reaction from plasmid vectors encoding cloned fragments of the HERC1 gene (gifted by J. L. Rosa). In order to anneal each of the fragments to the next, the primers designed to amplify each region added an approximately 20 nucleotide overhang complementary to the sequence of the subsequent fragment (see Figure 4.10A and Table 4.2). The forward primer for amplification of the L2G region comprised an *EcoRI* restriction site and nucleotide sequence for a FLAG-tag (amino acid sequence DYKDDDDK), for protein detection and purification, at the 5' end. The 3' end of the reverse primer for amplification of the HECT region coded for a 6xHis-tag (for identification and western blot) and *SalI* and *NotI* restriction sites for subcloning into the pMAL-C2 and pcDNA vectors, respectively, with the 5' *EcoRI* restriction site. Each of the fragments was amplified using the Velocity polymerase (Bioline) and the reactions performed at three different annealing temperatures (52,

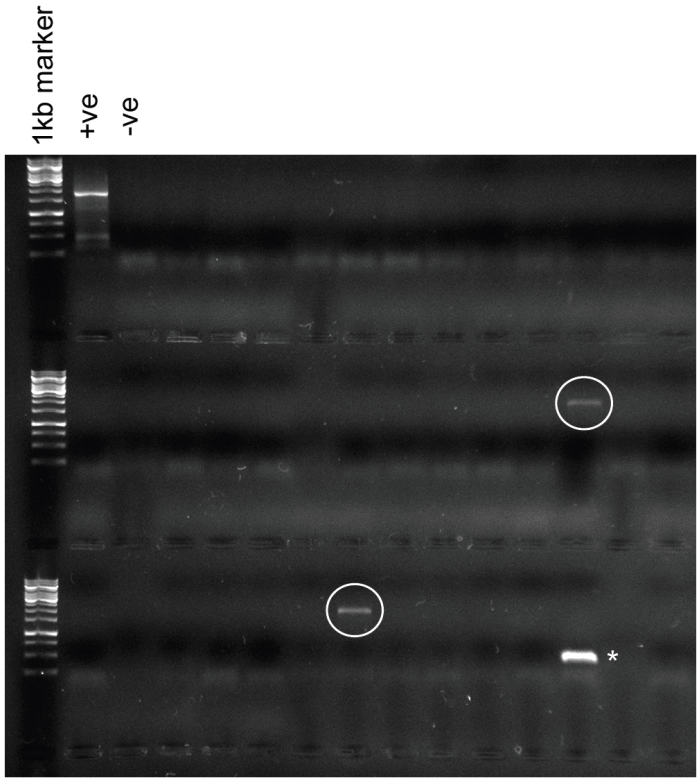
Figure 4.10 Construction of the HERC1 mini-gene

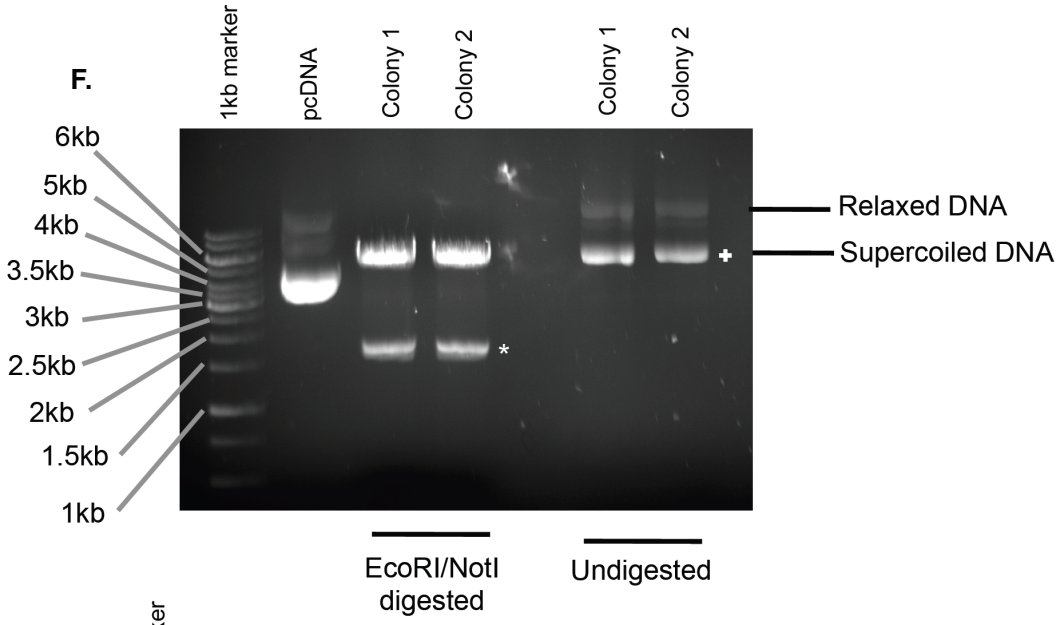


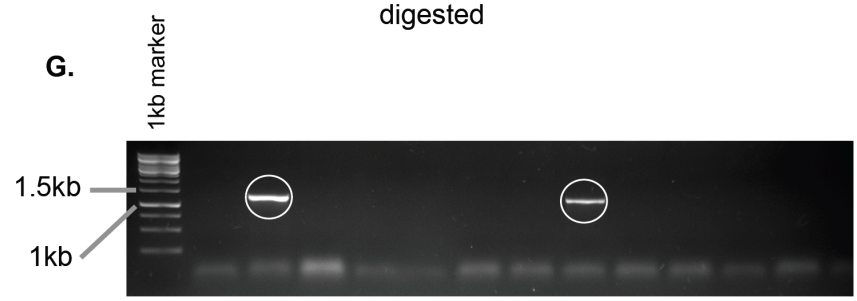
D.


EcoRI
NotI
EcoRI
HpaI
NotI
EcoRI
HpaI
NotI
HpaI
NotI
EcoRI
HpaI
NotI

E.


1kb marker
+ve
-ve
*


F.
1kb marker
pcDNA
Colony 1
Colony 2
Colony 1
Colony 2
6kb
5kb
4kb
3.5kb
3kb
2.5kb
2kb
1.5kb
1kb
Relaxed DNA
Supercoiled DNA
*
+
EcoRI/NotI digested
Undigested


G.
1kb marker
1.5kb
1kb

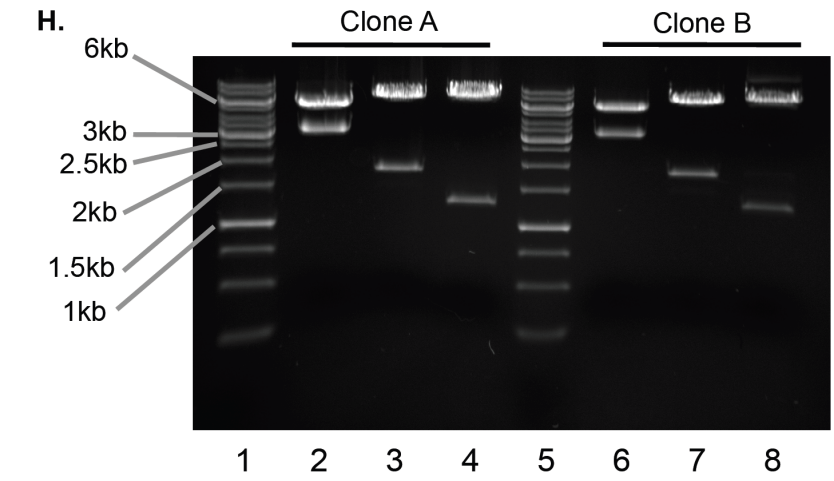

H.
Clone A
Clone B
6kb
3kb
2.5kb
2kb
1.5kb
1kb
1 2 3 4 5 6 7 8

Figure 4.10 legend

A. Schematic of the HERC1 mini-gene domains and the PCR products with primer overhangs designed to anneal the three products. Amino acids refer to those of the full length HERC1 protein.

B. Each of the PCR fragments shown in (A) was amplified by PCR at three different annealing temperatures (51, 55 and 60^{o}C). * indicates product of expected length by agarose gel electrophoresis.

C. The BH3/WD40 fragment was annealed to the L2G product in a PCR reaction. A longer product than the BH3/WD40 product alone, of the expected size (1760bp), was detected by agarose gel electrophoresis.

D. Schematic of the sequential cloning strategy used to construct the HERC1 mini-gene. A *HpaI* restriction site was inserted into the L2G/BH3/WD40 PCR fragment and a *NotI* restricton site added to the 3' end (represented by the red fragment). Using EcoR1 and NotI, the fragment was cloned into the pcDNA vector. The vector and HECT fragment with a 5' *HpaI* restriction site were digested with HpaI and NotI and the HECT fragment cloned in (represented by the blue fragment).

E. The L2G/BH3/WD40 fragment was first cloned into the pcDNA vector using the *EcoRI* and *NotI* restriction sites. A direct PCR screen from bacterial colonies for successful clones was performed. Bacterial colonies from selective plates were suspended in PBS. Two microlitres of the suspension was added to a PCR reaction with primers specific for amplification of the L2G/BH3/WD40 domain. The indicated lanes show the 1kb marker, a positive control reaction using the L2G/BH3/WD40 PCR fragment as a template (expected size 1760bp) and a negative control replacing the bacterial suspension with water in the reaction. All other lanes are PCR products from bacterial clones. Two potentially successful clones are circled. * indicates a false positive as the PCR product was smaller than expected.

F. The two bacterial clones identified in (F) were expanded, the plasmid DNA was extracted and subjected to a diagnostic restriction digest for the L2G/BH3/WD40 fragment by EcoRI and NotI. In the digested vectors a band of approximately 1.7kb can be detected (*) possibly corresponding to the L2G/BH3/WD40 fragment (expected 1760bp). The band at ~6kb (**+**) is likely to correspond to supercoiled undigested vector (in the linear conformation, expected to be 7.16kb). The undigested pcDNA plasmid is expected to be 5.4kb. The discrepancies between these expected and observed sizes may be explained by the use of linear markers and supercoiled DNA. Both clones were subsequently sequenced.

G. The HECT domain fragment was cloned into the pcDNA vector containing the L2G/BH3/WD40 fragment, using HpaI and NotI. Successful clones were again screened using direct PCR from transformed bacterial colonies. Reactions were performed using primers to the HECT domain. Identification of a PCR product of 1200bp, corrresponding to the size of the HECT domain fragment, was used to isolate bacterial clones likely to express the complete mini-gene. The indicated lane shows 1kb markers. All other lanes contain PCR reactions for the HECT domain fragment using bacterial suspension of isolated clones as a template. Two products of the expected size were detected.

H. The two clones isolated in (G) were subjected to diagnostic restriction digest. Lane 1 and 5; 1kb markers, Lane 2 and 6; EcoRI and NotI for the complete mini-gene sequence (expected 2960bp), Lane 3 and 7; EcoRI and HpaI for the L2G/BH3/WD40 domain (expected 1760bp), Lane 4 and 8, HpaI and NotI for the HECT domain (expected 1200bp). The complete mini-gene was checked by DNA sequencing.

---

55 and 60^{o}C). As some of the primers introduced a long non-templated sequence three initial cycles with an annealing temperature of 45^{o}C were used to increase initial primer annealing before a remaining 27 cycles using the indicated annealing temperatures.

The reactions at all three temperatures showed an amplified product when analysed by agarose gel (Figure 4.10B). For the BH3/WD40 and HECT region the PCR products were specific, however all three annealing temperatures gave a non-specific product for the L2G region. Consequently the products of the correct size for the L2G region were excised from the gel and extracted using the Qiagen Gel Extraction kit. The BH3/WD40 and HECT region reactions were cleaned by PCR purification (Qiagen). For all three fragments, products from the reactions at the differing annealing temperatures were pooled and cleaned by phenol/chloroform extraction. A PCR reaction was then performed to anneal the L2G region to the BH3/WD40 region. The L2G and BH3/WD40 fragments were used as the template in a molar ratio in a PCR reaction with the primers A and D (Table 4.2). Again, three initial cycles with an annealing temperature of 45^{o}C before increasing to 60^{o}C for the remaining 27 cycles was used to aid initial annealing of the two fragment overhangs.

```
E6AP_human      ESPLKYLFRPEEIELLICGSRNLDFQALEETTEYDGGYTRDSVLIREFWEIVHSFTDEQKRLFLQ
HERC1_human     PVPLLSLLTAKQLEQMVCGMPEISVEVLKKVVRYR-EVDEQHQLVQWFWHTLEEFSNEERVLFMR
                  **  *: .:::* ::**  ::..:.*::...*     .:  *:: **. :..*::*:: **::
```

Figure 4.11 HERC1 and E6AP C-terminus alignment

The amino acid sequences of HERC1 and E6AP were aligned using the T-Coffee alignment program. The alignment of the sequence surrounding the active cysteine is shown. The active cysteines are shown in bold and underlined. * identical : conserved substitution . semi-conserved substitution.

The product was analysed by agarose gel electrophoresis and an increase in size in the product could be detected when compared to that of the BH3/WD40 region alone (Figure 4.10C).

The product was excised from the gel and phenol/chloroform extracted and used with the HECT domain fragment in a molar ratio as a template in a PCR reaction to anneal the two fragments with the primers A and F. This reaction, however, failed to anneal the two fragments. Consequently new primers were designed to extend the overhangs on the 3' end of the L2G/BH3/WD40 fragment and the 5' end of the HECT domain region to approximately 40 nucleotides (primers G & H). PCR reactions were performed using the L2G/BH3/WD40 fragment as a template with primers A and H, and the HECT region template with primers G & F. The reaction to anneal the L2G/BH3/WD40 and HECT region was then performed again as previous, however this also failed to give a product of the correct size. Consequently a sequential cloning approach was taken, using codon redundancy (schematic in Figure 4.10D).

A *Hpa*I restriction site was identified as not being present in the pcDNA vector as well as not changing the amino acid sequence in the mini-gene. Consequently a primer was designed to introduce a *HpaI* and *NotI* restriction site at the 3' end of the L2G/BH3/WD40 fragment, a PCR reaction was performed using this new primer (I) and primer A and the original L2G/BH3/WD40 fragment as template DNA (without

Table 4.2 HERC1 mini-gene construction primers

Primers were designed in order to construct the HERC1 mini-gene.

	Primer name	Description	Sequence (5'→3')
A	EcoR1 FLAG L2G FWD	Adds an *EcoRI* restriction site and FLAG-tag to amplify the L2G region	CTCGAATTCACCATGGAT TACAAGGATGACGACGAT AAGTCAGAAATCAGAGCA GT
B	L2G BH3/WD40 RVE	Adds an overhang complementary to the start of the BH3 segment to the end of the L2G region	TGTACAAGCAGTTTGGCT TCAGCCAGAACTTTTGG
C	L2G BH3/WD40 FWD	Adds an overhang complementary to the end of the L2G segment to the beginning of the BH3/WD40 segment	CCAAAAGTTCTGGCTGAA GCCAAACTGCTTGTACA
D	BH3/WD40 HECT RVE	Adds an overhang complementary to the beginning of the HECT region to the end of the BH3/WD40 segment	ATGGTTTTTCCTATGGAT GCTGTACAATTCACGA
E	BH3/WD40 HECT FWD	Add an overhang complementary to the end of the BH3/WD40 segment to the beginning of the HECT region	TCGTGAATTGTACAGCAT CCATAGGAAAAACCAT
F	SalI NotI His-tag RVE	Adds *SalI* and *NotI* restriction sites and His-tag to the 3' end of the HECT domain	GAGGCGGCCGCGTCGAC TCAATGATGATGATGATG ATGGTAGTCAGTGTCGGA GC
G	HECT overhang FWD	Extends the overhang of the 5' end of the HECT fragment	GCTGCTTGCTCAAATAGA TCAAAGGATGTTTTGGTC GTGAATTGTACAGCA
H	BH3/WD40 overhang RVE	Extends the overhang of the 3' end of the L2G/BH3/WD40 fragment	GGTCCATAGTTTTTGCCT TGAACCATGGTTTTTCCT ATGGA
I	L2G/BH3/WD40 *Hpa*I and *NotI* RVE	Introduces the *HpaI* and *NotI* restriction sites at the 3' end of the L2G/BH3/WD40 fragment	GGTGCGGCCGCACAGTT AACGACCAAAACATCCTT TG
J	HECT *Hpa*I FWD	Introduces *HpaI* restriction site at the 5' end of the HECT region.	TCAGTTAACTGTACAGCA TCCATAGG
K	HERC1 MG STOP FWD Mutation primer	Introduces a stop codon to remove the C-terminal His-tag. Codon change from CAT to TAA	GCTCCGACACTGACTACT AACATCATCATCATCATT G
L	HERC1 MG STOP RVE Mutation primer		CAATGATGATGATGATGT TAGTAGTCAGTGTCGGAG C

M	HERC1 MG C to A FWD Mutation primer	Mutates the active cysteine of HERC1 to alanine. Codon change of TGT to GCT	AACTGGAGCAGATGGTG GCTGGGATGCCCGAGAT CTC
N	HERC1 MG C to A RVE Mutation primer		GAGATCTCGGGCATCCC AGCCACCATCTGCTCCAG TT

the extended overhang). Using the *EcoRI* and *NotI* restriction sites, the L2G/BH3/WD40 fragment was cloned into the pcDNA vector. Transformation of the reaction into BL21 bacteria gave a large number of false positive clones, therefore a direct PCR for the fragment from bacterial colonies was utilised as a higher throughput screening approach.

Bacterial colonies were picked from selective plates and resuspended in 15µl PBS. Two microlitres of this suspension was used in a Taq polymerase PCR reaction as a template with primers A and I. Products from the reactions were examined by agarose gel electrophoresis (Figure 4.10E). Two clones producing a product of the expected size were identified, the bacteria were expanded to a 5ml culture and the plasmid extracted using Qiagen QIAprep miniprep kit. This DNA was subjected to a test restriction digest with EcoRI and NotI (Figure 4.10F). Both clones, when digested, gave a fragment of the expected size of the L2G/BH3/WD40 fragment and were sent for sequencing using the sequencing primers pcDNA seq fwd and HERC1 MG seq1 given in Table 2.16. Only one of the clones had the correct sequence.

The HECT domain region PCR product with the extended 5' overhang was used as a template in a PCR reaction with primer F and a new forward primer to introduce a *HpaI* restriction site at the 5' end of the product (primer J). The product with the extended 5' overhang was used to provide sufficient template for the primer introducing the *HpaI* restriction site to anneal. This product and the pcDNA vector encoding the L2G/BH3/WD40 domain were digested with NotI and HpaI and used to clone the HECT fragment into the L2G/BH3/WD40 containing plasmid. Again, a direct PCR bacterial colony screening approach was taken using primers F and J to screen for insertion of the HECT domain. Analysis by agarose gel electrophoresis for products correlating with the expected size of the HECT domain identified two

positive clones (Figure 4.10G). These clones were expanded to 5ml cultures, the DNA extracted as previous and subjected to a series of diagnostic restriction digests.

For test restriction digests the DNA was digested with EcoRI and NotI to check for insertion of the complete mini-gene (L2G/BH3/WD40/HECT), EcoRI and HpaI for the L2G/BH3/WD40 fragment, and HpaI and NotI to check the HECT domain insertion (Figure 4.10H). Both clones appeared correct, with fragments of the expected size given for all digests. The construct insert was therefore sequenced using nine sequencing primers designed ~300bp apart (Table 2.16), again only one clone provided the complete correct sequence. A naturally occurring single nucleotide polymorphism was identified, differing from the reference sequence for *herc1* (Gene ID: 8925), resulting in a codon change of GAG to GAC and an amino acid substitution of E3722D in the full length HERC1 protein.

Having constructed the mini-gene, attempts were made to transiently express it in both HEK293 and HCT116 cells for *in vivo* assays however, using an anti-FLAG antibody by western blot, expression could not be detected in cellular lysates.

For use in *in vitro* assays, for expression and purification from bacteria, the coding sequence was subcloned into the bacterial expression pMAL-C2 vector using the *EcoRI* and *SalI* restriction sites. Correct insertion was verified by sequencing. Use of the pMAL-C2 vector fuses the mini-gene to the maltose binding protein (MBP) and leads to cytoplasmic expression, resulting in a higher yield and a more soluble fusion protein (Riggs, 2001). Furthermore, after discussion with P. Howley, previous work with HERC2 suggested a C-terminal tag may interfere with HECT domain activity. Consequently mutational primers were designed to mutate the first histidine codon of the His-tag (CAT) to a STOP codon (TAA; primers K & L in Table 4.2) using the QuikChangeII XL site directed mutagenesis kit as previously described (Stratagene). In order to generate a non-functional control for the mini-gene, mutational primers were also designed to mutate the active cysteine to alanine (HERC1 mini-gene mutant C859A) in the HERC1 mini-gene fusion protein sequence

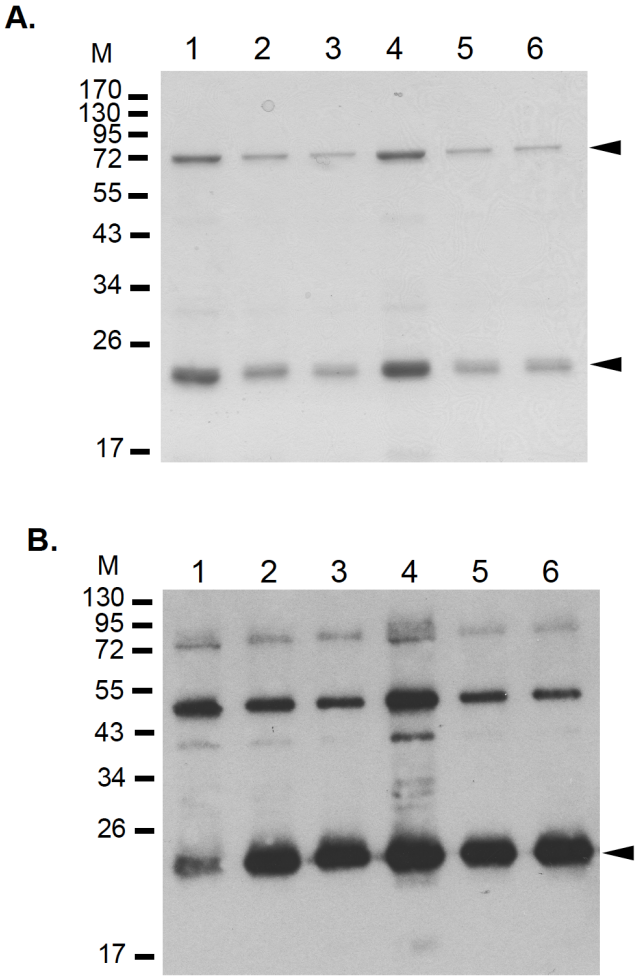
by codon change from TGT to GCT. The resultant HERC1 mini-gene was verified by DNA sequencing. The final sequences of the wild type HERC1 mini-gene construct and protein are given in Appendix 1.

4.3.7 *In vitro* HPV5 E6-mediated ubiquitination assay of BAK using the HERC1 mini-gene

In order to test the HERC1 protein expressed from the mini-gene construct for ubiquitination activity towards BAK, an *in vitro* ubiquitination assay was designed based on previous reports (Woelk et al., 2006, Okamoto et al., 2009). In order to perform the experiment human recombinant ubiquitin processing enzymes (E1 enzyme for ubiquitin activation and E2 ubiquitin conjugating enzymes), along with recombinant ubiquitin, were obtained from Boston Biochemicals. Only one human E1 enzyme is available. However, E2 enzymes are more numerous and show interacting preferences with E3 enzymes. The HERC1 HECT domain active cysteine has previously been shown to preferentially form a thioester bond with UbcH5a (Schwarz et al., 1998), therefore this E2 was selected. In addition to the purchased E1, E2 enzymes, ubiquitin and buffers, additional components of the ubiquitination assay were expressed and purified from bacteria as described in Materials and Methods.

As a substrate, His-tagged BAK lacking the C-terminal transmembrane domain (His-BAKΔC; Figure 4.12) was produced from bacteria. Coomassie staining of the purified proteins (Figure 4.12A) revealed that the His-BAKΔC protein existed in a monomeric form, but in addition a higher molecular weight band of ~70kDa was also observed. Western blotting of these samples (Figure 4.12B) revealed that both species reacted with the BAK monoclonal antibody, suggesting that the ~70kDa species was likely to be an aggregated form of the protein generated either during expression or purification. Western blotting also revealed a BAK species of ~50kDa that was not readily visible on the stained gel. For the ubiquitination reactions using His-BAKΔC as substrate, the concentrated elution 3 (Figure 4.12 lane 6) was used.

Figure 4.12 Purification of His-BAKΔC protein



A. The His-BAKΔC protein was eluted in three fractions from His-Select Nickel affinity gel using 200mM imidazole, elutions E1-E3 (lanes 1-3) each in 750µl volumes. A 20µl sample of each elution was analysed. Eluted fractions E1-E3 were then dialysed and concentrated to generate fractions E4-E6 respectively (lanes 4-6), and a 1µl sample of each was analysed on a 12% acrylamide SDS-PAGE gel and coomassie staining. Monomeric BAK as well as a slower migrating species are indicated by arrowheads.

B. Elution fractions E1-E6 were analysed by western blotting using the anti-BAK [Y164] antibody. As well as monomeric BAK, indicated by an arrowhead, higher molecular species were also detected. Fraction E6 was used in subsequent ubiquitination assays.

GST-E6, GST, MBP (Figure 4.13) and the MBP-HERC1 and the inactive C to A mutant protein (Figure 4.14) were also expressed and purified from bacteria. For the MBP-HERC1 fusion protein, the three elution fractions show a band of approximately 150kDa corresponding to the expected size of the MBP-HERC1 fusion protein, however a large number of lower molecular mass contaminants are also observed. Western blot with an anti-FLAG antibody (Figure 4.14D) showed that, for the wild type protein, many of these appeared to be C-terminal truncation/breakdown products of the MBP-HERC1 fusion protein.

To perform the ubiquitination assay 0.5µl of the His-BAKΔC concentrated solution from Figure 4.12 (lane 6), 1µl of the GST-HPV5 E6 protein fraction (Figure 4.13C, lane 3) or 1µl of GST (Figure 4.13D lane 4), 0.25µl of MBP (Figure 4.13A lane 7), or 1µl of the wild type or C859A mutant HERC1 mini-gene (Figure 4.14C, lanes 1 and 2 respectively), were mixed in the indicated combinations with 5µg human recombinant ubiquitin, 150ng E1, 100ng UbcH5a, 1x final concentration of Mg^{2+}-ATP solution and 1x final concentration of reaction buffer in a total reaction volume of 20µl and incubated at 37^{o}C for 1 hour. Negative control reactions were performed using either the mutant HERC1, or lacking either ubiquitin or the BAK substrate. After incubation, the reactions were stopped by addition of 2x Laemmli buffer to a final concentration of 1x. The samples were then heated for 4 minutes at 90^{o}C and separated on a 12% acrylamide gel by SDS-PAGE followed by western blotting for BAK using the rabbit anti-BAK monoclonal antibody. Multiple ubiquitinations are normally indicated by a smear and monoubiquitination by a species with an increased molecular weight of 8kDa (the molecular mass of ubiquitin). Using the His-BAKΔC as substrate no specific ubiquitination of BAK could be observed when the wild type MBP-HERC1 protein was used either alone or in combination with E6, even after a longer exposure of the film (Figure 4.15).

As it is possible that the BAK protein produced in bacteria may not be in a

Figure 4.13 Purification of MBP, GST-5E6, and GST proteins

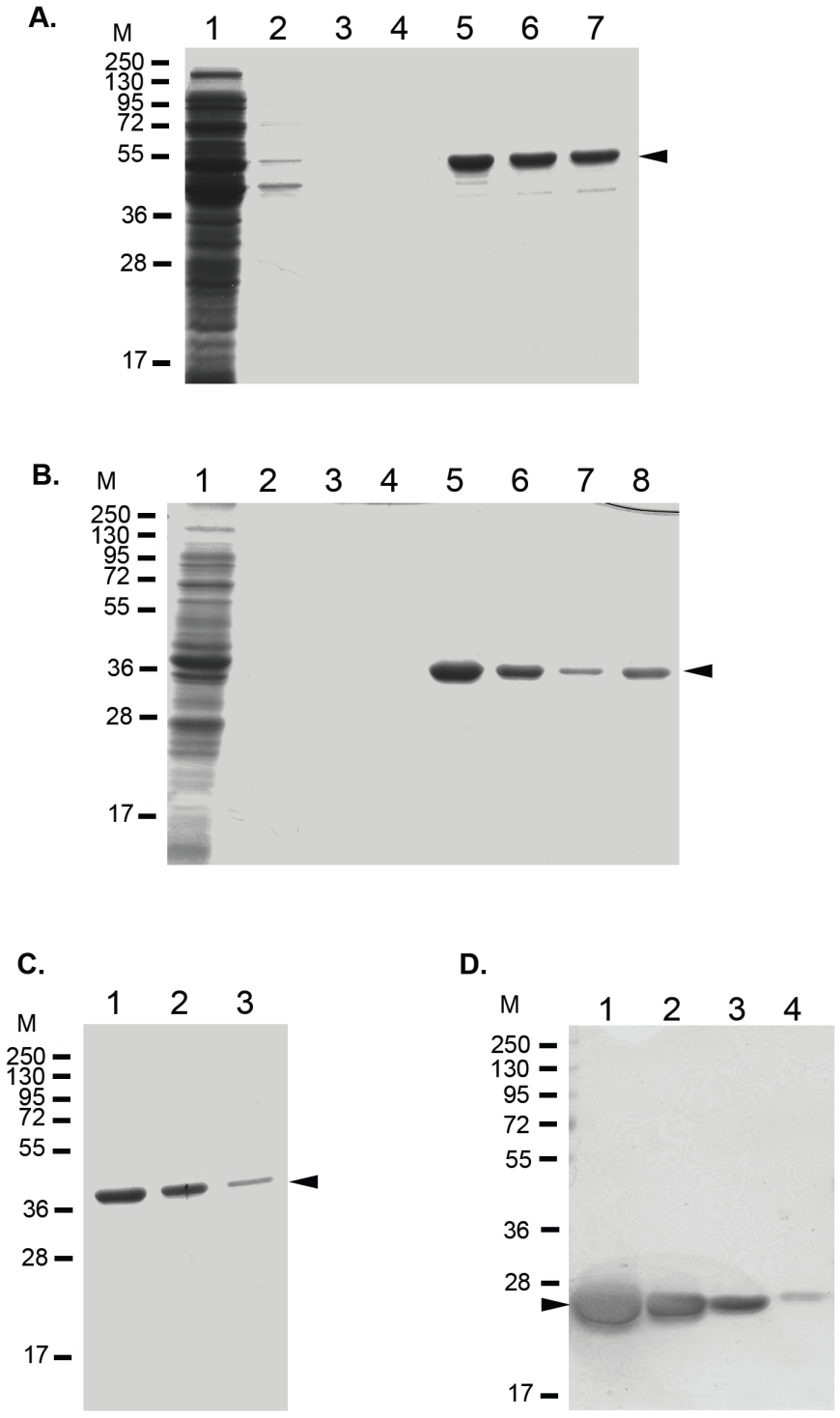


Figure 4.13 legend

A. Purification of MBP. MBP in bacterial lysates was bound to amylose resin in a volume of 40ml. Beads were harvested and a 20µl sample of unbound proteins retained for analysis (lane 1). The beads were washed three times in 40ml MBP buffer, a 20µl sample of each was step was analysed (lanes 2-4). Bound MBP was serially eluted in three steps, each performed with 1ml buffer containing maltose (lanes 5-7). A 1µl sample of each elution was analysed. Samples of each stage of purification were analysed by SDS-PAGE and coomassie staining as before. As the MBP was highly expressed, samples were dialysed but not concentrated. Elution E3 (lane 7) was used in subsequent ubiquitination assays. The purified protein is indicated with an arrowhead.

B. Purification of GST-5E6. GST-5E6 in bacterial lysates was bound to SuperGlu resin in a volume of 40ml GST binding buffer. Beads were harvested and a 20µl sample of unbound proteins retained for analysis (lane 1). The beads were washed three times in 40ml GST binding buffer, and a 20µl sample of each step was analysed (lanes 2-4). Bound GST-5E6 was serially eluted in three steps, each performed with 1ml GST binding buffer containing reduced glutathione. A 20µl sample of each elution was retained (lanes 5-7). A 20µl sample of the remaining beads was also analysed to monitor retained GST-5E6 protein. Samples of each stage of purification were analysed by SDS-PAGE and coomassie staining as before. The purified protein is indicated with an arrowhead.

C. Elutions 1-3 of the GST-5E6 protein produced in (B) above were dialysed and concentrated to a final volume of 50µl. A 1µl sample of each elution was subsequently analysed by SDS-PAGE and coomassie staining as before (lanes 1-3; concentrated elutions E1-E3 respectively). Fraction E3 was used in subsequent ubiquitination assays. The purified protein is indicated with an arrowhead.

D. GST purification. The GST protein was highly expressed in bacteria and was purified from 50ml culture using SuperGlu resin as described above. Bound GST was eluted in three fractions with reduced glutathione in 500µl volumes. A 1µl sample of each sequential elution was analysed by SDS gel electrophoresis as above. Lanes 1-3; elutions 1-3, lane 4; 20µl sample of remaining beads. The purified protein is indicated with an arrowhead.

For all proteins here SDS-PAGE was performed using a 12% acrylamide gel.

Figure 4.14 Purification of MBP-HERC1 fusion proteins

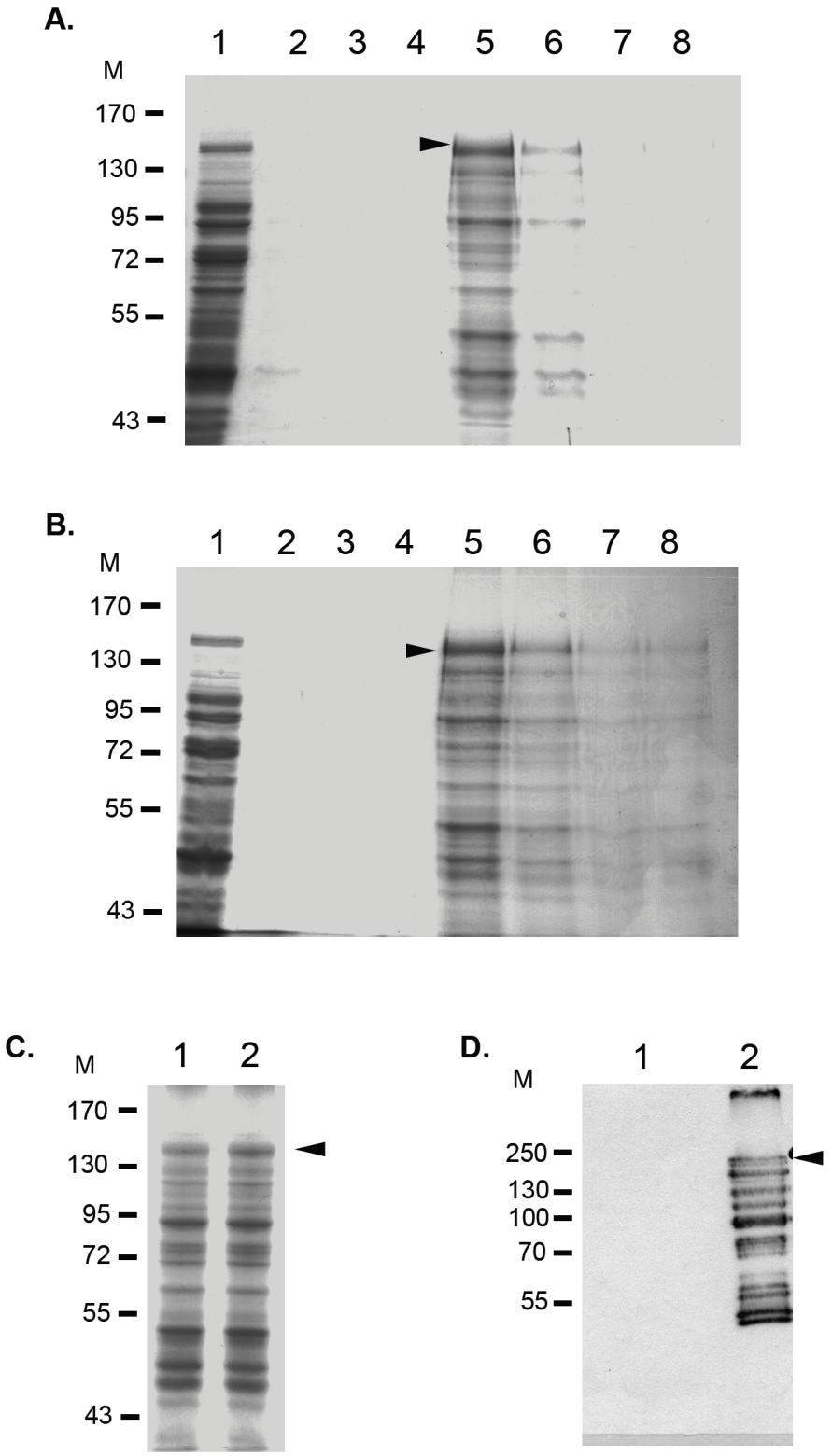


Figure 4.14 legend

The wild type (A) or mutant MBP-HERC1 (B) proteins were prepared as described for MBP. MBP fusion proteins in bacterial lysates obtained from 800ml cultures were bound to amylose resin in a volume of 40ml. Beads were harvested and a 20µl sample of unbound proteins retained for analysis (lane 1). The beads were washed three times in 40ml MBP buffer, a 20µl sample of each was step was analysed (lanes 2-4). Bound MBP was serially eluted in three steps, each performed with 1ml buffer containing maltose (lanes 5-7). A 20µl sample of each elution was retained. A 20µl sample of beads was also analysed for retained proteins (lane 8). Samples of each stage of purification were analysed by SDS-PAGE on a 8% acrylamide gel and coomassie staining as before.

C. Eluted fractions E1 and E2 (lanes 5 and 6) of (A) or (B) were pooled, dialysed and concentrated. A 0.5µl of each was then analysed by SDS-PAGE on a 8% acrylamide gel and coomassie staining as before. The full-length MBP-HERC1 fusion protein is indicated with an arrowhead. Lane 1; MBP-HERC1 wild type, lane 2; MBP-HERC1 inactive C to A mutant.

D. A fraction of MBP and the MBP-HERC1 wild type protein was eluted in a 20µl volume of 2x Laemlli buffer from 20µl of beads and analysed by western blotting using a FLAG M2 mouse monoclonal antibody. The full-length MBP-HERC1 fusion protein is indicated with an arrowhead. Lane 1; MBP, lane 2; MBP-HERC1 wild type. SDS-PAGE was performed on a 10% acrylamide gel.

---

conformation able to be recognised by HERC1, a second experiment was performed where the BAK substrate was obtained from mitochondrial-enriched sub-cellular fractions of irradiated HCT116-BAK cells. Mitochondrial preparations were prepared from cells 8 hours post-UV irradiation, as previous experiments had shown that at this time point S117 has undergone dephosphorylation thereby affording access to the hydrophobic groove on the surface of BAK, and BAK has also undergone N-terminal conformational change associated with activation. However, as with the His-BAKΔC substrate, no specific ubiquitinated forms of BAK could be detected following incubation with the HERC1 and E6 recombinant proteins (Figure 4.16).

GST		+		+				
MBP						+		
GST-E6			+		+	+	+	+
HERCmt				+	+			
HERCwt		+	+				+	+
Ubi	+	+	+	+	+	+	+	
E2	+	+	+	+	+	+	+	+
E1	+	+	+	+	+	+	+	+
His-BAK	+	+	+	+	+	+		+

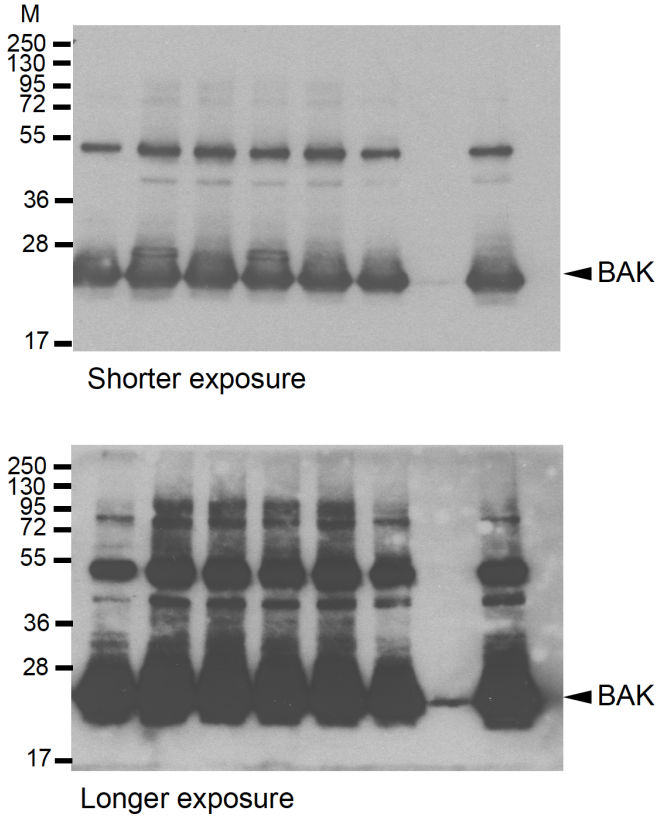


Figure 4.15 Ubiquitination assay using His-BAKΔC protein

Ubiquitination assays were performed in a total volume of 20µl for 1hr at 37^0C. Reactions were initiated by the addition of Mg^{2+}-ATP solution.

All reactions contained reaction buffer, Mg^{2+}-ATP, and the E1 and E2 enzymes, together with the individual components listed in the table with His-BAKΔC acting as substrate. HERC1wt or HERC1mt indicate the wild type or mutant MBP-HERC1 fusion protein used. Reactions were terminated by the addition of an equal volume SDS sample buffer, and were analysed by western blotting using the anti-BAK [Y164] antibody. Monomeric BAK species are indicated with an arrowhead.

The upper panel is a 5 second exposure of the X-ray film, the lower panel is a 2 minute exposure of the same blot.

GST		+		+				
MBP						+		
GST-E6			+		+	+	+	+
HERCmt				+	+			
HERCwt		+	+				+	+
Ubi	+	+	+	+	+	+		+
E2	+	+	+	+	+	+	+	+
E1	+	+	+	+	+	+	+	+
Mito BAK	+	+	+	+	+	+	+	

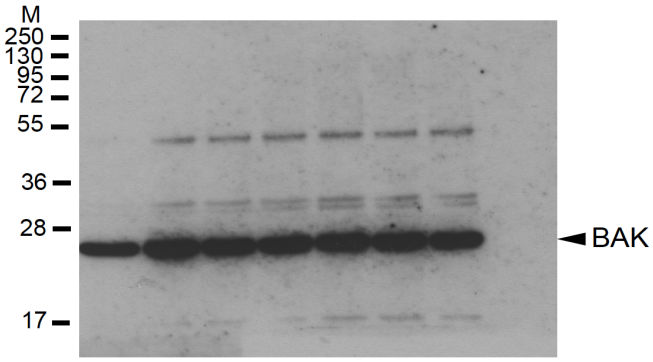


Figure 4.16 Ubiquitination assay using mitochondrial sub-cellular fractions

Ubiquitination assays were performed as before in a total volume of 20µl for 1 hour at 37^0C. Reactions were initiated by the addition of Mg^{2+}-ATP solution.

All reactions contained reaction buffer, Mg^{2+}-ATP, and the E1 and E2 enzymes, together with the individual components listed in the table. In these experiments 5µl of a mitochondrial-enriched cellular fractions was used in place of the bacterially expressed His-BAKΔC protein. As above, HERC1wt or HERC1mt indicate the wild type or mutant MBP-HERC1 fusion protein used. Reactions were terminated by the addition of an equal volume SDS sample buffer, then analysed by western blotting using the anti-BAK [Y164] antibody. Monomeric BAK species are indicated with an arrowhead.

4.4 Discussion

A number of substrates targeted to the proteasome by E6 have been shown to do so in an E6AP independent manner. After the original identification of HERC1 as a possible novel β-HPV E6 associated ligase by a previous member of the group, the work here supports the involvement of HERC1 in E6-mediated degradation of BAK in a cell type independent manner. An interaction between HERC1 and BAK *in vivo* has also been identified and preliminary work, when complemented by previous work in this thesis, suggests a potential mechanism of interaction between HERC1 and BAK.

It is interesting that HERC1 shows little homology to E6AP outside of the HECT domain yet both α- and β-HPV both associate with HECT domain ligases. Whilst α-HPV E6 targeting of p53 through the use of E6AP is constitutive, it appears that here the β-HPV5 E6 protein recruits a specialised HECT domain ligase with a putative BH3 domain to target a BCL-2 protein. It remains to be investigated whether HERC1 plays a role in the degradation of BAK by other β- and α-HPV E6 proteins and therefore whether the use of ligases by the E6 proteins are substrate specific.

It may be hypothesised that an ancestor of E6-associated ligases was a HECT ligase which then evolved to target different substrates. This is particularly interesting as the HERC1 relative, HERC2 has been identified as an E6 interacting protein, albeit only of α- and not β-HPV (Vos et al., 2009, White et al., 2012). It has subsequently been demonstrated that this interaction is dependent on E6AP (Martinez-Noel et al., 2012). HERC2 has been shown to regulate E6AP in the absence of the E6 protein (Kuhnle et al., 2011, Martinez-Noel et al., 2012). Similarly, the HECT domain ligase EDD was identified as an interacting protein of the HPV18 E6 protein, shown to regulate the activity of E6AP ubiquitin ligase activity, both in the absence and presence of E6 activity (Tomaic et al., 2011).

Furthermore E6AP and HERC1 have both been implicated in the turnover of TSC2. HERC1 regulation of TSC2 has only been examined in the absence of E6, whilst E6AP is implicated in both the presence and absence of E6 (Zheng et al., 2008, Spangle and Munger, 2010). Together, these reports suggest an evolutionary connection between the E6 proteins, E6 substrates and E6-associated HECT domain ligases. Based on this, it is easy to speculate that other substrates targeted for degradation by E6 in an E6AP independent manner (some PDZ domain proteins, TIP60, p300) may be done so using a HECT domain ligase. Interestingly only the Cullin family of the SCF E3 ligases have so far been associated with the E7 protein in targeting substrates such as p130, pRB as well as E7 itself (Huh et al., 2007, Oh et al., 2004) to further support the idea that HPV proteins associate with specific E3 ligase protein families.

The recent identification of the β-HPV38 and HPV92 E6 proteins as being able to interact with p53 (White et al., 2012), as well as the ability of the β-HPV49 E6 protein to target p53 for degradation (Cornet et al., 2012), raises the possibility of these HPV E6 types being ancestral relatives of the α- and β-HPV before further specialisation. Furthermore it is interesting that knockdown of E6AP appeared to recover only the codon 72 proline wild type p53 isoform in the presence of the HPV49 E6 protein (Cornet et al., 2012), suggesting that HPV49 E6 targets only the proline isoform using E6AP. This contrasts with previous studies showing that HPV18 E6 targets the p53 arginine isoform more efficiently than the p53 proline isoform (Storey et al., 1998). Previously two point mutations in the HPV5 E6 protein induced the protein to swap specificity from targeting BAK to p53 in a codon 72 isoform dependent manner, therefore it will be of interest to establish if HPV49 E6 targets BAK for degradation (as both α- and β-HPV E6 proteins do) and, if so, which ligase(s) it is able to interact with. It was not established for the HPV5 E6 point mutants as to whether the mutations altered the interacting ligase or the substrate specificity of the E3 ligase from BAK to the p53 isoforms but this activity was shown to be independent of E6AP (Simmonds and Storey, 2008). Consequently

investigation of the involvement of HERC1 in these activities would further the understanding of E6 protein interactions.

The work presented here complements previous work in this thesis which indicated that BAK must become active in order to be targeted by the E6 protein. The PLISA assay was performed using the Ab1 antibody, and therefore only BAK which has undergone the N-terminal conformational change and was interacting with HERC1 was detected in the assay. These findings furthered investigations into a mechanism of how HERC1 and BAK may interact. The interaction between another hydrophobic groove containing BCL-2 family member, MCL-1, and its E3 ligase MULE has been shown to be mediated by a BH3 sequence in MULE which can bind to the hydrophobic grove of MCL-1 (Zhong et al., 2005, Warr et al., 2005), thus highlighting that BH3 domain sequences are not restricted to BCL-2 proteins.

Using this as a precedent, it was explored whether a similar mechanism may be used by HERC1 and BAK. A sequence resembling that of a BH3 sequence could be identified in HERC1 with homology to the BAK sequence extending beyond the core amino acids required for BH3 homology. Consequently peptides corresponding to the BH3 sequence of the BCL-2 protein BID, MULE and the putative BH3 sequence of HERC1 were generated to test their ability to bind to WT BAK. The S117E BAK mutant was used to test requirement of the hydrophobic pocket as it has previously been characterised and shown to prevent access of BH3 domains to the hydrophobic pocket on BAK. The ability of the HERC1, BAK and BID BH3 peptides, and the inability of the MULE peptide, to pull-down WT BAK in response to UVB suggests that the putative BH3 sequence identified in HERC1 is able to bind the BH3 groove of BAK selectively and that this is not just due to the hydrophobicity of the peptide sequences. Furthermore, the non-binding of the HERC1-4E mutant peptide suggests that the same core amino acids, important for BH3 domain binding between other BCL-2 proteins, may be used by HERC1 to interact with BAK. This correlates with the known hierarchy of binding preferences of BCL-2 family proteins where, though BH3 sequences have a consensus motif, BCL-2 family proteins have

certain binding preferences for each other. Further exploration of the relative binding affinities of these peptides could be achieved through the use of isothermal calorimetry or BiaCore.

The knockdown experiments (Figure 4.3 and Figure 4.4) suggest that, like p53 and E6AP, HERC1 is not involved in BAK degradation in the absence of HPV5 E6 under the conditions of this assay. However, whether HERC1 is involved in promoting BAK turnover under different conditions of cell stress remains to be investigated. Furthermore, the role of E6 in the interaction also remains to be elucidated, and the PLISA assay may be used to interrogate this further with the use of HPV5 E6 mutations in order to determine the regions of the E6 protein required for the interaction between HERC1 and BAK. Comparison of this with the previously characterised HPV5 E6 point mutants, which have identified regions in the HPV5 E6 protein required to mediate BAK proteolysis (Simmonds and Storey, 2008), would further enlighten how these regions of HPV5 E6 contribute to the anti-apoptotic activity of the protein.

Interestingly HERC1 has a role in the regulation of TSC2 which in turn regulates the mTOR pathway which can promote cell survival and proliferation or autophagy. Current research in the group suggests that HPV5 E6-expressing cells have higher levels of autophagy (personal communication with G. Almuhaini), a pathway thought to prolong cell survival in the presence of stress such as hypoxia and nutrient deprivation. HERC1 is able to destabilise the interaction of TSC2 with TSC1 to inhibit mTOR and promote autophagy. E6 enhancing HERC1 activity towards BAK to prevent apoptosis may divert HERC1 away from TSC2 destabilisation, driving cells towards autophagy to promote survival under stress.

The HERC1 HECT domain has been previously isolated and shown to be competent in ubiquitin thioester formation (Schwarz et al., 1998) however substrate ubiquitination has not been shown. Since an interaction between BAK and HERC1 could be detected here, in order to elucidate the role of HERC1 in E6-mediated BAK degradation an attempt was made to elucidate how HERC1 mediates BAK

degradation in the presence of E6. The aim was to determine whether HERC1 was able to directly ubiquitinate BAK, rather than HERC1 acting as a scaffold protein or regulating levels of E6 or another ligase, as previously shown for EDD (Tomaic et al., 2011). Efforts to explore whether HERC1 is able to directly ubiquitinate BAK have been challenging. Here, an *in vitro* ubiquitination assay was attempted using a HERC1 protein produced from a mini-gene construct. This construct comprised regions of the HERC1 protein that may be required to interact with the E6 protein and to ubiquitinate the His-BAKΔC and mitochondrial sub-cellular fraction substrates (Figure 4.15 and Figure 4.16). These HERC1 regions included the L2G motif, the putative BH3 domain and the HECT domain. However detection of any higher molecular mass species, possibly corresponding to ubiquitinated BAK, were not detected. Reasons for this might be the use of truncated BAK where the C-terminus, along with the BH3 binding groove of BAK, may be required for correct interaction between BAK and HERC1. The BAK and HERC1 proteins purified from bacteria may also be in the incorrect conformations and/or lack the necessary post-translational modifications required for the ubiquitination reaction to occur. Furthermore, the HERC1 fusion protein may fold incorrectly or lack regions of the full length HERC1 protein necessary to interact with other components of the ubiquitin pathway, such as the E2 enzyme. In addition, a subsequent experiment using mitochondrial-enriched cell fractions where BAK is likely to be in a correct conformation, also failed to show any specific ubiquitinated products. Further work will be required to investigate whether HERC1 can ubiquitinate BAK *in vivo* and whether this occurs only in response to UV and in the presence of the E6 protein. It may be possible to express a recombinant HERC1 protein in other *in vitro* systems, or purify full-length native protein from large-scale mammalian cell cultures. Investigation of the requirement of the L2G motif, included here but not investigated due to the lack of ubiquitinated species, would also provide insight into the requirement of this motif and interaction with the E6 protein for HERC1 ubiquitination of BAK. Such systems would also allow further exploration of the role of the putative

HERC1 BH3 sequence with the use of competing peptides, for example. Detection of ubiquitinated species using the HERC1 fusion protein expressed from the mini-gene would also have permitted further exploration of the putative HERC1 BH3 sequence through mutation of the key residues believed to be required for an interaction with BAK.

Taken together, the data here suggest a model of HPV5 E6-mediated BAK degradation where, in response to UVB, BAK undergoes the early stages of activation to dephosphorylate Y108, bind p53 and undergo its N-terminal conformational change. Dephosphorylation of S117 is also required to expose the hydrophobic pocket on BAK, not only to permit the transient binding of BH3 only proteins to induce the N-terminal conformational change, but also, as proposed here, to permit interaction of HERC1 with BAK through the binding of a putative BH3 domain in HERC1 to the hydrophobic groove of BAK. This suggests that the timing of the interaction between HERC1 with BAK is crucial in the interaction. Binding of HERC1 here would also mean HERC1 would be in proximity to K113, although it is not clear which regions of the proteins interact: whether the active cysteine residue of HERC1 would be in proximity to K113 for ubiquitin transfer. In Chapter 3 it was shown that mutation of K113 to arginine did not affect BAK dimerisation therefore, in this model, mutation of K113 to arginine should not prevent BAK degradation by E6 through blocking access of the HERC1 BH3 sequence to the hydrophobic groove.

Since BAK dimers and subsequent oligomers are very stable, it may be difficult for E6 to destabilise them. This is an especially important point if access to the hydrophobic pocket was required for BAK and HERC1 to interact as dimerisation would mean the hydrophobic pocket is occluded. Therefore it is hypothesised that E6 and HERC1 target the dephosphorylated BAK S117 in a monomeric form (summarised in Figure 4.17). Furthermore, targeting only this conformation of BAK would permit sufficient levels of BAK to persist in the cell required to fulfil the other roles of BAK in the cell such as mitochondrial maintenance, preserving cell viability.

Whether HERC1 is required for BAK degradation by other HPV E6 types and for other known β-HPV E6 substrates which have been shown to be E6AP independent such as p300 and TIP60 remains to be explored. Further work to determine if HERC1 knockdown is able to restore apoptotic death to HPV5 E6-expressing cells would also elucidate the contribution of E6-mediated BAK degradation to cell survival.

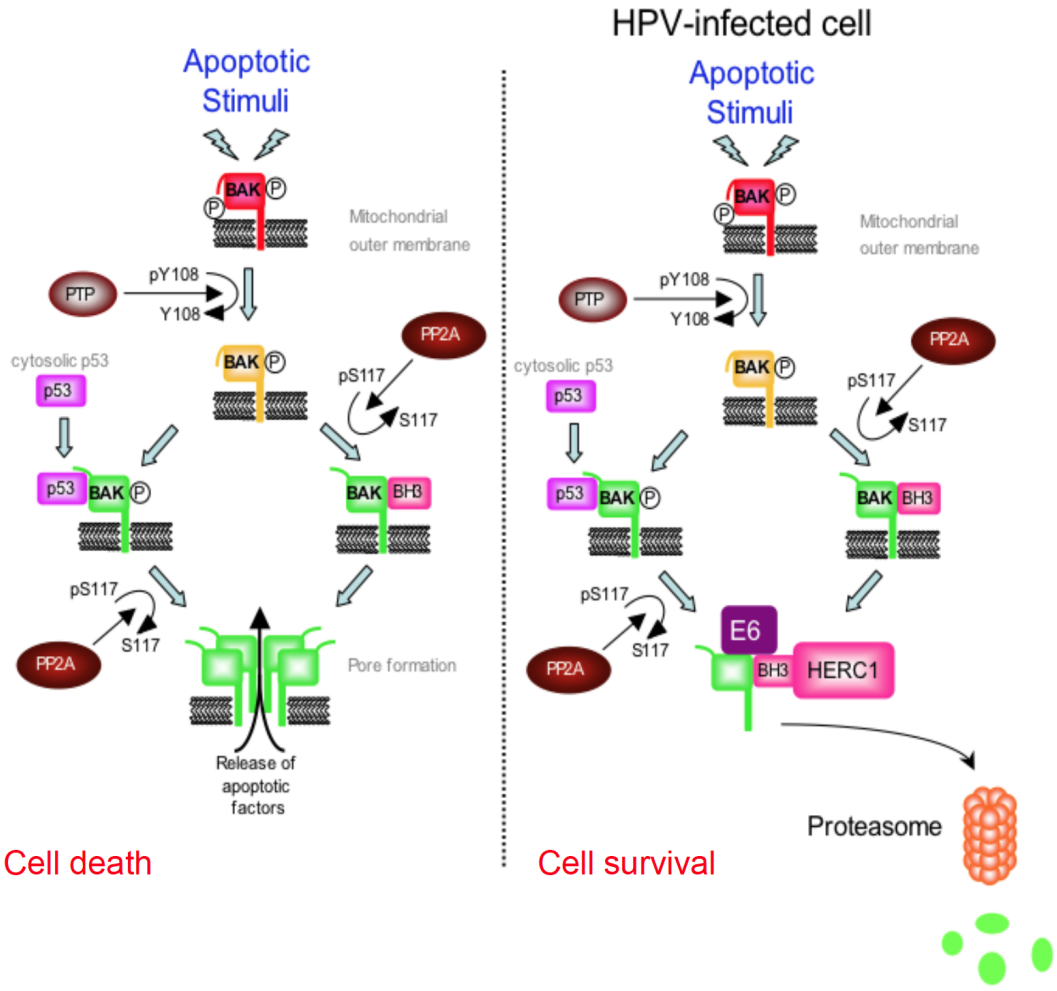


Figure 4.17 Schematic of HPV E6-mediated cell survival through BAK proteolysis

In uninfected cells, upon receipt of apoptotic stimulus, BAK is activated to result in permeabilisation of the mitochondria to result in cell death. In HPV E6 infected cells it appears the early stages of BAK activation progress normally. However, upon achieving the S117 dephosphorylated conformation, E6 targets HERC1 to BAK. HERC1 subsequently interacts with BAK via a putative BH3 domain in HERC1 and the hydrophobic groove on BAK. This targets BAK for proteolysis to promote the survival of damaged cells. The K113 residue of BAK is important for this process.

Chapter 5 Identification of binding partners of the HPV5 E6 C-terminal motif

5.1 Introduction

Cell adhesion to surrounding tissues is essential for epithelial structure and integrity, restriction of cell motility and providing locational information to cells. Deregulation of these processes has important implications for cancer and metastasis. There are many kinds of cell junctions which mediate adhesion and cell-cell communication. Focal adhesions and hemidesmosomes are integrin-based junctions which mediate cell attachment to the basement membrane, therefore they are enriched in the basal cells of the epithelia. In physiological processes their breakdown leads to detachment from the ECM and leads to anoikis that prevents anchorage independent growth, or terminal differentiation.

The BPV has been used as a prototype virus in papillomavirus studies and the BPV1 E6 protein can transform mouse cells (Neary and DiMaio, 1989). Along with high-risk mucosal HPV, the BPV1 E6 protein has been shown to target proteins involved in cell adhesion and polarity, such as paxillin, a scaffold protein in focal adhesions, which interacts with E6 via a L2G motif in paxillin. Loss of this interaction reduces the transforming ability of BPV1 E6 (Wade et al., 2008, Vande Pol et al., 1998). The high-risk α-HPV E6 proteins are also able to target proteins containing PDZ domains which are predominantly involved in cell adhesion and polarity and are considered tumour suppressor proteins. As previously mentioned, these include Dlg, the MAGI family of proteins (Thomas et al., 2002), MUPP1 and Scribble (Kranjec and Banks, 2010, Lee et al., 2000b, Gardiol et al., 1999, Nakagawa and Huibregtse, 2000). The E6 proteins recognise PDZ domains through a conserved C-terminal ETQV/L motif. The HPV16 E6 protein has an ETQL motif at the C-terminus and consequently shows less efficient binding and degradation of the PDZ protein Dlg compared to the ETQV motif of HPV18 E6 (Pim et al., 2000). The reports for the requirement of E6AP in this process depend on the PDZ protein,

while others are conflicting with the degradation of some substrates, such as Scribble and Dlg, being reported as both E6AP dependent (Nakagawa and Huibregtse, 2000, Kuballa et al., 2007) and independent (Massimi et al., 2008).

The ability of E6 proteins to degrade PDZ proteins has been shown to disrupt cell junction formation and actin cytoskeleton organisation, and correlate with transformation of keratinocytes (Watson et al., 2003). Scribble co-localises with the tight junction protein ZO1 and HPV16 E6 expression resulted in loss of ZO1 localisation to suggest tight junction disruption (Nakagawa and Huibregtse, 2000). Furthermore mice transgenically expressing α-HPV E6 C-terminal truncation mutants, which are still able to inactivate p53 but are unable to target PDZ proteins, do not exhibit epithelial hyperplasia (Nguyen et al., 2003) to suggest the interaction of E6 proteins, through the C-terminal motif, with PDZ proteins contributes to hyperplasia. HPV16 E6 expression, through loss of PTPN13 in a PDZ binding dependent manner, also promotes anchorage independent growth (Spanos et al., 2008).

Whilst cutaneous HPV lack the ETQV/L motif, HPV8 E6 has been shown to repress expression of the PDZ protein syntenin-2 (Lazic et al., 2012), increasing keratinocyte proliferation and reducing differentiation. Whilst HPV16 E6 also inhibited syntenin-2 transcription, it was less effective than HPV8 E6. Although this was not the case for other PDZ domain containing proteins, including MAGI, Scribble and Dlg, this suggests that targeting of such proteins involved in epithelial integrity is a conserved activity across the E6 proteins.

The high-risk cutaneous HPV E6 proteins (HPV5 and 8) also have four conserved amino acids (YHDW, Figure 5.1) at their C-terminus whilst other cutaneous HPV E6 proteins retain some degree of similarity in this motif, however no function has currently been attributed to the motif (Nomine et al., 2006).

Figure 5.1 High-risk cutaneous HPV E6 proteins have a conserved C-terminal YHDW motif

The high-risk mucosal HPV E6 proteins have a conserved ETQV/L motif which has been shown to be involved in the binding and degradation of PDZ domain containing host proteins which are involved in cell adhesion and polarity. The high-risk cutaneous HPV E6 proteins also have a conserved YHDW motif which has not been previously investigated. The C-terminal amino acid sequence, starting with the final conserved CXXC zinc binding motif, of β-HPV E6 proteins is shown.

Genus	Species	C-terminal sequence
β1	HPV5	CRQCKHFYHDW
	HPV8	CRLCKHLYHDW
	HPV14	CRLCKHFQYDW
	HPV19	CRLCKHFYNDW
	HPV25	CRLCKHFYNDW
	HPV36	CRQCKHFYNDW
	HPV47	CRQCKHFYNDW
	HPV99	CRLCKHLYNDW
	HPV105	CRHCKHLYNDW
	HPV12	CRQCKHLYLNNDR
	HPV15	CRHCRAIE
	HPV20	CRLCKHFQ
	HPV21	CRLCKHFQ
	HPV24	CRQCKQI
	HPV98	CRQCKQI
	HPV93	CRQCK
	HPV124	CKYCK
β2	HPV38	CRHCKAIE
β3	HPV49	CRHCRVIE
β4	HPV92	CRFCTEI
β5	HPV96	CRYCREI
	HPV108	CKFCK

5.2 Aim

The function of the conserved YHDW cutaneous HPV E6 protein C-terminal motif has not been previously investigated. Therefore, the aim here was to firstly use a HA-tagged peptide of the YHDW motif and mass spectrometric analysis to identify any interacting cellular proteins. Secondly, the aim was to characterise function of the motif with respect to potential involvement in disease processes.

5.3 Results

5.3.1 Identification of the YHDW motif interacting proteins

In order to investigate which proteins the YHDW motif of cutaneous type E6 proteins bind to in host cells a haemagglutinin (HA) tagged YHDW peptide was synthesised. A flexible glycine-serine-serine repeat was used as a linker between the tag and motif. The final sequence was YPYDVPDYAGSSGSSGSSYHDW (HA-tag sequence is underlined) and was used in pull-down assays. A peptide lacking the YHDW motif was also synthesised as a control to identify non-specific binding to the backbone. A lysate was prepared from the N-TERT keratinocyte cell line cultured in low calcium EpiLife media (Life Technologies) using TAP lysis buffer and freeze/thaw cycles. The lysate was pre-cleared with anti-HA agarose beads and then incubated with anti-HA agarose beads and either the control peptide or the YHDW peptide overnight (schematic shown in Figure 5.2A). The beads were precipitated and the interacting proteins were separated by SDS-PAGE (NuPAGE, Life Technologies) and silver-stained (FOCUS FASTsilver, G-Biosciences, Figure 5.2B). Areas of the gel where protein bands unique to the YHDW peptide could be observed were extracted, subjected to tryptic digest and the resultant peptides analysed by liquid chromatography tandem mass spectrometry to identify the interacting proteins (performed by B. Kessler, Wellcome Trust Centre for Human Genetics, Oxford).

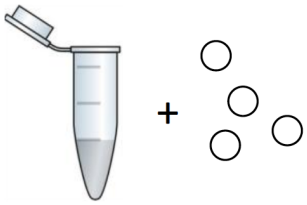
The proteins pulled down by the YHDW peptide were cross-referenced with those pulled down by the control peptide. Any proteins identified as binding to both

Figure 5.2 Isolation of YHDW interacting proteins

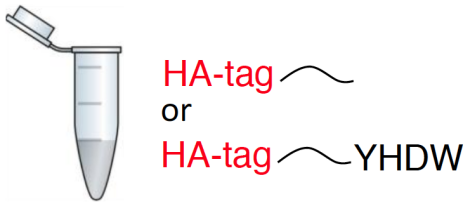
A.

Control peptide: HA-tag – $(GSS)_3$

Test peptide: HA-tag – $(GSS)_3$ - YHDW



i. N-TERT lysate pre-cleared with sepharose beads



ii. Pre-cleared lysate incubated with peptide



iii. Pull-down peptides with anti-HA antibody conjugated agarose beads.

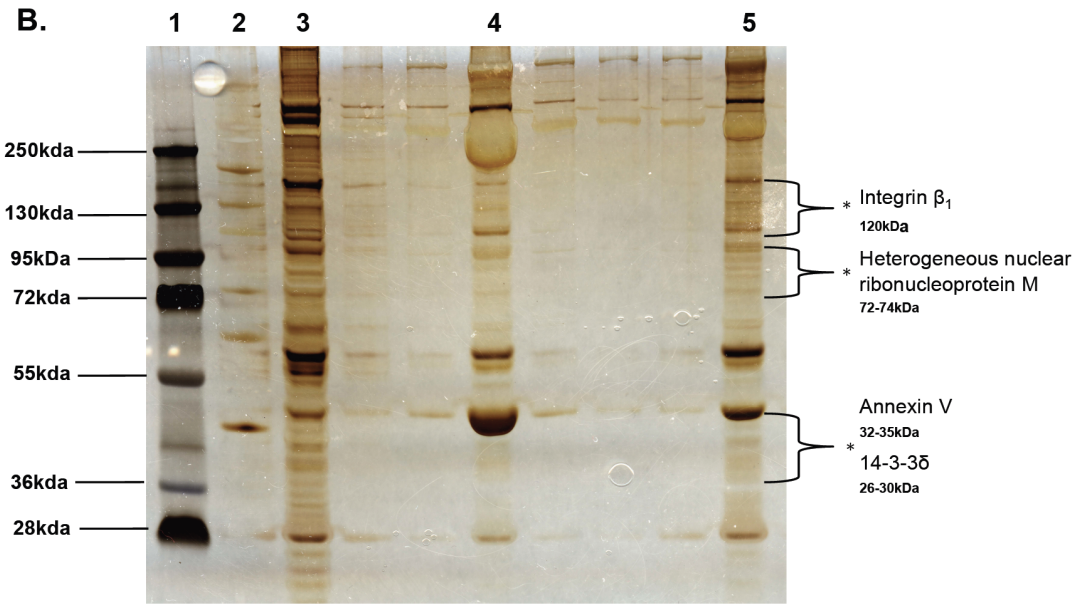


Figure 5.2 legend

A lysate was prepared from N-TERT cells grown in low calcium EpiLife media using TAP lysis buffer and protocol.

A. The lysate was pre-cleared with sepharose beads for 1 hour then incubated overnight with either HA-tagged control peptide or a HA-tagged peptide with the YHDW motif. The peptides and any bound proteins were precipitated using anti-HA agarose beads.

B. Interacting proteins were eluted in 2x SDS buffer and separated on a 4-12% NUPAGE gel. The gel was fixed and silver stained. Areas where differences in silver staining between the control peptide and the YHDW peptide could be detected were isolated and sent for analysis by liquid chromatography coupled mass spectrometry. Lanes: 1) Markers 2) High molecular weight markers 3) Lysate pre-clear with beads only 4) Control peptide lacking YHDW motif 5) YHDW peptide. All other lanes are empty, the bands observed are the result of background staining and possible carry over from adjacent lanes.

* Indicates areas cut out of lanes 4 and 5 for analysis by mass spectrometry.

The unique proteins identified from the YHDW peptide pull-down are indicated on the right with the expected molecular weight.

Table 5.1 Unique interacting proteins of the YHDW peptide

Proteins uniquely interacting with the YHDW motif were identified by peptide pull-down and mass spectrometric analysis of peptides generated by tryptic digest. Only proteins identified by at least two peptides, with at least one peptide match with a significance of $p \leq 0.05$ (to indicate identity or extensive homology) are shown below.

Protein Name	PubMed accession number	No. of matching peptides	MW (kDa)	Gel area cut from (kDa)	Function
Integrin-β_1	P05556	3 2 peptides $p \leq 0.05$	130	100-250	Cell adhesion and migration (Huttenlocher and Horwitz, 2011)
Heterogeneous nuclear ribonucleoprotein M	P52272	2 1 peptide $p \leq 0.05$	72-74	70-100	Involved in mRNA processing in the nucleus, altering splice sites (Dreyfuss et al., 1993, Han et al., 2010)
14-3-3δ	P31947	4 2 peptides $p \leq 0.05$	26-30	25-55	Seven 14-3-3 isoforms exist between which there is a large amount of redundancy. 14-3-3δ binds phosphoserine proteins and is a p53 inducible regulator of the cell cylcle at G2/M arrest (Li et al., 2009). Is epigenetically dysregulated in cancer (Oshiro et al., 2005), downregulated in stem cells (Fuchs and Raghavan, 2002).
Annexin V	P08758	2 2 peptides $p \leq 0.05$	32-35	25-55	Possible inhibitor of blood coagulation by competition for phosphatidylserine binding. Inhibits PKC (Schlaepfer et al., 1992, Dubois et al., 1996) Mediates chondrocyte binding to collagen II (Reid et al., 2000)

peptides were excluded. Any proteins identified by only one peptide from the tryptic digest or lacking any peptides with a significance of $p \leq 0.05$, to indicate identity or extensive homology, were also excluded. The four unique proteins identified by at least two peptides are summarised in Table 5.1. Peptide sequences identified in the mass spectrometric analysis by the Mascot software are given in Appendix 2. Only two or three peptides were matched for each protein identified, at least one of which had a significance of $p \leq 0.05$ to indicate identity or extensive homology.

Annexin V was identified as an interacting protein of the YHDW peptide. The function of Annexin V is poorly understood but it has been shown to inhibit Protein Kinase C (PKC; Dubois et al., 1996, Schlaepfer et al., 1992) and be involved in chondrocyte adhesion to collagen (Reid et al., 2000). Also identified was Heterogeneous nuclear ribonucleoprotein M, a protein involved in altering mRNA splice sites in the nucleus (Han et al., 2010) whilst 14-3-3δ is a p53-inducible regulator of the cell cycle which is downregulated in keratinocyte stem cells (Li et al., 2009, Fuchs and Raghavan, 2002).

Integrin-β_1 was a particularly intriguing interacting protein since it is a transmembrane receptor binding extracellular matrix proteins, regulating cell polarity, migration and adhesion. It is also interesting as it is enriched in keratinocyte stem cells (Jones and Watt, 1993) which are thought to be the reservoir of HPV in latent infections (Moody and Laimins, 2010). As β_1-integrin is a cell adhesion molecule it is also consistent with the profile of proteins targeted by the conserved C-terminal motif of the high-risk E6 proteins. Integrin-β_1 has recently been identified as an interactor of the α-HPV6, 11, 16 and 18 E5 proteins (Rozenblatt-Rosen et al., 2012) as well as of the β-HPV8 E6 protein (2011). In this study interactions of HPV5, 38 and 16 E6 proteins were also investigated however only β_4-integrin was identified an interactor of them all, not β_1-integrin. Furthermore cutaneous HPV have previously been shown to target cytoskeletal proteins (Akgul et al., 2009) and the high-risk anogenital α-HPV E6 proteins can bind paxillin *in vitro* (Tong and Howley, 1997), a focal adhesion protein able to bind to β-integrins. It was therefore decided

to further explore the effect of cutaneous HPV E6 expression, and the requirement of the YHDW motif, towards β_1-integrin activity.

5.3.2 Point mutation of the HPV5 E6 YHDW motif

In order to assess activity towards β_1-integrin of other cutaneous HPV E6 proteins N-TERT cell lines were retrovirally infected with the pLXSN vector or the pLXSN vector encoding the HPV5, 8 and 20 E6 genes (pLXSN-5E6, -8E6 and -20E6 respectively; constructs previously described Akgul et al., 2010, Akgul et al., 2007). HPV8 E6 was chosen as this shares the YHDW motif found at the C-terminus of HPV5 E6 (HPV β1) and has also been associated with high-risk for progression to malignancy in EV individuals (Orth, 1986). HPV20 E6 was chosen as it is a β1 HPV type and one of the most commonly detected HPV types identified in NMSC of renal transplant recipients (de Villiers et al., 1997) and does not share the YHDW consensus, replaced by the amino acids KHFQ. Successfully transduced cells were selected with 500µg/ml neomycin for 5 days or until parental cells were dead. Selected cells were expanded and cell line pool stocks frozen in liquid nitrogen.

To further investigate the contribution of the YHDW amino acids N-TERT cell lines expressing the HPV5 E6 protein with point mutations in the YHDW motif were also generated. The Quikchange II XL site directed mutagenesis kit (Stratagene; as previously described in chapter 2.5.3) and the primers listed in Table 2.15 were used to mutate the HPV5 E6 gene in the pLXSN vector. Aspartic acid 156 and tryptophan 157 were both mutated to alanine to generate pLXSN-D156A (GAT to GCT) and pLXSN-W157A respectively (TGG to GCG). Mutation schematics are shown in Figure 5.3A. Mutation reactions were transformed into *E.coli* bacteria (XL-Gold Ultracompetent, Stratagene) and successful transformants selected by sequencing (Figure 5.3B shows sequencing traces confirming the nucleotide mutations).

Mutation of these two residues was chosen as the alignment in Figure 5.1 shows

Figure 5.3 Expression of HPV E6 transcripts in N-TERT cells

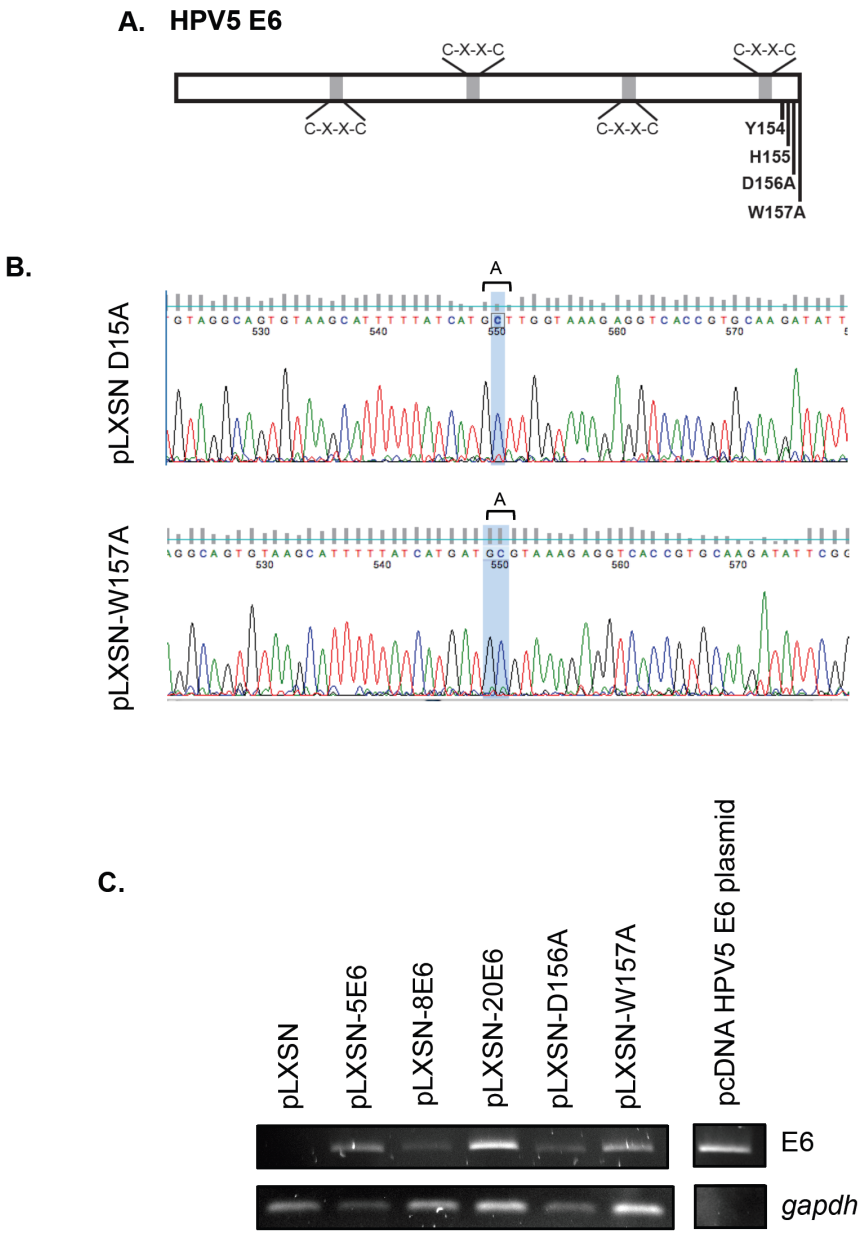


Figure 5.3 legend

A. Schematic of the HPV5 E6 protein which contains four conserved C-X-X-C motifs. Point mutations were made in the HPV5 E6 YHDW motif at D156 and W157 (D156A or W157A, respectively).

B. Example sequencing traces showing successful nucleotide mutation to change the amino acid codons for D156A and W157A from GAT to GCT and TGG to GCG, respectively.

C. mRNA was extracted from N-TERT cells retrovirally transduced with three different HPV E6 proteins (HPV5, 8, 20), the empty vector (pLXSN) or the HPV5 E6 protein with mutations in the C-terminal YHDW motif (HPV5 E6 D156A and W157A). cDNA was synthesised and PCR reactions performed as described below. Products were analysed by agarose gel electrophoresis. Primers for HPV5 E6 were used in the PCR reactions with cDNA synthesised from N-TERT cells expressing pLXSN, HPV5 E6, HPV5 E6 D156A and HPV5 E6 W157A and a positive control reaction replacing cDNA with pcDNA HPV5 E6 plasmid template. Primers for HPV8 and HPV20 E6 were used in reactions with cDNA from cells expressing the corresponding protein. HPV5 E6 and mutants; 474bp, HPV8 E6; 468bp, HPV20 E6; 497bp, *gapdh*; 261bp.

D. All cDNAs and the pcDNA HPV5 E6 vector were used in PCR reactions with primers for *gapdh* to check cDNA quality.

---

that these are the most highly conserved residues across the β-HPV E6 proteins along with tyrosine 154, however a successful mutant construct could not be isolated for this residue. Mutation of histidine was not performed as it is substituted by asparagine in some cutaneous E6 protein C-termini, although this is a conserved substitution suggesting the placement of a basic residue here could be important for function of the motif. The pLXSN-D156A and pLXSN-W157A constructs were used to generate viral supernatant by transfection into the PT67 packaging cell line, as previously described, and the supernatant used to retrovirally infect N-TERT cells. Cell line pools expressing the mutant HPV5 E6 proteins were selected as discussed above.

Expression of the E6 constructs in the cell lines, along with those of the N-TERT cells selected to express pLXSN, pLXSN-5E6, pLXSN-8E6 and pLXSN-20E6 was checked by mRNA extraction to generate a cDNA template which was used in a PCR reaction with primers specific to the HPV5, 8 or 20 E6 protein (Table 2.12).

Figure 5.3C shows the PCR reactions separated by agarose gel electrophoresis and that expression of the relevant E6 mRNA could be detected. cDNA from pLXSN-expressing cells was used in a PCR reaction with primers against HPV5 E6 as a negative control and a pcDNA plasmid encoding the HPV5 E6 gene as a positive control. All cDNA templates were used in PCR reactions with primers specific to the *gapdh* reference gene to check the quality of the cDNA in the event expression of the E6 transcripts could not be detected.

5.3.3 Western blot for junctional and cytoskeletal proteins in N-TERT cells expressing HPV E6 constructs

To begin to probe the effects of HPV E6 expression and the potential involvement of the YHDW motif on β_1-integrin function, each of the cell lines expressing pLXSN, pLXSN-5E6, pLXSN-8E6, pLXSN-20E6 and the two HPV5 E6 mutants were seeded in 100mm dishes at $1x10^6$ cells and grown to ~80% confluence in RM+ 10% FCS media for at least 72 hours. RM+ supplement and FCS were used to culture cells in a higher calcium concentration to stimulate cellular differentiation and cell junction formation. Cells were lysed in RIPA buffer and proteins separated by SDS-PAGE and transferred to nitrocellulose membranes. The membranes were western blotted for a variety of different cell junctional proteins, plaque proteins and cytoskeletal proteins: β_1-integrin, FAK, vinculin, paxillin, ZO1, desmoplakin, F-actin, β-actin and GAPDH as a loading control. The location of the cell junctions and these proteins are shown in Figure 1.2.

Figure 5.4A shows that β_1-integrin levels were higher by western blot in N-TERT cells expressing pLXSN-5E6 and -8E6 compared to cells expressing any other constructs whilst cells expressing pLXSN-20E6 appeared to have reduced levels of β_1-integrin. HPV5 E6 W157A mutant-expressing cells also appeared to have low levels of β_1-integrin whilst cells expressing pLXSN-D156A had slightly lower levels compared to those expressing pLXSN-5E6.

Figure 5.4 Western blot of N-TERT lysates expressing HPV E6 constructs for plaque, junctional and cytoskeletal proteins

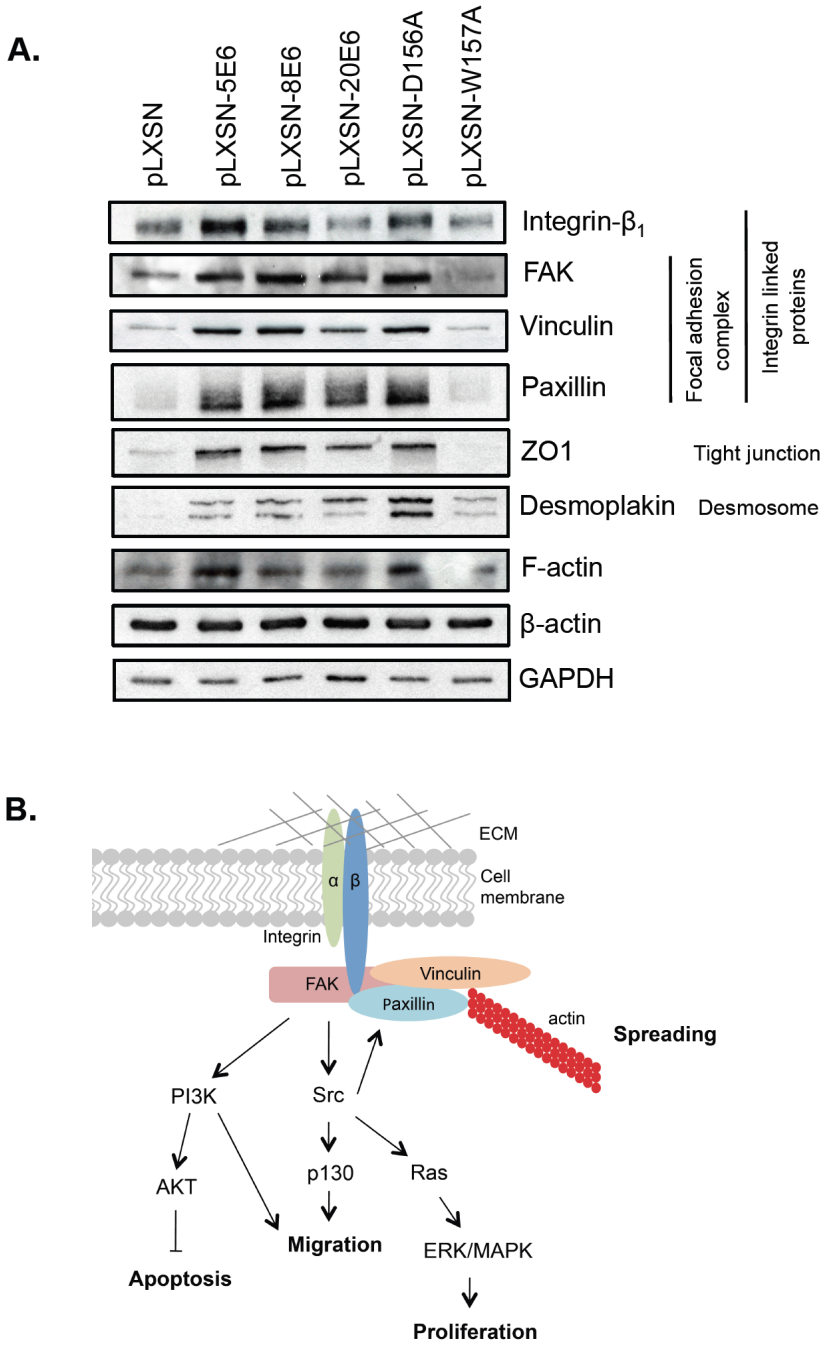


Figure 5.4 legend

A. N-TERT cell lines expressing the indicated pLXSN E6 constructs were grown to ~80% confluence in RM+ 10% FCS media and lysed in RIPA buffer and western blotted for the indicated proteins. Integrin-β_1 (125kDa, P5D2, Covance), FAK (120kDa, Cell Signalling), vinculin (120kDa, SPM227, Abcam) and paxillin (~65kDa, BD Bioscience) are focal adhesion associated proteins. ZO1 (240kDa, Life Technologies) and desmoplakin (isoforms I & II, 210kDa and 225kDa respectively, Serotec) are plaque proteins associated with tight junctions and desmosomes respectively. F-actin is filamentous actin, β-actin represents the cellular pool of actin and GAPDH is used as a loading control. Blots performed three times.

B. Integrin signalling. Upon activation of integrin receptors, FAK is recruited via its N-terminus to the cytoplasmic tail of β-integrins. Upon interaction with integrins, FAK autophosphorylates at tyrosine 397. This recruits Src kinase causing a positive feedback loop for further FAK phosphorylation to result in full kinase activity and the recruitment of other focal adhesion proteins. Paxillin and vinculin are important for localisation of FAK to integrin tails. Adapted from van Nimwegen and van de Water (2007)

FAK is a tyrosine kinase through which integrins signal, hence it was of interest to determine if there were changes in downstream signalling pathways. Western blotting the lysates above for FAK showed that, amongst the different E6 types, cells expressing HPV5 and 8 E6 exhibited the highest levels of FAK. Cells expressing HPV20 E6 showed higher levels of FAK compared to the empty vector-expressing cells, but slightly lower levels than those observed in pLXSN-5E6 and -8E6-expressing cells. Cells expressing the HPV5 E6 D156A mutant had similar levels of FAK to those expressing the WT HPV5 E6 protein. However, cells expressing the W157A mutant showed lower FAK levels compared to those expressing the pLXSN-5E6 construct. Vinculin and paxillin are focal adhesion plaque proteins mediating the interaction between the transmembrane α2/α3 β1-integrin complex and the actin cytoskeleton. Expression levels of vinculin and paxillin by western blot in the E6-expressing N-TERT cells showed a similar pattern to that of FAK.

The proteins of other cell junction complexes were also analysed: ZO1 is a plaque protein in tight junctions, mediating transmembrane protein attachment to the

cytoskeleton. The levels of ZO1 were almost undetectable in pLXSN-expressing N-TERT cells compared to that of cells expressing pLXSN-5E6, -8E6, -20E6, which were much higher by comparison. The level of ZO1 in pLXSN-D156A N-TERT cells was comparable to that in cells expressing the WT HPV5 E6 protein whilst cells expressing pLXSN-W157A had almost undetectable levels of ZO1. Desmoplakin mediates connection of transmembrane proteins to the intermediate cytoskeleton (keratins in the skin epithelium) in desmosomes. Western blotting the lysates for desmoplakin showed a small increase in all HPV E6-expressing cell lines compared to cells expressing the empty vector. Cells expressing the pLXSN-W157A mutant showed comparable desmoplakin levels to WT HPV5 E6-expressing cells, however expression of the HPV5 E6 D156A mutant resulted in higher desmoplakin levels than those observed in cells expressing the WT HPV5 E6 protein. Western blotting for β-actin as an indicator of the cellular pool of actin monomers indicates that this is unchanged across the cell lines, in a similar manner to GAPDH as the loading control. However probing for filamentous actin (F-actin) reveals that higher levels can be detected in pLXSN-5E6-expressing cells compared to those expressing pLXSN, -8E6 or -20E6. Comparable F-actin levels were observed between cells expressing the HPV5 E6 D156A mutant and the WT HPV5 E6 protein. In contrast, pLXSN-W157A-expressing cells exhibited lower F-actin levels in comparison to WT HPV5 E6-expressing cells.

From these data it appears that mutation of W157 abrogates the effects of HPV5 E6 expression on β_1-integrin, FAK, vinculin, paxillin, ZO1 and F-actin, hence subsequent investigations focused on the effects of the HPV E6 protein on β_1-integrin and the well established downstream targets, FAK, paxillin and F-actin (Figure 5.4B) as they showed a correlation with β_1-integrin levels. In addition, components of this pathway have previously been shown to be disrupted by infection with high-risk anogenital HPV and targeted by the BPV1 E6 protein (Wade et al., 2008, McCormack et al., 1997).

5.3.4 Immunofluorescent staining of β_1-integrin and FAK in keratinocyte cell lines

Given the differences in the levels of β_1-integrin by western blot in N-TERT cells expressing the different HPV E6 constructs, it was of interest to investigate if there was any observable difference in β_1-integrin localisation by immunofluorescence among the different E6-expressing cell lines. As many downstream events of β_1-integrin signalling are mediated through FAK, FAK localisation was investigated simultaneously. N-TERT cells expressing the E6 and mutant pLXSN constructs were seeded on coverslips in 12 well plates at $1.5x10^5$ cells per well and grown to 80% confluence for ~72 hours in RM+ supplemented media with 10% FCS. Cells were fixed in 4% PFA, permeabilised with 0.5% Triton X-100 and stained for FAK (rabbit polyclonal antibody) and revealed using an Alexafluor568 conjugated goat anti-rabbit secondary antibody. Cells were then stained for β_1-integrin (mouse monoclonal antibody) using a rabbit anti-mouse Alexafluor488 conjugated secondary antibody and imaged by Z-stack confocal microscopy. Compressed Z-stack images are shown in Figure 5.5.

The images show that the β_1-integrin staining pattern in pLXSN-expressing N-TERT cells was that of the characteristic 'paving' plasma membrane staining. In contrast, the staining for β_1-integrin in cells expressing the HPV5 E6 protein appeared much reduced at the plasma membrane. N-TERT cells expressing pLXSN-8E6 showed a similar β_1-integrin staining pattern to that of cells expressing pLXSN-5E6 with reduced β_1-integrin levels, whilst cells expressing pLXSN-20E6 had a β_1-integrin staining pattern similar to that of pLXSN-expressing cells, albeit slightly more diffuse around cell margins. Mutation of D156 and W157 to alanine appeared to restore β_1-integrin staining to N-TERT cells compared to those expressing the WT HPV5 E6 protein, however the staining pattern was slightly more diffuse compared to that of cells expressing pLXSN.

Staining for FAK showed an inverse relationship with β_1-integrin staining: pLXSN

Figure 5.5 Immunofluorescent staining of β_1-integrin and FAK levels in HPV E6-expressing N-TERT cells

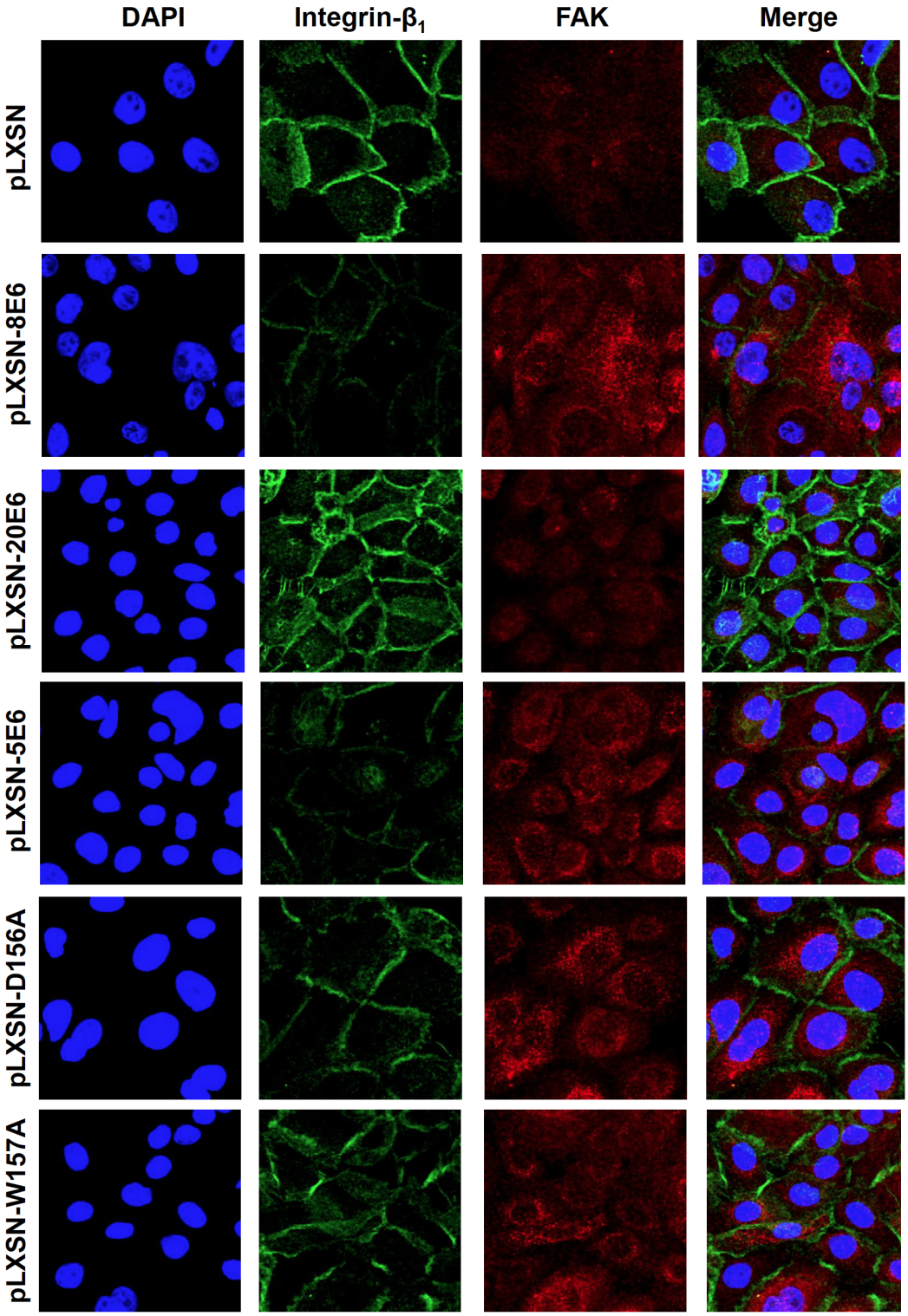


Figure 5.5 legend

N-TERT cells retrovirally transduced to express pLXSN, -8E6, 20E6, -5E6 and the HPV5 E6 D156A and W157A mutants were grown in RM+ media for 72 hours, fixed in 4% PFA and doubly stained for immunofluorescence with antibodies against FAK (rabbit, Cell Signalling) and, subsequently, β_1-integrin (mouse, P5D2, Covance). Representative compiled Z-stack images are shown. Blue; nuclear DAPI staining, green; β_1-integrin, red; FAK. Experiment performed three times.

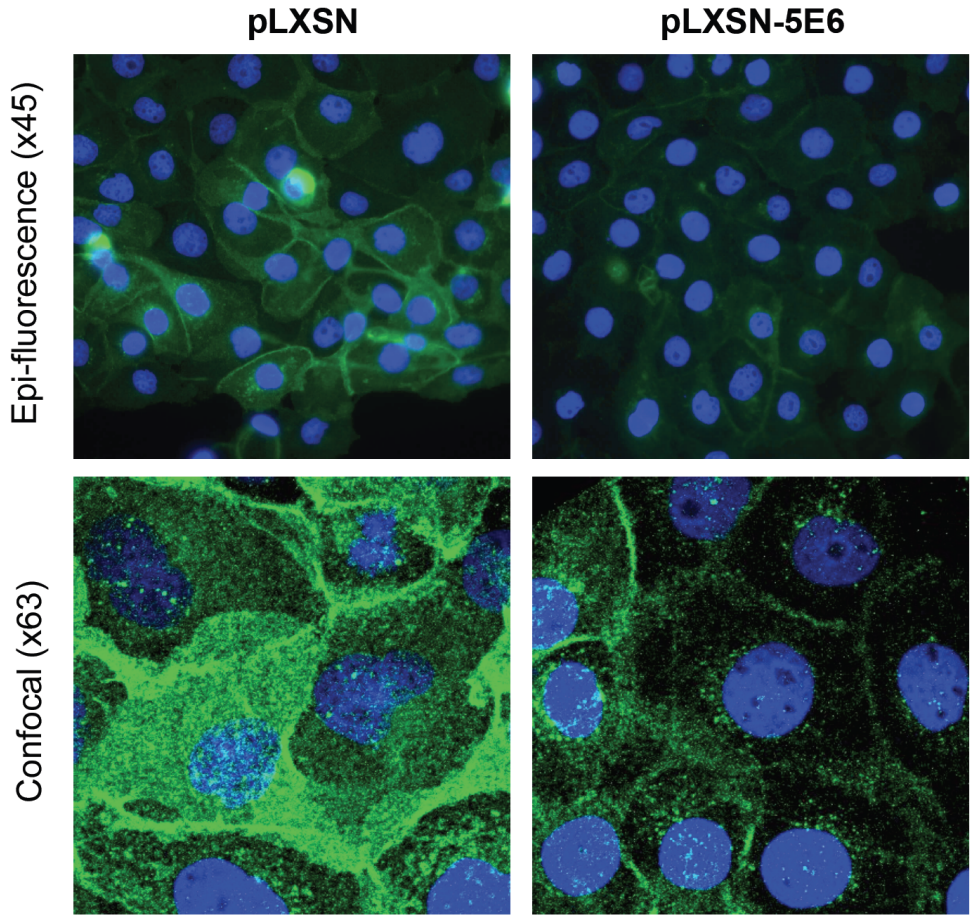
---

and pLXSN-20E6-expressing cells exhibited a lower staining intensity for FAK compared to pLXSN-5E6 and pLXSN-8E6-expressing cells. Compared to cells expressing the WT HPV5 E6 protein, FAK levels in pLXSN-D156A-expressing cells appeared similar whilst FAK levels appeared lower in cells expressing pLXSN-W157A. Whilst the increased FAK staining in HPV E6-expressing cells correlated with the western blot results in Figure 5.4, that of β_1-integrin did not.

5.3.5 Integrin-β_1 immunofluorescence in PM1 cells

Given the differing results for β_1-integrin immunofluorescence and western blot, β_1-integrin immunofluorescence was investigated in a different keratinocyte cell line; the spontaneously immortalised pre-malignant keratinocyte cell line PM1 (Proby et al., 2000). pLXSN and pLXSN-5E6-expressing cell line pools were established as previously described for N-TERT cells and cells were stained for β_1-integrin as above. Examination of the staining by epi-fluorescence microscopy (Figure 5.6), again, revealed a lower level and less distinctive staining pattern in HPV5 E6-expressing cells compared to empty vector. Z-stack confocal microscopy of these cells revealed a concentration of β_1-integrin staining at cell-cell contacts but a more diffuse staining pattern throughout the cell compared to the N-TERT cells. This may be a cell specific effect, however, in agreement with the N-TERT cells, those expressing HPV5 E6 had lower overall levels of β_1-integrin staining. These data suggest the lower staining levels of β_1-integrin in cells expressing the HPV5 E6 protein is not a cell line specific occurrence.

Figure 5.6 Immunofluorescent β_1-integrin staining in the PM1 cell line expressing HPV5 E6



The PM1 cell line was retrovirally infected to express pLXSN or pLXSN-5E6. After selection cells were seeded on coverslips and grown in RM+ media to ~80% confluence for 72 hours. Cells were fixed in 4% PFA, permeabilised with 0.5% Triton X-100 and stained for β_1-integrin (P5D2, Covance).

Top row; imaging by epi-fluorescence microscopy at x40 magnification using a ZEISS Axioskop microscope, bottom row; imaging by a ZEISS LSM 510 confocal microscope showing compressed Z-stack images. Blue; nuclear DAPI staining, Green; β_1-integrin staining.

Experiment performed twice. Representative images shown.

5.3.6 Integrin-β_1 immunofluorescence using saponin permeabilisation

Given the contrasting results of the β_1-integrin immunofluorescence staining and total cellular β_1-integrin levels by western blot, it was hypothesised that the E6 proteins may be altering β_1-integrin localisation such that less was located at the cell surface and more located in intracellular vesicles (Vassilieva et al., 2008) which Triton X-100 permeabilisation did not reveal (Goldenthal et al., 1985). N-TERT cells were therefore treated as previous and stained for β_1-integrin by immunofluorescence using the same antibody but permeabilsed with 0.1% saponin for 5 minutes and imaged as previously described using Z-stack confocal microscopy (Figure 5.7). This revealed a differing β_1-integrin staining pattern to that observed using Triton X-100.

Using saponin permeabilisation, cells expressing pLXSN-5E6 or -8E6 showed greater staining for β_1-integrin than cells expressing pLXSN or pLXSN-20E6. Cells expressing the HPV5 E6 D156A mutant showed a similar pattern of β_1-integrin staining to those expressing the WT HPV5 E6 protein, however, cells expressing pLXSN-W157A showed a lower level of β_1-integrin staining compared to those expressing the WT HPV5 E6 protein using saponin permeabilisation. Whilst β_1-integrin staining was more concentrated around the cell membrane to give the 'paving stone' patterning in those cells with higher β_1-integrin staining, the overall distribution of β_1-integrin was more diffuse and could be detected throughout the cytosol compared to that observed when using Triton X-100. These data suggest that cells expressing HPV E6 proteins have a greater β_1-integrin cytoplasmic localisation. The restoration of the β_1-integrin membrane staining may indicate vesicle encapsulated, endocytosed β_1-integrin below the membrane surface.

5.3.7 Paxillin localisation by immunofluorescence

Paxillin is a downstream effector of FAK previously shown to be targeted by the BPV1 E6 protein (Tong and Howley, 1997, Tong et al., 1997). Paxillin localises FAK to integrins, both directly and indirectly, and is itself a substrate for phosphorylation

Figure 5.7 Integrin-β_1 immunofluorescence by saponin permeabilisation in N-TERT cells expressing HPV E6 constructs

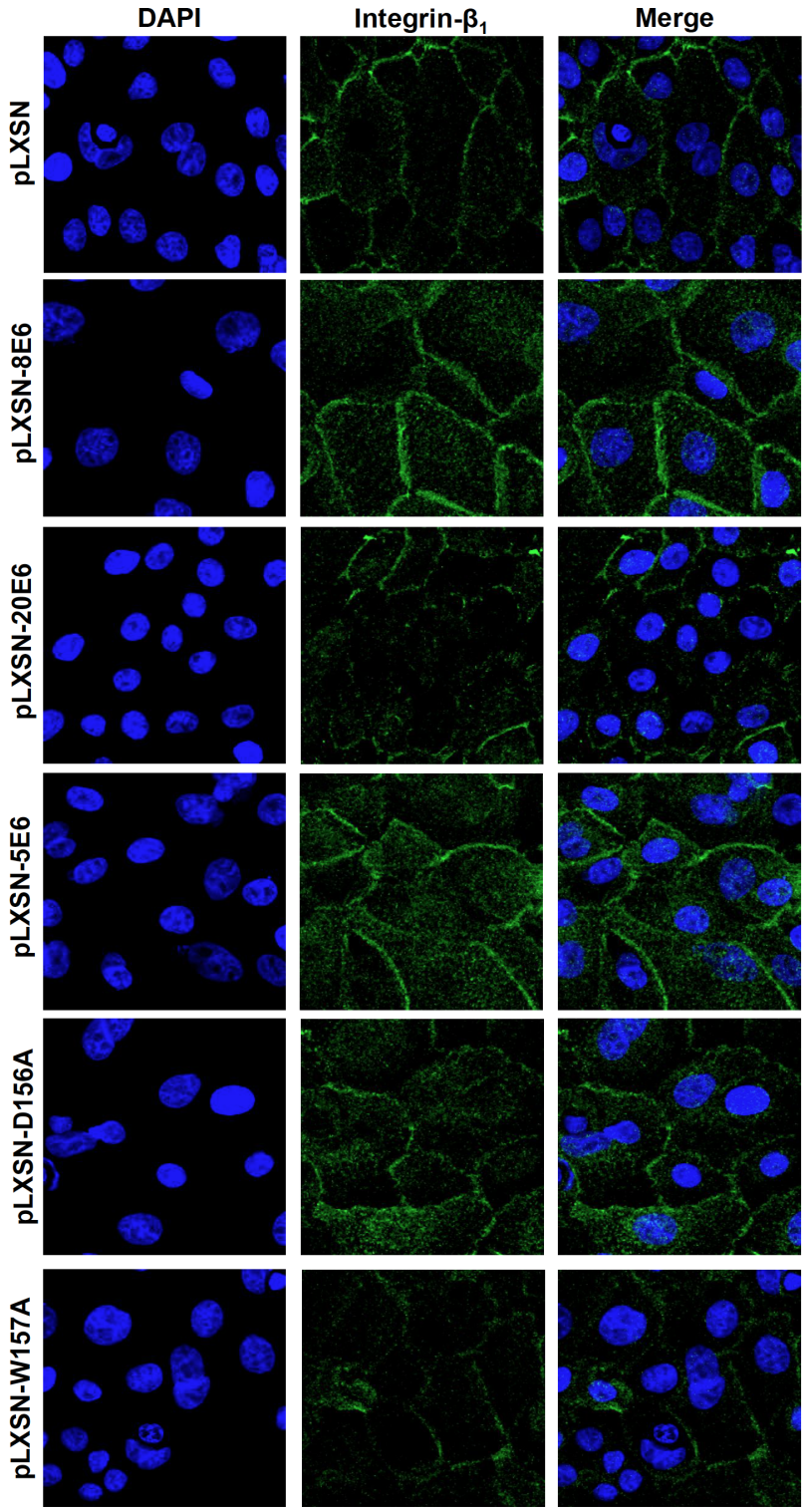


Figure 5.7 legend

N-TERT cells expressing pLXSN, -8E6, -20E6, -5E6, -D156A and W157A were seeded on coverslips and grown to 80% confluence in RM+ media for 72 hours. Cells were fixed in 4% PFA and permeabilised with 0.1% saponin for 5 minutes. Immunofluorescence staining was performed against β_1-integrin (P5D2, Covance) using the rabbit anti-mouse Alexafluor488 conjugated secondary antibody. Experiment performed three times. Representitive images are shown.

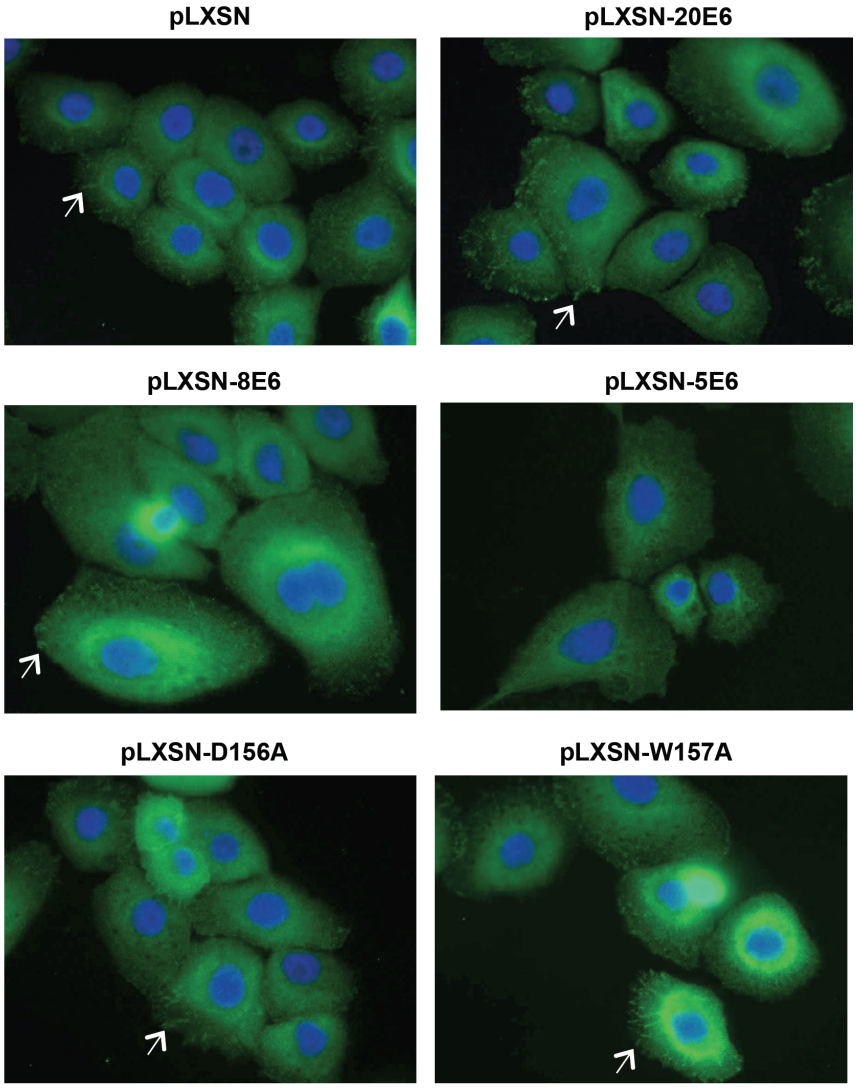
upon FAK activation. The western blot for paxillin in Figure 5.4 indicated that HPV E6-expressing cells may affect paxillin which is abrogated by the HPV5 E6 W157A mutant. Immunofluorescent staining of paxillin localisation was performed in order to further probe the effect of β_1-integrin on downstream focal adhesion complex formation.

The N-TERT cell lines expressing the HPV E6 constructs were seeded on coverslips, fixed in 4% PFA and stained with an antibody against paxillin. Staining was imaged by epi-flourescence microscopy (Figure 5.8) as this gave better imaging of the distinctive paxillin localisation at focal adhesions, seen in the images as staining 'flecks' consistent with those previously reported (Gupton et al., 2007). N-TERT cells expressing pLXSN and pLXSN-W157A showed a number of flecks per cell which appeared fine and long in structure. N-TERT cells expressing pLXSN-20E6 also showed a number of these flecks per cell however the structures appear more compact compared to that of pLXSN. Cells expressing pLXSN-8E6 and -D156A appeared to have fewer paxillin foci per cell with those of pLXSN-8E6 appearing more diffuse. Cells expressing pLXSN-5E6 had few distinguishable flecks, suggesting that expression of E6 proteins may alter paxillin localisation.

5.3.8 Investigation of filamentous actin cytoskeletal arrangement in N-TERT cells expressing HPV E6 constructs during migration

The previous data suggested that HPV E6 proteins were affecting β1-integrin localisation and the downstream effectors FAK and paxillin. These are mediators of actin cytoskeleton re-arrangement and migration and cutaneous HPV E7 proteins have also previously been shown to affect the actin cytoskeleton (Akgul et al., 2009), hence it was of interest to investigate whether E6 altered actin cytoskeleton

Figure 5.8 Paxillin immunofluorescence in N-TERT cells expressing pLXSN HPV E6 constructs



N-TERT cells were seeded on coverslips and grown for 72 hours in RM+ media. Cells were fixed in 4% PFA for 10 minutes, permeabilised with 0.5% Triton X-100 for 4 minutes and blocked in 3% BSA for 1 hour at room temperature. Cells were stained with anti-paxillin primary antibody (BD Bioscience, #612405) in 1% BSA for 1 hour, washed three times with PBS and then labelled with rabbit anti-mouse AlexaFluor488 conjugated secondary antibody for 1 hour. Cells were washed three times with PBS and mounted on glass slides in mounting media with DAPI. Images taken with Carl Zeiss Axiovert microscope at x63 magnification. All images were taken using the same exposure. Arrows indicate paxillin staining in focal adhesions. Blue; nuclear DAPI staining, Green; paxillin staining. Experiment performed twice. Representative images shown.

arrangement in migrating N-TERT cells. N-TERT cells expressing the E6 constructs were seeded on coverslips and grown to 100% confluence in 10% FCS RM+ media. Proliferation was inhibited by treatment with 10µg/ml mitomycin C for one hour at 37^{o}C and a scratch created amongst the cells using a 10µl pipette tip. Any detached cells were washed away with PBS and the media was replaced. Six hours later cells were fixed and stained for F-actin using Alexafluor635 conjugated phalloidin, a toxin specifically targeting F-actin.

Figure 5.9 shows that, in migrating keratinocytes at the wound edge, the actin belt was compact with linear stress fibres forming on the leading edge of cells adjacent to the wound in cells expressing pLXSN. The actin fibres in the confluent cells behind the cells forming the wound edge also appear compact and concentrated at the cell edges. Furthermore, very few protrusions into the wound could be observed in cells expressing pLXSN. By comparison, the actin staining in migratory HPV5 E6-expressing cells appeared more disorganised and less compact with a greater number of protrusions around the cells. The actin fibres of the confluent cells behind these wound edge cells also showed a greater number of cellular protrusions. A similar phenotype could be observed in cells expressing pLXSN-8E6 and pLXSN-D156A. pLXSN-20E6 and pLXSN-W157A-expressing cells appeared to show a F-actin phenotype most similar to that of pLXSN-expressing cells. However, there appeared to be a slightly increased number of cellular protrusions into the wound and the actin filaments appeared to be organised less compactly. These data suggest that expression of the HPV5 or 8 E6 proteins leads to disruption of the cytoskeleton and that W157 of the HPV5 E6 protein contributes to this phenotype.

5.3.9 Investigation of migration rates in N-TERT cells expressing HPV E6 constructs

It was hypothesised that high-risk cutaneous E6 proteins, through use of the YHDW motif, could modulate β_1-integrin localisation, subsequently affecting downstream effector levels and localisation, in order to promote a more migratory phenotype. In order to assess whether the YHDW motif had an effect on cellular migration N-TERT

Figure 5.9 Actin cytoskeleton in migrating N-TERT cells expressing HPV E6 constructs

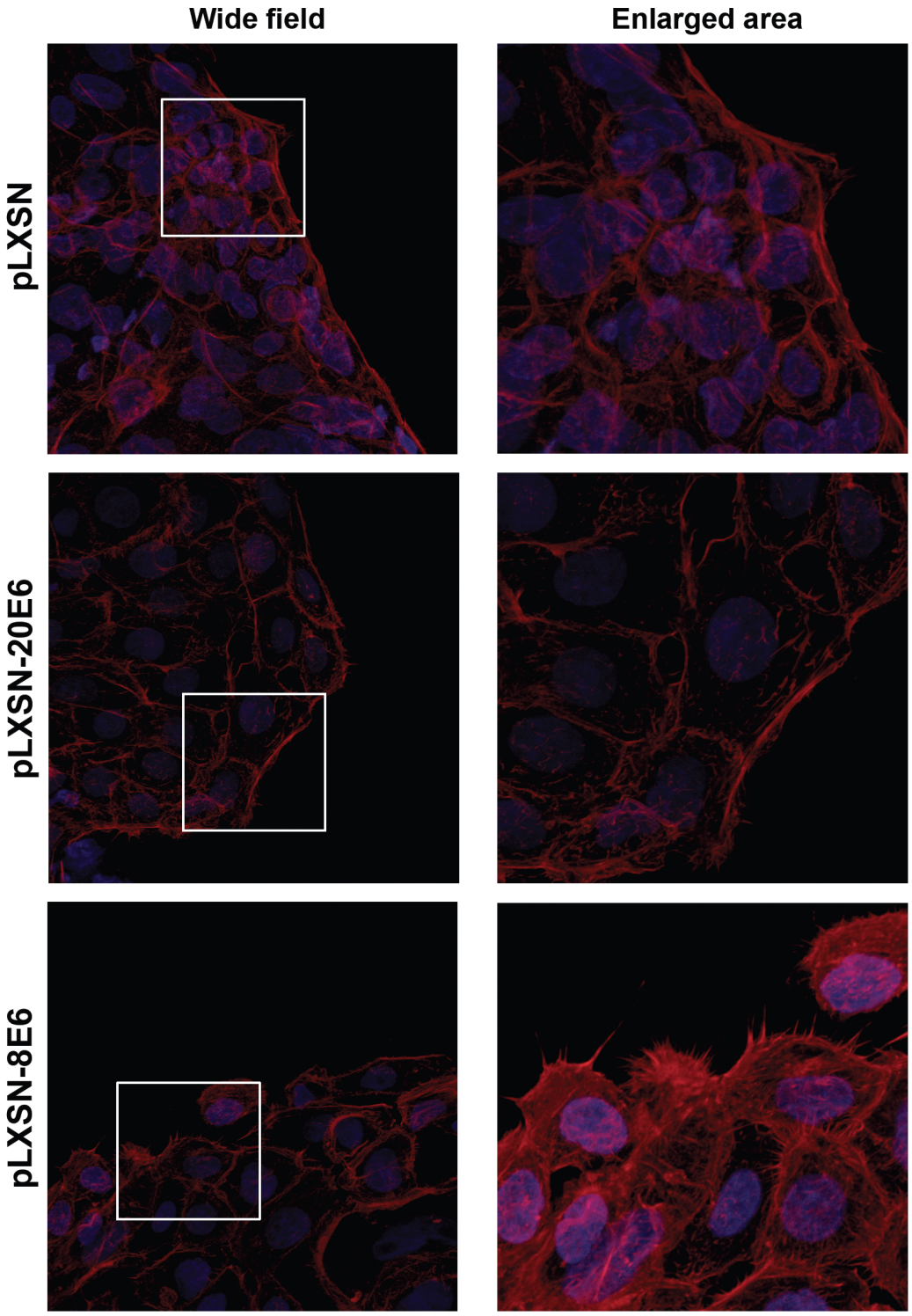


Figure 5.9 continued

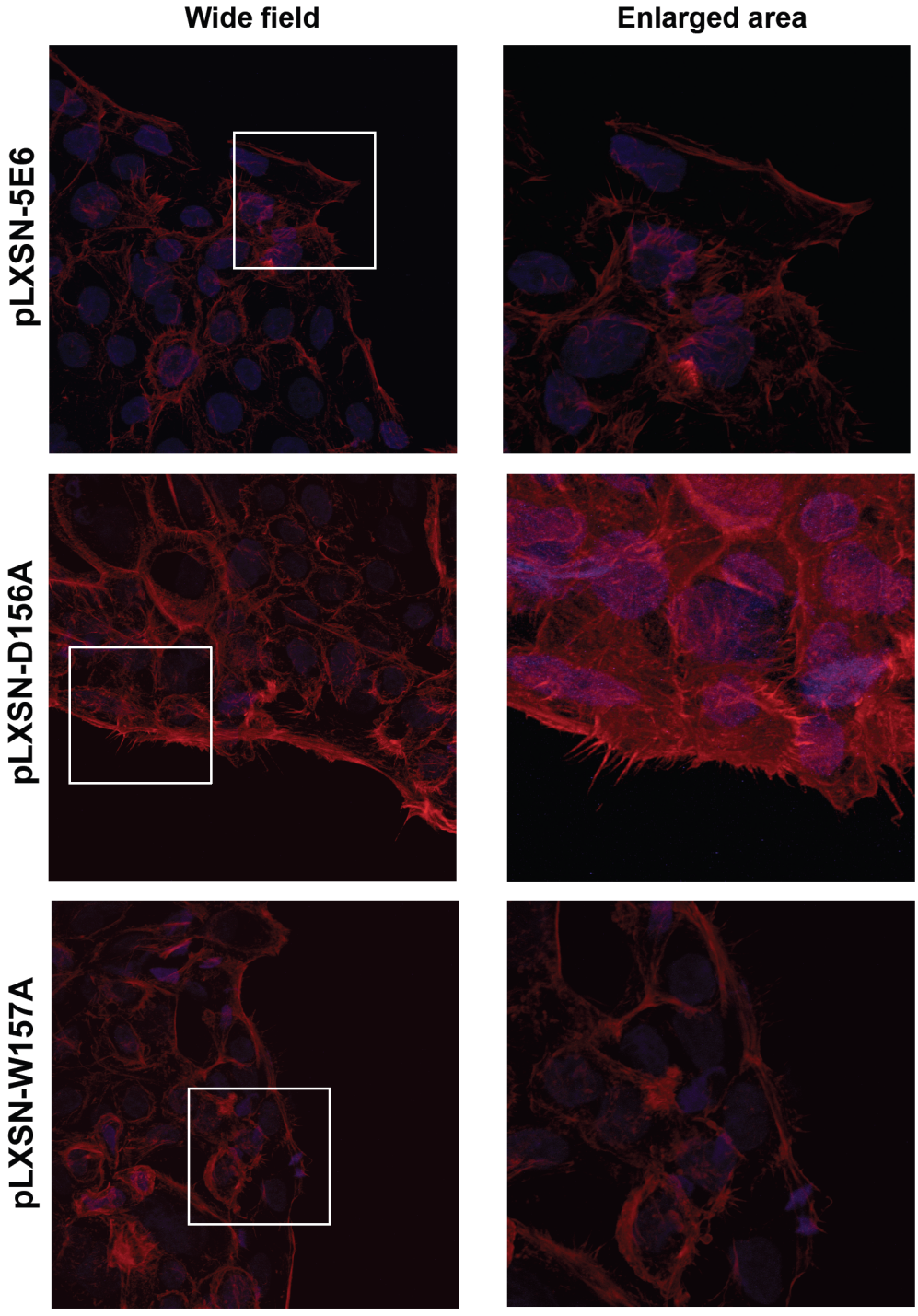


Figure 5.9 legend

N-TERT cells stably expressing pLXSN, -5E6, -8E6, -20E6, -D156A or -W157A were grown to confluence in RM+ media. After treatment with 10µg/ml mitomycin C for 1 hour, a scratch was made using a 10µl pipette tip. Detached cells were removed by washing with PBS. Culture media was replaced and 6 hours later cells were fixed in 4% PFA, permeabilised with 0.5% Triton X-100 and stained with AlexaFluor635 conjugated phalloidin to stain for F-actin. Cells imaged by Zeiss LSM 510 confocal microscopy. Representative compressed Z-stack images are shown. The white squares in the left hand column show the area selected for enhancement on the right. Blue; nuclear DAPI staining, red; F-actin.

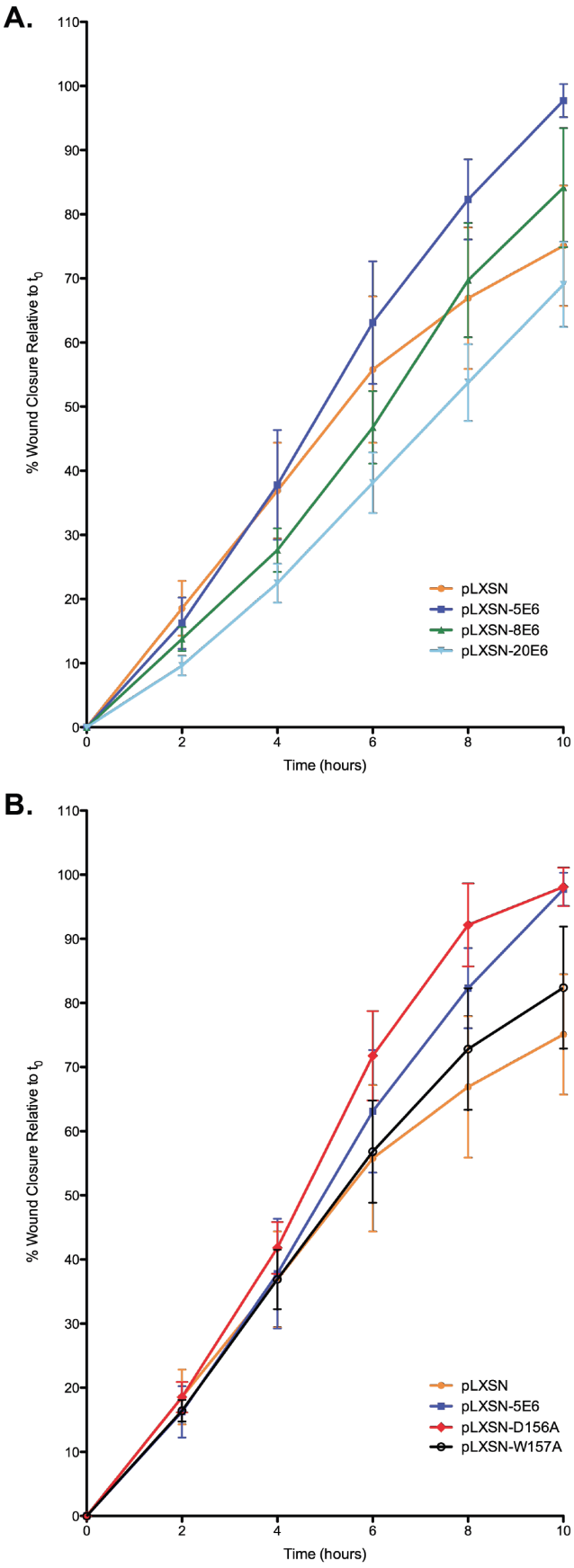
Experiment performed twice.

---

cells expressing pLXSN, -5E6, -8E6, -20E6, -D156A and -W157A were seeded at $2x10^5$ cells per well in collagen coated 24 well EssenBio ImageLock plates and grown to 100% confluence in RM+ 10% FCS supplemented media. Cells were treated with mitomycin C for 1 hour and scratched using 10µl pipette tips as before. Detached cells were washed away with PBS and new RM+ 10% FCS media added. Wound closure was monitored by Incucyte phase contrast imaging (Essen BioScience) at 2 hour intervals for a total of 10 hours.

The percentage wound closure, calculated by the Incucyte software, at each time point is plotted in Figure 5.10. Figure 5.10A shows migration of N-TERT cells expressing E6 proteins from the different HPV types (pLXSN-5E6, -8E6 and -20E6). It can be seen that cells expressing the HPV5 E6 protein migrated fastest, achieving complete wound closure by 10 hours. Cells expressing the HPV8 E6 protein or empty vector reached approximately 85% and 70% wound closure by 10 hours, respectively. It is noteworthy that the migration of cells expressing the HPV8 E6 protein was initially slower than that of cells expressing the empty vector, however 6-8 hours after scratching the migration rate of HPV8 E6-expressing cells increased to result in the higher percentage wound closure observed at 10 hours. Cells expressing pLXSN-20E6 consistently exhibited the slowest migration throughout the assay, achieving only 55-70% wound closure after 10 hours.

Figure 5.10 Percentage wound closure in N-TERT cells expressing HPV E6 constructs



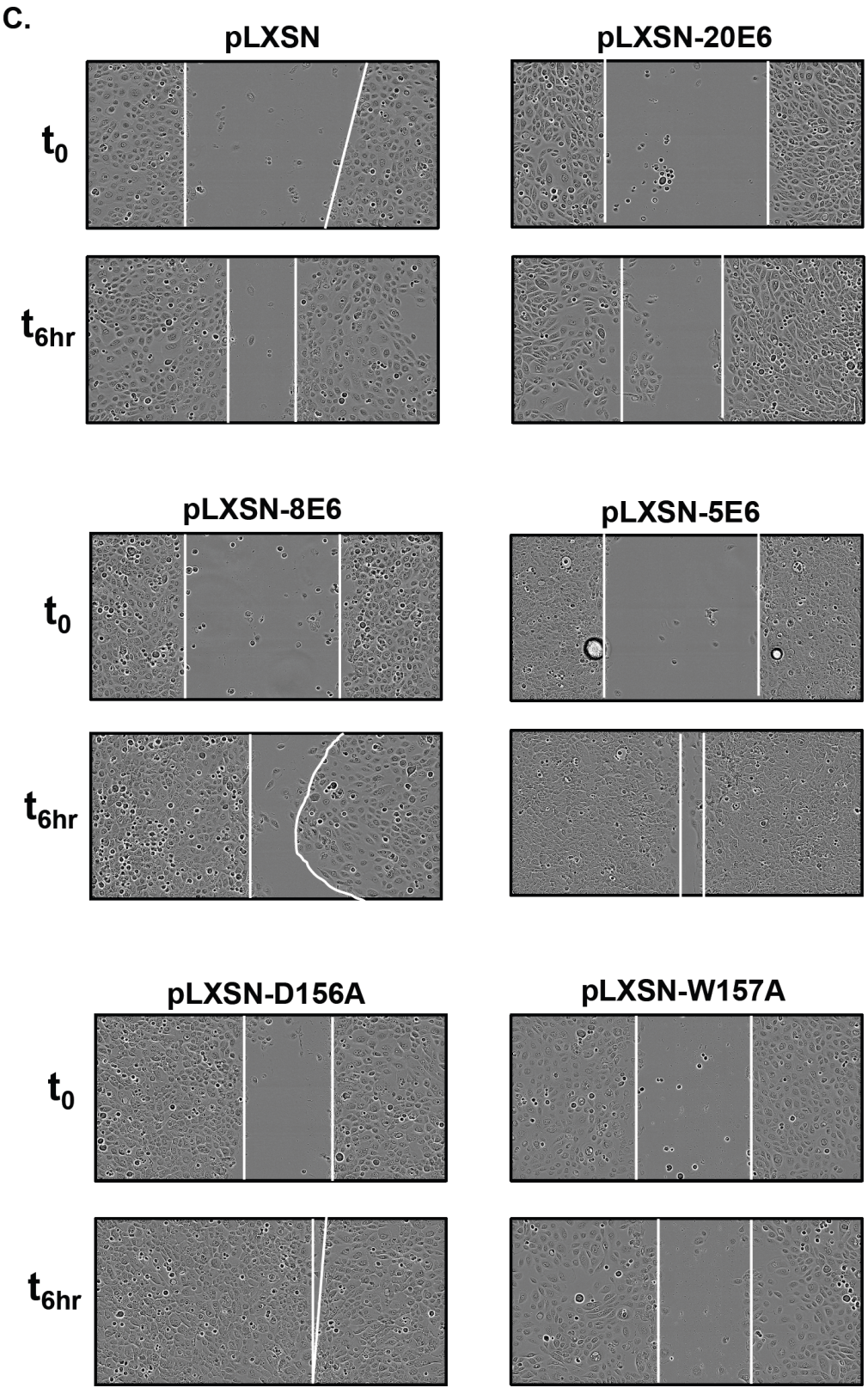

C.
pLXSN
pLXSN-20E6
t_0
t_{6hr}
pLXSN-8E6
pLXSN-5E6
t_0
t_{6hr}
pLXSN-D156A
pLXSN-W157A
t_0
t_{6hr}

Figure 5.10 legend

N-TERT cell lines expressing the indicated constructs were seeded on coverslips and grown to confluence in RM+ media. Cells were treated with 10µg/ml mitomycin C for 1 hour and then a scratch made with a 10µl pipette tip. Wound closure was monitored at 2 hour intervals by the Incucyte Live Imaging system (EssenBio).

A. Percentage wound closure of N-TERT cells expressing pLXSN, -5E6, -8E6 or -20E6, relative to the wound at t_0, at 2 hour intervals over a 10 hour period calculated by the Incucyte. n=6, mean wound closure ± SEM.

B. Percentage wound closure of N-TERT cells expressing pLXSN, -5E6, -D156A or -W157A, relative to the wound at t_0, at 2 hour intervals over a 10 hour period calculated by the Incucyte. n=6, mean wound closure ± SEM.

C. Representative images showing the initial wound (t_0) and closure 6 hours later (t_{6hr}).

NB. For comparison, the same data for pLXSN and pLXSN-5E6-expressing N-TERT cells has been plotted on the graphs in (A) and (B).

Figure 5.10B shows the migration of N-TERT cells expressing the WT HPV5 E6 protein and the mutants. For comparison, the same data for pLXSN and -5E6-expressing cells shown in Figure 5.10A is re-plotted in Figure 5.10B. The data show that N-TERT cells expressing pLXSN-D156A exhibited the most rapid migration over the 10 hour period reaching complete wound closure by 8-10 hours, migrating slightly faster than cells expressing the WT HPV5 E6 protein. Expression of the W157A mutant resulted in a reduced rate of migration compared to those cells expressing the WT HPV5 E6 protein 4 hours after the initial wounding. Cells expressing pLXSN-W157A achieved 70-90% wound closure by 10 hours. Migration of cells expressing these three constructs was faster than those expressing the empty vector. However it is noteworthy that the migration rate of cells expressing pLXSN-W157A only diverged from that of cells expressing pLXSN 6 hours after wounding.

Figure 5.10C shows representative images of the initial wound and closure 6 hours later, as this is where greatest difference in wound closure could be observed. These data suggest that expression of the E6 proteins of the high-risk cutaneous HPV5 and 8 increases the cell migratory phenotype and that W157 within the

C-terminal YHDW motif makes an important contribution to this effect of the HPV5 E6 protein expression.

5.4 Discussion

The C-terminus of the β-HPV5 and 8 E6 proteins, which are associated with the highest risk of progression to malignancy in NMSC in EV individuals, have a conserved YHDW sequence. Y-DW residues are perfectly conserved in the C-terminus of 7 other β1 HPV E6 proteins in Figure 5.1 (HPV14, 19, 25, 36, 47, 99 and 105) where histidine shows conserved substitution with asparagine. The remaining β-HPV E6 proteins do not retain any conservation of this motif.

Integrin-β_1 was identified as an interacting protein of this motif using peptide pull-down. It must be noted that the peptide pull-down was performed in lysates prepared from N-TERT cells grown in low calcium EpiLife media whilst subsequent experiments were performed in differentiated N-TERT cells by culture in RM+ media. Reasoning for this was that immunofluorescence of β_1-integrin in the undifferentiated N-TERT cells showed a diffuse staining pattern with no observable difference between E6-expressing and control cells (data not shown). Only upon differentiation did β_1-integrin localisation to the plasma membrane occur, showing the difference in β_1-integrin immunofluorescence between the control and E6-expressing cells. This suggests that E6 can bind β_1-integrin in the undifferentiated cells but that the effects of E6 on β_1-integrin localisation, by immunofluorescence, are only apparent when β_1-integrin is stimulated to localise upon induction of cell differentiation and junction formation. Performing the pull-down in differentiated N-TERT cells may identify other cutaneous E6 interacting proteins and further work to investigate the effect of E6 expression on β1-integrin in undifferentiated keratinocytes may contribute to understanding of the E6 interaction with β_1-integrin.

Integrin-β_1 has been previously identified as a protein that interacts with the α-HPV E5 and β-HPV8 E6 proteins although the significance of these interactions has not

been explored (Howie et al., 2011, Rozenblatt-Rosen et al., 2012). As the β-HPV do not encode the E5 protein, it is possible the E6 protein of cutaneous HPV may have evolved to disrupt β_1-integrin. In light of previous reports that other cell adhesion complexes are targeted by both HPV and BPV proteins (Tong and Howley, 1997, Kranjec and Banks, 2010), it appears that disruption of cell junctions is an important target in the activity of HPV encoded proteins so that both α- and β-HPV have evolved to disturb their protective function. An interaction between a GST fusion HPV5 E6 protein and β_1-integrin could not be detected through incubation of the GST protein with a N-TERT cell lysate and western blotting for β_1-integrin. The inability to detect an interaction in this manner may be a result of the altered ratio of the molarity of the YHDW peptide to β_1-integrin, less sensitive techniques compared to mass spectrometry or a reflection of a weak interaction. It is also feasible that the motif is not exposed in an incorrectly folded protein purified from bacteria.

Subsequently N-TERT cell lines expressing the HPV5, 8 and 20 E6 proteins and HPV5 E6 point mutants D156A and W157A were generated to probe the effects and requirement of this motif on β_1-integrin. Western blotting of lysates from these cell lines for β_1-integrin revealed a correlating pattern between the levels of β_1-integrin, F-actin, FAK, vinculin, paxillin and ZO1 suggesting a connection between the modulation of β_1-integrin and the E6 proteins. The W157 residue of HPV5 E6 showed the greatest contribution to these observed differences as mutation of this residue appeared to abrogate the effects of expression of the HPV5 E6 protein. Mutation of D156 had less of an effect, compared to mutation of W157, on the activities of the HPV5 E6 protein in these assays, suggesting D156 does not strongly contribute to the observed effects of HPV5 E6 expression, however misfolding of the HPV5 E6 D156A mutant protein cannot be excluded.

ZO1 is tight junction protein not immediately associated with β_1-integrin, however there are common regulators of the two proteins. Both are found in proximity and ZO1 also interacts with F-actin (Fanning et al., 1998, Taliana et al., 2005, Tafazoli et

al., 2000, Mandicourt et al., 2007), therefore a disruption of β_1-integrin having an effect on ZO1 cannot be excluded.

As the relationship between β_1-integrin, FAK and paxillin has been well characterised, the effects on this pathway were further probed. Immunofluorescent staining for β_1-integrin with different detergents (Figure 5.5 and Figure 5.7) suggested that expression of HPV5, 8 and HPV5 D156A E6 increased vesicular β_1-integrin. To confirm reduced β_1-integrin surface levels in E6-expressing cells, an antibody specific to the extracellular β_1-integrin domain and flow cytometry analysis could be employed. Investigation of co-localisation of β_1-integrin with endocytosis vesicle markers would also further enhance understanding.

The mechanism of how β-HPV E6 expression results in reduced surface β_1-integrin levels remains to be elucidated: does E6 expression increase β_1-integrin flux by increasing the rate of removal and internalisation from the plasma membrane or prevention of it reaching the membrane? It has previously been shown that β_1-integrin internalisation and trafficking plays a large role in cell migration: removing integrins from focal adhesions at one point and trafficking them to a different location on the plasma membrane to lay down new adhesion points. Endocytosis of integrin heterodimers, containing β_1-integrin, is required to allow focal adhesion dissembly (Vassilieva et al., 2008, Ezratty et al., 2009), and blocking integrin trafficking blocks cell migration (Ng et al., 1999, Shen et al., 2012). Use of a function-blocking antibody to β_1-integrin blocks β_1-integrin internalisation, suggesting internalisation occurs in response to activation (Du et al., 2011). Integrins are internalised to endocytic recycling pathways and endosomes by Rab proteins, a family of GTPases that regulate membrane trafficking (Pellinen et al., 2006). Therefore E6 may increase integrin activation or promote signalling for Rab-mediated internalisation. Fluorescently tagged β_1-integrin and live cell imaging would elucidate the effect of E6 expression on these processes.

Interestingly, integrins expressed exclusively on leukocytes, such as β_2 and β_7 have an endocytic signal in their cytoplasmic tail, proximal to the plasma membrane,

which is required for recycling to the plasma membrane surface. This motif is YXXΦ where Y represents tyrosine, X any amino acid and Φ any amino acid with a bulky hydrophobic moiety, resembling the YHDW motif. Mutation of Y in this motif in β_2-integrin diverted the integrin from a recycling compartment to a degradatory one leading to a marked decrease in cell migration (Fabbri et al., 1999). It would therefore be interesting to investigate the activity of the HPV5 E6 with a point mutation of Y154.

The increased levels of FAK observed here in E6-expressing cell lines has been previously observed in HPV18 positive cells, along with increased paxillin phosphorylation, and is associated with anchorage independent growth through anoikis abrogation (McCormack et al., 1997). Attempts to detect phosphorylated FAK at tyrosine 397 by western blot, as an indicator of FAK activation, were unsuccessful. However, activity of FAK is essential to cell migration, the role of FAK in focal adhesion is not only essential for focal adhesion assembly but also disassembly. FAK knock out mice cells show increased focal adhesion stability and reduced migration (Ilic et al., 1995) and dominant negative FAK blocks integrin internalisation suggesting FAK activation could be coupled to integrin endocytosis (Agerer et al., 2005, Alrutz and Isberg, 1998).

BPV E6 has been shown to directly interact with paxillin, which is necessary for the transforming ability of BPV E6, for high-risk HPV the purpose of the interaction has not been clarified (Wade et al., 2008). Here, the disruption of β_1-integrin, again dependent on residue W157 of the HPV5 E6 protein, appears to affect the localisation of paxillin and increase levels of the protein. As for β_1-integrin, there appears to be an inverse correlation between the cell lines with higher levels of paxillin observed by western blot and immunofluorescence (Figure 5.4 and Figure 5.8). Similar to β_1-integrin, this may be a result of the permeabilisation detergent used in immunofluorescence, alternatively it is possible that in E6-expressing cells, if integrins and focal adhesions are less stable, focal adhesions do not mature to the same extent so less paxillin concentrates at contact points. Further work to probe

this would require investigation of focal adhesion maturity markers, such as zyxin (Zaidel-Bar et al., 2003).

Other proteins identified in the interaction screen, taken together with these observations, may further elucidate how the E6 proteins contribute to the phenotype observed here. Annexin V has been shown to mediate chondrocyte adhesion, as well as being an inhibitor of PKC which has been shown to regulate integrin trafficking (Ng et al., 1999). In addition the identification of 14-3-3σ is intriguing as it is implicated in the regulation of stem cell proliferation (Chang et al., 2012, Fuchs and Raghavan, 2002) and other 14-3-3 isoforms have been previously identified as interacting with high-risk mucosal HPV E6 proteins (Boon and Banks, 2013). Therefore further work to investigate this interaction with the E6 protein may further contribute to the understanding of how HPV may promote tumour formation.

In summary, the high-risk cutaneous E6 proteins via the YHDW motif, of which the W157 residue seems of most importance here, appear to target β_1-integrin. In turn, this affects markers of downstream focal adhesion formation, actin cytoskeletal arrangement and cell migration. Through the targeting of β_1-integrin, potentially by alteration of β_1-integrin endocytosis and recycling to the plasma membrane, E6 has the potential to alter many cell pathways which may contribute to malignancy (keratinocyte differentiation, proliferation, adhesion and migration). Furthermore, the recent observation that cells expressing high levels of $\alpha_6\beta_1$-integrin with increased FAK signalling, isolated from SCC, meet criteria for definition as a cancer stem cell suggests further exploration of β_1-integrin modulation by the E6 protein may be warranted (Schober and Fuchs, 2011).

Though the exact effect and mechanism of the E6 interaction with β_1-integrin remains to be clarified, it is hypothesised here that expression of the high-risk HPV E6 proteins (5 and 8) results in increased β_1-integrin turnover and trafficking from the plasma membrane, resulting in increased focal adhesion turnover to result in the observed disruption of focal adhesion and β_1-integrin associated proteins. This subsequently leads to an increased migratory phenotype and actin cytoskeleton

disorganisation. Further work would be required to determine if this also affects anchorage independent growth, proliferation, invasion and adhesion. Further work to elucidate the recognition site of the YHDW motif would also be of interest, since the C-terminal ETQV/L motif of high risk α-HPV E6 proteins specifically recognises PDZ domains.

Investigation of E6 targeting of β_1-integrin in 3D skin cultures, such as organotypic rafts, would also prove insightful since the expression and function of E6 is predominantly in suprabasal keratinocytes whilst β_1-integrins mediate cell adhesion in the basal cells. PDZ proteins are disrupted at different stages of HPV-induced malignancy and Banks et al. (2012) propose that disruption of cell polarity is an early event and driving force in tumourigenesis. Therefore organotypic cultures would also provide a model in which to investigate the effects of E6 modulation of β_1-integrins throughout the differing epidermal strata.

In conclusion, these data suggest that high-risk cutaneous HPV E6 proteins target similar pathways to BPV and α-HPV E6 proteins, as has been observed for other pathways. This indicates that disruption of cell junction proteins may be important for HPV-mediated tumourigenesis and that further work into targeting of such proteins may have significant consequences for cutaneous HPV E6-mediated malignancy.

General Discussion

The increasing incidence of NMSC in the fair skinned population is a large burden on healthcare resources. Mounting evidence from epidemiological studies conducted in EV and immune suppressed individuals, as well as biological data, suggests that infection with β-HPV may contribute to the early stages of NMSC development. The work presented in this thesis primarily aimed to better understand how the β-HPV5 E6 protein, in co-operativity with UV-induced DNA damage, acted to target BAK for degradation. Investigations focussed on interrogating the BAK activation process in UV-irradiated E6-expressing cells, the requirement of a BAK lysine residue for E6-mediated BAK proteolysis and the role of a novel β-HPV E6 associated E3 ubiquitin ligase.

The data presented here elucidates the mechanism of BAK degradation, mediated by the β-HPV5 E6 protein, in response to UV DNA damage. This work showed that the residue K113 in the BAK amino acid sequence is required for E6-mediated BAK proteolysis and that mutation of this residue prevented E6-mediated degradation which resulted in decreased cell survival.

Experiments were initiated to determine which point of the BAK activation process is targeted by the E6. Investigations into the early steps of BAK activation involving the dephosphorylation of BAK at Y108 and S117, as well as binding of p53 in E6-expressing cells indicated that the early stages of activation proceeded normally in E6-expressing cells. These events are required for the BAK N-terminal conformational change. Further experimental data supported the idea that E6 targets the later stages of BAK activation. Using a well characterised BAK mutant, BAK S117E, where a negative charge prevents access of BH3 helices to a hydrophobic binding pocket, it was established that targeting of BAK by the E6 protein requires access of this hydrophobic pocket. Building on this information, the interaction of BAK with a novel β-HPV associated E3 ligase, HERC1, was investigated. HERC1 was found to be required for E6-mediated BAK proteolysis in both HCT116 and HEKa cells by siRNA knockdown of *herc1* expression.

Furthermore, an interaction between HERC1 and BAK could be identified using a proximity ligation *in situ* assay in HCT116 cells, showing that HERC1 and BAK interact only in E6-expressing cells, and that this required DNA damage generated by UV irradiation.

Identification of a putative BH3 domain sequence in HERC1 suggested a potential mechanism by which HERC1 may interact with BAK. To test this, peptides corresponding to the BH3 sequence of BAK, BID, HERC1 and MULE were used to pull-down BAK from cell extracts. The results showed that binding of the putative HERC1 BH3 peptide to BAK only occurred after DNA damage by UV irradiation, complementing previous work presented here that dephosphorylation of S117 is required to allow access to the BAK hydrophobic pocket for E6-mediated BAK degradation.

These data confirm previous findings from the laboratory that BAK is only targeted by the E6 protein in response to UV exposure, suggesting that there is only a small time frame in which E6 can target activated BAK for degradation once the BAK activation process has been initiated. This is in contrast to the constitutive degradation of p53 observed by the expression of high-risk anogenital α-HPV E6 proteins where E6 functions as a dimer and targets multiple p53 molecules for degradation at once. It remains to be elucidated whether the α-HPV E6 proteins also use HERC1 and the same mechanism to target BAK as that of β-HPV E6 proteins. Nevertheless, these experiments provide novel insight into the mechanism of the interaction of β-HPV E6 targeting of specific forms of BAK. Further work on this matter would emphasise how the E6 protein from HPV of differing genera are able to contribute to cell survival in response to mutagenic and apoptotic stimuli which may have implications for models and treatment of α- vs β-HPV-associated malignancies.

Together, the identification of the K113 residue within BAK as being important for E6-mediated BAK degradation and HERC1 as an E3 ligase able to interact with BAK may have wider implications for non-HPV-associated pathologies. The role of

ubiquitin conjugation to lysine residues in BAK degradation and the deregulation of BAK proteolysis in conditions where aberrant cell death, or BCL-2 protein levels, are observed has not been previously investigated. Such conditions include melanomas which exhibit lower levels of BAK and BAX (Tchernev and Orfanos, 2007). Reduced levels of BAK and increased levels of MCL-1 have also been observed in Multiple Sclerosis, associated with a failure in apoptosis of self-reactive immune cells (Mandel et al., 2012). As yet, the cause of these changes in protein levels remain unexplained. Therefore it is possible that BCL-2 protein proteolysis may play a role in such diseases. Furthermore, in the case of some cancers, higher levels of autophagy are observed (reviewed in Rosenfeldt and Ryan, 2011). Autophagy induction may also contribute to cell survival under adverse conditions, such as hypoxia. It is possible that this induction of autophagy may be a cell survival mechanism in the event of an inability of a cell to execute apoptosis in response to a stress-inducing environment. Potentially, loss of BAK activity as a result of active BAK proteolysis may contribute to such apoptosis suppression. Therefore identification of the K113 residue within BAK and the identification of HERC1 as a BAK-associated E3 ligase in HPV E6-mediated BAK proteolysis may have implications for future studies in the crosstalk between apoptosis and autophagy (reviewed in Maiuri et al., 2007) and associated diseases.

In additional work, β_1-integrin was identified as a novel interacting protein of HPV5 E6, via a β-HPV conserved YHDW C-terminal motif. Expression of the HPV5, and to a lesser extent, HPV8 E6 proteins appeared to reduce cell surface expression of β_1-integrin. These cells also showed altered levels of the β_1-integrin downstream proteins FAK and paxillin, which mediate cell attachment via focal adhesion formation. Furthermore cells expressing the HPV5 E6 proteins showed faster migration rates and increased actin cytoskeleton disorganisation compared to control cells. Mutation of residue W157, but not D156, in this motif of the HPV5 E6 protein reduced these effects. α-HPV E5 proteins have previously been reported to interact with β_1-integrin and other components of these pathways have previously

been shown to be disrupted by expression of HPV proteins. As the α-HPV E5 proteins have been shown to interact with β_1-integrin yet the β-type HPV do not encode the E5 protein these data suggest a conservation of function between α- and β-type HPV but through different proteins. This indicates that perturbation of cell adherence through junction proteins is an important activity of the HPV life cycle and subsequent carcinogenesis.

Together these data support a role for β-HPV in the progression of NMSC and help to elucidate the understanding of the contribution the E6 proteins may make to the early stages of the progression of NMSC. Targeting of activated BAK in order to lower levels of apoptosis in response to UV damage, promoting genomic instability, and increased migration through β_1-integrin disruption may contribute towards NMSC development. Further investigations, based on the findings presented here, will strengthen comprehension of HPV-mediated pathology leading to the development of new intervention strategies aimed at effective and efficient treatment.

Appendices

Appendix 1 HERC1 mini-gene nucleotide and translated amino acid sequence

ctcgaattcaccatggattacaaggatgacgacgataagtcagaaatcagagcagtccag
M D Y K D D D D K S E I R A V Q
ctgtcctatctttacctcggtgctatgaagtcacttagtgcccttcttggctgtagtaaa
L S Y L Y L G A M K S **L** S A **L L G** C S K
tatgctgagctgttgctgataccaaaagttctggctgaagccaaactgcttgtacagttg
Y A E L L L I P K V L A E A K L L V Q L
tgtacacagaacttgatttctgctgcaacaggtgtaaatctaaccacagttgatgactca
C T Q N L I S A A **T G V N L T T V D D S**
attcagcgaaagtttctacccagctttctccgaggaattgctgaagagaacaagcttgtg
I Q R K F L P S F L R G I A E E N K L V
acctccccaaactttgttgtaacacaggcccttgtggcattgctagcagacaaaggggcc
T S P N F V V T Q A L V A L L A D K G A
aaactaagacctaactatgataagtcagaagttgaaaagaaaggccctctggagttggct
K L R P N Y D K S E V E K K G P L E L A
aatgccctggcagcctgctgcctctcctccaggctgtcctcacagcatcggcaatgggca
N A L A A C C L S S R L S S Q H R Q W A
gctcagcaactcgtgcgcactcttgctgcacacgaccgtgacaaccaaactactctgcag
A Q Q L V R T L A A H D R D N Q T T L Q
acacttgctgatatgggaggagatcttagaaaatgctcctttatcaaattggaggctcat
T L A D M G G D L R K C S F I K L E A H
cagaacagagtaatgacatgtgtttggtgtaataaaaaaggtcttttggctacaagtggc
Q N R V M T C V W C N K K G L L A T S G
aatgatggcaccatccgcgtatggaatgttaccaagaagcaatattcactgcaacagacc
N D G T I R V W N V T K K Q Y S L Q Q T
tgtgtgttcaacagattggaaggggatgctgaggaaagcctgggatcacccagtgatcca
C V F N R L E G D A E E S L G S P S D P
agtttctcaccagtttcctggagtatcagtggcaaatatctagcaggcgctttggaaaag
S F S P V S W S I S G K Y L A G A L E K
atggtgaatatctggcaagttaatggaggaaaaggattagtagatattcagcctcattgg
M V N I W Q V N G G K G L V D I Q P H W
gtatctgccctggcttggccagaagagggtccggctacagcctggtcaggagagtctcca
V S A L A W P E E G P A T A W S G E S P
gaattgttgttggtgggacggatggatggatctctgggactgattgaagttgttgatgtg
E L L L V G R M D G S L G L I E V V D V
tccaccatgcaccgtcgagaattggagcattgctatcgaaaggatgtgtctgttacttgc
S T M H R R E L E H C Y R K D V S V T C
attgcatggttcagtgaagacagaccatttgcagtgggatattttgatggaaaactgtta
I A W F S E D R P F A V G Y F D G K L L
ctgggaacaaaggaaccacttgagaaaggaggcattgttctaattgatgcacataaggat
L G T K E P L E K G G I V L I D A H K D
actcttattagcatgaagtgggaccctacaggtcatattcttatgacatgtgccaaagaa
T L I S M K W D P T G H I L M T C A K E
gacagtgtgaaactctggggctctatttcgggatgctggtgctgtctacattcactctgc
D S V K L W G S I S G C W C C L H S L C
catccatctattgtaaatggcattgcttggtgccgccttccagggaaaggatccaagttg

H P S I V N G I A W C R L P G K G S K L
cagttactgatggctactggctgtcagagtggcttagtatgtgtttggcgcattcctcaa
Q L L M A T G C Q S G L V C V W R I P Q
gatactacacagaccaatgtgactagtgcagaaggatggtgg**gac**caggaatcaaattgc
D T T Q T N V T S A E G W W **D** Q E S N C
caggatggatataggaaatcatcaggagccaagtgtgtttatcagctgcggggacacatc
Q D G Y R K S S G A K C V Y Q L R G H I
actcctgttcggactgttgcctttagttctgatgggttggccctggtgtctggtggacta
T P V R T V A F S S D G L A L V S G G L
ggtgggctcatgaacatttggtctttaagggatggctctgtcttgcaaactgttgtgata
G G L M N I W S L R D G S V L Q T V V I
ggctctggagctattcagaccacagtatggattccagaagttggagtagctgcttgctca
G S G A I Q T T V W I P E V G V A A C S
aatagatcaaaggatgttttggtc**gttaac**tgtacagcatccataggaaaaaccatggtt
N R S K D V L V V N C T A S I G K T M V
caaggcaaaaactatggacctcagataactgtaaagaggatatcaaccagaggacggaag
Q G K N Y G P Q I T V K R I S T R G R K
tgtaagcctatttttgtccaaatagcgagacaagtagttaagctgaatgcttcagacctc
C K P I F V Q I A R Q V V K L N A S D L
cgcctgccttcccgagcgtggaaggttaagctggttggagaaggggctgatgatgctgga
R L P S R A W K V K L V G E G A D D A G
ggagtgtttgatgacaccatcacagagatgtgccaggaacttgaaactggtattgttgac
G V F D D T I T E M C Q E L E T G I V D
cttcttataccctctcccaatgccaccgcagaagtgggttacaatagggacaggttcctt
L L I P S P N A T A E V G Y N R D R F L
tttaacccttctgcctgcctcgatgaacacttaatgcagtttaagtttttaggaatttta
F N P S A C L D E H L M Q F K F L G I L
atgggggttgccattcgcacaaagaagcctctggacctccacttggcccctctggtgtgg
M G V A I R T K K P L D L H L A P L V W
aagcagctgtgctgtgtcccactcaccctagaggacctggaggaggtggatctgctctac
K Q L C C V P L T L E D L E E V D L L Y
gtgcagactctcaacagcattcttcacattgaagacagtgggattaccgaggagagtttc
V Q T L N S I L H I E D S G I T E E S F
catgagatgattcctcttgattcttttgttggccagagtgctgatggcaaaatggttcct
H E M I P L D S F V G Q S A D G K M V P
ataatccctggtggaaatagtatcccactcacattttccaacaggaaggaatatgtggag
I I P G G N S I P L T F S N R K E Y V E
agggccattgaatatcgacttcatgagatggacagacaggtggctgcagtccgagaaggg
R A I E Y R L H E M D R Q V A A V R E G
atgtcctggattgttcctgtgccgctgctgtccctcctcacagcaaaacaactggagcag
M S W I V P V P L L S L L T A K Q L E Q
atggtgtgtgggatgcccgagatctctgtggaagtcttgaagaaagtggtgcggtaccgt
M V **C** G M P E I S V E V L K K V V R Y R
gaggtggatgagcagcatcagctggtgcagtggttctggcacacgctggaagagttctcc
E V D E Q H Q L V Q W F W H T L E E F S
aatgaggagcgggtgcttttcatgaggtttgtgtcaggaagatctcgactaccagccaac
N E E R V L F M R F V S G R S R L P A N
actgctgacatttctcagagatttcaaatcatgaaggttgataggccttacgacagtctg

```
 T  A  D  I  S  Q  R  F  Q  I  M  K  V  D  R  P  Y  D  S  L
cctacctcacagacctgcttcttccagctgaggctgcccccgtactccagccagctggtc
 P  T  S  Q  T  C  F  F  Q  L  R  L  P  P  Y  S  S  Q  L  V
atggccgagcgcctgcgctatgccatcaacaactgccgctcaatcgacatggacaactac
 M  A  E  R  L  R  Y  A  I  N  N  C  R  S  I  D  M  D  N  Y
atgctctcgagaaacgtggacaacgccgagggctccgacactgactactaacatcatcat
 M  L  S  R  N  V  D  N  A  E  G  S  D  T  D  Y  -  H  H  H
catcattgagtcgacgcggccgcctc
 H  H  -
```

Restriction sites FLAG-tag L2G containing region
BH3/WD40 domain HECT domain His-tag

TGVNLTTVDDSIQRKF – HERC1 putative BH3 domain

GAC - naturally occurring single nucleotide polymorphism resulting in an amino acid change from the reference sequence. Codon change from GAG to GAC resulting in amino acid change E3722D in the full length HERC1 protein sequence[2].

GTTAAC – mutated from GTTAAT to encode a *HpaI* restriction site for sequential cloning, preserving the amino acid.

C – active cysteine. Codon mutated to GCT for mutation to alanine in the C895A HERC1 mini-gene mutant.

TAA – mutated from CAT in order to remove the originally encoded His-tag.

[2] http://www.ncbi.nlm.nih.gov/SNP/snp_ref.cgi?locusId=8925

Appendix 2 Mascot search results of tryptic digest

14-3-3δ

P31947 **Mass:** 27757 **Score:** 183 **Queries matched:** 5 **emPAI:** 0.25
RecName: Full=14-3-3 protein sigma; AltName: Full=Stratifin; AltName: Full=Epithelial cell marker protein 1;
Check to include this hit in error tolerant search or archive report

Query	Observed	Mr(expt)	Mr(calc)	Delta	Miss	Score	Expect	Rank	Peptide
50	452.3600	902.7054	902.5073	0.1982	0	43	0.35	2	R.VLSSIEQK.S
51	454.3760	906.7374	906.5174	0.2200	0	34	2.3	1	R.NLLSVAYK.N
52	454.4300	906.8454	906.5174	0.3280	0	(33)	3	2	R.NLLSVAYK.N
254	796.9330	1591.8514	1591.7148	0.1367	1	61	0.0067	1	K.GAVEKGEELSCEER.N + Carbamidomethyl (C)
417	813.7870	2438.3392	2438.2727	0.0665	0	60	0.011	1	K.VETELQGVCDTVLGLLDSHLIK.E + Carbamidomethyl (C)

Annexin V

Q4R4H7 **Mass:** 35824 **Score:** 155 **Queries matched:** 4 **emPAI:** 0.19
RecName: Full=Annexin A5; AltName: Full=Annexin-5; AltName: Full=Annexin V;
Check to include this hit in error tolerant search or archive report

Query	Observed	Mr(expt)	Mr(calc)	Delta	Miss	Score	Expect	Rank	Peptide
260	807.1310	1612.2474	1612.9036	-0.6561	0	68	0.0031	1	R.ETSGNLEQLLLAVVK.S
284	852.6890	1703.3634	1703.8941	-0.5307	0	87	2e-05	1	K.GLGTDEESILTLLTSR.S
285	853.0940	1704.1734	1703.8941	0.2793	0	(84)	3.7e-05	1	K.GLGTDEESILTLLTSR.S
286	853.1600	1704.3054	1703.8941	0.4113	0	(81)	7.9e-05	1	K.GLGTDEESILTLLTSR.S

Proteins matching the same set of peptides:
Q5R1W0 **Mass:** 35914 **Score:** 155 **Queries matched:** 4
RecName: Full=Annexin A5; AltName: Full=Annexin-5; AltName: Full=Annexin V;
P08758 **Mass:** 35914 **Score:** 155 **Queries matched:** 4
RecName: Full=Annexin A5; AltName: Full=Annexin-5; AltName: Full=Annexin V; AltName: Full=Lipocortin V;

Heterogeneous nuclear ribonucleoprotein M

P52272 **Mass:** 77464 **Score:** 86 **Queries matched:** 3 **emPAI:** 0.04
RecName: Full=Heterogeneous nuclear ribonucleoprotein M; Short=hnRNP M;
Check to include this hit in error tolerant search or archive report

Query	Observed	Mr(expt)	Mr(calc)	Delta	Miss	Score	Expect	Rank	Peptide
130	563.4950	1124.9754	1124.5107	0.4648	0	29	7.6	1	R.MGAGMGFGLER.M
177	632.9930	1263.9714	1263.6863	0.2851	0	66	0.0018	1	R.AFITNIPFDVK.W
178	633.0620	1264.1094	1263.6863	0.4231	0	(56)	0.017	1	R.AFITNIPFDVK.W

Proteins matching the same set of peptides:
Q62826 **Mass:** 73733 **Score:** 86 **Queries matched:** 3
RecName: Full=Heterogeneous nuclear ribonucleoprotein M; Short=hnRNP M; AltName: Full=M4 protein;
Q9D0E1 **Mass:** 77597 **Score:** 83 **Queries matched:** 3
RecName: Full=Heterogeneous nuclear ribonucleoprotein M; Short=hnRNP M;

Integrin β_1

Q5RCA9 **Mass:** 88327 **Score:** 128 **Queries matched:** 4 **emPAI:** 0.08
RecName: Full=Integrin beta-1; AltName: Full=Fibronectin receptor subunit beta; AltName: Full=VLA-4 subunit beta; AltName: CD_antigen=CD29;
Check to include this hit in error tolerant search or archive report

Query	Observed	Mr(expt)	Mr(calc)	Delta	Miss	Score	Expect	Rank	Peptide
70	492.4670	982.9194	982.5124	0.4071	0	37	0.93	1	R.IGFGSFVEK.T
89	508.4040	1014.7934	1014.5710	0.2225	0	67	0.0014	1	K.SAVTTVVNPK.Y
90	508.4180	1014.8214	1015.5550	-0.7335	0	(55)	0.02	1	K.SAVTTVVNPK.Y + Deamidated (NQ)
313	615.7820	1844.3242	1844.9091	-0.5849	1	31	8.2	5	R.DKLPQPVQPDPVSHCK.E + Carbamidomethyl (C); Deamidated (NQ)

Proteins matching the same set of peptides:
P05556 **Mass:** 88357 **Score:** 128 **Queries matched:** 4
RecName: Full=Integrin beta-1; AltName: Full=Fibronectin receptor subunit beta; AltName: Full=VLA-4 subunit beta; AltName: CD_antigen=CD29;

References

Accardi, R., Dong, W., Smet, A., Cui, R., Hautefeuille, A., Gabet, A. S., Sylla, B. S., Gissmann, L., Hainaut, P. & Tommasino, M. 2006. Skin human papillomavirus type 38 alters p53 functions by accumulation of deltaNp73. EMBO Rep, 7, 334-40.

Acehan, D., Jiang, X., Morgan, D. G., Heuser, J. E., Wang, X. & Akey, C. W. 2002. Three-dimensional structure of the apoptosome: implications for assembly, procaspase-9 binding, and activation. Mol Cell, 9, 423-32.

Agerer, F., Lux, S., Michel, A., Rohde, M., Ohlsen, K. & Hauck, C. R. 2005. Cellular invasion by Staphylococcus aureus reveals a functional link between focal adhesion kinase and cortactin in integrin-mediated internalisation. J Cell Sci, 118, 2189-200.

Agrawal, N., Frederick, M. J., Pickering, C. R., Bettegowda, C., Chang, K., Li, R. J., Fakhry, C., Xie, T. X., Zhang, J., Wang, J., Zhang, N., El-Naggar, A. K., Jasser, S. A., Weinstein, J. N., Trevino, L., Drummond, J. A., Muzny, D. M., Wu, Y., Wood, L. D., Hruban, R. H., Westra, W. H., Koch, W. M., Califano, J. A., Gibbs, R. A., Sidransky, D., Vogelstein, B., Velculescu, V. E., Papadopoulos, N., Wheeler, D. A., Kinzler, K. W. & Myers, J. N. 2011. Exome sequencing of head and neck squamous cell carcinoma reveals inactivating mutations in NOTCH1. Science, 333, 1154-7.

Ahdieh, L., Munoz, A., Vlahov, D., Trimble, C. L., Timpson, L. A. & Shah, K. 2000. Cervical neoplasia and repeated positivity of human papillomavirus infection in human immunodeficiency virus-seropositive and -seronegative women. Am J Epidemiol, 151, 1148-57.

Akgul, B., Bostanci, N., Westphal, K., Nindl, I., Navsaria, H., Storey, A. & Pfister, H. 2010. Human papillomavirus 5 and 8 E6 downregulate interleukin-8 secretion in primary human keratinocytes. J Gen Virol, 91, 888-92.

Akgul, B., Garcia-Escudero, R., Ekechi, C., Steger, G., Navsaria, H., Pfister, H. & Storey, A. 2011. The E2 protein of human papillomavirus type 8 increases the expression of matrix metalloproteinase-9 in human keratinocytes and organotypic skin cultures. Med Microbiol Immunol, 200, 127-35.

Akgul, B., Garcia-Escudero, R., Ghali, L., Pfister, H. J., Fuchs, P. G., Navsaria, H. & Storey, A. 2005a. The E7 protein of cutaneous human papillomavirus type 8 causes invasion of human keratinocytes into the dermis in organotypic cultures of skin. Cancer Res, 65, 2216-23.

Akgul, B., Ghali, L., Davies, D., Pfister, H., Leigh, I. M. & Storey, A. 2007. HPV8 early genes modulate differentiation and cell cycle of primary human adult keratinocytes. Exp Dermatol, 16, 590-9.

Akgul, B., Lemme, W., Garcia-Escudero, R., Storey, A. & Pfister, H. J. 2005b. UV-B irradiation stimulates the promoter activity of the high-risk, cutaneous human papillomavirus 5 and 8 in primary keratinocytes. Arch Virol, 150, 145-51.

Akgul, B., Pfefferle, R., Marcuzzi, G. P., Zigrino, P., Krieg, T., Pfister, H. & Mauch, C. 2006. Expression of matrix metalloproteinase (MMP)-2, MMP-9, MMP-13, and MT1-MMP in skin tumors of human papillomavirus type 8 transgenic mice. Exp Dermatol, 15, 35-42.

Akgul, B., Zigrino, P., Frith, D., Hanrahan, S. & Storey, A. 2009. Proteomic analysis reveals the actin cytoskeleton as cellular target for the human papillomavirus type 8. Virology, 386, 1-5.

Alam, H., Sehgal, L., Kundu, S. T., Dalal, S. N. & Vaidya, M. M. 2011. Novel function of keratins 5 and 14 in proliferation and differentiation of stratified epithelial cells. Mol Biol Cell, 22, 4068-78.

Alotaibi, L., Provost, N., Gagnon, S., Franco, E. L. & Coutlee, F. 2006. Diversity of cutaneous human papillomavirus types in individuals with and without skin lesion. J Clin Virol, 36, 133-40.

Alrutz, M. A. & Isberg, R. R. 1998. Involvement of focal adhesion kinase in invasin-mediated uptake. Proc Natl Acad Sci U S A, 95, 13658-63.

Ambrosini, G., Adida, C. & Altieri, D. C. 1997. A novel anti-apoptosis gene, survivin, expressed in cancer and lymphoma. Nat Med, 3, 917-21.

Ansari, T., Brimer, N. & Vande Pol, S. B. 2012. Peptide interactions stabilize and restructure human papillomavirus type 16 E6 to interact with p53. J Virol, 86, 11386-91.

Antonsson, A., Erfurt, C., Hazard, K., Holmgren, V., Simon, M., Kataoka, A., Hossain, S., Hakangard, C. & Hansson, B. G. 2003. Prevalence and type spectrum of human papillomaviruses in healthy skin samples collected in three continents. J Gen Virol, 84, 1881-6.

Antonsson, A., Forslund, O., Ekberg, H., Sterner, G. & Hansson, B. G. 2000. The ubiquity and impressive genomic diversity of human skin papillomaviruses suggest a commensalic nature of these viruses. J Virol, 74, 11636-41.

Aplin, A. E. & Juliano, R. L. 1999. Integrin and cytoskeletal regulation of growth factor signaling to the MAP kinase pathway. J Cell Sci, 112 (Pt 5), 695-706.

Aragane, Y., Kulms, D., Metze, D., Wilkes, G., Poppelmann, B., Luger, T. A. & Schwarz, T. 1998. Ultraviolet light induces apoptosis via direct activation of CD95 (Fas/APO-1) independently of its ligand CD95L. J Cell Biol, 140, 171-82.

Arbeit, J. M., Howley, P. M. & Hanahan, D. 1996. Chronic estrogen-induced cervical and vaginal squamous carcinogenesis in human papillomavirus type 16 transgenic mice. Proc Natl Acad Sci U S A, 93, 2930-5.

Arbeit, J. M., Munger, K., Howley, P. M. & Hanahan, D. 1994. Progressive squamous epithelial neoplasia in K14-human papillomavirus type 16 transgenic mice. J Virol, 68, 4358-68.

Arias-Pulido, H., Peyton, C. L., Joste, N. E., Vargas, H. & Wheeler, C. M. 2006. Human papillomavirus type 16 integration in cervical carcinoma in situ and in invasive cervical cancer. J Clin Microbiol, 44, 1755-62.

Armstrong, B. K. & Kricker, A. 2001. The epidemiology of UV induced skin cancer. J Photochem Photobiol B, 63, 8-18.

Asgari, M. M., Kiviat, N. B., Critchlow, C. W., Stern, J. E., Argenyi, Z. B., Raugi, G. J., Berg, D., Odland, P. B., Hawes, S. E. & de Villiers, E. M. 2008. Detection of human papillomavirus DNA in cutaneous squamous cell carcinoma among immunocompetent individuals. J Invest Dermatol, 128, 1409-17.

Astori, G., Lavergne, D., Benton, C., Hockmayr, B., Egawa, K., Garbe, C. & de Villiers, E. M. 1998. Human papillomaviruses are commonly found in normal skin of immunocompetent hosts. J Invest Dermatol, 110, 752-5.

Auluck, A., Hislop, G., Bajdik, C., Poh, C., Zhang, L. & Rosin, M. 2010. Trends in oropharyngeal and oral cavity cancer incidence of human papillomavirus (HPV)-related and HPV-unrelated sites in a multicultural population: the British Columbia experience. Cancer, 116, 2635-44.

Azad, A., Fox, J., Leverrier, S. & Storey, A. 2012. Blockade of the BAK Hydrophobic Groove by Inhibitory Phosphorylation Regulates Commitment to Apoptosis. PLoS One, 7, e49601.

Baker, C. C., Phelps, W. C., Lindgren, V., Braun, M. J., Gonda, M. A. & Howley, P. M. 1987. Structural and transcriptional analysis of human papillomavirus type 16 sequences in cervical carcinoma cell lines. J Virol, 61, 962-71.

Banks, L., Pim, D. & Thomas, M. 2003. Viruses and the 26S proteasome: hacking into destruction. Trends Biochem Sci, 28, 452-9.

Banks, L., Pim, D. & Thomas, M. 2012. Human tumour viruses and the deregulation of cell polarity in cancer. Nat Rev Cancer, 12, 877-86.

Bastien, N. & McBride, A. A. 2000. Interaction of the papillomavirus E2 protein with mitotic chromosomes. Virology, 270, 124-34.

Batista, L. F., Kaina, B., Meneghini, R. & Menck, C. F. 2009. How DNA lesions are turned into powerful killing structures: insights from UV-induced apoptosis. Mutat Res, 681, 197-208.

Batonnet, S., Leibovitch, M. P., Tintignac, L. & Leibovitch, S. A. 2004. Critical role for lysine 133 in the nuclear ubiquitin-mediated degradation of MyoD. J Biol Chem, 279, 5413-20.

Bedard, K. M., Underbrink, M. P., Howie, H. L. & Galloway, D. A. 2008. The E6 oncoproteins from human betapapillomaviruses differentially activate telomerase through an E6AP-dependent mechanism and prolong the lifespan of primary keratinocytes. J Virol, 82, 3894-902.

Bell, I., Martin, A. & Roberts, S. 2007. The E1circumflexE4 protein of human papillomavirus interacts with the serine-arginine-specific protein kinase SRPK1. J Virol, 81, 5437-48.

Bergant Marusic, M., Ozbun, M. A., Campos, S. K., Myers, M. P. & Banks, L. 2012. Human papillomavirus L2 facilitates viral escape from late endosomes via sorting nexin 17. Traffic, 13, 455-67.

Bernard, H. U., Burk, R. D., Chen, Z., van Doorslaer, K., Hausen, H. & de Villiers, E. M. 2010. Classification of papillomaviruses (PVs) based on 189 PV types and proposal of taxonomic amendments. Virology, 401, 70-9.

Besaratinia, A., Kim, S. I. & Pfeifer, G. P. 2008. Rapid repair of UVA-induced oxidized purines and persistence of UVB-induced dipyrimidine lesions determine the mutagenicity of sunlight in mouse cells. FASEB J, 22, 2379-92.

Blanpain, C. & Fuchs, E. 2009. Epidermal homeostasis: a balancing act of stem cells in the skin. Nat Rev Mol Cell Biol, 10, 207-17.

Boon, S. S. & Banks, L. 2013. High-risk human papillomavirus E6 oncoproteins interact with 14-3-3zeta in a PDZ binding motif-dependent manner. J Virol, 87, 1586-95.

Borgogna, C., Zavattaro, E., De Andrea, M., Griffin, H. M., Dell'Oste, V., Azzimonti, B., Landini, M. M., Peh, W. L., Pfister, H., Doorbar, J., Landolfo, S. & Gariglio, M. 2012. Characterization of beta papillomavirus E4 expression in tumours from Epidermodysplasia Verruciformis patients and in experimental models. Virology, 423, 195-204.

Borradori, L. & Sonnenberg, A. 1999. Structure and function of hemidesmosomes: more than simple adhesion complexes. J Invest Dermatol, 112, 411-8.

Borzacchiello, G., Roperto, F., Campo, M. S. & Venuti, A. 2010. 1st International Workshop on Papillomavirus E5 Oncogene-a report. Virology, 408, 135-7.

Bousarghin, L., Touze, A., Sizaret, P. Y. & Coursaget, P. 2003. Human papillomavirus types 16, 31, and 58 use different endocytosis pathways to enter cells. J Virol, 77, 3846-50.

Bouvard, V., Storey, A., Pim, D. & Banks, L. 1994. Characterization of the human papillomavirus E2 protein: evidence of trans-activation and trans-repression in cervical keratinocytes. EMBO J, 13, 5451-9.

Bouwes Bavinck, J. N., Hardie, D. R., Green, A., Cutmore, S., MacNaught, A., O'Sullivan, B., Siskind, V., Van Der Woude, F. J. & Hardie, I. R. 1996. The risk of skin cancer in renal transplant recipients in Queensland, Australia. A follow-up study. Transplantation, 61, 715-21.

Bouwes Bavinck, J. N., Neale, R. E., Abeni, D., Euvrard, S., Green, A. C., Harwood, C. A., de Koning, M. N., Naldi, L., Nindl, I., Pawlita, M., Pfister, H., Proby, C. M., Quint, W. G., ter Schegget, J., Waterboer, T., Weissenborn, S. & Feltkamp, M. C. 2010. Multicenter study of the association between betapapillomavirus infection and cutaneous squamous cell carcinoma. Cancer Res, 70, 9777-86.

Boxman, I. L., Berkhout, R. J., Mulder, L. H., Wolkers, M. C., Bouwes Bavinck, J. N., Vermeer, B. J. & ter Schegget, J. 1997. Detection of human papillomavirus DNA in plucked hairs from renal transplant recipients and healthy volunteers. J Invest Dermatol, 108, 712-5.

Boxman, I. L., Mulder, L. H., Noya, F., de Waard, V., Gibbs, S., Broker, T. R., ten Kate, F., Chow, L. T. & ter Schegget, J. 2001. Transduction of the E6 and E7 genes of epidermodysplasia-verruciformis-associated human papillomaviruses alters human keratinocyte growth and differentiation in organotypic cultures. J Invest Dermatol, 117, 1397-404.

Brake, T. & Lambert, P. F. 2005. Estrogen contributes to the onset, persistence, and malignant progression of cervical cancer in a human papillomavirus-transgenic mouse model. Proc Natl Acad Sci U S A, 102, 2490-5.

Brakebusch, C., Grose, R., Quondamatteo, F., Ramirez, A., Jorcano, J. L., Pirro, A., Svensson, M., Herken, R., Sasaki, T., Timpl, R., Werner, S. & Fassler, R. 2000. Skin and hair follicle integrity is crucially dependent on beta 1 integrin expression on keratinocytes. EMBO J, 19, 3990-4003.

Brandner, J. M. 2009. Tight junctions and tight junction proteins in mammalian epidermis. Eur J Pharm Biopharm, 72, 289-94.

Branzei, D. & Foiani, M. 2008. Regulation of DNA repair throughout the cell cycle. Nat Rev Mol Cell Biol, 9, 297-308.

Brash, D. E., Rudolph, J. A., Simon, J. A., Lin, A., McKenna, G. J., Baden, H. P., Halperin, A. J. & Ponten, J. 1991. A role for sunlight in skin cancer: UV-induced p53 mutations in squamous cell carcinoma. Proc Natl Acad Sci U S A, 88, 10124-8.

Brehm, A., Miska, E., Reid, J., Bannister, A. & Kouzarides, T. 1999. The cell cycle-regulating transcription factors E2F-RB. Br J Cancer, 80 Suppl 1, 38-41.

Brehm, A., Miska, E. A., McCance, D. J., Reid, J. L., Bannister, A. J. & Kouzarides, T. 1998. Retinoblastoma protein recruits histone deacetylase to repress transcription. Nature, 391, 597-601.

Brimer, N., Lyons, C., Wallberg, A. E. & Vande Pol, S. B. 2012. Cutaneous papillomavirus E6 oncoproteins associate with MAML1 to repress transactivation and NOTCH signaling. Oncogene.

Broemer, M. & Meier, P. 2009. Ubiquitin-mediated regulation of apoptosis. Trends Cell Biol, 19, 130-40.

Buitrago-Perez, A., Hachimi, M., Duenas, M., Lloveras, B., Santos, A., Holguin, A., Duarte, B., Santiago, J. L., Akgul, B., Rodriguez-Peralto, J. L., Storey, A., Ribas, C., Larcher, F., del Rio, M., Paramio, J. M. & Garcia-Escudero, R. 2012. A humanized mouse model of HPV-associated pathology driven by E7 expression. PLoS One, 7, e41743.

Cadet, J. & Douki, T. 2011. Oxidatively generated damage to DNA by UVA radiation in cells and human skin. J Invest Dermatol, 131, 1005-7.

Caldeira, S., de Villiers, E. M. & Tommasino, M. 2000. Human papillomavirus E7 proteins stimulate proliferation independently of their ability to associate with retinoblastoma protein. Oncogene, 19, 821-6.

Campbell, C., Quinn, A. G., Angus, B., Farr, P. M. & Rees, J. L. 1993. Wavelength specific patterns of p53 induction in human skin following exposure to UV radiation. Cancer Res, 53, 2697-9.

Candi, E., Rufini, A., Terrinoni, A., Dinsdale, D., Ranalli, M., Paradisi, A., De Laurenzi, V., Spagnoli, L. G., Catani, M. V., Ramadan, S., Knight, R. A. & Melino, G. 2006. Differential roles of p63 isoforms in epidermal development: selective genetic complementation in p63 null mice. Cell Death Differ, 13, 1037-47.

Cartron, P. F., Priault, M., Oliver, L., Meflah, K., Manon, S. & Vallette, F. M. 2003. The N-terminal end of Bax contains a mitochondrial-targeting signal. J Biol Chem, 278, 11633-41.

Castellsague, X. 2008. Natural history and epidemiology of HPV infection and cervical cancer. Gynecol Oncol, 110, S4-7.

Castle, P. E., Schiffman, M., Wheeler, C. M. & Solomon, D. 2009. Evidence for frequent regression of cervical intraepithelial neoplasia-grade 2. Obstet Gynecol, 113, 18-25.

Caswell, P. T. & Norman, J. C. 2006. Integrin trafficking and the control of cell migration. Traffic, 7, 14-21.

Certo, M., Del Gaizo Moore, V., Nishino, M., Wei, G., Korsmeyer, S., Armstrong, S. A. & Letai, A. 2006. Mitochondria primed by death signals determine cellular addiction to antiapoptotic BCL-2 family members. Cancer Cell, 9, 351-65.

Chang, T. C., Liu, C. C., Hsing, E. W., Liang, S. M., Chi, Y. H., Sung, L. Y., Lin, S. P., Shen, T. L., Ko, B. S., Yen, B. L., Yet, S. F., Wu, K. K. & Liou, J. Y. 2012. 14-3-3sigma

regulates beta-catenin-mediated mouse embryonic stem cell proliferation by sequestering GSK-3beta. PLoS One, 7, e40193.

Chaturvedi, A. K., Engels, E. A., Pfeiffer, R. M., Hernandez, B. Y., Xiao, W., Kim, E., Jiang, B., Goodman, M. T., Sibug-Saber, M., Cozen, W., Liu, L., Lynch, C. F., Wentzensen, N., Jordan, R. C., Altekruse, S., Anderson, W. F., Rosenberg, P. S. & Gillison, M. L. 2011. Human papillomavirus and rising oropharyngeal cancer incidence in the United States. J Clin Oncol, 29, 4294-301.

Chen, A. C., McMillan, N. A. & Antonsson, A. 2008. Human papillomavirus type spectrum in normal skin of individuals with or without a history of frequent sun exposure. J Gen Virol, 89, 2891-7.

Chinnaiyan, A. M., O'Rourke, K., Tewari, M. & Dixit, V. M. 1995. FADD, a novel death domain-containing protein, interacts with the death domain of Fas and initiates apoptosis. Cell, 81, 505-12.

Chipuk, J. E., Kuwana, T., Bouchier-Hayes, L., Droin, N. M., Newmeyer, D. D., Schuler, M. & Green, D. R. 2004. Direct activation of Bax by p53 mediates mitochondrial membrane permeabilization and apoptosis. Science, 303, 1010-4.

Chipuk, J. E., Moldoveanu, T., Llambi, F., Parsons, M. J. & Green, D. R. 2010. The BCL-2 family reunion. Mol Cell, 37, 299-310.

Chong-Kopera, H., Inoki, K., Li, Y., Zhu, T., Garcia-Gonzalo, F. R., Rosa, J. L. & Guan, K. L. 2006. TSC1 stabilizes TSC2 by inhibiting the interaction between TSC2 and the HERC1 ubiquitin ligase. J Biol Chem, 281, 8313-6.

Christian, P. A., Fiandalo, M. V. & Schwarze, S. R. 2011. Possible role of death receptor-mediated apoptosis by the E3 ubiquitin ligases Siah2 and POSH. Mol Cancer, 10, 57.

Ciechanover, A. & Ben-Saadon, R. 2004. N-terminal ubiquitination: more protein substrates join in. Trends Cell Biol, 14, 103-6.

Cleaver, J. E. 2000. Common pathways for ultraviolet skin carcinogenesis in the repair and replication defective groups of xeroderma pigmentosum. J Dermatol Sci, 23, 1-11.

Cleland, M. M., Norris, K. L., Karbowski, M., Wang, C., Suen, D. F., Jiao, S., George, N. M., Luo, X., Li, Z. & Youle, R. J. 2011. Bcl-2 family interaction with the mitochondrial morphogenesis machinery. Cell Death Differ, 18, 235-47.

Clifford, G. M., Polesel, J., Rickenbach, M., Dal Maso, L., Keiser, O., Kofler, A., Rapiti, E., Levi, F., Jundt, G., Fisch, T., Bordoni, A., De Weck, D. & Franceschi, S. 2005. Cancer risk in the Swiss HIV Cohort Study: associations with immunodeficiency, smoking, and highly active antiretroviral therapy. J Natl Cancer Inst, 97, 425-32.

Clifford, G. M., Smith, J. S., Aguado, T. & Franceschi, S. 2003. Comparison of HPV type distribution in high-grade cervical lesions and cervical cancer: a meta-analysis. Br J Cancer, 89, 101-5.

Cobrinik, D. 2005. Pocket proteins and cell cycle control. Oncogene, 24, 2796-809.

Cogliano, V., Baan, R., Straif, K., Grosse, Y., Secretan, B. & El Ghissassi, F. 2005. Carcinogenicity of human papillomaviruses. Lancet Oncol, 6, 204.

Cornet, I., Bouvard, V., Campo, M. S., Thomas, M., Banks, L., Gissmann, L., Lamartine, J., Sylla, B. S., Accardi, R. & Tommasino, M. 2012. Comparative analysis of

transforming properties of E6 and E7 from different beta human papillomavirus types. J Virol, 86, 2366-70.

Crish, J. F. & Eckert, R. L. 2008. Synergistic activation of human involucrin gene expression by Fra-1 and p300--evidence for the presence of a multiprotein complex. J Invest Dermatol, 128, 530-41.

CRUK. 2010. London, UK. Available: http://www.cancerresearchuk.org/cancer-info/cancerstats/types/cervix/incidence/uk-cervical-cancer-incidence-statistics [Accessed November 2012].

Culp, T. D., Budgeon, L. R. & Christensen, N. D. 2006. Human papillomaviruses bind a basal extracellular matrix component secreted by keratinocytes which is distinct from a membrane-associated receptor. Virology, 347, 147-59.

Dai, C. & Gu, W. 2010. p53 post-translational modification: deregulated in tumorigenesis. Trends Mol Med, 16, 528-36.

Davy, C. E., Ayub, M., Jackson, D. J., Das, P., McIntosh, P. & Doorbar, J. 2006. HPV16 E1--E4 protein is phosphorylated by Cdk2/cyclin A and relocalizes this complex to the cytoplasm. Virology, 349, 230-44.

Day, P. M., Lowy, D. R. & Schiller, J. T. 2003. Papillomaviruses infect cells via a clathrin-dependent pathway. Virology, 307, 1-11.

de Villiers, E. M., Fauquet, C., Broker, T. R., Bernard, H. U. & zur Hausen, H. 2004. Classification of papillomaviruses. Virology, 324, 17-27.

de Villiers, E. M., Lavergne, D., McLaren, K. & Benton, E. C. 1997. Prevailing papillomavirus types in non-melanoma carcinomas of the skin in renal allograft recipients. Int J Cancer, 73, 356-61.

DePry, J. L., Reed, K. B., Cook-Norris, R. H. & Brewer, J. D. 2011. Iatrogenic immunosuppression and cutaneous malignancy. Clin Dermatol, 29, 602-13.

Dewson, G., Kratina, T., Czabotar, P., Day, C. L., Adams, J. M. & Kluck, R. M. 2009. Bak activation for apoptosis involves oligomerization of dimers via their alpha6 helices. Mol Cell, 36, 696-703.

Dewson, G., Kratina, T., Sim, H. W., Puthalakath, H., Adams, J. M., Colman, P. M. & Kluck, R. M. 2008. To trigger apoptosis, Bak exposes its BH3 domain and homodimerizes via BH3:groove interactions. Mol Cell, 30, 369-80.

Dickson, M. A., Hahn, W. C., Ino, Y., Ronfard, V., Wu, J. Y., Weinberg, R. A., Louis, D. N., Li, F. P. & Rheinwald, J. G. 2000. Human keratinocytes that express hTERT and also bypass a p16(INK4a)-enforced mechanism that limits life span become immortal yet retain normal growth and differentiation characteristics. Mol Cell Biol, 20, 1436-47.

Dong, G., Broker, T. R. & Chow, L. T. 1994. Human papillomavirus type 11 E2 proteins repress the homologous E6 promoter by interfering with the binding of host transcription factors to adjacent elements. J Virol, 68, 1115-27.

Dong, W., Kloz, U., Accardi, R., Caldeira, S., Tong, W. M., Wang, Z. Q., Jansen, L., Durst, M., Sylla, B. S., Gissmann, L. & Tommasino, M. 2005. Skin hyperproliferation and susceptibility to chemical carcinogenesis in transgenic mice expressing E6 and E7 of human papillomavirus type 38. J Virol, 79, 14899-908.

Doorbar, J., Ely, S., Sterling, J., McLean, C. & Crawford, L. 1991. Specific interaction between HPV-16 E1-E4 and cytokeratins results in collapse of the epithelial cell intermediate filament network. Nature, 352, 824-7.

Doorbar, J., Quint, W., Banks, L., Bravo, I. G., Stoler, M., Broker, T. R. & Stanley, M. A. 2012. The biology and life-cycle of human papillomaviruses. Vaccine, 30 Suppl 5, F55-70.

Dostatni, N., Lambert, P. F., Sousa, R., Ham, J., Howley, P. M. & Yaniv, M. 1991. The functional BPV-1 E2 trans-activating protein can act as a repressor by preventing formation of the initiation complex. Genes Dev, 5, 1657-71.

Dowhanick, J. J., McBride, A. A. & Howley, P. M. 1995. Suppression of cellular proliferation by the papillomavirus E2 protein. J Virol, 69, 7791-9.

Dreyfuss, G., Matunis, M. J., Pinol-Roma, S. & Burd, C. G. 1993. hnRNP proteins and the biogenesis of mRNA. Annu Rev Biochem, 62, 289-321.

Du, J., Chen, G. G., Vlantis, A. C., Chan, P. K., Tsang, R. K. & van Hasselt, C. A. 2004. Resistance to apoptosis of HPV 16-infected laryngeal cancer cells is associated with decreased Bak and increased Bcl-2 expression. Cancer Lett, 205, 81-8.

Du, J., Chen, X., Liang, X., Zhang, G., Xu, J., He, L., Zhan, Q., Feng, X. Q., Chien, S. & Yang, C. 2011. Integrin activation and internalization on soft ECM as a mechanism of induction of stem cell differentiation by ECM elasticity. Proc Natl Acad Sci U S A, 108, 9466-71.

Dubois, T., Oudinet, J. P., Mira, J. P. & Russo-Marie, F. 1996. Annexins and protein kinases C. Biochim Biophys Acta, 1313, 290-4.

Duensing, S., Lee, L. Y., Duensing, A., Basile, J., Piboonniyom, S., Gonzalez, S., Crum, C. P. & Munger, K. 2000. The human papillomavirus type 16 E6 and E7 oncoproteins cooperate to induce mitotic defects and genomic instability by uncoupling centrosome duplication from the cell division cycle. Proc Natl Acad Sci U S A, 97, 10002-7.

Dumont, P., Leu, J. I., Della Pietra, A. C., 3rd, George, D. L. & Murphy, M. 2003. The codon 72 polymorphic variants of p53 have markedly different apoptotic potential. Nat Genet, 33, 357-65.

Dunkern, T. R., Fritz, G. & Kaina, B. 2001. Ultraviolet light-induced DNA damage triggers apoptosis in nucleotide excision repair-deficient cells via Bcl-2 decline and caspase-3/-8 activation. Oncogene, 20, 6026-38.

Edlich, F., Banerjee, S., Suzuki, M., Cleland, M. M., Arnoult, D., Wang, C., Neutzner, A., Tjandra, N. & Youle, R. J. 2011. Bcl-x(L) retrotranslocates Bax from the mitochondria into the cytosol. Cell, 145, 104-16.

Egawa, K. 2003. Do human papillomaviruses target epidermal stem cells? Dermatology, 207, 251-4.

Elbel, M., Carl, S., Spaderna, S. & Iftner, T. 1997. A comparative analysis of the interactions of the E6 proteins from cutaneous and genital papillomaviruses with p53 and E6AP in correlation to their transforming potential. Virology, 239, 132-49.

Elson, D. A., Riley, R. R., Lacey, A., Thordarson, G., Talamantes, F. J. & Arbeit, J. M. 2000. Sensitivity of the cervical transformation zone to estrogen-induced squamous carcinogenesis. Cancer Res, 60, 1267-75.

Elston, R. C., Napthine, S. & Doorbar, J. 1998. The identification of a conserved binding motif within human papillomavirus type 16 E6 binding peptides, E6AP and E6BP. J Gen Virol, 79 (Pt 2), 371-4.

Erster, S., Mihara, M., Kim, R. H., Petrenko, O. & Moll, U. M. 2004. In vivo mitochondrial p53 translocation triggers a rapid first wave of cell death in response to DNA damage that can precede p53 target gene activation. Mol Cell Biol, 24, 6728-41.

Evander, M., Frazer, I. H., Payne, E., Qi, Y. M., Hengst, K. & McMillan, N. A. 1997. Identification of the alpha6 integrin as a candidate receptor for papillomaviruses. J Virol, 71, 2449-56.

Ezratty, E. J., Bertaux, C., Marcantonio, E. E. & Gundersen, G. G. 2009. Clathrin mediates integrin endocytosis for focal adhesion disassembly in migrating cells. J Cell Biol, 187, 733-47.

Fabbri, M., Fumagalli, L., Bossi, G., Bianchi, E., Bender, J. R. & Pardi, R. 1999. A tyrosine-based sorting signal in the beta2 integrin cytoplasmic domain mediates its recycling to the plasma membrane and is required for ligand-supported migration. EMBO J, 18, 4915-25.

Fang, L., Budgeon, L. R., Doorbar, J., Briggs, E. R. & Howett, M. K. 2006. The human papillomavirus type 11 E1ΛE4 protein is not essential for viral genome amplification. Virology, 351, 271-9.

Fanning, A. S., Jameson, B. J., Jesaitis, L. A. & Anderson, J. M. 1998. The tight junction protein ZO-1 establishes a link between the transmembrane protein occludin and the actin cytoskeleton. J Biol Chem, 273, 29745-53.

Fehrmann, F., Klumpp, D. J. & Laimins, L. A. 2003. Human papillomavirus type 31 E5 protein supports cell cycle progression and activates late viral functions upon epithelial differentiation. J Virol, 77, 2819-31.

Feltkamp, M. C., Broer, R., di Summa, F. M., Struijk, L., van der Meijden, E., Verlaan, B. P., Westendorp, R. G., ter Schegget, J., Spaan, W. J. & Bouwes Bavinck, J. N. 2003. Seroreactivity to epidermodysplasia verruciformis-related human papillomavirus types is associated with nonmelanoma skin cancer. Cancer Res, 63, 2695-700.

Feng, H., Shuda, M., Chang, Y. & Moore, P. S. 2008. Clonal integration of a polyomavirus in human Merkel cell carcinoma. Science, 319, 1096-100.

Filippova, M., Parkhurst, L. & Duerksen-Hughes, P. J. 2004. The human papillomavirus 16 E6 protein binds to Fas-associated death domain and protects cells from Fas-triggered apoptosis. J Biol Chem, 279, 25729-44.

Fox, J., Azad, A., Ismail, F. & Storey, A. 2011. "Licensed to kill": tyrosine dephosphorylation and Bak activation. Cell Cycle, 10, 598-603.

Fox, J. L., Ismail, F., Azad, A., Ternette, N., Leverrier, S., Edelmann, M. J., Kessler, B. M., Leigh, I. M., Jackson, S. & Storey, A. 2010. Tyrosine dephosphorylation is required for Bak activation in apoptosis. EMBO J, 29, 3853-68.

Fradet-Turcotte, A., Bergeron-Labrecque, F., Moody, C. A., Lehoux, M., Laimins, L. A. & Archambault, J. 2011. Nuclear accumulation of the papillomavirus E1 helicase blocks S-phase progression and triggers an ATM-dependent DNA damage response. J Virol, 85, 8996-9012.

Francis, D. A., Schmid, S. I. & Howley, P. M. 2000. Repression of the integrated papillomavirus E6/E7 promoter is required for growth suppression of cervical cancer cells. J Virol, 74, 2679-86.

Frazer, I. H., Leggatt, G. R. & Mattarollo, S. R. 2011. Prevention and treatment of papillomavirus-related cancers through immunization. Annu Rev Immunol, 29, 111-38.

Fuchs, E. 1990. Epidermal differentiation: the bare essentials. J Cell Biol, 111, 2807-14.

Fuchs, E. & Raghavan, S. 2002. Getting under the skin of epidermal morphogenesis. Nat Rev Genet, 3, 199-209.

Furniss, C. S., McClean, M. D., Smith, J. F., Bryan, J., Nelson, H. H., Peters, E. S., Posner, M. R., Clark, J. R., Eisen, E. A. & Kelsey, K. T. 2007. Human papillomavirus 16 and head and neck squamous cell carcinoma. Int J Cancer, 120, 2386-92.

Gallenne, T., Gautier, F., Oliver, L., Hervouet, E., Noel, B., Hickman, J. A., Geneste, O., Cartron, P. F., Vallette, F. M., Manon, S. & Juin, P. 2009. Bax activation by the BH3-only protein Puma promotes cell dependence on antiapoptotic Bcl-2 family members. J Cell Biol, 185, 279-90.

Gardiol, D., Kuhne, C., Glaunsinger, B., Lee, S. S., Javier, R. & Banks, L. 1999. Oncogenic human papillomavirus E6 proteins target the discs large tumour suppressor for proteasome-mediated degradation. Oncogene, 18, 5487-96.

Garnett, T. O., Filippova, M. & Duerksen-Hughes, P. J. 2006. Accelerated degradation of FADD and procaspase 8 in cells expressing human papilloma virus 16 E6 impairs TRAIL-mediated apoptosis. Cell Death Differ, 13, 1915-26.

Garrison, J. B., Correa, R. G., Gerlic, M., Yip, K. W., Krieg, A., Tamble, C. M., Shi, R., Welsh, K., Duggineni, S., Huang, Z., Ren, K., Du, C. & Reed, J. C. 2011. ARTS and Siah collaborate in a pathway for XIAP degradation. Mol Cell, 41, 107-16.

Genther, S. M., Sterling, S., Duensing, S., Munger, K., Sattler, C. & Lambert, P. F. 2003. Quantitative role of the human papillomavirus type 16 E5 gene during the productive stage of the viral life cycle. J Virol, 77, 2832-42.

Genther Williams, S. M., Disbrow, G. L., Schlegel, R., Lee, D., Threadgill, D. W. & Lambert, P. F. 2005. Requirement of epidermal growth factor receptor for hyperplasia induced by E5, a high-risk human papillomavirus oncogene. Cancer Res, 65, 6534-42.

Giampieri, S. & Storey, A. 2004. Repair of UV-induced thymine dimers is compromised in cells expressing the E6 protein from human papillomaviruses types 5 and 18. Br J Cancer, 90, 2203-9.

Giglia-Mari, G. & Sarasin, A. 2003. TP53 mutations in human skin cancers. Hum Mutat, 21, 217-28.

Gil, J. & Peters, G. 2006. Regulation of the INK4b-ARF-INK4a tumour suppressor locus: all for one or one for all. Nat Rev Mol Cell Biol, 7, 667-77.

Gillespie, K. A., Mehta, K. P., Laimins, L. A. & Moody, C. A. 2012. Human papillomaviruses recruit cellular DNA repair and homologous recombination factors to viral replication centers. J Virol, 86, 9520-6.

Goldenthal, K. L., Hedman, K., Chen, J. W., August, J. T. & Willingham, M. C. 1985. Postfixation detergent treatment for immunofluorescence suppresses localization of some integral membrane proteins. J Histochem Cytochem, 33, 813-20.

Goldstein, J. C., Waterhouse, N. J., Juin, P., Evan, G. I. & Green, D. R. 2000. The coordinate release of cytochrome c during apoptosis is rapid, complete and kinetically invariant. Nat Cell Biol, 2, 156-62.

Gonzalez, S. L., Stremlau, M., He, X., Basile, J. R. & Munger, K. 2001. Degradation of the retinoblastoma tumor suppressor by the human papillomavirus type 16 E7 oncoprotein is important for functional inactivation and is separable from proteasomal degradation of E7. J Virol, 75, 7583-91.

Griffiths, G. J., Dubrez, L., Morgan, C. P., Jones, N. A., Whitehouse, J., Corfe, B. M., Dive, C. & Hickman, J. A. 1999. Cell damage-induced conformational changes of the pro-apoptotic protein Bak in vivo precede the onset of apoptosis. J Cell Biol, 144, 903-14.

Grm, H. S. & Banks, L. 2004. Degradation of hDlg and MAGIs by human papillomavirus E6 is E6-AP-independent. J Gen Virol, 85, 2815-9.

Gruener, M., Bravo, I. G., Momburg, F., Alonso, A. & Tomakidi, P. 2007. The E5 protein of the human papillomavirus type 16 down-regulates HLA-I surface expression in calnexin-expressing but not in calnexin-deficient cells. Virol J, 4, 116.

Gupton, S. L., Eisenmann, K., Alberts, A. S. & Waterman-Storer, C. M. 2007. mDia2 regulates actin and focal adhesion dynamics and organization in the lamella for efficient epithelial cell migration. J Cell Sci, 120, 3475-87.

Hagglund, R. & Roizman, B. 2002. Characterization of the novel E3 ubiquitin ligase encoded in exon 3 of herpes simplex virus-1-infected cell protein 0. Proc Natl Acad Sci U S A, 99, 7889-94.

Hagglund, R., Van Sant, C., Lopez, P. & Roizman, B. 2002. Herpes simplex virus 1-infected cell protein 0 contains two E3 ubiquitin ligase sites specific for different E2 ubiquitin-conjugating enzymes. Proc Natl Acad Sci U S A, 99, 631-6.

Halliday, G. M., Byrne, S. N. & Damian, D. L. 2011. Ultraviolet A radiation: its role in immunosuppression and carcinogenesis. Semin Cutan Med Surg, 30, 214-21.

Han, S. P., Tang, Y. H. & Smith, R. 2010. Functional diversity of the hnRNPs: past, present and perspectives. Biochem J, 430, 379-92.

Hanahan, D. & Weinberg, R. A. 2011. Hallmarks of cancer: the next generation. Cell, 144, 646-74.

Harburger, D. S. & Calderwood, D. A. 2009. Integrin signalling at a glance. J Cell Sci, 122, 159-63.

Hartevelt, M. M., Bavinck, J. N., Kootte, A. M., Vermeer, B. J. & Vandenbroucke, J. P. 1990. Incidence of skin cancer after renal transplantation in The Netherlands. Transplantation, 49, 506-9.

Harwood, C. A., McGregor, J. M., Proby, C. M. & Breuer, J. 1999. Human papillomavirus and the development of non-melanoma skin cancer. J Clin Pathol, 52, 249-53.

Harwood, C. A., Surentheran, T., McGregor, J. M., Spink, P. J., Leigh, I. M., Breuer, J. & Proby, C. M. 2000. Human papillomavirus infection and non-melanoma skin cancer in immunosuppressed and immunocompetent individuals. J Med Virol, 61, 289-97.

Haupt, Y., Rowan, S., Shaulian, E., Vousden, K. H. & Oren, M. 1995. Induction of apoptosis in HeLa cells by trans-activation-deficient p53. Genes Dev, 9, 2170-83.

He, W., Staples, D., Smith, C. & Fisher, C. 2003. Direct activation of cyclin-dependent kinase 2 by human papillomavirus E7. J Virol, 77, 10566-74.

Helt, A. M. & Galloway, D. A. 2003. Mechanisms by which DNA tumor virus oncoproteins target the Rb family of pocket proteins. Carcinogenesis, 24, 159-69.

Herber, R., Liem, A., Pitot, H. & Lambert, P. F. 1996. Squamous epithelial hyperplasia and carcinoma in mice transgenic for the human papillomavirus type 16 E7 oncogene. J Virol, 70, 1873-81.

Hicke, L. 2001. Protein regulation by monoubiquitin. Nat Rev Mol Cell Biol, 2, 195-201.

Hill, L. L., Ouhtit, A., Loughlin, S. M., Kripke, M. L., Ananthaswamy, H. N. & Owen-Schaub, L. B. 1999. Fas ligand: a sensor for DNA damage critical in skin cancer etiology. Science, 285, 898-900.

Ho, G. Y., Bierman, R., Beardsley, L., Chang, C. J. & Burk, R. D. 1998. Natural history of cervicovaginal papillomavirus infection in young women. N Engl J Med, 338, 423-8.

Hobbs, S., Jitrapakdee, S. & Wallace, J. C. 1998. Development of a bicistronic vector driven by the human polypeptide chain elongation factor 1alpha promoter for creation of stable mammalian cell lines that express very high levels of recombinant proteins. Biochem Biophys Res Commun, 252, 368-72.

Hoffman, W. H., Biade, S., Zilfou, J. T., Chen, J. & Murphy, M. 2002. Transcriptional repression of the anti-apoptotic survivin gene by wild type p53. J Biol Chem, 277, 3247-57.

Holick, M. F., MacLaughlin, J. A., Clark, M. B., Holick, S. A., Potts, J. T., Jr., Anderson, R. R., Blank, I. H., Parrish, J. A. & Elias, P. 1980. Photosynthesis of previtamin D3 in human skin and the physiologic consequences. Science, 210, 203-5.

Hopfl, R., Heim, K., Christensen, N., Zumbach, K., Wieland, U., Volgger, B., Widschwendter, A., Haimbuchner, S., Muller-Holzner, E., Pawlita, M., Pfister, H. & Fritsch, P. 2000. Spontaneous regression of CIN and delayed-type hypersensitivity to HPV-16 oncoprotein E7. Lancet, 356, 1985-6.

Hou, S. Y., Wu, S. Y. & Chiang, C. M. 2002. Transcriptional activity among high and low risk human papillomavirus E2 proteins correlates with E2 DNA binding. J Biol Chem, 277, 45619-29.

Housman, T. S., Feldman, S. R., Williford, P. M., Fleischer, A. B., Jr., Goldman, N. D., Acostamadiedo, J. M. & Chen, G. J. 2003. Skin cancer is among the most costly of all cancers to treat for the Medicare population. J Am Acad Dermatol, 48, 425-9.

Howie, H. L., Koop, J. I., Weese, J., Robinson, K., Wipf, G., Kim, L. & Galloway, D. A. 2011. Beta-HPV 5 and 8 E6 promote p300 degradation by blocking AKT/p300 association. PLoS Pathog, 7, e1002211.

Hsu, H., Xiong, J. & Goeddel, D. V. 1995. The TNF receptor 1-associated protein TRADD signals cell death and NF-kappa B activation. Cell, 81, 495-504.

Hu, B., Castillo, E., Harewood, L., Ostano, P., Reymond, A., Dummer, R., Raffoul, W., Hoetzenecker, W., Hofbauer, G. F. & Dotto, G. P. 2012. Multifocal epithelial tumors and field cancerization from loss of mesenchymal CSL signaling. Cell, 149, 1207-20.

Hu, L. & Ceresa, B. P. 2009. Characterization of the plasma membrane localization and orientation of HPV16 E5 for cell-cell fusion. Virology, 393, 135-43.

Hu, L., Potapova, T. A., Li, S., Rankin, S., Gorbsky, G. J., Angeletti, P. C. & Ceresa, B. P. 2010. Expression of HPV16 E5 produces enlarged nuclei and polyploidy through endoreplication. Virology, 405, 342-51.

Hughes, F. J. & Romanos, M. A. 1993. E1 protein of human papillomavirus is a DNA helicase/ATPase. Nucleic Acids Res, 21, 5817-23.

Huh, K., Zhou, X., Hayakawa, H., Cho, J. Y., Libermann, T. A., Jin, J., Harper, J. W. & Munger, K. 2007. Human papillomavirus type 16 E7 oncoprotein associates with the cullin 2 ubiquitin ligase complex, which contributes to degradation of the retinoblastoma tumor suppressor. J Virol, 81, 9737-47.

Huibregtse, J. M., Scheffner, M., Beaudenon, S. & Howley, P. M. 1995. A family of proteins structurally and functionally related to the E6-AP ubiquitin-protein ligase. Proc Natl Acad Sci U S A, 92, 5249.

Huibregtse, J. M., Scheffner, M. & Howley, P. M. 1991. A cellular protein mediates association of p53 with the E6 oncoprotein of human papillomavirus types 16 or 18. EMBO J, 10, 4129-35.

Huibregtse, J. M., Scheffner, M. & Howley, P. M. 1993a. Cloning and expression of the cDNA for E6-AP, a protein that mediates the interaction of the human papillomavirus E6 oncoprotein with p53. Mol Cell Biol, 13, 775-84.

Huibregtse, J. M., Scheffner, M. & Howley, P. M. 1993b. Localization of the E6-AP regions that direct human papillomavirus E6 binding, association with p53, and ubiquitination of associated proteins. Mol Cell Biol, 13, 4918-27.

Huttenlocher, A. & Horwitz, A. R. 2011. Integrins in cell migration. Cold Spring Harb Perspect Biol, 3, a005074.

Iannacone, M. R., Wang, W., Stockwell, H. G., O'Rourke, K., Giuliano, A. R., Sondak, V. K., Messina, J. L., Roetzheim, R. G., Cherpelis, B. S., Fenske, N. A., Michael, K. M., Waterboer, T., Pawlita, M. & Rollison, D. E. 2012. Sunlight exposure and cutaneous human papillomavirus seroreactivity in basal cell and squamous cell carcinomas of the skin. J Infect Dis, 206, 399-406.

Iftner, A., Klug, S. J., Garbe, C., Blum, A., Stancu, A., Wilczynski, S. P. & Iftner, T. 2003. The prevalence of human papillomavirus genotypes in nonmelanoma skin cancers of nonimmunosuppressed individuals identifies high-risk genital types as possible risk factors. Cancer Res, 63, 7515-9.

Iftner, T., Elbel, M., Schopp, B., Hiller, T., Loizou, J. I., Caldecott, K. W. & Stubenrauch, F. 2002. Interference of papillomavirus E6 protein with single-strand break repair by interaction with XRCC1. EMBO J, 21, 4741-8.

Iftner, T., Fuchs, P. G. & Pfister, H. 1989. Two independently transforming functions of human papillomavirus 8. Curr Top Microbiol Immunol, 144, 167-73.

Iftner, T., Iftner, A., Buttner, P., Harrison, S., Glasby, M., Raasch, B. & Garbe, C. 2009. Human Papillomavirus in Basal Cel Carcinoma - A Pilot Study. Journal of Rural and Tropical Public Health, 8, 42-44.

Ilic, D., Furuta, Y., Kanazawa, S., Takeda, N., Sobue, K., Nakatsuji, N., Nomura, S., Fujimoto, J., Okada, M. & Yamamoto, T. 1995. Reduced cell motility and enhanced focal adhesion contact formation in cells from FAK-deficient mice. Nature, 377, 539-44.

Jackson, S., Ghali, L., Harwood, C. & Storey, A. 2002. Reduced apoptotic levels in squamous but not basal cell carcinomas correlates with detection of cutaneous human papillomavirus. Br J Cancer, 87, 319-23.

Jackson, S., Harwood, C., Thomas, M., Banks, L. & Storey, A. 2000. Role of Bak in UV-induced apoptosis in skin cancer and abrogation by HPV E6 proteins. Genes Dev, 14, 3065-73.

Jackson, S. & Storey, A. 2000. E6 proteins from diverse cutaneous HPV types inhibit apoptosis in response to UV damage. Oncogene, 19, 592-8.

Jariel-Encontre, I., Bossis, G. & Piechaczyk, M. 2008. Ubiquitin-independent degradation of proteins by the proteasome. Biochim Biophys Acta, 1786, 153-77.

Jayaprakash, V., Reid, M., Hatton, E., Merzianu, M., Rigual, N., Marshall, J., Gill, S., Frustino, J., Wilding, G., Loree, T., Popat, S. & Sullivan, M. 2011. Human papillomavirus types 16 and 18 in epithelial dysplasia of oral cavity and oropharynx: a meta-analysis, 1985-2010. Oral Oncol, 47, 1048-54.

Jesenberger, V. & Jentsch, S. 2002. Deadly encounter: ubiquitin meets apoptosis. Nat Rev Mol Cell Biol, 3, 112-21.

Jha, S., Vande Pol, S., Banerjee, N. S., Dutta, A. B., Chow, L. T. & Dutta, A. 2010. Destabilization of TIP60 by human papillomavirus E6 results in attenuation of TIP60-dependent transcriptional regulation and apoptotic pathway. Mol Cell, 38, 700-11.

Jiang, P., Du, W., Heese, K. & Wu, M. 2006. The Bad guy cooperates with good cop p53: Bad is transcriptionally up-regulated by p53 and forms a Bad/p53 complex at the mitochondria to induce apoptosis. Mol Cell Biol, 26, 9071-82.

Jiang, W., Ananthaswamy, H. N., Muller, H. K. & Kripke, M. L. 1999. p53 protects against skin cancer induction by UV-B radiation. Oncogene, 18, 4247-53.

Jimenez, G. S., Nister, M., Stommel, J. M., Beeche, M., Barcarse, E. A., Zhang, X. Q., O'Gorman, S. & Wahl, G. M. 2000. A transactivation-deficient mouse model provides insights into Trp53 regulation and function. Nat Genet, 26, 37-43.

Johnson, B. N., Berger, A. K., Cortese, G. P. & Lavoie, M. J. 2012. The ubiquitin E3 ligase parkin regulates the proapoptotic function of Bax. Proc Natl Acad Sci U S A, 109, 6283-8.

Jonason, A. S., Kunala, S., Price, G. J., Restifo, R. J., Spinelli, H. M., Persing, J. A., Leffell, D. J., Tarone, R. E. & Brash, D. E. 1996. Frequent clones of p53-mutated keratinocytes in normal human skin. Proc Natl Acad Sci U S A, 93, 14025-9.

Jones, D. L., Alani, R. M. & Munger, K. 1997. The human papillomavirus E7 oncoprotein can uncouple cellular differentiation and proliferation in human keratinocytes by abrogating p21Cip1-mediated inhibition of cdk2. Genes Dev, 11, 2101-11.

Jones, P. H., Harper, S. & Watt, F. M. 1995. Stem cell patterning and fate in human epidermis. Cell, 80, 83-93.

Jones, P. H. & Watt, F. M. 1993. Separation of human epidermal stem cells from transit amplifying cells on the basis of differences in integrin function and expression. Cell, 73, 713-24.

Joyce, J. G., Tung, J. S., Przysiecki, C. T., Cook, J. C., Lehman, E. D., Sands, J. A., Jansen, K. U. & Keller, P. M. 1999. The L1 major capsid protein of human papillomavirus type 11 recombinant virus-like particles interacts with heparin and cell-surface glycosaminoglycans on human keratinocytes. J Biol Chem, 274, 5810-22.

Kabsch, K. & Alonso, A. 2002. The human papillomavirus type 16 E5 protein impairs TRAIL- and FasL-mediated apoptosis in HaCaT cells by different mechanisms. J Virol, 76, 12162-72.

Kadaja, M., Isok-Paas, H., Laos, T., Ustav, E. & Ustav, M. 2009. Mechanism of genomic instability in cells infected with the high-risk human papillomaviruses. PLoS Pathog, 5, e1000397.

Kadish, A. S., Timmins, P., Wang, Y., Ho, G. Y., Burk, R. D., Ketz, J., He, W., Romney, S. L., Johnson, A., Angeletti, R. & Abadi, M. 2002. Regression of cervical intraepithelial neoplasia and loss of human papillomavirus (HPV) infection is associated with cell-mediated immune responses to an HPV type 16 E7 peptide. Cancer Epidemiol Biomarkers Prev, 11, 483-8.

Kamper, N., Day, P. M., Nowak, T., Selinka, H. C., Florin, L., Bolscher, J., Hilbig, L., Schiller, J. T. & Sapp, M. 2006. A membrane-destabilizing peptide in capsid protein L2 is required for egress of papillomavirus genomes from endosomes. J Virol, 80, 759-68.

Kannan, K., Kaminski, N., Rechavi, G., Jakob-Hirsch, J., Amariglio, N. & Givol, D. 2001. DNA microarray analysis of genes involved in p53 mediated apoptosis: activation of Apaf-1. Oncogene, 20, 3449-55.

Kao, W. H., Beaudenon, S. L., Talis, A. L., Huibregtse, J. M. & Howley, P. M. 2000. Human papillomavirus type 16 E6 induces self-ubiquitination of the E6AP ubiquitin-protein ligase. J Virol, 74, 6408-17.

Karagas, M. R., Nelson, H. H., Sehr, P., Waterboer, T., Stukel, T. A., Andrew, A., Green, A. C., Bavinck, J. N., Perry, A., Spencer, S., Rees, J. R., Mott, L. A. & Pawlita, M. 2006. Human papillomavirus infection and incidence of squamous cell and basal cell carcinomas of the skin. J Natl Cancer Inst, 98, 389-95.

Karagas, M. R., Stukel, T. A., Greenberg, E. R., Baron, J. A., Mott, L. A. & Stern, R. S. 1992. Risk of subsequent basal cell carcinoma and squamous cell carcinoma of the skin among patients with prior skin cancer. Skin Cancer Prevention Study Group. JAMA, 267, 3305-10.

Karbowski, M., Norris, K. L., Cleland, M. M., Jeong, S. Y. & Youle, R. J. 2006. Role of Bax and Bak in mitochondrial morphogenesis. Nature, 443, 658-62.

Kerr, J. F., Wyllie, A. H. & Currie, A. R. 1972. Apoptosis: a basic biological phenomenon with wide-ranging implications in tissue kinetics. Br J Cancer, 26, 239-57.

Kim, H., Rafiuddin-Shah, M., Tu, H. C., Jeffers, J. R., Zambetti, G. P., Hsieh, J. J. & Cheng, E. H. 2006. Hierarchical regulation of mitochondrion-dependent apoptosis by BCL-2 subfamilies. Nat Cell Biol, 8, 1348-58.

Kim, H., Tu, H. C., Ren, D., Takeuchi, O., Jeffers, J. R., Zambetti, G. P., Hsieh, J. J. & Cheng, E. H. 2009. Stepwise activation of BAX and BAK by tBID, BIM, and PUMA initiates mitochondrial apoptosis. Mol Cell, 36, 487-99.

Kim, K., Garner-Hamrick, P. A., Fisher, C., Lee, D. & Lambert, P. F. 2003. Methylation patterns of papillomavirus DNA, its influence on E2 function, and implications in viral infection. J Virol, 77, 12450-9.

Kim, S. H., Kim, K. S., Lee, E. J., Kim, M. O., Park, J. H., Cho, K. I., Imakawa, K., Hyun, B. H., Chang, K. T., Lee, H. T. & Ryoo, Z. Y. 2004. Human keratin 14 driven HPV 16 E6/E7 transgenic mice exhibit hyperkeratinosis. Life Sci, 75, 3035-42.

Kines, R. C., Thompson, C. D., Lowy, D. R., Schiller, J. T. & Day, P. M. 2009. The initial steps leading to papillomavirus infection occur on the basement membrane prior to cell surface binding. Proc Natl Acad Sci U S A, 106, 20458-63.

Kirnbauer, R., Booy, F., Cheng, N., Lowy, D. R. & Schiller, J. T. 1992. Papillomavirus L1 major capsid protein self-assembles into virus-like particles that are highly immunogenic. Proc Natl Acad Sci U S A, 89, 12180-4.

Kischkel, F. C., Hellbardt, S., Behrmann, I., Germer, M., Pawlita, M., Krammer, P. H. & Peter, M. E. 1995. Cytotoxicity-dependent APO-1 (Fas/CD95)-associated proteins form a death-inducing signaling complex (DISC) with the receptor. EMBO J, 14, 5579-88.

Kishino, T., Lalande, M. & Wagstaff, J. 1997. UBE3A/E6-AP mutations cause Angelman syndrome. Nat Genet, 15, 70-3.

Kisselev, A. & Goldberg, A. 2001. Proteasome inhibitors: from research tools to drug candidates. Chemistry & Biology, 8, 739-758.

Kiyono, T., Foster, S. A., Koop, J. I., McDougall, J. K., Galloway, D. A. & Klingelhutz, A. J. 1998. Both Rb/p16INK4a inactivation and telomerase activity are required to immortalize human epithelial cells. Nature, 396, 84-8.

Klingelhutz, A. J., Foster, S. A. & McDougall, J. K. 1996. Telomerase activation by the E6 gene product of human papillomavirus type 16. Nature, 380, 79-82.

Klingelhutz, A. J. & Roman, A. 2012. Cellular transformation by human papillomaviruses: lessons learned by comparing high- and low-risk viruses. Virology, 424, 77-98.

Knight, G. L., Pugh, A. G., Yates, E., Bell, I., Wilson, R., Moody, C. A., Laimins, L. A. & Roberts, S. 2011. A cyclin-binding motif in human papillomavirus type 18 (HPV18) E1^E4 is necessary for association with CDK-cyclin complexes and G2/M cell cycle arrest of keratinocytes, but is not required for differentiation-dependent viral genome amplification or L1 capsid protein expression. Virology, 412, 196-210.

Kovach, B. T. & Stasko, T. 2009. Skin cancer after transplantation. Transplant Rev (Orlando), 23, 178-89.

Kraemer, K. H. 1997. Sunlight and skin cancer: another link revealed. Proc Natl Acad Sci U S A, 94, 11-4.

Krajewski, S., Krajewska, M. & Reed, J. C. 1996. Immunohistochemical analysis of in vivo patterns of Bak expression, a proapoptotic member of the Bcl-2 protein family. Cancer Res, 56, 2849-55.

Krajewski, S., Krajewska, M., Shabaik, A., Miyashita, T., Wang, H. G. & Reed, J. C. 1994. Immunohistochemical determination of in vivo distribution of Bax, a dominant inhibitor of Bcl-2. Am J Pathol, 145, 1323-36.

Kranjec, C. & Banks, L. 2010. A systematic analysis of HPV E6 PDZ substrates identifies MAGI-1 as a major target of HPV-16 and HPV-18 whose loss accompanies disruption of Tight Junctions. J Virol.

Kravtsova-Ivantsiv, Y. & Ciechanover, A. 2012. Non-canonical ubiquitin-based signals for proteasomal degradation. J Cell Sci, 125, 539-48.

Kroemer, G., Galluzzi, L., Vandenabeele, P., Abrams, J., Alnemri, E. S., Baehrecke, E. H., Blagosklonny, M. V., El-Deiry, W. S., Golstein, P., Green, D. R., Hengartner, M., Knight, R. A., Kumar, S., Lipton, S. A., Malorni, W., Nunez, G., Peter, M. E., Tschopp, J., Yuan, J., Piacentini, M., Zhivotovsky, B. & Melino, G. 2009. Classification of cell death: recommendations of the Nomenclature Committee on Cell Death 2009. Cell Death Differ, 16, 3-11.

Kuballa, P., Matentzoglu, K. & Scheffner, M. 2007. The role of the ubiquitin ligase E6-AP in human papillomavirus E6-mediated degradation of PDZ domain-containing proteins. J Biol Chem, 282, 65-71.

Kuhne, C. & Banks, L. 1998. E3-ubiquitin ligase/E6-AP links multicopy maintenance protein 7 to the ubiquitination pathway by a novel motif, the L2G box. J Biol Chem, 273, 34302-9.

Kuhnle, S., Kogel, U., Glockzin, S., Marquardt, A., Ciechanover, A., Matentzoglu, K. & Scheffner, M. 2011. Physical and functional interaction of the HECT ubiquitin-protein ligases E6AP and HERC2. J Biol Chem, 286, 19410-6.

Kulms, D., Poppelmann, B., Yarosh, D., Luger, T. A., Krutmann, J. & Schwarz, T. 1999. Nuclear and cell membrane effects contribute independently to the induction of apoptosis in human cells exposed to UVB radiation. Proc Natl Acad Sci U S A, 96, 7974-9.

Kuo, S. R., Liu, J. S., Broker, T. R. & Chow, L. T. 1994. Cell-free replication of the human papillomavirus DNA with homologous viral E1 and E2 proteins and human cell extracts. J Biol Chem, 269, 24058-65.

Kurasawa, M., Maeda, T., Oba, A., Yamamoto, T. & Sasaki, H. 2011. Tight junction regulates epidermal calcium ion gradient and differentiation. Biochem Biophys Res Commun, 406, 506-11.

Lalier, L., Cartron, P. F., Juin, P., Nedelkina, S., Manon, S., Bechinger, B. & Vallette, F. M. 2007. Bax activation and mitochondrial insertion during apoptosis. Apoptosis, 12, 887-96.

Lane, D. P. 1992. Cancer. p53, guardian of the genome. Nature, 358, 15-6.

Lazarczyk, M., Pons, C., Mendoza, J. A., Cassonnet, P., Jacob, Y. & Favre, M. 2008. Regulation of cellular zinc balance as a potential mechanism of EVER-mediated protection against pathogenesis by cutaneous oncogenic human papillomaviruses. J Exp Med, 205, 35-42.

Lazarou, M., Stojanovski, D., Frazier, A. E., Kotevski, A., Dewson, G., Craigen, W. J., Kluck, R. M., Vaux, D. L. & Ryan, M. T. 2010. Inhibition of Bak activation by VDAC2 is dependent on the Bak transmembrane anchor. J Biol Chem, 285, 36876-83.

Lazic, D., Hufbauer, M., Zigrino, P., Buchholz, S., Kazem, S., Feltkamp, M. C., Mauch, C., Steger, G., Pfister, H. & Akgul, B. 2012. Human papillomavirus type 8 e6 oncoprotein inhibits transcription of the PDZ protein syntenin-2. J Virol, 86, 7943-52.

Lee, C. & Laimins, L. A. 2004. Role of the PDZ domain-binding motif of the oncoprotein E6 in the pathogenesis of human papillomavirus type 31. J Virol, 78, 12366-77.

Lee, D., Lee, B., Kim, J., Kim, D. W. & Choe, J. 2000a. cAMP response element-binding protein-binding protein binds to human papillomavirus E2 protein and activates E2-dependent transcription. J Biol Chem, 275, 7045-51.

Lee, J. T. & Gu, W. 2010. The multiple levels of regulation by p53 ubiquitination. Cell Death Differ, 17, 86-92.

Lee, S. S., Glaunsinger, B., Mantovani, F., Banks, L. & Javier, R. T. 2000b. Multi-PDZ domain protein MUPP1 is a cellular target for both adenovirus E4-ORF1 and high-risk papillomavirus type 18 E6 oncoproteins. J Virol, 74, 9680-93.

Lee, S. W., Seong, M. W., Jeon, Y. J. & Chung, C. H. 2012. Ubiquitin E3 ligases controlling p53 stability. Animal Cells and Systems, 16, 173-182.

Leechanachai, P., Banks, L., Moreau, F. & Matlashewski, G. 1992. The E5 gene from human papillomavirus type 16 is an oncogene which enhances growth factor-mediated signal transduction to the nucleus. Oncogene, 7, 19-25.

Lessene, G., Czabotar, P. E. & Colman, P. M. 2008. BCL-2 family antagonists for cancer therapy. Nat Rev Drug Discov, 7, 989-1000.

Letai, A., Bassik, M. C., Walensky, L. D., Sorcinelli, M. D., Weiler, S. & Korsmeyer, S. J. 2002. Distinct BH3 domains either sensitize or activate mitochondrial apoptosis, serving as prototype cancer therapeutics. Cancer Cell, 2, 183-92.

Leu, J. I., Dumont, P., Hafey, M., Murphy, M. E. & George, D. L. 2004. Mitochondrial p53 activates Bak and causes disruption of a Bak-Mcl1 complex. Nat Cell Biol, 6, 443-50.

Leverrier, S., Bergamaschi, D., Ghali, L., Ola, A., Warnes, G., Akgul, B., Blight, K., Garcia-Escudero, R., Penna, A., Eddaoudi, A. & Storey, A. 2007. Role of HPV E6 proteins in preventing UVB-induced release of pro-apoptotic factors from the mitochondria. Apoptosis, 12, 549-60.

Levy, L., Broad, S., Diekmann, D., Evans, R. D. & Watt, F. M. 2000. beta1 integrins regulate keratinocyte adhesion and differentiation by distinct mechanisms. Mol Biol Cell, 11, 453-66.

Li, J., Uchida, T., Todo, T. & Kitagawa, T. 2006. Similarities and differences between cyclobutane pyrimidine dimer photolyase and (6-4) photolyase as revealed by resonance Raman spectroscopy: Electron transfer from the FAD cofactor to ultraviolet-damaged DNA. J Biol Chem, 281, 25551-9.

Li, M., Brooks, C. L., Wu-Baer, F., Chen, D., Baer, R. & Gu, W. 2003. Mono- versus polyubiquitination: differential control of p53 fate by Mdm2. Science, 302, 1972-5.

Li, W., Bengtson, M. H., Ulbrich, A., Matsuda, A., Reddy, V. A., Orth, A., Chanda, S. K., Batalov, S. & Joazeiro, C. A. 2008. Genome-wide and functional annotation of human E3 ubiquitin ligases identifies MULAN, a mitochondrial E3 that regulates the organelle's dynamics and signaling. PLoS One, 3, e1487.

Li, X. & Coffino, P. 1996. High-risk human papillomavirus E6 protein has two distinct binding sites within p53, of which only one determines degradation. J Virol, 70, 4509-16.

Li, Z., Jing-Yuan & Zhang, J.-T. 2009. 14-3-3σ, the double-edged sword of human cancers. American Journal of Translational Research, 1, 326-340.

Lippens, S., Denecker, G., Ovaere, P., Vandenabeele, P. & Declercq, W. 2005. Death penalty for keratinocytes: apoptosis versus cornification. Cell Death Differ, 12 Suppl 2, 1497-508.

Llambi, F., Moldoveanu, T., Tait, S. W., Bouchier-Hayes, L., Temirov, J., McCormick, L. L., Dillon, C. P. & Green, D. R. 2011. A unified model of mammalian BCL-2 protein family interactions at the mitochondria. Mol Cell, 44, 517-31.

Longworth, M. S., Wilson, R. & Laimins, L. A. 2005. HPV31 E7 facilitates replication by activating E2F2 transcription through its interaction with HDACs. EMBO J, 24, 1821-30.

Luo, X., Budihardjo, I., Zou, H., Slaughter, C. & Wang, X. 1998. Bid, a Bcl2 interacting protein, mediates cytochrome c release from mitochondria in response to activation of cell surface death receptors. Cell, 94, 481-90.

Lustbader, E. D., Williams, W. R., Bondy, M. L., Strom, S. & Strong, L. C. 1992. Segregation analysis of cancer in families of childhood soft-tissue-sarcoma patients. Am J Hum Genet, 51, 344-56.

Ma, T., Zou, N., Lin, B. Y., Chow, L. T. & Harper, J. W. 1999. Interaction between cyclin-dependent kinases and human papillomavirus replication-initiation protein E1 is required for efficient viral replication. Proc Natl Acad Sci U S A, 96, 382-7.

MacLachlan, T. K. & El-Deiry, W. S. 2002. Apoptotic threshold is lowered by p53 transactivation of caspase-6. Proc Natl Acad Sci U S A, 99, 9492-7.

Maecker, H. L., Koumenis, C. & Giaccia, A. J. 2000. p53 promotes selection for Fas-mediated apoptotic resistance. Cancer Res, 60, 4638-44.

Magal, S. S., Jackman, A., Ish-Shalom, S., Botzer, L. E., Gonen, P., Schlegel, R. & Sherman, L. 2005. Downregulation of Bax mRNA expression and protein stability by the E6 protein of human papillomavirus 16. J Gen Virol, 86, 611-21.

Maiuri, M. C., Zalckvar, E., Kimchi, A. & Kroemer, G. 2007. Self-eating and self-killing: crosstalk between autophagy and apoptosis. Nat Rev Mol Cell Biol, 8, 741-52.

Majewski, S. & Jablonska, S. 1995. Epidermodysplasia verruciformis as a model of human papillomavirus-induced genetic cancer of the skin. Arch Dermatol, 131, 1312-8.

Mandel, I., Paperna, T. & Miller, A. 2012. Aberrant expression of the apoptosis-related proteins BAK and MCL1 in T cells in multiple sclerosis. J Neuroimmunol, 244, 51-6.

Mandicourt, G., Iden, S., Ebnet, K., Aurrand-Lions, M. & Imhof, B. A. 2007. JAM-C regulates tight junctions and integrin-mediated cell adhesion and migration. J Biol Chem, 282, 1830-7.

Marcil, I. & Stern, R. S. 2000. Risk of developing a subsequent nonmelanoma skin cancer in patients with a history of nonmelanoma skin cancer: a critical review of the literature and meta-analysis. Arch Dermatol, 136, 1524-30.

Marcuzzi, G. P., Hufbauer, M., Kasper, H. U., Weissenborn, S. J., Smola, S. & Pfister, H. 2009. Spontaneous tumour development in human papillomavirus type 8 E6 transgenic mice and rapid induction by UV-light exposure and wounding. J Gen Virol, 90, 2855-64.

Margadant, C., Charafeddine, R. A. & Sonnenberg, A. 2010. Unique and redundant functions of integrins in the epidermis. FASEB J, 24, 4133-52.

Martinez-Noel, G., Galligan, J. T., Sowa, M. E., Arndt, V., Overton, T. M., Harper, J. W. & Howley, P. M. 2012. Identification and proteomic analysis of distinct UBE3A/E6AP protein complexes. Mol Cell Biol, 32, 3095-106.

Mashimo, T., Hadjebi, O., Amair-Pinedo, F., Tsurumi, T., Langa, F., Serikawa, T., Sotelo, C., Guenet, J. L. & Rosa, J. L. 2009. Progressive Purkinje cell degeneration in tambaleante mutant mice is a consequence of a missense mutation in HERC1 E3 ubiquitin ligase. PLoS Genet, 5, e1000784.

Masini, C., Fuchs, P. G., Gabrielli, F., Stark, S., Sera, F., Ploner, M., Melchi, C. F., Primavera, G., Pirchio, G., Picconi, O., Petasecca, P., Cattaruzza, M. S., Pfister, H. J. & Abeni, D. 2003. Evidence for the association of human papillomavirus infection and cutaneous squamous cell carcinoma in immunocompetent individuals. Arch Dermatol, 139, 890-4.

Massimi, P., Gammoh, N., Thomas, M. & Banks, L. 2004. HPV E6 specifically targets different cellular pools of its PDZ domain-containing tumour suppressor substrates for proteasome-mediated degradation. Oncogene, 23, 8033-9.

Massimi, P., Shai, A., Lambert, P. & Banks, L. 2008. HPV E6 degradation of p53 and PDZ containing substrates in an E6AP null background. Oncogene, 27, 1800-4.

Masson, M., Hindelang, C., Sibler, A. P., Schwalbach, G., Trave, G. & Weiss, E. 2003. Preferential nuclear localization of the human papillomavirus type 16 E6 oncoprotein in cervical carcinoma cells. J Gen Virol, 84, 2099-104.

McCormack, S. J., Brazinski, S. E., Moore, J. L., Jr., Werness, B. A. & Goldstein, D. J. 1997. Activation of the focal adhesion kinase signal transduction pathway in cervical carcinoma cell lines and human genital epithelial cells immortalized with human papillomavirus type 18. Oncogene, 15, 265-74.

McIntosh, P. B., Laskey, P., Sullivan, K., Davy, C., Wang, Q., Jackson, D. J., Griffin, H. M. & Doorbar, J. 2010. E1--E4-mediated keratin phosphorylation and ubiquitylation: a mechanism for keratin depletion in HPV16-infected epithelium. J Cell Sci, 123, 2810-22.

McIntyre, M. C., Ruesch, M. N. & Laimins, L. A. 1996. Human papillomavirus E7 oncoproteins bind a single form of cyclin E in a complex with cdk2 and p107. Virology, 215, 73-82.

McLaughlin-Drubin, M. E. & Munger, K. 2009. Oncogenic activities of human papillomaviruses. Virus Res, 143, 195-208.

Melendy, T., Sedman, J. & Stenlund, A. 1995. Cellular factors required for papillomavirus DNA replication. J Virol, 69, 7857-67.

Menkel, A. R., Kroemker, M., Bubeck, P., Ronsiek, M., Nikolai, G. & Jockusch, B. M. 1994. Characterization of an F-actin-binding domain in the cytoskeletal protein vinculin. J Cell Biol, 126, 1231-40.

Mihara, M., Erster, S., Zaika, A., Petrenko, O., Chittenden, T., Pancoska, P. & Moll, U. M. 2003. p53 has a direct apoptogenic role at the mitochondria. Mol Cell, 11, 577-90.

Mitra, R. S., Wrone-Smith, T., Simonian, P., Foreman, K. E., Nunez, G. & Nickoloff, B. J. 1997. Apoptosis in keratinocytes is not dependent on induction of differentiation. Lab Invest, 76, 99-107.

Mitra, S. K., Hanson, D. A. & Schlaepfer, D. D. 2005. Focal adhesion kinase: in command and control of cell motility. Nat Rev Mol Cell Biol, 6, 56-68.

Miyashita, T., Krajewski, S., Krajewska, M., Wang, H. G., Lin, H. K., Liebermann, D. A., Hoffman, B. & Reed, J. C. 1994. Tumor suppressor p53 is a regulator of bcl-2 and bax gene expression in vitro and in vivo. Oncogene, 9, 1799-805.

Modis, Y., Trus, B. L. & Harrison, S. C. 2002. Atomic model of the papillomavirus capsid. EMBO J, 21, 4754-62.

Moll, U. M., Erster, S. & Zaika, A. 2001. p53, p63 and p73--solos, alliances and feuds among family members. Biochim Biophys Acta, 1552, 47-59.

Moloney, F. J., Comber, H., O'Lorcain, P., O'Kelly, P., Conlon, P. J. & Murphy, G. M. 2006. A population-based study of skin cancer incidence and prevalence in renal transplant recipients. Br J Dermatol, 154, 498-504.

Moody, C. A. & Laimins, L. A. 2009. Human papillomaviruses activate the ATM DNA damage pathway for viral genome amplification upon differentiation. PLoS Pathog, 5, e1000605.

Moody, C. A. & Laimins, L. A. 2010. Human papillomavirus oncoproteins: pathways to transformation. Nat Rev Cancer, 10, 550-60.

Morandell, D., Kaiser, A., Herold, S., Rostek, U., Lechner, S., Mitterberger, M. C., Jansen-Durr, P., Eilers, M. & Zwerschke, W. 2012. The human papillomavirus type 16 E7 oncoprotein targets Myc-interacting zinc-finger protein-1. Virology, 422, 242-53.

Morris, S., Cox, B. & Bosanquet, N. 2009. Cost of skin cancer in England. Eur J Health Econ, 10, 267-73.

Moscicki, A. B., Ma, Y., Wibbelsman, C., Darragh, T. M., Powers, A., Farhat, S. & Shiboski, S. 2010. Rate of and risks for regression of cervical intraepithelial neoplasia 2 in adolescents and young women. Obstet Gynecol, 116, 1373-80.

Muench, P., Hiller, T., Probst, S., Florea, A. M., Stubenrauch, F. & Iftner, T. 2009. Binding of PDZ proteins to HPV E6 proteins does neither correlate with epidemiological risk classification nor with the immortalization of foreskin keratinocytes. Virology, 387, 380-7.

Muench, P., Probst, S., Schuetz, J., Leiprecht, N., Busch, M., Wesselborg, S., Stubenrauch, F. & Iftner, T. 2010. Cutaneous papillomavirus E6 proteins must interact with p300 and block p53-mediated apoptosis for cellular immortalization and tumorigenesis. Cancer Res, 70, 6913-24.

Munger, K., Phelps, W. C., Bubb, V., Howley, P. M. & Schlegel, R. 1989. The E6 and E7 genes of the human papillomavirus type 16 together are necessary and sufficient for transformation of primary human keratinocytes. J Virol, 63, 4417-21.

Munger, K., Yee, C. L., Phelps, W. C., Pietenpol, J. A., Moses, H. L. & Howley, P. M. 1991. Biochemical and biological differences between E7 oncoproteins of the high- and

low-risk human papillomavirus types are determined by amino-terminal sequences. J Virol, 65, 3943-8.

Munoz, N. 2000. Human papillomavirus and cancer: the epidemiological evidence. J Clin Virol, 19, 1-5.

Munoz, N., Bosch, F. X., Castellsague, X., Diaz, M., de Sanjose, S., Hammouda, D., Shah, K. V. & Meijer, C. J. 2004. Against which human papillomavirus types shall we vaccinate and screen? The international perspective. Int J Cancer, 111, 278-85.

Munoz, N., Bosch, F. X., de Sanjose, S., Herrero, R., Castellsague, X., Shah, K. V., Snijders, P. J. & Meijer, C. J. 2003. Epidemiologic classification of human papillomavirus types associated with cervical cancer. N Engl J Med, 348, 518-27.

Murata, S., Yashiroda, H. & Tanaka, K. 2009. Molecular mechanisms of proteasome assembly. Nat Rev Mol Cell Biol, 10, 104-15.

Murphy, M., Ahn, J., Walker, K. K., Hoffman, W. H., Evans, R. M., Levine, A. J. & George, D. L. 1999. Transcriptional repression by wild-type p53 utilizes histone deacetylases, mediated by interaction with mSin3a. Genes Dev, 13, 2490-501.

Murray-Zmijewski, F., Lane, D. P. & Bourdon, J. C. 2006. p53/p63/p73 isoforms: an orchestra of isoforms to harmonise cell differentiation and response to stress. Cell Death Differ, 13, 962-72.

Muschik, D., Braspenning-Wesch, I., Stockfleth, E., Rosl, F., Hofmann, T. G. & Nindl, I. 2011. Cutaneous HPV23 E6 prevents p53 phosphorylation through interaction with HIPK2. PLoS One, 6, e27655.

Muzio, M., Chinnaiyan, A. M., Kischkel, F. C., O'Rourke, K., Shevchenko, A., Ni, J., Scaffidi, C., Bretz, J. D., Zhang, M., Gentz, R., Mann, M., Krammer, P. H., Peter, M. E. & Dixit, V. M. 1996. FLICE, a novel FADD-homologous ICE/CED-3-like protease, is recruited to the CD95 (Fas/APO-1) death-inducing signaling complex. Cell, 85, 817-27.

Nakagawa, S. & Huibregtse, J. M. 2000. Human scribble (Vartul) is targeted for ubiquitin-mediated degradation by the high-risk papillomavirus E6 proteins and the E6AP ubiquitin-protein ligase. Mol Cell Biol, 20, 8244-53.

Nakahara, T., Peh, W. L., Doorbar, J., Lee, D. & Lambert, P. F. 2005. Human papillomavirus type 16 E1circumflexE4 contributes to multiple facets of the papillomavirus life cycle. J Virol, 79, 13150-65.

Nakano, K. & Vousden, K. H. 2001. PUMA, a novel proapoptotic gene, is induced by p53. Mol Cell, 7, 683-94.

Neary, K. & DiMaio, D. 1989. Open reading frames E6 and E7 of bovine papillomavirus type 1 are both required for full transformation of mouse C127 cells. J Virol, 63, 259-66.

Ng, T., Shima, D., Squire, A., Bastiaens, P. I., Gschmeissner, S., Humphries, M. J. & Parker, P. J. 1999. PKCalpha regulates beta1 integrin-dependent cell motility through association and control of integrin traffic. EMBO J, 18, 3909-23.

Nguyen, M. L., Nguyen, M. M., Lee, D., Griep, A. E. & Lambert, P. F. 2003. The PDZ ligand domain of the human papillomavirus type 16 E6 protein is required for E6's induction of epithelial hyperplasia in vivo. J Virol, 77, 6957-64.

Nguyen, T. H. & Ho, D. Q. 2002. Nonmelanoma skin cancer. Curr Treat Options Oncol, 3, 193-203.

Nicolaides, L., Davy, C., Raj, K., Kranjec, C., Banks, L. & Doorbar, J. 2011. Stabilization of HPV16 E6 protein by PDZ proteins, and potential implications for genome maintenance. Virology, 414, 137-45.

Nomine, Y., Charbonnier, S., Ristriani, T., Stier, G., Masson, M., Cavusoglu, N., Van Dorsselaer, A., Weiss, E., Kieffer, B. & Trave, G. 2003. Domain substructure of HPV E6 oncoprotein: biophysical characterization of the E6 C-terminal DNA-binding domain. Biochemistry, 42, 4909-17.

Nomine, Y., Masson, M., Charbonnier, S., Zanier, K., Ristriani, T., Deryckere, F., Sibler, A. P., Desplancq, D., Atkinson, R. A., Weiss, E., Orfanoudakis, G., Kieffer, B. & Trave, G. 2006. Structural and functional analysis of E6 oncoprotein: insights in the molecular pathways of human papillomavirus-mediated pathogenesis. Mol Cell, 21, 665-78.

Nuber, U., Schwarz, S. E. & Scheffner, M. 1998. The ubiquitin-protein ligase E6-associated protein (E6-AP) serves as its own substrate. Eur J Biochem, 254, 643-9.

Oda, E., Ohki, R., Murasawa, H., Nemoto, J., Shibue, T., Yamashita, T., Tokino, T., Taniguchi, T. & Tanaka, N. 2000. Noxa, a BH3-only member of the Bcl-2 family and candidate mediator of p53-induced apoptosis. Science, 288, 1053-8.

Oh, J. M., Kim, S. H., Cho, E. A., Song, Y. S., Kim, W. H. & Juhnn, Y. S. 2010a. Human papillomavirus type 16 E5 protein inhibits hydrogen-peroxide-induced apoptosis by stimulating ubiquitin-proteasome-mediated degradation of Bax in human cervical cancer cells. Carcinogenesis, 31, 402-10.

Oh, K. J., Kalinina, A., Wang, J., Nakayama, K., Nakayama, K. I. & Bagchi, S. 2004. The papillomavirus E7 oncoprotein is ubiquitinated by UbcH7 and Cullin 1- and Skp2-containing E3 ligase. J Virol, 78, 5338-46.

Oh, K. J., Singh, P., Lee, K., Foss, K., Lee, S., Park, M., Aluvila, S., Kim, R. S., Symersky, J. & Walters, D. E. 2010b. Conformational changes in BAK, a pore-forming proapoptotic Bcl-2 family member, upon membrane insertion and direct evidence for the existence of BH3-BH3 contact interface in BAK homo-oligomers. J Biol Chem, 285, 28924-37.

Oh, S. T., Kyo, S. & Laimins, L. A. 2001. Telomerase activation by human papillomavirus type 16 E6 protein: induction of human telomerase reverse transcriptase expression through Myc and GC-rich Sp1 binding sites. J Virol, 75, 5559-66.

Okamoto, K., Taya, Y. & Nakagama, H. 2009. Mdmx enhances p53 ubiquitination by altering the substrate preference of the Mdm2 ubiquitin ligase. FEBS Lett, 583, 2710-4.

Oldak, M., Maksym, R. B., Sperling, T., Yaniv, M., Smola, H., Pfister, H. J., Malejczyk, J. & Smola, S. 2010. Human papillomavirus type 8 E2 protein unravels JunB/Fra-1 as an activator of the beta4-integrin gene in human keratinocytes. J Virol, 84, 1376-86.

Oldak, M., Smola, H., Aumailley, M., Rivero, F., Pfister, H. & Smola-Hess, S. 2004. The human papillomavirus type 8 E2 protein suppresses beta4-integrin expression in primary human keratinocytes. J Virol, 78, 10738-46.

Orth, G. 1986. Epidermodysplasia verruciformis: a model for understanding the oncogenicity of human papillomaviruses. Ciba Found Symp, 120, 157-74.

Orth, G., Jablonska, S., Favre, M., Croissant, O., Jarzabek-Chorzelska, M. & Rzesa, G. 1978. Characterization of two types of human papillomaviruses in lesions of epidermodysplasia verruciformis. Proc Natl Acad Sci U S A, 75, 1537-41.

Oshiro, M. M., Futscher, B. W., Lisberg, A., Wozniak, R. J., Klimecki, W. T., Domann, F. E. & Cress, A. E. 2005. Epigenetic regulation of the cell type-specific gene 14-3-3sigma. Neoplasia, 7, 799-808.

Ottinger, M., Smith, J. A., Schweiger, M. R., Robbins, D., Powell, M. L., You, J. & Howley, P. M. 2009. Cell-type specific transcriptional activities among different papillomavirus long control regions and their regulation by E2. Virology, 395, 161-71.

Owen-Schaub, L. B., Zhang, W., Cusack, J. C., Angelo, L. S., Santee, S. M., Fujiwara, T., Roth, J. A., Deisseroth, A. B., Zhang, W. W., Kruzel, E. & et al. 1995. Wild-type human p53 and a temperature-sensitive mutant induce Fas/APO-1 expression. Mol Cell Biol, 15, 3032-40.

Owens, D. M., Broad, S., Yan, X., Benitah, S. A. & Watt, F. M. 2005. Suprabasal alpha 5 beta1 integrin expression stimulates formation of epidermal squamous cell carcinomas without disrupting TGFbeta signaling or inducing spindle cell tumors. Mol Carcinog, 44, 60-6.

Owens, D. M., Romero, M. R., Gardner, C. & Watt, F. M. 2003. Suprabasal alpha6beta4 integrin expression in epidermis results in enhanced tumourigenesis and disruption of TGFbeta signalling. J Cell Sci, 116, 3783-91.

Ozbun, M. A. & Meyers, C. 1997. Characterization of late gene transcripts expressed during vegetative replication of human papillomavirus type 31b. J Virol, 71, 5161-72.

Pandya, R. K., Partridge, J. R., Love, K. R., Schwartz, T. U. & Ploegh, H. L. 2010. A structural element within the HUWE1 HECT domain modulates self-ubiquitination and substrate ubiquitination activities. J Biol Chem, 285, 5664-73.

Parkin, D. M. 2006. The global health burden of infection-associated cancers in the year 2002. Int J Cancer, 118, 3030-44.

Peh, W. L., Brandsma, J. L., Christensen, N. D., Cladel, N. M., Wu, X. & Doorbar, J. 2004. The viral E4 protein is required for the completion of the cottontail rabbit papillomavirus productive cycle in vivo. J Virol, 78, 2142-51.

Pellinen, T., Arjonen, A., Vuoriluoto, K., Kallio, K., Fransen, J. A. & Ivaska, J. 2006. Small GTPase Rab21 regulates cell adhesion and controls endosomal traffic of beta1-integrins. J Cell Biol, 173, 767-80.

Perciavalle, R. M., Stewart, D. P., Koss, B., Lynch, J., Milasta, S., Bathina, M., Temirov, J., Cleland, M. M., Pelletier, S., Schuetz, J. D., Youle, R. J., Green, D. R. & Opferman, J. T. 2012. Anti-apoptotic MCL-1 localizes to the mitochondrial matrix and couples mitochondrial fusion to respiration. Nat Cell Biol, 14, 575-83.

Pfefferle, R., Marcuzzi, G. P., Akgul, B., Kasper, H. U., Schulze, F., Haase, I., Wickenhauser, C. & Pfister, H. 2008. The human papillomavirus type 8 E2 protein induces skin tumors in transgenic mice. J Invest Dermatol, 128, 2310-5.

Pfeifer, G. P. 2000. p53 mutational spectra and the role of methylated CpG sequences. Mutat Res, 450, 155-66.

Pfeifer, G. P. & Besaratinia, A. 2012. UV wavelength-dependent DNA damage and human non-melanoma and melanoma skin cancer. Photochem Photobiol Sci, 11, 90-7.

Pfister, H., Fuchs, P. G., Majewski, S., Jablonska, S., Pniewska, I. & Malejczyk, M. 2003. High prevalence of epidermodysplasia verruciformis-associated human papillomavirus DNA in actinic keratoses of the immunocompetent population. Arch Dermatol Res, 295, 273-9.

Pfister, H., Gassenmaier, A., Nurnberger, F. & Stuttgen, G. 1983. Human papilloma virus 5-DNA in a carcinoma of an epidermodysplasia verruciformis patient infected with various human papillomavirus types. Cancer Res, 43, 1436-41.

Pickart, C. M. 2001. Mechanisms underlying ubiquitination. Annu Rev Biochem, 70, 503-33.

Pietsch, E. C., Perchiniak, E., Canutescu, A. A., Wang, G., Dunbrack, R. L. & Murphy, M. E. 2008a. Oligomerization of BAK by p53 utilizes conserved residues of the p53 DNA binding domain. J Biol Chem, 283, 21294-304.

Pietsch, E. C., Sykes, S. M., McMahon, S. B. & Murphy, M. E. 2008b. The p53 family and programmed cell death. Oncogene, 27, 6507-21.

Pim, D. & Banks, L. 1999. HPV-18 E6*I protein modulates the E6-directed degradation of p53 by binding to full-length HPV-18 E6. Oncogene, 18, 7403-8.

Pim, D., Thomas, M., Javier, R., Gardiol, D. & Banks, L. 2000. HPV E6 targeted degradation of the discs large protein: evidence for the involvement of a novel ubiquitin ligase. Oncogene, 19, 719-25.

Pincelli, C. & Marconi, A. 2010. Keratinocyte stem cells: friends and foes. J Cell Physiol, 225, 310-5.

Polager, S. & Ginsberg, D. 2009. p53 and E2f: partners in life and death. Nat Rev Cancer, 9, 738-48.

Proby, C. M., Harwood, C. A., Neale, R. E., Green, A. C., Euvrard, S., Naldi, L., Tessari, G., Feltkamp, M. C., de Koning, M. N., Quint, W. G., Waterboer, T., Pawlita, M., Weissenborn, S., Wieland, U., Pfister, H., Stockfleth, E., Nindl, I., Abeni, D., Schegget, J. T. & Bouwes Bavinck, J. N. 2011. A case-control study of betapapillomavirus infection and cutaneous squamous cell carcinoma in organ transplant recipients. Am J Transplant, 11, 1498-508.

Proby, C. M., Purdie, K. J., Sexton, C. J., Purkis, P., Navsaria, H. A., Stables, J. N. & Leigh, I. M. 2000. Spontaneous keratinocyte cell lines representing early and advanced stages of malignant transformation of the epidermis. Exp Dermatol, 9, 104-17.

Qin, J. Z., Chaturvedi, V., Denning, M. F., Bacon, P., Panella, J., Choubey, D. & Nickoloff, B. J. 2002. Regulation of apoptosis by p53 in UV-irradiated human epidermis, psoriatic plaques and senescent keratinocytes. Oncogene, 21, 2991-3002.

Radoja, N., Gazel, A., Banno, T., Yano, S. & Blumenberg, M. 2006. Transcriptional profiling of epidermal differentiation. Physiol Genomics, 27, 65-78.

Ramoz, N., Rueda, L. A., Bouadjar, B., Montoya, L. S., Orth, G. & Favre, M. 2002. Mutations in two adjacent novel genes are associated with epidermodysplasia verruciformis. Nat Genet, 32, 579-81.

Rank, N. M. & Lambert, P. F. 1995. Bovine papillomavirus type 1 E2 transcriptional regulators directly bind two cellular transcription factors, TFIID and TFIIB. J Virol, 69, 6323-34.

Reid, D. L., Aydelotte, M. B. & Mollenhauer, J. 2000. Cell attachment, collagen binding, and receptor analysis on bovine articular chondrocytes. J Orthop Res, 18, 364-73.

Reinson, T., Toots, M., Kadaja, M., Pipitch, R., Allik, M., Ustav, E. & Ustav, M. 2012. Engagement of the ATR-dependent DNA damage response at the HPV18 replication centers during the initial amplification. J Virol.

Reinstein, E., Scheffner, M., Oren, M., Ciechanover, A. & Schwartz, A. 2000. Degradation of the E7 human papillomavirus oncoprotein by the ubiquitin-proteasome system: targeting via ubiquitination of the N-terminal residue. Oncogene, 19, 5944-50.

Ren, Z. P., Ahmadian, A., Ponten, F., Nister, M., Berg, C., Lundeberg, J., Uhlen, M. & Ponten, J. 1997. Benign clonal keratinocyte patches with p53 mutations show no genetic link to synchronous squamous cell precancer or cancer in human skin. Am J Pathol, 150, 1791-803.

Ren, Z. P., Hedrum, A., Ponten, F., Nister, M., Ahmadian, A., Lundeberg, J., Uhlen, M. & Ponten, J. 1996. Human epidermal cancer and accompanying precursors have identical p53 mutations different from p53 mutations in adjacent areas of clonally expanded non-neoplastic keratinocytes. Oncogene, 12, 765-73.

Riggs, P. 2001. Expression and purification of maltose-binding protein fusions. Curr Protoc Mol Biol, Chapter 16, Unit16 6.

Riley, R. R., Duensing, S., Brake, T., Munger, K., Lambert, P. F. & Arbeit, J. M. 2003. Dissection of human papillomavirus E6 and E7 function in transgenic mouse models of cervical carcinogenesis. Cancer Res, 63, 4862-71.

Roberts, S., Ashmole, I., Johnson, G. D., Kreider, J. W. & Gallimore, P. H. 1993. Cutaneous and mucosal human papillomavirus E4 proteins form intermediate filament-like structures in epithelial cells. Virology, 197, 176-87.

Rodriguez, M. S., Desterro, J. M., Lain, S., Lane, D. P. & Hay, R. T. 2000. Multiple C-terminal lysine residues target p53 for ubiquitin-proteasome-mediated degradation. Mol Cell Biol, 20, 8458-67.

Rosa, J. L., Casaroli-Marano, R. P., Buckler, A. J., Vilaro, S. & Barbacid, M. 1996. p619, a giant protein related to the chromosome condensation regulator RCC1, stimulates guanine nucleotide exchange on ARF1 and Rab proteins. EMBO J, 15, 4262-73.

Rosenfeldt, M. T. & Ryan, K. M. 2011. The multiple roles of autophagy in cancer. Carcinogenesis, 32, 955-63.

Rosso, S., Zanetti, R., Martinez, C., Tormo, M. J., Schraub, S., Sancho-Garnier, H., Franceschi, S., Gafa, L., Perea, E., Navarro, C., Laurent, R., Schrameck, C., Talamini, R., Tumino, R. & Wechsler, J. 1996. The multicentre south European study 'Helios'. II: Different sun exposure patterns in the aetiology of basal cell and squamous cell carcinomas of the skin. Br J Cancer, 73, 1447-54.

Rozenblatt-Rosen, O., Deo, R. C., Padi, M., Adelmant, G., Calderwood, M. A., Rolland, T., Grace, M., Dricot, A., Askenazi, M., Tavares, M., Pevzner, S. J., Abderazzaq, F., Byrdsong, D., Carvunis, A. R., Chen, A. A., Cheng, J., Correll, M., Duarte, M., Fan, C., Feltkamp, M. C., Ficarro, S. B., Franchi, R., Garg, B. K., Gulbahce, N., Hao, T., Holthaus, A. M., James, R., Korkhin, A., Litovchick, L., Mar, J. C., Pak, T. R., Rabello, S., Rubio, R., Shen, Y., Singh, S., Spangle, J. M., Tasan, M., Wanamaker, S., Webber, J. T., Roecklein-Canfield, J., Johannsen, E., Barabasi, A. L., Beroukhim, R., Kieff, E., Cusick, M. E., Hill, D. E., Munger, K., Marto, J. A., Quackenbush, J.,

Roth, F. P., DeCaprio, J. A. & Vidal, M. 2012. Interpreting cancer genomes using systematic host network perturbations by tumour virus proteins. Nature, 487, 491-5.

Runswick, S. K., O'Hare, M. J., Jones, L., Streuli, C. H. & Garrod, D. R. 2001. Desmosomal adhesion regulates epithelial morphogenesis and cell positioning. Nat Cell Biol, 3, 823-30.

Sakakibara, N., Mitra, R. & McBride, A. A. 2011. The papillomavirus E1 helicase activates a cellular DNA damage response in viral replication foci. J Virol, 85, 8981-95.

Salomon, D., Masgrau, E., Vischer, S., Ullrich, S., Dupont, E., Sappino, P., Saurat, J. H. & Meda, P. 1994. Topography of mammalian connexins in human skin. J Invest Dermatol, 103, 240-7.

Salvesen, G. S. & Duckett, C. S. 2002. IAP proteins: blocking the road to death's door. Nat Rev Mol Cell Biol, 3, 401-10.

Sasagawa, T., Kondoh, G., Inoue, M., Yutsudo, M. & Hakura, A. 1994. Cervical/vaginal dysplasias of transgenic mice harbouring human papillomavirus type 16 E6-E7 genes. J Gen Virol, 75 (Pt 11), 3057-65.

Sattler, M., Liang, H., Nettesheim, D., Meadows, R. P., Harlan, J. E., Eberstadt, M., Yoon, H. S., Shuker, S. B., Chang, B. S., Minn, A. J., Thompson, C. B. & Fesik, S. W. 1997. Structure of Bcl-xL-Bak peptide complex: recognition between regulators of apoptosis. Science, 275, 983-6.

Sax, J. K. & El-Deiry, W. S. 2003. p53-induced gene expression analysis. Methods Mol Biol, 234, 65-71.

Sax, J. K., Fei, P., Murphy, M. E., Bernhard, E., Korsmeyer, S. J. & El-Deiry, W. S. 2002. BID regulation by p53 contributes to chemosensitivity. Nat Cell Biol, 4, 842-9.

Scaffidi, C., Fulda, S., Srinivasan, A., Friesen, C., Li, F., Tomaselli, K. J., Debatin, K. M., Krammer, P. H. & Peter, M. E. 1998. Two CD95 (APO-1/Fas) signaling pathways. EMBO J, 17, 1675-87.

Schaller, M. D. 2010. Cellular functions of FAK kinases: insight into molecular mechanisms and novel functions. J Cell Sci, 123, 1007-13.

Schaper, I. D., Marcuzzi, G. P., Weissenborn, S. J., Kasper, H. U., Dries, V., Smyth, N., Fuchs, P. & Pfister, H. 2005. Development of skin tumors in mice transgenic for early genes of human papillomavirus type 8. Cancer Res, 65, 1394-400.

Schapiro, F., Sparkowski, J., Adduci, A., Suprynowicz, F., Schlegel, R. & Grinstein, S. 2000. Golgi alkalinization by the papillomavirus E5 oncoprotein. J Cell Biol, 148, 305-15.

Scheffner, M., Huibregtse, J. M., Vierstra, R. D. & Howley, P. M. 1993. The HPV-16 E6 and E6-AP complex functions as a ubiquitin-protein ligase in the ubiquitination of p53. Cell, 75, 495-505.

Scheffner, M., Werness, B. A., Huibregtse, J. M., Levine, A. J. & Howley, P. M. 1990. The E6 oncoprotein encoded by human papillomavirus types 16 and 18 promotes the degradation of p53. Cell, 63, 1129-36.

Scheffner, M. & Whitaker, N. J. 2003. Human papillomavirus-induced carcinogenesis and the ubiquitin-proteasome system. Semin Cancer Biol, 13, 59-67.

Schiffman, M., Castle, P. E., Jeronimo, J., Rodriguez, A. C. & Wacholder, S. 2007. Human papillomavirus and cervical cancer. Lancet, 370, 890-907.

Schile, A. J., Garcia-Fernandez, M. & Steller, H. 2008. Regulation of apoptosis by XIAP ubiquitin-ligase activity. Genes Dev, 22, 2256-66.

Schipper, J. H., Frixen, U. H., Behrens, J., Unger, A., Jahnke, K. & Birchmeier, W. 1991. E-cadherin expression in squamous cell carcinomas of head and neck: inverse correlation with tumor dedifferentiation and lymph node metastasis. Cancer Res, 51, 6328-37.

Schlaepfer, D. D., Jones, J. & Haigler, H. T. 1992. Inhibition of protein kinase C by annexin V. Biochemistry, 31, 1886-91.

Schmitt, A., Harry, J. B., Rapp, B., Wettstein, F. O. & Iftner, T. 1994. Comparison of the properties of the E6 and E7 genes of low- and high-risk cutaneous papillomaviruses reveals strongly transforming and high Rb-binding activity for the E7 protein of the low-risk human papillomavirus type 1. J Virol, 68, 7051-9.

Schober, M. & Fuchs, E. 2011. Tumor-initiating stem cells of squamous cell carcinomas and their control by TGF-beta and integrin/focal adhesion kinase (FAK) signaling. Proc Natl Acad Sci U S A, 108, 10544-9.

Schwarz, A., Bhardwaj, R., Aragane, Y., Mahnke, K., Riemann, H., Metze, D., Luger, T. A. & Schwarz, T. 1995. Ultraviolet-B-induced apoptosis of keratinocytes: evidence for partial involvement of tumor necrosis factor-alpha in the formation of sunburn cells. J Invest Dermatol, 104, 922-7.

Schwarz, S. E., Rosa, J. L. & Scheffner, M. 1998. Characterization of human hect domain family members and their interaction with UbcH5 and UbcH7. J Biol Chem, 273, 12148-54.

Searle, P. F., Thomas, D. P., Faulkner, K. B. & Tinsley, J. M. 1994. Stomach cancer in transgenic mice expressing human papillomavirus type 16 early region genes from a keratin promoter. J Gen Virol, 75 (Pt 5), 1125-37.

Sen, E., Alam, S. & Meyers, C. 2004. Genetic and biochemical analysis of cis regulatory elements within the keratinocyte enhancer region of the human papillomavirus type 31 upstream regulatory region during different stages of the viral life cycle. J Virol, 78, 612-29.

Shafti-Keramat, S., Handisurya, A., Kriehuber, E., Meneguzzi, G., Slupetzky, K. & Kirnbauer, R. 2003. Different heparan sulfate proteoglycans serve as cellular receptors for human papillomaviruses. J Virol, 77, 13125-35.

Shamanin, V., zur Hausen, H., Lavergne, D., Proby, C. M., Leigh, I. M., Neumann, C., Hamm, H., Goos, M., Haustein, U. F., Jung, E. G., Plewig, G., Wolff, H. & de Villiers, E. M. 1996. Human papillomavirus infections in nonmelanoma skin cancers from renal transplant recipients and nonimmunosuppressed patients. J Natl Cancer Inst, 88, 802-11.

Shen, X., Li, C. C., Aponte, A. M., Shen, R. F., Billings, E. M., Moss, J. & Vaughan, M. 2012. Brefeldin A-inhibited ADP-ribosylation factor activator BIG2 regulates cell migration via integrin beta1 cycling and actin remodeling. Proc Natl Acad Sci U S A, 109, 14464-9.

Shiozaki, H., Iihara, K., Oka, H., Kadowaki, T., Matsui, S., Gofuku, J., Inoue, M., Nagafuchi, A., Tsukita, S. & Mori, T. 1994. Immunohistochemical detection of alpha-catenin expression in human cancers. Am J Pathol, 144, 667-74.

Simmonds, M. & Storey, A. 2008. Identification of the regions of the HPV 5 E6 protein involved in Bak degradation and inhibition of apoptosis. Int J Cancer, 123, 2260-6.

Simonson, S. J., Difilippantonio, M. J. & Lambert, P. F. 2005. Two distinct activities contribute to human papillomavirus 16 E6's oncogenic potential. Cancer Res, 65, 8266-73.

Simpson, C. L., Patel, D. M. & Green, K. J. 2011. Deconstructing the skin: cytoarchitectural determinants of epidermal morphogenesis. Nat Rev Mol Cell Biol, 12, 565-80.

Sinha, R. P. & Hader, D. P. 2002. UV-induced DNA damage and repair: a review. Photochem Photobiol Sci, 1, 225-36.

Slominski, A. 2005. Neuroendocrine system of the skin. Dermatology, 211, 199-208.

Smith, J. A., White, E. A., Sowa, M. E., Powell, M. L., Ottinger, M., Harper, J. W. & Howley, P. M. 2010. Genome-wide siRNA screen identifies SMCX, EP400, and Brd4 as E2-dependent regulators of human papillomavirus oncogene expression. Proc Natl Acad Sci U S A, 107, 3752-7.

Smith, J. L., Campos, S. K. & Ozbun, M. A. 2007a. Human papillomavirus type 31 uses a caveolin 1- and dynamin 2-mediated entry pathway for infection of human keratinocytes. J Virol, 81, 9922-31.

Smith, J. S., Lindsay, L., Hoots, B., Keys, J., Franceschi, S., Winer, R. & Clifford, G. M. 2007b. Human papillomavirus type distribution in invasive cervical cancer and high-grade cervical lesions: a meta-analysis update. Int J Cancer, 121, 621-32.

Solary, E., Dubrez, L. & Eymin, B. 1996. The role of apoptosis in the pathogenesis and treatment of diseases. Eur Respir J, 9, 1293-305.

Song, S., Liem, A., Miller, J. A. & Lambert, P. F. 2000. Human papillomavirus types 16 E6 and E7 contribute differently to carcinogenesis. Virology, 267, 141-50.

Spangle, J. M. & Munger, K. 2010. The human papillomavirus type 16 E6 oncoprotein activates mTORC1 signaling and increases protein synthesis. J Virol, 84, 9398-407.

Spanos, W. C., Hoover, A., Harris, G. F., Wu, S., Strand, G. L., Anderson, M. E., Klingelhutz, A. J., Hendriks, W., Bossler, A. D. & Lee, J. H. 2008. The PDZ binding motif of human papillomavirus type 16 E6 induces PTPN13 loss, which allows anchorage-independent growth and synergizes with ras for invasive growth. J Virol, 82, 2493-500.

Sperling, T., Oldak, M., Walch-Ruckheim, B., Wickenhauser, C., Doorbar, J., Pfister, H., Malejczyk, M., Majewski, S., Keates, A. C. & Smola, S. 2012. Human papillomavirus type 8 interferes with a novel C/EBPbeta-mediated mechanism of keratinocyte CCL20 chemokine expression and Langerhans cell migration. PLoS Pathog, 8, e1002833.

Spoden, G., Freitag, K., Husmann, M., Boller, K., Sapp, M., Lambert, C. & Florin, L. 2008. Clathrin- and caveolin-independent entry of human papillomavirus type 16--involvement of tetraspanin-enriched microdomains (TEMs). PLoS One, 3, e3313.

Stambolic, V., MacPherson, D., Sas, D., Lin, Y., Snow, B., Jang, Y., Benchimol, S. & Mak, T. W. 2001. Regulation of PTEN transcription by p53. Mol Cell, 8, 317-25.

Stauffer, Y., Raj, K., Masternak, K. & Beard, P. 1998. Infectious human papillomavirus type 18 pseudovirions. J Mol Biol, 283, 529-36.

Stege, H., Roza, L., Vink, A. A., Grewe, M., Ruzicka, T., Grether-Beck, S. & Krutmann, J. 2000. Enzyme plus light therapy to repair DNA damage in ultraviolet-B-irradiated human skin. Proc Natl Acad Sci U S A, 97, 1790-5.

Steger, G. & Corbach, S. 1997. Dose-dependent regulation of the early promoter of human papillomavirus type 18 by the viral E2 protein. J Virol, 71, 50-8.

Steger, G. & Pfister, H. 1992. In vitro expressed HPV 8 E6 protein does not bind p53. Arch Virol, 125, 355-60.

Steller, M. A., Zou, Z., Schiller, J. T. & Baserga, R. 1996. Transformation by human papillomavirus 16 E6 and E7: role of the insulin-like growth factor 1 receptor. Cancer Res, 56, 5087-91.

Stewart, D., Kazemi, S., Li, S., Massimi, P., Banks, L., Koromilas, A. E. & Matlashewski, G. 2004. Ubiquitination and proteasome degradation of the E6 proteins of human papillomavirus types 11 and 18. J Gen Virol, 85, 1419-26.

Stiewe, T. & Putzer, B. M. 2000. Role of the p53-homologue p73 in E2F1-induced apoptosis. Nat Genet, 26, 464-9.

Stockfleth, E., Ulrich, C., Meyer, T., Arndt, R. & Christophers, E. 2001. Skin diseases following organ transplantation--risk factors and new therapeutic approaches. Transplant Proc, 33, 1848-53.

Stoler, M. H., Rhodes, C. R., Whitbeck, A., Wolinsky, S. M., Chow, L. T. & Broker, T. R. 1992. Human papillomavirus type 16 and 18 gene expression in cervical neoplasias. Hum Pathol, 23, 117-28.

Storey, A. 2002. Papillomaviruses: death-defying acts in skin cancer. Trends Mol Med, 8, 417-21.

Storey, A., Thomas, M., Kalita, A., Harwood, C., Gardiol, D., Mantovani, F., Breuer, J., Leigh, I. M., Matlashewski, G. & Banks, L. 1998. Role of a p53 polymorphism in the development of human papillomavirus-associated cancer. Nature, 393, 229-34.

Stransky, N., Egloff, A. M., Tward, A. D., Kostic, A. D., Cibulskis, K., Sivachenko, A., Kryukov, G. V., Lawrence, M. S., Sougnez, C., McKenna, A., Shefler, E., Ramos, A. H., Stojanov, P., Carter, S. L., Voet, D., Cortes, M. L., Auclair, D., Berger, M. F., Saksena, G., Guiducci, C., Onofrio, R. C., Parkin, M., Romkes, M., Weissfeld, J. L., Seethala, R. R., Wang, L., Rangel-Escareno, C., Fernandez-Lopez, J. C., Hidalgo-Miranda, A., Melendez-Zajgla, J., Winckler, W., Ardlie, K., Gabriel, S. B., Meyerson, M., Lander, E. S., Getz, G., Golub, T. R., Garraway, L. A. & Grandis, J. R. 2011. The mutational landscape of head and neck squamous cell carcinoma. Science, 333, 1157-60.

Struijk, L., van der Meijden, E., Kazem, S., ter Schegget, J., de Gruijl, F. R., Steenbergen, R. D. & Feltkamp, M. C. 2008. Specific betapapillomaviruses associated with squamous cell carcinoma of the skin inhibit UVB-induced apoptosis of primary human keratinocytes. J Gen Virol, 89, 2303-14.

Suprynowicz, F. A., Disbrow, G. L., Krawczyk, E., Simic, V., Lantzky, K. & Schlegel, R. 2008. HPV-16 E5 oncoprotein upregulates lipid raft components caveolin-1 and ganglioside GM1 at the plasma membrane of cervical cells. Oncogene, 27, 1071-8.

Suzuki, M., Youle, R. J. & Tjandra, N. 2000. Structure of Bax: coregulation of dimer formation and intracellular localization. Cell, 103, 645-54.

Swindle, C. S., Zou, N., Van Tine, B. A., Shaw, G. M., Engler, J. A. & Chow, L. T. 1999. Human papillomavirus DNA replication compartments in a transient DNA replication system. J Virol, 73, 1001-9.

Tada, J. & Hashimoto, K. 1997. Ultrastructural localization of gap junction protein connexin 43 in normal human skin, basal cell carcinoma, and squamous cell carcinoma. J Cutan Pathol, 24, 628-35.

Tafazoli, F., Holmstrom, A., Forsberg, A. & Magnusson, K. E. 2000. Apically exposed, tight junction-associated beta1-integrins allow binding and YopE-mediated perturbation of epithelial barriers by wild-type Yersinia bacteria. Infect Immun, 68, 5335-43.

Taliana, L., Benezra, M., Greenberg, R. S., Masur, S. K. & Bernstein, A. M. 2005. ZO-1: lamellipodial localization in a corneal fibroblast wound model. Invest Ophthalmol Vis Sci, 46, 96-103.

Tan, C. L., Gunaratne, J., Lai, D., Carthagena, L., Wang, Q., Xue, Y. Z., Quek, L. S., Doorbar, J., Bachelerie, F., Thierry, F. & Bellanger, S. 2012a. HPV-18 E2^E4 chimera: 2 new spliced transcripts and proteins induced by keratinocyte differentiation. Virology, 429, 47-56.

Tan, J. M., Wong, E. S., Kirkpatrick, D. S., Pletnikova, O., Ko, H. S., Tay, S. P., Ho, M. W., Troncoso, J., Gygi, S. P., Lee, M. K., Dawson, V. L., Dawson, T. M. & Lim, K. L. 2008. Lysine 63-linked ubiquitination promotes the formation and autophagic clearance of protein inclusions associated with neurodegenerative diseases. Hum Mol Genet, 17, 431-9.

Tan, M. J., White, E. A., Sowa, M. E., Harper, J. W., Aster, J. C. & Howley, P. M. 2012b. Cutaneous beta-human papillomavirus E6 proteins bind Mastermind-like coactivators and repress Notch signaling. Proc Natl Acad Sci U S A.

Tchernev, G. & Orfanos, C. E. 2007. Downregulation of cell cycle modulators p21, p27, p53, Rb and proapoptotic Bcl-2-related proteins Bax and Bak in cutaneous melanoma is associated with worse patient prognosis: preliminary findings. J Cutan Pathol, 34, 247-56.

Thain, A., Jenkins, O., Clarke, A. R. & Gaston, K. 1996. CpG methylation directly inhibits binding of the human papillomavirus type 16 E2 protein to specific DNA sequences. J Virol, 70, 7233-5.

Thierry, F. 2009. Transcriptional regulation of the papillomavirus oncogenes by cellular and viral transcription factors in cervical carcinoma. Virology, 384, 375-9.

Thomas, M. & Banks, L. 1998. Inhibition of Bak-induced apoptosis by HPV-18 E6. Oncogene, 17, 2943-54.

Thomas, M. & Banks, L. 1999. Human papillomavirus (HPV) E6 interactions with Bak are conserved amongst E6 proteins from high and low risk HPV types. J Gen Virol, 80 (Pt 6), 1513-7.

Thomas, M., Laura, R., Hepner, K., Guccione, E., Sawyers, C., Lasky, L. & Banks, L. 2002. Oncogenic human papillomavirus E6 proteins target the MAGI-2 and MAGI-3 proteins for degradation. Oncogene, 21, 5088-96.

Thomas, M., Tomaic, V., Pim, D., Myers, M. P., Tommasino, M. & Banks, L. 2013. Interactions between E6AP and E6 proteins from alpha and beta HPV types. Virology, 435, 357-62.

Thomas, M. C. & Chiang, C. M. 2005. E6 oncoprotein represses p53-dependent gene activation via inhibition of protein acetylation independently of inducing p53 degradation. Mol Cell, 17, 251-64.

Tomaic, V., Pim, D., Thomas, M., Massimi, P., Myers, M. P. & Banks, L. 2011. Regulation of the human papillomavirus type 18 E6/E6AP ubiquitin ligase complex by the HECT domain-containing protein EDD. J Virol, 85, 3120-7.

Tomlins, C. & Storey, A. 2010. Cutaneous HPV5 E6 causes increased expression of Osteoprotegerin and Interleukin 6 which contribute to evasion of UV-induced apoptosis. Carcinogenesis, 31, 2155-64.

Tommasino, M., Adamczewski, J. P., Carlotti, F., Barth, C. F., Manetti, R., Contorni, M., Cavalieri, F., Hunt, T. & Crawford, L. 1993. HPV16 E7 protein associates with the protein kinase p33CDK2 and cyclin A. Oncogene, 8, 195-202.

Tong, X. & Howley, P. M. 1997. The bovine papillomavirus E6 oncoprotein interacts with paxillin and disrupts the actin cytoskeleton. Proc Natl Acad Sci U S A, 94, 4412-7.

Tong, X., Salgia, R., Li, J. L., Griffin, J. D. & Howley, P. M. 1997. The bovine papillomavirus E6 protein binds to the LD motif repeats of paxillin and blocks its interaction with vinculin and the focal adhesion kinase. J Biol Chem, 272, 33373-6.

Ullrich, S. E. 2005. Mechanisms underlying UV-induced immune suppression. Mutat Res, 571, 185-205.

Underbrink, M. P., Howie, H. L., Bedard, K. M., Koop, J. I. & Galloway, D. A. 2008. E6 proteins from multiple human betapapillomavirus types degrade Bak and protect keratinocytes from apoptosis after UVB irradiation. J Virol, 82, 10408-17.

Uren, R. T., Dewson, G., Chen, L., Coyne, S. C., Huang, D. C., Adams, J. M. & Kluck, R. M. 2007. Mitochondrial permeabilization relies on BH3 ligands engaging multiple prosurvival Bcl-2 relatives, not Bak. J Cell Biol, 177, 277-87.

Vaeteewoottacharn, K., Chamutpong, S., Ponglikitmongkol, M. & Angeletti, P. C. 2005. Differential localization of HPV16 E6 splice products with E6-associated protein. Virol J, 2, 50.

Vallejo-Torres, L., Morris, S., Kinge, J., Poirier, V. & Verne, J. 2011. Cost of skin cancer in England. *The Economics of Cancer Workshop.* The Ambassadors Bloomsbury, Upper Woburn Place, London.

van Dam, R. M., Huang, Z., Rimm, E. B., Weinstock, M. A., Spiegelman, D., Colditz, G. A., Willett, W. C. & Giovannucci, E. 1999. Risk factors for basal cell carcinoma of the skin in men: results from the health professionals follow-up study. Am J Epidemiol, 150, 459-68.

van Nimwegen, M. J. & van de Water, B. 2007. Focal adhesion kinase: a potential target in cancer therapy. Biochem Pharmacol, 73, 597-609.

van Wijk, S. J., de Vries, S. J., Kemmeren, P., Huang, A., Boelens, R., Bonvin, A. M. & Timmers, H. T. 2009. A comprehensive framework of E2-RING E3 interactions of the human ubiquitin-proteasome system. Mol Syst Biol, 5, 295.

Vande Pol, S. B., Brown, M. C. & Turner, C. E. 1998. Association of Bovine Papillomavirus Type 1 E6 oncoprotein with the focal adhesion protein paxillin through a conserved protein interaction motif. Oncogene, 16, 43-52.

Vassilieva, E. V., Gerner-Smidt, K., Ivanov, A. I. & Nusrat, A. 2008. Lipid rafts mediate internalization of beta1-integrin in migrating intestinal epithelial cells. Am J Physiol Gastrointest Liver Physiol, 295, G965-76.

Vaux, D. L., Cory, S. & Adams, J. M. 1988. Bcl-2 gene promotes haemopoietic cell survival and cooperates with c-myc to immortalize pre-B cells. Nature, 335, 440-2.

Vaux, D. L. & Korsmeyer, S. J. 1999. Cell death in development. Cell, 96, 245-54.

Veness, M. J. 2007. High-risk cutaneous squamous cell carcinoma of the head and neck. J Biomed Biotechnol, 2007, 80572.

Venuti, A., Paolini, F., Nasir, L., Corteggio, A., Roperto, S., Campo, M. S. & Borzacchiello, G. 2011. Papillomavirus E5: the smallest oncoprotein with many functions. Mol Cancer, 10, 140.

Viarisio, D., Mueller-Decker, K., Kloz, U., Aengeneyndt, B., Kopp-Schneider, A., Grone, H. J., Gheit, T., Flechtenmacher, C., Gissmann, L. & Tommasino, M. 2011. E6 and E7 from beta HPV38 cooperate with ultraviolet light in the development of actinic keratosis-like lesions and squamous cell carcinoma in mice. PLoS Pathog, 7, e1002125.

Villa, L. L. 2011. HPV prophylactic vaccination: The first years and what to expect from now. Cancer Lett, 305, 106-12.

Vos, R. M., Altreuter, J., White, E. A. & Howley, P. M. 2009. The ubiquitin-specific peptidase USP15 regulates human papillomavirus type 16 E6 protein stability. J Virol, 83, 8885-92.

Wade, R., Brimer, N. & Vande Pol, S. 2008. Transformation by bovine papillomavirus type 1 E6 requires paxillin. J Virol, 82, 5962-6.

Walboomers, J. M., Jacobs, M. V., Manos, M. M., Bosch, F. X., Kummer, J. A., Shah, K. V., Snijders, P. J., Peto, J., Meijer, C. J. & Munoz, N. 1999. Human papillomavirus is a necessary cause of invasive cervical cancer worldwide. J Pathol, 189, 12-9.

Wallace, N. A., Robinson, K., Howie, H. L. & Galloway, D. A. 2012. HPV 5 and 8 E6 abrogate ATR activity resulting in increased persistence of UVB induced DNA damage. PLoS Pathog, 8, e1002807.

Wang, J., Sampath, A., Raychaudhuri, P. & Bagchi, S. 2001. Both Rb and E7 are regulated by the ubiquitin proteasome pathway in HPV-containing cervical tumor cells. Oncogene, 20, 4740-9.

Warr, M. R., Acoca, S., Liu, Z., Germain, M., Watson, M., Blanchette, M., Wing, S. S. & Shore, G. C. 2005. BH3-ligand regulates access of MCL-1 to its E3 ligase. FEBS Lett, 579, 5603-8.

Waterhouse, N. J. & Trapani, J. A. 2003. A new quantitative assay for cytochrome c release in apoptotic cells. Cell Death Differ, 10, 853-5.

Watson, M., Saraiya, M., Ahmed, F., Cardinez, C. J., Reichman, M. E., Weir, H. K. & Richards, T. B. 2008. Using population-based cancer registry data to assess the burden of human papillomavirus-associated cancers in the United States: overview of methods. Cancer, 113, 2841-54.

Watson, R. A., Thomas, M., Banks, L. & Roberts, S. 2003. Activity of the human papillomavirus E6 PDZ-binding motif correlates with an enhanced morphological transformation of immortalized human keratinocytes. J Cell Sci, 116, 4925-34.

Watt, F. M. 2002. Role of integrins in regulating epidermal adhesion, growth and differentiation. EMBO J, 21, 3919-26.

Watt, F. M., Estrach, S. & Ambler, C. A. 2008. Epidermal Notch signalling: differentiation, cancer and adhesion. Curr Opin Cell Biol, 20, 171-9.

Wehner, M. R., Shive, M. L., Chren, M. M., Han, J., Qureshi, A. A. & Linos, E. 2012. Indoor tanning and non-melanoma skin cancer: systematic review and meta-analysis. British Medical Journal, 345, e5909.

Wei, M. C., Lindsten, T., Mootha, V. K., Weiler, S., Gross, A., Ashiya, M., Thompson, C. B. & Korsmeyer, S. J. 2000. tBID, a membrane-targeted death ligand, oligomerizes BAK to release cytochrome c. Genes Dev, 14, 2060-71.

Weinkauf, B., Rukwied, R., Quiding, H., Dahllund, L., Johansson, P. & Schmelz, M. 2012. Local gene expression changes after UV-irradiation of human skin. PLoS One, 7, e39411.

Weissenborn, S., Neale, R. E., Waterboer, T., Abeni, D., Bavinck, J. N., Green, A. C., Harwood, C. A., Euvrard, S., Feltkamp, M. C., de Koning, M. N., Naldi, L., Quint, W. G., Tessari, G., Proby, C. M., Wieland, U. & Pfister, H. 2012. Beta-papillomavirus DNA loads in hair follicles of immunocompetent people and organ transplant recipients. Med Microbiol Immunol, 201, 117-25.

Weissenborn, S. J., Nindl, I., Purdie, K., Harwood, C., Proby, C., Breuer, J., Majewski, S., Pfister, H. & Wieland, U. 2005. Human papillomavirus-DNA loads in actinic keratoses exceed those in non-melanoma skin cancers. J Invest Dermatol, 125, 93-7.

Weissman, A. M. 2001. Themes and variations on ubiquitylation. Nat Rev Mol Cell Biol, 2, 169-78.

Welsh, M. M., Karagas, M. R., Kuriger, J. K., Houseman, A., Spencer, S. K., Perry, A. E. & Nelson, H. H. 2011. Genetic determinants of UV-susceptibility in non-melanoma skin cancer. PLoS One, 6, e20019.

Westphal, K., Akgul, B., Storey, A. & Nindl, I. 2009. Cutaneous human papillomavirus E7 type-specific effects on differentiation and proliferation of organotypic skin cultures. Cell Oncol, 31, 213-26.

Wetherill, L. F., Holmes, K. K., Verow, M., Muller, M., Howell, G., Harris, M., Fishwick, C., Stonehouse, N., Foster, R., Blair, G. E., Griffin, S. & Macdonald, A. 2012. High-risk human papillomavirus E5 oncoprotein displays channel-forming activity sensitive to small-molecule inhibitors. J Virol, 86, 5341-51.

White, E. A., Kramer, R. E., Tan, M. J., Hayes, S. D., Harper, J. W. & Howley, P. M. 2012. Comprehensive Analysis of Host Cellular Interactions with Human Papillomavirus E6 Proteins Identifies New E6 Binding Partners and Reflects Viral Diversity. J Virol.

Willis, S. N., Chen, L., Dewson, G., Wei, A., Naik, E., Fletcher, J. I., Adams, J. M. & Huang, D. C. 2005. Proapoptotic Bak is sequestered by Mcl-1 and Bcl-xL, but not Bcl-2, until displaced by BH3-only proteins. Genes Dev, 19, 1294-305.

Willis, S. N., Fletcher, J. I., Kaufmann, T., van Delft, M. F., Chen, L., Czabotar, P. E., Ierino, H., Lee, E. F., Fairlie, W. D., Bouillet, P., Strasser, A., Kluck, R. M., Adams, J. M. & Huang, D. C. 2007. Apoptosis initiated when BH3 ligands engage multiple Bcl-2 homologs, not Bax or Bak. Science, 315, 856-9.

Wilson, R., Fehrmann, F. & Laimins, L. A. 2005. Role of the E1--E4 protein in the differentiation-dependent life cycle of human papillomavirus type 31. J Virol, 79, 6732-40.

Wilson, R., Ryan, G. B., Knight, G. L., Laimins, L. A. & Roberts, S. 2007. The full-length E1E4 protein of human papillomavirus type 18 modulates differentiation-dependent viral DNA amplification and late gene expression. Virology, 362, 453-60.

Wilson, V. G., West, M., Woytek, K. & Rangasamy, D. 2002. Papillomavirus E1 proteins: form, function, and features. Virus Genes, 24, 275-90.

Wisgerhof, H. C., Edelbroek, J. R., de Fijter, J. W., Feltkamp, M. C., Willemze, R. & Bouwes Bavinck, J. N. 2010. Trends of skin diseases in organ-transplant recipients transplanted between 1966 and 2006: a cohort study with follow-up between 1994 and 2006. Br J Dermatol, 162, 390-6.

Woelk, T., Oldrini, B., Maspero, E., Confalonieri, S., Cavallaro, E., Di Fiore, P. P. & Polo, S. 2006. Molecular mechanisms of coupled monoubiquitination. Nat Cell Biol, 8, 1246-54.

Wong, P. P., Pickard, A. & McCance, D. J. 2010. p300 alters keratinocyte cell growth and differentiation through regulation of p21(Waf1/CIP1). PLoS One, 5, e8369.

Wu, S. Y., Lee, A. Y., Hou, S. Y., Kemper, J. K., Erdjument-Bromage, H., Tempst, P. & Chiang, C. M. 2006. Brd4 links chromatin targeting to HPV transcriptional silencing. Genes Dev, 20, 2383-96.

Yamamoto, Y., Huibregtse, J. M. & Howley, P. M. 1997. The human E6-AP gene (UBE3A) encodes three potential protein isoforms generated by differential splicing. Genomics, 41, 263-6.

Yamashita, T., Segawa, K., Fujinaga, Y., Nishikawa, T. & Fujinaga, K. 1993. Biological and biochemical activity of E7 genes of the cutaneous human papillomavirus type 5 and 8. Oncogene, 8, 2433-41.

You, J., Croyle, J. L., Nishimura, A., Ozato, K. & Howley, P. M. 2004. Interaction of the bovine papillomavirus E2 protein with Brd4 tethers the viral DNA to host mitotic chromosomes. Cell, 117, 349-60.

Youle, R. J. & Strasser, A. 2008. The BCL-2 protein family: opposing activities that mediate cell death. Nat Rev Mol Cell Biol, 9, 47-59.

Yu, J., Zhang, L., Hwang, P. M., Rago, C., Kinzler, K. W. & Vogelstein, B. 1999. Identification and classification of p53-regulated genes. Proc Natl Acad Sci U S A, 96, 14517-22.

Zaidel-Bar, R., Ballestrem, C., Kam, Z. & Geiger, B. 2003. Early molecular events in the assembly of matrix adhesions at the leading edge of migrating cells. J Cell Sci, 116, 4605-13.

Zanier, K., ould M'hamed ould Sidi, A., Boulade-Ladame, C., Rybin, V., Chappelle, A., Atkinson, A., Kieffer, B. & Trave, G. 2012. Solution structure analysis of the HPV16 E6 oncoprotein reveals a self-association mechanism required for E6-mediated degradation of p53. Structure, 20, 604-17.

Zerfass-Thome, K., Zwerschke, W., Mannhardt, B., Tindle, R., Botz, J. W. & Jansen-Durr, P. 1996. Inactivation of the cdk inhibitor p27KIP1 by the human papillomavirus type 16 E7 oncoprotein. Oncogene, 13, 2323-30.

Zhang, B., Chen, W. & Roman, A. 2006. The E7 proteins of low- and high-risk human papillomaviruses share the ability to target the pRB family member p130 for degradation. Proc Natl Acad Sci U S A, 103, 437-42.

Zhang, B., Spandau, D. F. & Roman, A. 2002. E5 protein of human papillomavirus type 16 protects human foreskin keratinocytes from UV B-irradiation-induced apoptosis. J Virol, 76, 220-31.

Zheng, L., Ding, H., Lu, Z., Li, Y., Pan, Y., Ning, T. & Ke, Y. 2008. E3 ubiquitin ligase E6AP-mediated TSC2 turnover in the presence and absence of HPV16 E6. Genes Cells, 13, 285-94.

Zhong, Q., Gao, W., Du, F. & Wang, X. 2005. Mule/ARF-BP1, a BH3-only E3 ubiquitin ligase, catalyzes the polyubiquitination of Mcl-1 and regulates apoptosis. Cell, 121, 1085-95.

Zhou, J., Stenzel, D. J., Sun, X. Y. & Frazer, I. H. 1993. Synthesis and assembly of infectious bovine papillomavirus particles in vitro. J Gen Virol, 74 (Pt 4), 763-8.

Ziegler, A., Jonason, A. S., Leffell, D. J., Simon, J. A., Sharma, H. W., Kimmelman, J., Remington, L., Jacks, T. & Brash, D. E. 1994. Sunburn and p53 in the onset of skin cancer. Nature, 372, 773-6.

Ziegler, A., Leffell, D. J., Kunala, S., Sharma, H. W., Gailani, M., Simon, J. A., Halperin, A. J., Baden, H. P., Shapiro, P. E., Bale, A. E. & et al. 1993. Mutation hotspots due to sunlight in the p53 gene of nonmelanoma skin cancers. Proc Natl Acad Sci U S A, 90, 4216-20.